UAB

Universitat Autònoma de Barcelona

Universitat Autònoma de Barcelona

Estudis de Doctorat en Química

Facultat de Ciències

Departament de Química

Metal Nanoparticles (Pt, Ni, Au, Rh) Stabilized by Imidazolium Salts. Synthesis, Characterization and Catalytic Applications

Ph.D. Thesis

Ph. D. in Chemistry

Guillem Fernández Freixes

2020

Supervisor:

Prof. Roser Pleixats i Rovira

Memòria presentada per aspirar al grau de Doctor per:

Guillem Fernández Freixes

Vist i plau,

Prof. Roser Pleixats i Rovira

Bellaterra, 15 de setembre de 2020

I. TABLE OF CONTENTS

II.   PUBLICATIONS

The results obtained in this Thesis have been reported in the following publications:

- Fernández, G., Sort, J., Pleixats, R., Nickel Nanoparticles stabilized by Tris-imidazolium Salts: Synthesis, Characterization and Application as Recyclable Catalysts for the Reduction of Nitroarenes. *ChemistrySelect* **2018**, *3*, 8597.

- Fernández, G., Pleixats, R., Soluble Pt Nanoparticles Stabilized by a Tris-imidazolium Tetrafluoroborate as Efficient and Recyclable Catalyst for the Stereoselective Hydrosilylation of Alkynes. *ChemistrySelect* **2018**, *3*, 11486.

- Fernández, G., Bernardo, L., Villanueva, A., Pleixats, R., Gold nanoparticles stabilized by PEG-tagged imidazolium salts as recyclable catalysts for the synthesis of propargylamines and the cycloisomerization of γ-alkynoic acids. *New J. Chem.* **2020**, *44*, 6130. (**Front Cover**)

- Another publication is under preparation.

III.   COMMUNICATIONS

During my PhD thesis, I have attended several scientific meetings:

- Guillem Fernández, Ana Villanueva, Roser Pleixats*. *Hydrosilylation of internal alkynes catalyzed by rhodium nanoparticles stabilized by PEG-tagged imidazolium salt*. XXXVI Reunión Bienal de Química. Sitges, June **2017**. **Poster**.
- Guillem Fernández, Roser Pleixats*. *Synthesis and Catalytic Applications of Platinum Nanoparticles Stabilized by a Tris-imidazolium Tetrafluoroborate*. X International School on Organometallic Chemistry Marcial Moreno Mañas. Ciudad Real, July **2017**. **Poster**.
- Guillem Fernández, Roser Pleixats*. *Síntesi i aplicacions catalítiques de nanopartícules de níquel i platí*. Desena Trobada de Joves Investigadors dels Països Catalans. Barcelona, January **2018**. **Oral presentation**.
- Guillem Fernández, Roser Pleixats*. *Nickel nanoparticles stabilized by tris-imidazolium salts: synthesis, characterization and applications as recyclable catalysts*. XI International School on Organometallic Chemistry Marcial Moreno Mañas. Oviedo, June **2018**. **Poster and flash presentation**.
- Guillem Fernández, Roser Pleixats*. *Selective reduction of nitroarenes catalyzed by nickel nanoparticles stabilized by tris-imidazolium salts*. XXVII Reunión Bienal de Química Orgánica. Santiago de Compostela, June **2018**. **Poster and flash presentation**.
- Guillem Fernández, Roser Pleixats*. *Synthesis and Catalytic Applications of Soluble Metal Nanoparticles*. Jornades Doctorals Department of Chemistry. Bellatera, May **2019**. **Poster and oral presentation**.
- Guillem Fernández**,** Ana Villanueva, Laura Bernardo, Roser Pleixats*. *Gold nanoparticles stabilized by PEG-tagged imidazolium salts: synthesis, characterization and applications as recyclable catalysis*. XII International School on Organometallic Chemistry Marcial Moreno Mañas. Castellón, June **2019**. **Poster and flash presentation**.
- Guillem Fernández, Laura Bernardo, Ana Villanueva, Roser Pleixats*. *Synthesis and Catalytic Applications of Soluble Rhodium Nanoparticles*. Onzena Trobada de Joves Investigadors dels Països Catalans. Vilanova i la Geltrú, January **2020**. **Oral presentation**.

IV. ABBREVIATIONS

9-BBN	9-borabicyclo[3.3.1]nonane	**EDS**	Energy-dispersive X-ray spectroscopy
A³ coupling	Three-component coupling	**EG**	Ethylene glycol
Ab	Arbitrary	**emu**	Electromagnetic unit
AB	Ammonia borane	**Equiv.**	Equivalents
acac	Acetylacetonate	**ESI-HRMS**	Electrospray ionization high resolution mass spectrometry
Ar	Aryl	**ESI-TOF-MS**	Electrospray ionization time-of-flight mass spectrometry
atm	Atmosphere	**Et**	Ethyl
br s (NMR)	Broad singlet	**Et$_2$O**	Diethyl ether
Bu	Butyl	**EtOAc**	Ethyl acetate
Cat	Catalyst	**EtOH**	Ethanol
COD	1,5-cyclooctadiene	**FCC**	Face-centered cubic
COT	1,3,5-cyclooctatriene	**G3**	3rd generation
CuAAC	Copper-catalyzed azide-alkyne cycloaddition	**GC-MS**	Gas chromatography-mass spectrometry
Δ	Heating	**H**	Magnetic field strength
d (NMR)	Doublet	**hlk**	Miller indices for lattice plains
dba	Dibenzylideneacetone	**HRTEM**	High resolution transmission electron microscopy
DBU	1,8-diazabicyclo[5.4.0]undec-7-ene	**ICP-OES**	Inductively coupled plasma-optical emission spectroscopy
dd (NMR)	Double doublet	**IR**	Infrared spectroscopy
δ (NMR)	Chemical shift	**J (NMR)**	Coupling constant
DFT	Density functional theory	**LSPR**	Localized surface plasmon resonance
d$_{hlk}$	Interplanar distance	**M**	Concentration mol/L
DLVO	Derjaguin, Landau Verwey and Overbeek theory	**M (magnetic measurements)**	Magnetization
DMF	*N,N*.Dimethylformamide	**m (NMR)**	Multiplet
DMSO	Dimethyl sulfoxide	**MAA**	Methylacrylamide
ED	Electron diffraction		

Abbreviations

MALDI-TOF MS	Matrix-assisted laser desorption/ionization time-of-flight mass spectrometry	**Ph**	Phenyl
Me	Methyl	**PMHS**	Polymethylhydrosiloxane
MeO	Methoxy	**PNMA**	Poly-*N*-methylolacrylamide
MeOH	Methanol	**ppm**	Parts-per-million
mM	Concentration in mmol/L	**Pr**	Isopropyl
MOFs	Metal organic frameworks	**PVP**	Polyvinylpyrrolidone
mp	Melting point	**q (NMR)**	Quartet
M$_s$	Saturation magnetization	**rt**	Room temperature
MsCl	Methanesulfonyl chloride	**s (NMR)**	Singlet
MW	Microwave	**T**	Temperature
NaOAc	Sodium acetate	**t (NMR)**	Triplet
NBE	2-norbornene	**T$_B$**	Blocking temperature
NHC	*N*-heterocyclic carbene	**^{t}BuOH**	*Tert*-butanol
NHT	*N*-heterocyclic thiones	**TEM**	Transmission electron microscopy
NMA	*N*-methylolacrylamide	**THF**	Tetrahydrofuran
NMP	*N*-methylpyrrolidone	**TLC**	Thin layer chromatography
NMR	Nuclear magnetic resonance	**TOAB**	Tetraoctylammonium bromide
N-rich	Nitrogen-rich	**UV-vis**	Ultraviolet-visible spectroscopy
NPs	Nanoparticles	**wt**	Weight
Oe	Oersted	**XPS**	X-ray photoelectron spectroscopy
p	para	**ZFC/FC**	Zero field cooling/field cooling
ρ	Density		
PEG	Polyethyleneglycol		

V. FORMULA INDEX

1

2a

2b

3

4

5

6

7

8

9

10

11

12a

12b

12c

12d

12e

13

14

15

16

17

18

19

20

21a

21b

21c

21d

21e

22a

22b

22c

22d

22e

23aaa

23aba

23aca

23ada

23aea

23bba

23cba

23dba

23eba

Formula index

23abb

23abc

23abd

23abe

24a

24b

24c

25aaa

25aba

25bba

25caa

26

27

28

29

30

31

32

33

34

35

36

37

38

HSiEt$_3$

39

40

HSiPh$_3$

41

42

Bu ── ── Bu

43

44

45

46

47

(*E*)-**48a**

(*E*)-**48b**

(*E*)-**49a**

(*E*)-**49b**

(*E*)-**50a**

(*E*)-**50b**

51

52

53

54

(*E*)-**55a**

(*E*)-**55b**

(*E*)-**56a**

(*E*)-**56b**

(*E*)-**57a**

(*E*)-**57b**

(*Z*)-**57a**

(*E*)-**58a**

58b

(*Z*)-**58a**

(*E*)-**59a**

59b

60

Formula index

61 **62** **63** **64** **65** **66** **67**

68 **69** **70** **71** **72** **73**

74 **75** **76** **77** **78** **79**

80 **81** **82** **83** **84** **85**

86 **87** **88** **89** **90** **91**

92 **93** **94** **95** **96** **97**

STABILIZERS

S1A **S1B** **S2A** **S2B**

S3

Formula index

MATERIALS

$X = I, BF_4$
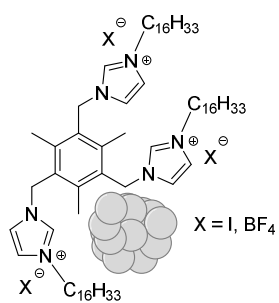
Pt NPs:
M2 : **S1A**/Pt = 2.5/1
M3 : **S1A**/Pt = 1/1
M4 : **S1B**/Pt = 1/1
M5 : **S1B**/Pt = 1/1
M6 : **S1B**/Pt = 0.5/1

Ni NPs:
M11 : **S1A**/Ni = 0.1/1
M12 : **S1A**/Ni = 0.05/1
M13 : **S1B**/Ni = 0.1/1

$X = Br, BF_4$
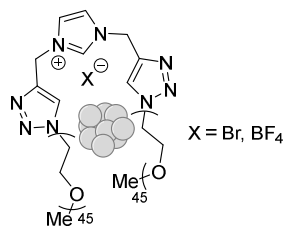
Au NPs:
M14 : **S2A**/Au = 0.3/1
M15 : **S2B**/Au = 0.3/1

Rh NPs:
M18 : **S2A**/Rh = 0.019/1
M19 : **S2B**/Rh = 0.019/1
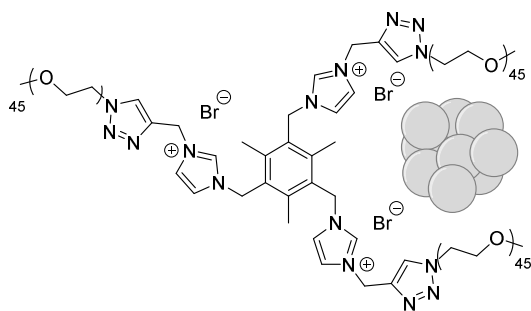
Au NPs:
M16 : **S3**/Au = 0.3/1
M17 : **S3**/Au = 0.3/1

Rh NPs:
M20 : **S3**/Rh = 0.025/1

VI. ABSTRACT

In the last years the research on metal nanoparticles (NPs) for catalytic purposes has grown exponentially. The small size of these materials provides unique properties, especially important for catalytic applications is their high surface/volume ratio. To ensure a complete control of the size of the metal NPs and to prevent their agglomeration, the effect of the stabilizing agent plays a key role. In this field, our group has been focused in the preparation of different kinds of ligands for the preparation of soluble metal NPs. Tris-imidazolium iodide and tetrafluoroborate bearing long alkyl chains (**S1A** and **S1B** respectively) have been reported as suitable stabilizers for the preparation of Pd NPs. Moreover, N-rich PEGylated ligands have been used as stabilizers for the obtention of water-soluble Au and Rh NPs. These NPs have been used as catalysts in cross-coupling reactions (Pd NPs), in the hydrosilylation of internal alkynes (Pd, Rh NPs) and in the reduction of nitroarenes (Au NPs).

We present herein the synthesis of three new PEG-tagged imidazolium salts (imidazolium bromide **S2A**, imidazolium tetrafluoroborate **S2B** and tris-imidazolium bromide **S3**). The key step of their synthesis involves the linking of the polyoxyethylenated chains and the imidazolium moieties through a triazole ring obtained by a copper-catalyzed [2+3] cycloaddition between alkynes and azides (CuAAC reaction).

The previously reported **S1A** and **S1B** have been used as stabilizers for the preparation of Pt and Ni NPs soluble in some organic solvents, such as dichloromethane, chloroform or THF and insoluble in diethyl ether or hexane. Besides, water-soluble Au and Rh NPs stabilized by the PEG-tagged imidazolium salts (**S2A**, **S2B** and **S3**) have also been prepared. All the nanomaterials were characterized by TEM, HRTEM, ED, EDS, XPS, ^{1}H NMR and ICP-OES. A study of the magnetic properties of Ni NPs was also performed (hysteresis loops and ZFC/FC).

These NPs were found catalytically active in different organic reactions. Thus, Au NPs were found effective catalysts for the synthesis of propargylamines via a three-component coupling reaction between aldehydes (or ketones), secondary amines and terminal alkynes. This nanocatalyst was also found active in the cycloisomerization of γ-alkynoic acids into enol lactones.

The hydrosilylation of internal alkynes was successfully performed under catalysis by Pt and Rh NPs. The reaction was stereolective and the *syn*-addition product was formed. When asymmetrically substituted alkynes were used, moderate regioselectivities were observed depending on the substrate and the catalyst used. In all cases high yields of the corresponding *(E)*-vinylsilanes were achieved. Platinum NPs gave faster reactions, but Rh NPs provided better regioselectivities.

Finally, the reduction of nitroarenes under catalysis by Ni and Rh NPs was carried out. The Ni NPs catalyzed the selective reduction of a wide number of substituted nitroarenes (bearing significant reducible functional groups) with hydrazine as hydrogen donor in refluxing THF. On the other hand the Rh nanocatalysts were able to catalyze the reduction of nitroarenes in THF-water (1:4) at room temperature using the hydrogen generated *in situ* in the hydrolysis of ammonia-borane.

In all cases the nanocatalysts could be reused for several cycles taking advantage of their different solubility properties and also the magnetic properties in the case of Ni NPs.

VII. RESUM

Durant els darrers anys la investigació basada en l'ús de nanopartícules metàl·liques (NPs) ha experimentat un creixement exponencial. La mida tant petita que tenen aquests materials els proporciona unes propietats úniques, sent especialment important, per les aplicacions catalítiques, la seva gran relació superfície/volum. Per assegurar un control complet de la mida de les NPs i evitar-ne la seva aglomeració, l'efecte dels estabilitzants és fonamental. En aquest sentit, el nostre grup ha centrat la seva investigació en la síntesi de diferents lligands per a la preparació de NPs metàl·liques solubles. Es va dur a terme la síntesi de NPs de Pd estabilitzades per iodur o tetrafluoroborat de tris-imidazoli amb llargues cadenes alquíliques (**S1A** o **S1B**, respectivament). A més, compostos rics en nitrogen amb cadenes polioxietilenades es van utilitzar com a estabilitzants per a la síntesi de NPs de Rh i Au solubles en aigua. Aquestes NPs es van usar com a catalitzador per reaccions d'acoblament creuat (NPs de Pd), per a la hidrosililació d'alquins interns (NPs de Pd i Rh) i per a la reducció de nitroarens (NPs d'Au).

Durant el transcurs d'aquesta tesi doctoral s'han sintetitzat tres noves sals d'imidazoli amb llargues cadenes de polietilenglicol (bromur d'imidazoli **S2A**, tetrafluoroborat d'imidazoli **S2B** i bromur de tris-imidazoli **S3**). El pas clau per a la síntesi d'aquests compostos implica l'enllaç de les sals de imidazoli i les cadenes de polietilenglicol a través d'un anell triazòlic format a partir d'una cicloaddició [2+3] catalitzada per coure entre alquins i azides (reacció de CuAAC).

Les sals de tris-imidzoli **S1A** i **S1B**, prèviament sintetitzades al nostre grup, es van utilitzar com a estabilitzants per a la síntesi de NPs de Pt i Ni, solubles en alguns dissolvents orgànics com ara clorur de metilè, cloroform o THF i insolubles en dietilèter o hexà. També es van sintetitzar NPs de Au i Rh solubles en aigua estabilitzades amb les sals d'imidazoli polioxietilenades (**S2A**, **S2B** i **S3**). Tots aquests nanomaterials van ser caracteritzats per TEM, HRTEM, ED, EDS, XPS, ^{1}H NMR i ICP-OES. A més, es va dur a terme un estudi de les propietats magnètiques de les NPS de Ni (corbes d'histèresi i ZFC/FC).

Aquestes NPS van ser catalíticament actives en diferents reaccions orgàniques. Així, les NPs d'or van presentar una gran efectivitat com a catalitzadors per a la síntesi de propargilamines a traves d'un acoblament triple entre aldehids (o cetones), amines secundàries, i alquins terminals. Aquests catalitzadors també van ser actius per a la cicloisomerització d'àcids γ-alquinoics a les corresponents enol-lactones.

La hidrosililació d'alquins interns es va dur a terme sota catàlisi per NPs de Pt i Rh. La reacció fou estereoselectiva, formant-se el producte d'addició *syn*. Partint d'alquins asimètrics es van observar diferents regioselectivitats depenent del substrat de partida així com del catalitzador emprat. En tots els casos es van obtenir els corresponents *(E)*-vinilsilans amb uns rendiments excel·lents. Amb les NPs de Pt els temps de reacció van ser menors, però les NPs de Rh van proporcionar millors regioselectivitats.

Finalment, es va dur a terme la reducció de nitroarens amb NPs de Ni i Pt. Les NPs de Ni van reduir de manera selectiva diversos nitroarens substituïts amb hidrazina com a font d'hidrogen a reflux de THF. Altres grups funcionals reduïbles presents en la molècula, van romandre inalterats. D'altra banda, amb les NPs de Rh es va catalitzar la reducció de nitroarens en el si de THF-aigua (1:4) a temperatura ambient fent servir l'hidrogen generat *in situ* en la hidròlisi del complex NH$_3$·BH$_3$.

En tots els casos els catalitzadors van ser reciclats varies vegades gràcies a la diferent solubilitat en diversos medis i a les propietats magnètiques en cas de les NPs de Ni.

VIII. RESUMEN

En los últimos años la investigación basada en el uso de nanopartículas metálicas (NPS) para aplicaciones catalíticas ha crecido exponencialmente. El pequeño tamaño de estos materiales proporciona unas propiedades únicas, siendo especialmente importante, en aplicaciones catalíticas, la gran relación superficie/volumen que poseen. Para asegurar un control completo del tamaño de partícula y evitar su aglomeración, el efecto del estabilizante es fundamental. En este sentido, nuestro grupo ha centrado su investigación en la síntesis de diferentes ligandos para la preparación de NPs metálicas solubles. Se sintetizaron NPs de Pd estabilizadas por ioduro o tetrafluoroborato de tris-imidazolio con largas cadenas hidrocarbonadas (**S1A** o **S1B**, respectivamente). Además, compuestos ricos en nitrógeno con cadenas polioxietilenadas se usaron como estabilizantes para la síntesis de NPs de Au y Rh solubles en agua. Estas NPs metálicas fueron empleadas como catalizadores para reacciones de acoplamiento cruzado (NPs de Pd), para la hidrosililación de alquinos internos (NPs de Pd y Rh) y para la reducción de nitroarenos (NPs de Au NPs).

En la presente tesis doctoral se han sintetizado tres nuevas sales de imidazolio con largas cadenas de polietilenglicol (bromuro de imidazolio **S2A**, tetrafluoroborato de imidazolio **S2B** y bromuro de tris-imidazolio **S3**). El paso clave de la síntesis de estos compuestos implica el enlace de las sales de imidazolio y las cadenas de polioxietilenglicol mediante un anillo triazólico obtenido a partir de una cicloadición [2+3] catalizada por cobre entre alquinos y azidas (reacción de CuAAC).

Las sales de tris-imidazolio **S1A** y **S1B**, previamente sintetizadas en nuestro grupo, se han utilizado como estabilizantes en la síntesis de NPs de Pt i Ni, solubles en algunos compuestos orgánicos como diclorometano, cloroformo o THF e insolubles en éter dietílico o hexano. También se han sintetizado NPs de Au y Rh solubles en agua con las sales de imidazolio polioxietilenadas (**S2A**, **S2B** y **S3**). Todos los nanomateriales obtenidos han sido caracterizados por TEM, HRTEM, ED, EDS, XPS, ^{1}H NMR y ICP-OES. Además, se realizó un estudio de las propiedades magnéticas de las NPs de Ni (curvas de histéresis y ZFC/FC).

Estas NPs metálicas fueron catalíticamente activas en diferentes reacciones orgánicas. Así, las NPs de Au presentaron una gran efectividad como catalizadores para la síntesis de propargilaminas a través un acoplamiento triple entre aldehídos (o cetonas), aminas secundarias y alquinos terminales. Estos catalizadores además fueron activos para la cicloisomerización de ácidos γ-alquinoicos a las correspondientes enol-lactonas.

La hidrosililación de alquinos internos se llevó a cabo bajo catálisis con NPs de Pt y Rh. La reacción fue estereoselectiva para la formación del producto de adición *syn*. Partiendo de alquinos asimétricos se observaron diferentes regioselectividades dependiendo del substrato de partida, así como del catalizador usado. En todos los casos se obtuvieron los correspondientes *(E)*-vinilsilanos con excelentes rendimientos. Con las NPs de Pt los tiempos de reacción fueron menores, pero las NPs de Rh proporcionaron mejores regioselectividades.

Finalmente, se llevó a cabo la reducción de nitroarenos con NPs de Ni y Rh. Las NPs de Ni redujeron de manera selectiva diversos nitroarenos sustituídos con hidracina como fuente de hidrogeno a reflujo de THF. Otros grupos funcionales reducibles presentes en la molécula se mantuvieron inalterados. Por otro lado, con las NPs de Rh se catalizó la reducción de nitroarenos en THF-agua (1:4) a temperatura ambiente usando el hidrógeno generado *in situ* en la hidrólisis del complejo $NH_3 \cdot BH_3$.

En todos los casos los catalizadores fueron reciclados varias veces gracias a la diferente solubilidad en diversos medios y a sus propiedades magnéticas en el caso de las NPs de Ni.

Chapter 1.   GENERAL INTRODUCTION

Catalysis has been playing a key role in the history of chemistry, in both industrial and academic research. Most of the common products that we use every day, from fuels or polymers to medicines, would not be affordable without the use of catalysts for their production. Depending on the nature of the catalyst, two major types can be distinguished: homogeneous and heterogeneous catalysts. Homogeneous catalysts are in general very active species present in the same phase as the reaction mixture. Nevertheless, they are not easily separated from the final products. This problem can be solved using heterogeneous catalysts which are present in a different phase than the reactants. However, as the active species are only present in the surface of the catalysts, their amount is much lower than in the homogeneous catalysts. In order to combine the advantages of both types of catalysts, the immobilization of the homogeneous active species into a solid support, such as metal oxides or polymers, has been proposed. In that way, these supported catalysts can be easily removed from the reaction mixture by filtration. Additionally, other options have been explored, such as the use of transition metal nanoparticles (NPs) in catalysis. These NPs can be supported or can be used in solution. The solubility of the NPs depends on the structure of the stabilizer surrounding the metal core, and these solubility properties can be useful for recycling the nanocatalyst. They can act as heterogeneous catalysts, but with a higher load of active species caused by their large surface/volume ratio.

1.1   METAL NANOPARTICLES

Metal NPs are defined as clusters of metal atoms with a size between 1 and 100 nm. These nanomaterials have applications in a wide range of fields such as electronics, energy, magnetism, biology, medicine and catalysis, among others.[1,2] The properties of the NPs are largely dependent of their size, especially in catalytic applications. In that way, it is desirable to obtain NPs as small as possible in order to maximize the amount of surface atoms. However, the high activity of these species increases the tendency of the nanoparticles to agglomerate forming larger and more stable particles, obtaining finally the bulk metal and, in consequence, losing most of their unique properties (they are thermodynamically unstable). In order to solve this problem, the NPs can be stabilized with different ligands or polymers surrounding the surface of the metal core of the NPs. Another option for the stabilization is the immobilization of the NPs on a solid support.

1.1.1 STABILIZATION OF METAL NANOPARTICLES

To prevent the agglomeration and increase the stability of the suspension in liquid phase the NPs should be stabilized. The stabilization of the NPs can tune their properties by changing their size and their solubility in different solvents. In that way, we can distinguish four major types of stabilization: (a) electrostatic stabilization; (b) steric stabilization; (c) electrosteric stabilization; (d) stabilization with ligands. Another option to avoid their agglomeration is their immobilization on solid supports.

1.1.1.1.   ELECTROSTATIC STABILIZATION

The basis of the electrostatic stabilization is the electric repulsion between the NPs generated by a double layer of electric charges surrounding the particles. This mutual repulsion between the particles and their neighbours is what prevents the agglomeration. The electrostatic stabilization was first defined in the

---

[1] Some selected monographies about NPs and nanotechnology: (a) *Nanoscale Materials in Chemistry;* Klabunde, K. J. Ed.: Wiley-Interscience, **2001.** (b) *Nanoparticles and catalysis*; Astruc, D. Ed.: Wiley-WCH, **2008.** (c) *Introduction to Nanoscience & Nanotechnology;* Hornyak, G. L., Tibbals, H. F., Dutta, J., Moore, J. J. Ed.: CRC press, **2009.** (d) *Nanostructures and Nanomaterials: Synthesis, Properties, and Applications*; Cao, G., Wang, Y. Ed.: World Scientific Publishing Co., **2011.** (e) *Noble Metal Nanoparticles: Synthesis and Optical Properties. Reference Module in Materials Science and Materials Engineering.* Hubental, F. Ed.: Elsevier Inc., **2016.**

[2] Some selected reviews about the preparation, properties, characterization and application of metal NPs: (a) Moreno-Mañas, M., Pleixats, R. *Acc. Chem. Res.* **2003**, *36*, 638. (b) Burda, C., Chen, X., Narayanan, R., El-Sayed, M. A. *Chem. Rev.* **2005**, *105*, 1025. (c) Astruc, D., Lu, F., Aranzaes, J. R. *Angew. Chem. Int. Ed.* **2005**, *44*, 7852. (d) Sau, T. K., Rogach, A. L., *Adv. Mater.* **2010**, *22*, 1781. (e) Alex, S., Tiwari, A. *J. Nanosci. Nanotechnol.* **2015**, *15*, 1869. (d) Khan, I., Saeed, K., Khan, I. *Arab. J. Chem.* **2019**, *12*, 908. (f) Jia, C.-J., Schüth, F. *Phys. Chem. Chem. Phys.* **2011**, *13*, 2457. (g) Campelo, J. M., Luna, D., Luque, R., Marinas, J. M., Romero, A. A. *ChemSusChem* **2009**, *2*, 18.

Chapter 1. General Introduction

Derjaguin, Landau, Verwey and Overbeek (DLVO) theory. According to that theory, there are two main forces that determine the interaction between the particles, the Van der Waals forces and the electrostatic double layer force. [3,4,5] These repulsive forces can prevent the agglomeration and stabilize the colloidal suspension of NPs.

The surfaces of metal NPs are, in general, electron-deficient, so the anions present in the solution can be adsorbed and generate a layer of anions around the NPs. A second layer of cations are generated to stabilize the formal charges in the clusters, forming a double layer structure. If the coulombic potential of this double layer is higher than the Van der Waals forces, the electric repulsion will prevent the agglomeration (**Figure 1**).[6] Nevertheless, this kind of stabilization is very pH dependant and sensitive to changes in the conductivity of the medium, producing not very stable colloidal solutions with trending to aggregation.

van der Waals attraction   van der Waals attraction

Electrostatic repulsion   Electrostatic repulsion
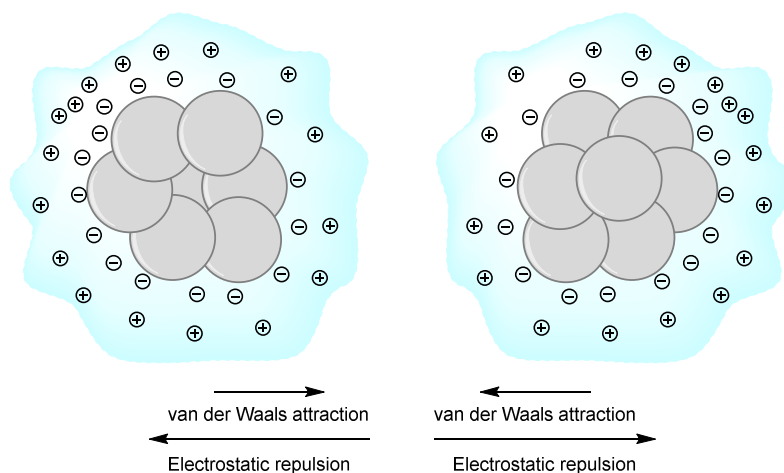
Figure 1 Electrostatic stabilization of metal NPs**.**[6]

One example of this kind of stabilization is the synthesis of Au NPs by the classical Turkevich method[7] developed at mid XX century. In that case the reducing agent for the Au(III) precursor was sodium citrate which also acts as stabilizer once the NPs are formed (**Scheme 1**).[8]
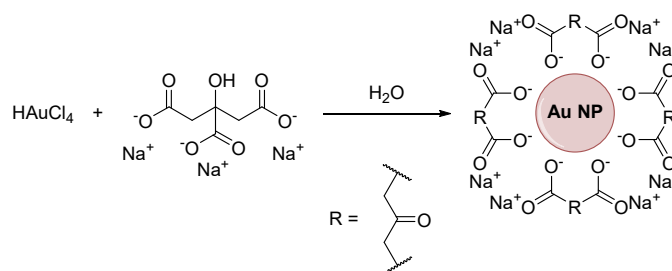
Scheme 1 Representation of Turkevich method.[8]

[3] *Concepts for the Stabilization of Metal Nanoparticles in Ionic Liquids, Applications of Ionic Liquids in Science and Technology*; Kraynov, A., Müller, T. E., Handy, S. (Ed.) Ed.: Intech, **2011.**

[4] Verwey, E. J. W. *J. Phys. Chem*. **1947**, *51* (3), 631.

[5] *Derjaguin, B., Landau, L. D. Zhurnal Eksperimentalnoi I Teoreticheskoi Fiziki* **1945**, *15*, 663.

[6] Wang, Y.-J., Zhao, N., Fang, B., Li, H., Bi, X. T., Wang, H. *Chem. Rev.* **2015**, *115*, 3433.

[7] (a) Turkevich, J., Stevenson, P. C., Hillier, J. Discuss. Faraday Soc. **1951,** *11*, 55. (b) Turkevich, J., Stevenson, P. C. Hillier, J. *J. Phys. Chem.* **1953**, *57*, 670.

[8] António, M., Nogueira, J., Vitorino, R., Daniel-da-Silva, A. L. *Nanomaterials* **2018**, *8*, 200.

1.1.1.2.   STERIC STABILIZATION

This kind of stabilization is based in the steric effect, caused by large molecules surrounding the NPs that prevent their agglomeration.[9] The most common molecules used for this purpose, due their big size, are polymers. These polymers can interact with the NPs by mainly two ways. The first option is their absorption into the NPs surface (**Figure 2 (A)**).[10,11] The other possibility is the generation of a network of crosslinked polymers, and suspending the metal NPs inside the network (**Figure 2 (B)**).[12,13,14] In both cases, the stabilization follows the same mechanism, when two NPs are close enough the absorbed molecules repel each other by the restriction in motion between them.
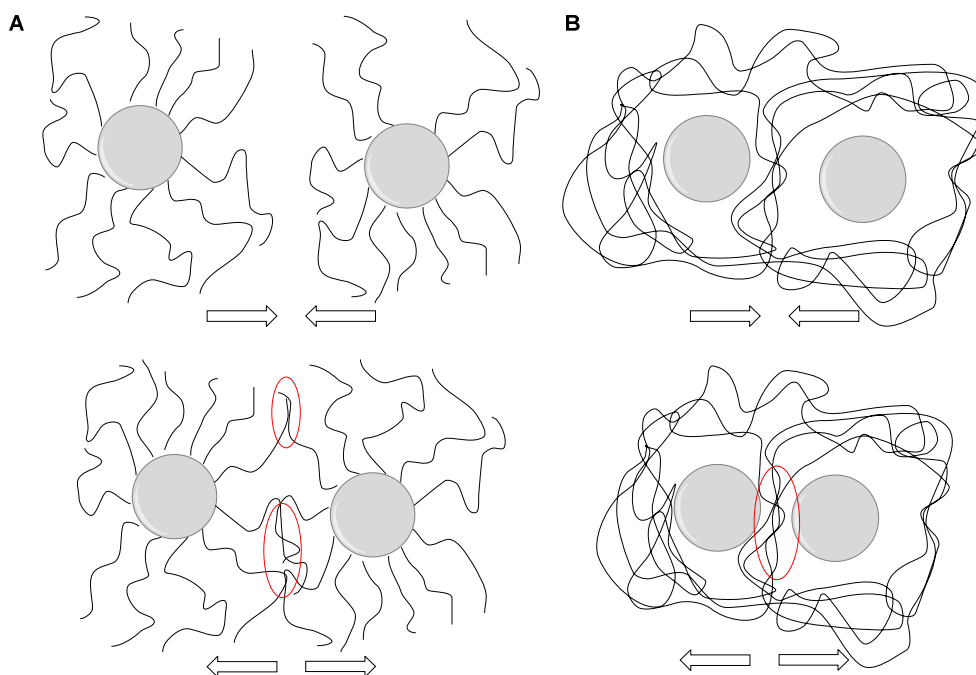
Figure 2 Steric stabilization of metal NPs: **(A)** NPs functionalized with polymer chains; **(B)** NPs inside a crosslinked polymer network.

Another good example of this kind of stabilization is the immobilization of metal NPs on a dendrimer.[15,16,17] In that way, the stabilization is similar to the encapsulation of NPs on the crosslinked polymers. The steric repulsion between the dendrimers prevents the agglomeration of the NPs (**Figure 3**).

[9] Saldías, C., Bonardd, S., Quezada, C., Radić, D., Leiva, A. *J. Nanosci. Nanotechnol.* **2017**, *17* (1), 87.

[10] Ortega-Muñoz, M., Blanco, V., Hernandez-Mateo, F., Lopez-Jaramillo, F. J., Santoyo-Gonzalez, F. *ChemCatChem* **2017**, *9*, 3965.

[11] Lü, J., Yang, Y., Gao, J., Duan, H., Lü, C. *Langmuir* **2018**, *34*, 8205.

[12] Farah, A. A., Alvarez-Puebla, R. A., Fenniri, H. *J. Colloid Interf. Sci* **2008**, *319*, 572.

[13] Murugan, E., Jebaranjitham, J. N. *J. Mol. Catal. A Chem.* **2012**, *365*, 128.

[14] Zhang, Y., Quek, X.-Y., Wu, L., Guan, Y., Hensen, E. J. *J. Mol. Catal. A Chem.* **2013**, *379*, 53.

[15] Crooks, R. M., Zhao, M., Sun, L., Chechik, V., Yeung, L. K. *Acc. Chem. Res.* **2001**, *34* (3), 181.

[16] Scott, R. W. J., Wilson, O. M., Crooks, R. M. *J. Phys. Chem. B* **2005**, *109*, 692.

[17] Yamamoto, K., Imaoka, T., Tanabe, M., Kambe, T. *Chem. Rev.* **2020**, *120*, 1397.
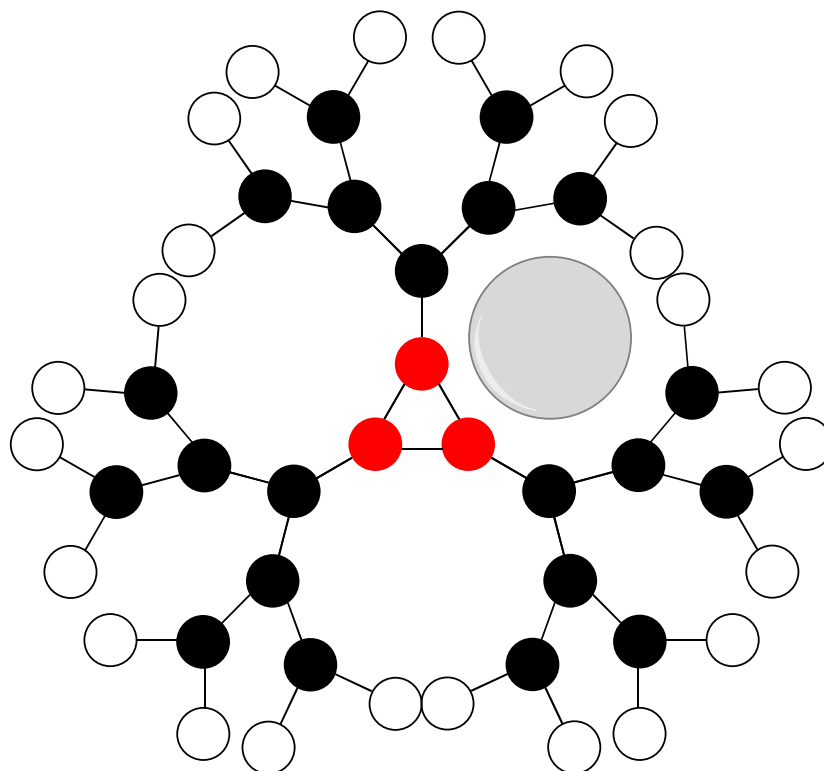
Figure 3 Representation of metal NP stabilized by a G3 dendrimer.

1.1.1.3.   ELECTROSTERIC STABILIZATION

There is another way to stabilize metal NPs that combines both methods previously described, obtaining a much better stabilization. Basically, electrosteric stabilization consists in surrounding the NPs with large molecules that contain ionic groups. The most common molecules used for this purpose are surfactants containing large polymeric chains.[18] Polymers containing ionic groups in their monomeric units can also be classified as electrosteric stabilizers.

1.1.1.4.   STABILIZATION WITH LIGANDS

The coordination of traditional ligands with the metal atoms have been extensively used for the preparation of metal NPs.[19,20] This type of stabilization allows a precise control of the size and shape by the robustness of the NP-ligand structure. One good example is the stabilization of gold NPs with thiol ligands, caused by the stability of the Au-S bond.[21] Other ligands with coordinating atoms such as phosphines[22] or amines[23] are also good examples of stabilizers for the obtention of different kinds of metal nanostructures. It should be

---

[18] Ghandi, K., Findlater, A. D., Mahimwalla, Z., MacNeil, C. S., Awoonor-Williams, E., Zahariev, F., Gordon, M. S. *Nanoscale* **2015**, *7*, 11545.

[19] Jin, R., Zeng, C., Zhou, M., Chen, Y. *Chem. Rev.* **2016**, *116*, 10346.

[20] (a) Lara, P., Philippot, K., Chaudret, B. *ChemCatChem* **2013**, *5*, 28. (b) Bronger, R., Le, T. D., Bastin, S., García-Antón, J., Citadelle, C., Chaudret, B., Lecante, P., Igau, A., Philippot, K. *New J. Chem.* **2011**, *35*, 2653.

[21] (a) Brust, M., Walker, M., Bethell, D., Schiffrin, D. J., Whyman, R. *J. Chem. Soc., Chem. Commun.* **1994**, 801. (b) Jin, R. *Nanoscale* **2010**, *2*, 343. (c) Wu, H., Zhu, H., Zhuang, J., Yang, S., Liu, C., Cao, Y. C. *Angew. Chem. Int. Ed.* **2008**, *47*, 3730.

[22] (a) Ibrahim, M., Wei, M. M., Deydier, E., Manoury, E., Poli, R., Lecante, P., Philippot, K. *Dalton Trans.* **2019**, *48*, 6777. (b) Castelbou, J. L., Bresó-Femenia, E., Blondeau, P., Chaudret, B., Castillón, S., Claver, C., Godard, C. *ChemCatChem* **2014**, *6*, 3160.

[23] a) Lacroix, L.-M., Gatel, C., Arenal, R., Garcia, C., Lachaize, S., Blon, T., Warot-Fonrose, B., Snoeck, E., Chaudret, B., Viau, G. *Angew. Chem. Int. Ed.* **2012**, *51*, 4690. b) Liu, Y., Wang, C., Wei, Y., Zhu, L., Li, D., Jiang, J. S., Markovic, N. M., Stamenkovic, V. R., Sun, S. *Nano Lett.* **2011**, *11*, 1614.

mentioned that some authors include the stabilization by coordinating ligands as a special type of electrosteric stabilization.

1.1.1.5. SUPPORTED METAL NPS

The use of solid materials as support for metal NPs have been extensively used in order to obtain stable and highly active nanomaterials.[24,25] Many types of materials can be used for the stabilization of metal NPs, such as insoluble polymers, carbon-based materials or inorganic oxides. This type of structures can be especially interesting in catalysis. After the reaction, the supported metal NPs can be easily removed from the reaction medium due to their heterogeneous nature.

Polymer-based supports have gained interest by their stability and reusability.[26] These materials present high porosity and surface area, which makes them perfect supports for NPs. Several examples have been reported with different metals: Pd,[27] Au,[28] or Ag.[29] The use of natural polymers for this purpose has also been described.[30,31]

Carbon-based materials present excellent properties as supports.[32,33,34,35,36] Nanostructures with a defined pore structure in shape and size can be synthesized, which give a high surface area to the nanomaterial. The most used carbon-based materials as supports for metal NPs are graphene[33] and nanotubes.[34]

Other materials suitable for the metal NPs immobilization are inorganic oxides.[37] Metal oxides provide high chemical and thermal stability, leading to very robust nanocomposites. The immobilization of small nanoclusters on the surface of the oxides creates heterogeneous materials with very active species that give many catalytic benefits. Among the metal oxides, alumina,[38] silicon oxides,[39] zinc oxides[29], are possibly the most used. Zeolites are also good supports for metal NPs due their high porosity.[40]

[24] Liu, L., Corma, A. *Chem. Rev.* **2018**, *118*, 4981.

[25] Hussain, M. A., Joseph, N., Kang, O., Cho, Y.-H., Um, B.-H., Kim, J. W. *Appl. Chem. Eng.* **2016**, *27*, 227.

[26] a) Bell, A. T. *Science* **2003**, *299*, 1688. b) Nasrollahzadeh, M., Sajjadi, M., Shokouhimehr, M., Varma, R. S. *Coord. Chem. Rev.* **2019**, *397*, 54. c) Dzhardimalieva, G. I., Zharmagambetova, A. K., Kudaibergenov, S. E., Uflyand *Kinet. and Catal.* **2020**, *61* (2), 198.

[27] a) Chen, X., Wang, W., Zhu, H., Yang, W., Ding, Y. *Molec. Catal.* **2018**, *456*, 49. b) Wang, K., Liu, J., Zhang, F., Zhang, Q., Jiang, H., Tong, M., Xiao, Y., Phan, N. T. S., Zhang, F. *ACS Appl. Mater. Interfaces* **2019**, *11* (44), 41238. (c) Shokouhimehr, M., Hong, K., Lee, T. H., Moon, C. W., Hong, S. P., Zhang, K., Suh, J. M., Choi, K. S., Varma, R. S., Jang, H. W. *Green Chem.* **2018**, *20*, 3809.

[28] a) Kaboudin, B., Khanmohammadi, H., Kazemi, F. *Appl. Surf. Sci.* **2017**, *425*, 400. b) Burguete, M. I., García-Verdugo, E., Luis, S. V., Restrepo, J. A. *Phys. Chem. Chem. Phys.* **2011**, *13*, 14831.

[29] Yesmurzayeva, N. N., Nurakhmetova, Z. A., Tatykhanova, G. S., Selenova, B. S., Kudaibergenov, S. E. *Supramol. Catal.* **2015**, *2*, 1.

[30] Khodadadi, B., Bordbar, M., Nasrollahzadeh, M. *J. Coloidl. Interf. Sci.* **2017**, *490*, 1.

[31] a) Lam, E., Hrapovic, S., Majid, E., Chong, J. H., Luong, J. H. T. *Nanoscale* **2012**, *4*, 997. b) Jebali, Z., Granados, A., Nabili, A., Boufi, S., do Rego, A. M. B., Majdoub, H., Vallribera, A. *Cellulose* **2018**, *25*, 6963. c) Ayad, M. M., Amer, W. A., Zaghlol, S., Maráková, N., Stejskal, J. *Cellulose* **2018**, *25*, 7393.

[32] Zhao, M., Wu, Y., Cao, J.-P. *Appl. Organometal. Chem.* **2020**, *34* (4), 5539.

[33] Kamat, P. V. *J. Phys. Chem. Lett.* **2010**, *1*, 520.

[34] Huang, K., Zhong, J., Huang, J., Tang, H., Fan, Y., Waqas, M., Yang, B., Chen, W., Yang, J. *Appl. Surf. Sci.* **2020**, *501*, 144260.

[35] *Preparation, Characterization, and Catalytic Activity of Carbon Nanotubes-Supported Metal or Metal Oxide*; Zhao, F.-q., Yi, J.-h., Hong, W.-l., An, T., Yang, Y.-j. Ed.: Elsevier Inc. **2016**.

[36] Zeng, L., Cui, X., Shi, J. *Sci. China Mat.* **2018**, *61*, 1557.

[37] *Supported Gold Nanoparticles Leading to Green Chemistry*; Ishida, T., Haruta, M. Ed.: Wiley-VCH. **2017**.

[38] Ohyama, J., Esaki, A., Koketsu, T., Yamamoto, Y., Arai, S., Satsuma, A. *J. Catal.* **2016**, *335*, 24

[39] Turner, M., Golovko, V. B., Vaughan, O. P. H., Abdulkin, P., Berenguer-Murcia, A., Tikhov, M. S., Johnson, B. F. G., Lambert, R. M. *Nature* **2008**, *454*, 981.

[40] Dutta, P., Wang, B. *Coord. Chem. Rev.* **2019**, *383*, 1.

1.1.2 Preparation of metal nanoparticles

As mentioned previously, metal NPs consist in clusters of metal atoms with a few nm of size. To achieve these structures there are two main approaches: top-down and bottom-up methods. Based in physical techniques, the top-down method consists in dividing a bulk metal into smaller portions. After successive steps reducing the size of the material, NPs can be obtained. The main techniques used for the top-down approach are microfluidics and lithography.[1b,41] These techniques are principally used in the preparation of polymeric nano and micromaterials with sizes bigger than 100 nm. Top down procedures are mainly used for the preparation of devices and electronic components, but they are not very useful for the obtention of reproducible metal NPs. Bottom–up techniques follow the opposite direction. The desired atoms are generated from the treatment of corresponding precursors with chemical processes. Then, the aggregation of the atoms can be controlled by the addition of a suitable stabilizer. These techniques allow an almost complete control of the synthesis, leading to the preparation of small clusters of metal NPs in a reproducible way. For these reasons, this section is mainly focused on the description of bottom-up techniques.

For the obtention of metal NPs, naked atoms generated in the reaction must group together to form stable clusters. In this process there are two key steps, first the nucleation of the atoms and then the growing and stabilization of the obtained clusters. Generally, the synthesis of metal NPs is a very sensitive process, for this reason a precise control of the reaction conditions is needed. Changes in the stabilizer, solvent, concentration of the reactants, temperature or reaction time may affect significantly the result. Even, in some cases, the stirring method or the shape of the reaction vessel should be considered as important factors.

To understand the process of nucleation is important to introduce the concept of Ostwald ripening.[42] As mentioned previously, as smaller the NPs are, they become more energetically unstable. This is caused by a higher proportion of surface atoms that the small NPs contain in comparison with bigger ones. This stability of the cluster of atoms is caused by the number of bonds that an atom can make with the neighbour atoms. The atoms present in the inner part of the particles are completely linked with other atoms. In contrast the surface atoms are only linked with a few atoms. In order to minimize their energy these atoms tend to interact with the surface atoms of other particles, forming bigger and more stable NPs. This is the basis of the Ostwald ripening effect.

This phenomenon occurs during the formation of the particles. Initially, the generated metal atoms form clusters of different sizes. After this first nucleation, the smallest clusters will lose their unstable surface atoms generating a saturated solution of metal(0) species. These species tend to deposit into the bigger NPs minimizing their energy (**Figure 4**). This process will occur until the interactions between the stabilizer and the metal NPs are strong enough to compensate the energy of the surface and stable particles will be formed. For this reason, in the absence of any stabilizer the nucleation process will continue until all the atoms form a macroscopic structure with the minimum energy possible.

---

[41] (a) Euliss, L. E., DuPont, J. A., Gratton, S., DeSimone, J. *Chem. Soc. Rev.* **2006**, *35*, 1095. (b) Gratton, S. E. A., Ropp, P. A., Pohlhaus, P. D., Luft, J. C., Madden, V. J., Napier, M. E., DeSimone, J. M. *Proceed. Nat. Acad. Sci.* **2008**, *105* (33), 11613.
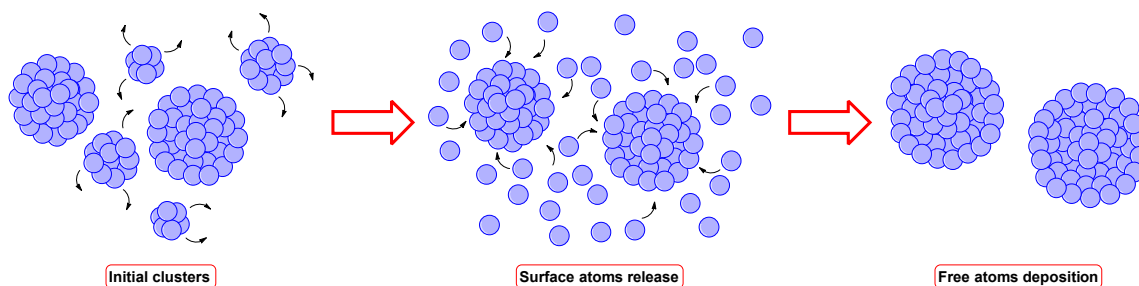[42] Baldan, A. *J. Mater. Sci.* **2002**, *37*, 2171.

Figure 4 Ostwald ripening schematic representation.

Even though Ostwald ripening is the most common theory for the formation of NPs, in recent years, other possibilities have been postulated for some concrete cases. The LaMer mechanism, Finke-Watsky two-step mechanism, coalescence attachment or interparticle growth are other possible theories for this phenomenon.[43]

The most common methods for the preparation of colloidal suspensions of metal NPs are: (i) chemical reduction of transition metal salts in the presence of a stabilizer; (ii) ligand reduction and displacement from organometallic complexes in the presence of a stabilizer. Other methods include: (iii) photochemical synthesis, (iv) thermal decomposition, (v) electrochemical reduction.

1.1.2.1. REDUCTION OF METAL SALTS IN THE PRESENCE OF A STABILIZER

The reduction of a metal salt in the presence of a stabilizer is the most common method for the synthesis of metal NPs.[1b] It is a very simple methodology that gives the desired NPs with a narrow size distribution and in high yield.

The first example of the reduction of a metal salt precursor for the preparation of metal NPs was reported by Turkevich in 1951.[7a] As mentioned previously, the Turkevich method consists in the reduction of $HAuCl_4$ by sodium citrate, which acts at the same time as reductant and stabilizer. Based in that methodology, the synthesis of NPs of other metals (Ag, Ir, Pd, Pt, Rh, Ni, Ru, etc.) and different kinds of reductants were studied. Hydrogen, $NaBH_4$, hydrazine, carbon monoxide, sodium citrate, oxidable alcohols or boranes are common reducing agents used for the synthesis of metal NPs. This methodology can be applied with any type of stabilizer, such as ionic species, polymers, surfactants or solid supports.[44]

The synthesis of metal NPs by chemical reduction can be summarized (**Figure 5**) in four steps: (**A**) obtention of the corresponding zerovalent metal atoms from the reduction of the metal salt; (**B**) nucleation and aggregation to generate the first small clusters; (**C**) clusters growth to generate NPs; (**D**) stop of the aggregation by the adsorption of the stabilizer on the particles surface.

---

[43] Thanh, N. T. K., Maclean, N., Mahiddine, S. *Chem. Rev.* **2014**, *114*, 7610.
[44] *Some examples of metal NPs obtained by metal salt chemical reduction:* (a) Wu, L., Ling, J., Wu, Z.-Q. *Adv. Synth. Catal.* **2011**, *353*, 1452. (b) Sanlés Sobrido, M., Pérez-Lorenzo, M., Rodríguez González, B., Salgueiriño, V., Correa-Duarte, M. A. *Angew. Chem. Int. Ed.* **2012**, *51*, 3877. (c) Bai, L., Yuan, F., Tang, Q., *Mater. Lett.* **2008**, *62*, 2267. (d) Wang, T., Shou, H., Kou, Y., Liu, H. *Green Chem.* **2009**, *11*, 562. See also: 2f, 23a,27a, 28, 31a,b.
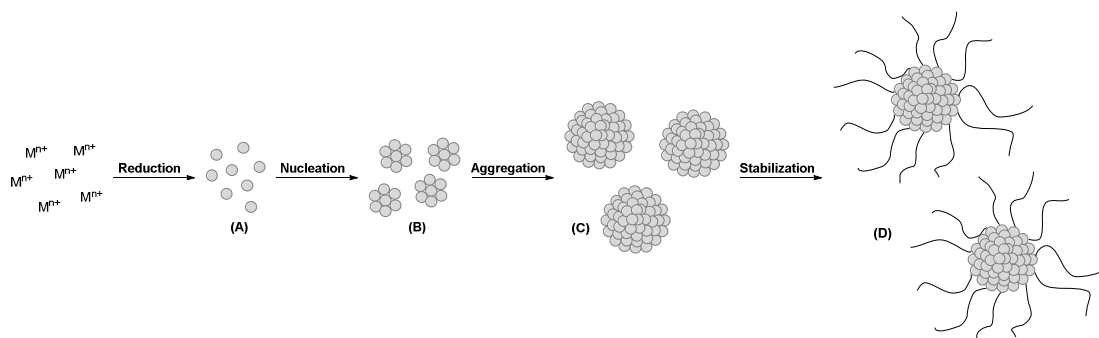
Figure 5 Preparation of a colloidal solution of metal NPs by reduction of metal salts**.**

1.1.2.2.   REDUCTION AND DISPLACEMENT OF LIGANDS FROM ORGANOMETALLIC COMPOUNDS

This method, known as the *organometallic approach*, was initially developed by Chaudret's group.[45] It consists in the reduction (mainly with H_2) and subsequent displacement of a ligand from a zerovalent organometallic complex. Then, metal atoms suspension was generated, which after nucleation and growing, and subsequent stabilization give the desired NPs. This method is, generally, highly reproducible and offers a complete control of the size, the shape and the surface of the nanoclusters.

Based on that methodology, NPs of different metals have been reported. In principle, the only requirement to obtain the metal NPs is the use of the corresponding zerovalent complex and a suitable stabilizer. For this purpose, different types of complexes can be used, but the most common are those bearing olefin ligands (such as dibenzylideneacetone (dba), cyclooctadiene (COD), or cyclooctatriene (COT)) or other ligands that can be easily reduced.

Following the *organometallic approach,* Pt NPs were prepared from the reduction of $Pt(dba)_2$ in the presence of NHC (*N*-heterocyclic carbene) ligands (**Scheme 2**).[46] Some other examples have been reported, such as the use of polyvinylpyrrolidone (PVP) for the stabilization of Ni NPs by the hydrogenation of $Ni(COD)_2$.[47] Ru NPs have also been obtained from [Ru(COD)(COT)] with different kinds of stabilizers.[20b,22b,48] Iron,[49] palladium[50] and cobalt[51] NPs have also been successfully obtained applying this methodology. Ferrocenyl phosphine ligands have also been reported for the stabilization of Rh NPs produced by the *organometallic approach*.[22a]

---

[45] (a) Cordente, N., Respaud, M., Senocq, F., Casanove, M.-J., Amiens, C., Chaudret, B. *Nano Lett.* **2001**, *1*, 565. (b) Philippot, K., Chaudret, B. *C. R. Chimie* **2003**, *6*, 1019.

[46] Lara, P., Suárez, A., Collière, V., Philippot, K., Chaudret, B. *ChemCatChem* **2014**, *6*, 87.

[47] Ely, T. O., Amiens, C., Chaudret, B. *Chem. Mater.* **1999**, *11*, 526.

[48] Philippot, K., Lignier, P., Chaudret, B. *Top. Organomet. Chem.* **2014**, 319.

[49] Kelsen, V., Wendt, B., Werkmeister, S., Junge, K., Beller, M., Chaudret, B. *Chem. Commun.* **2013**, *49*, 3416.

[50] Guerrero, M., García-Antón, J., Tristany, M., Pons, J., Ros, J., Philippot, K., Lecante, P., Chaudret, B. *Langmuir* **2010**, *26* (19), 15532

[51] Ciuculescu, D., Dumestre, F., Comesaña-Hermo, M., Chaudret, B., Spasova, M., Frale, M., Amiens, C. *Chem. Mater.* **2009**, *21*, 3987.
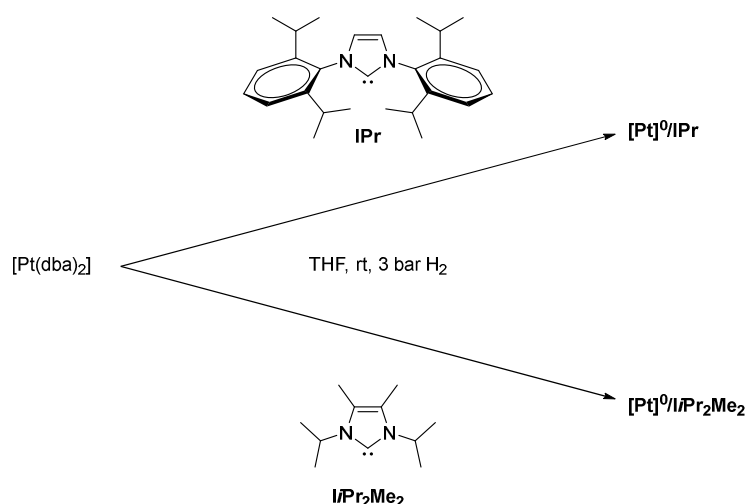
Scheme 2 Pt NPs synthesized by the *organometallic approach.*[46]

1.1.2.3. PHOTOCHEMICAL SYNTHESIS

In order to avoid the use of a reducing agent or aggressive conditions (high temperature or pressure), photochemical processes have found increasing interest.[52] These methods are based in the direct formation of metal atoms by the irradiation of metal salts or complexes. One of the first reports using this methodology was the synthesis of Ag NPs from the reduction of $AgNO_3$. The photochemical reduction for the synthesis of NPs was also successfully applied to Au and Cu NPs.[53,54]

1.1.2.4. THERMAL DECOMPOSITION

In some cases, metal NPs can be obtained by the decomposition of metal complexes under a thermal treatment, in the presence of the appropriate stabilizers. Some examples based in that procedure have been reported to obtain small monodisperse nanoclusters. Hyeon and collaborators postulated that the carbon monoxide generated by the decomposition of the organic species of the metal complex could act as reducing agent in that case.[55] Although the preparation of different metal NPs using this method have been reported (Ni, Pd, Ni-Pd, or Fe), [56,57,58,59] it is not as widely used as the other synthetic procedures described previously.

1.1.2.5. ELECTROCHEMICAL REDUCTION

The electrochemical reduction method was firstly reported by Reetz for the synthesis of Pd NPs stabilized by tetraoctylammonium bromide (TOAB).[60] This procedure consisted in a palladium sheet that acted as anode and a platinum sheet as cathode, with 5 mm of separation between them. The supporting electrolyte was a solution of TOAB in acetonitrile/THF. After the application of a certain current, the metal ions were generated from the anode. Then, the cathode reduces these ions to generate the Pd NPs.

---

[52] (a) Hada, H., Yonezawa, Y., Yoshida, A., Kurakake, A. *J. Phys. Chem.* **1976**, *80* (25), 2728. (b) Huang, H. H., Ni, X. P., Loy, G. L., Chew, C. H., Tan, K. L., Loh, F. C., Deng, J. F., Xu, G. Q. *Langmuir* **1996**, *12*, 909. (c) Murayama, H., Hashimoto, N., Tanaka, H. *Chem. Phys. Lett.* **2009**, *482*, 291.

[53] Filip, G. A., Moldovan, B., Baldea, I., Oletanu, D., Suharoschi, R., Decea, N., Cismaru, C. M., Gal, E., Cenariu, M., Clichici, S., David, L. *J. Photochem. Photobiol. B Biol.* **2019**, *191*, 26.

[54] Nishida, N., Miyashita, A., Hashimoto, N., Murayama, H., Tanaka, H. *Eur. Phys. J. D* **2011**, *63*, 307.

[55] Kim, S.-W., Park, J., Jang, Y., Chung, Y., Hwang, S., Hyeon, T. *Nano Lett.* **2003**, *3* (9), 1289.

[56] Akbarzadeh, R., Dehghani, H. *Dalton Trans.* **2014**, *43*, 5474.

[57] Asensio, J. M., Tricard, S., Coppel, Y., Andrés, R., Chaudret, B., de Jesús, E. *Chem. Eur. J.* **2017**, *23* (54), 13435.

[58] Son, S. U., Jang, Y., Park, J., Na, H. B., Park, H. M., Yun, H. J., Lee, J., Hyeon, T. *J. Am. Chem. Soc.* **2004**, *126*, 5026.

[59] Peng, S., Wang, C., Xie, J., Sun, S. *J. Am. Chem. Soc.* **2006**, *126*, 10676.

[60] Reetz, M. T., Helbig, W. *J. Am. Chem. Soc.* **1994**, *116*, 7401.

This method was successfully applied to other oxidable metals, such as the synthesis of gold nanocubes[61] or silver NPs.[62,63] The use of ionic liquids as electrolyte solution and stabilizer was reported for the synthesis of Pd NPs.[64] These reports show that this synthesis allows the control of the NPs size by adjusting the current density, in general the obtained particle size is inversely proportional to the current density.

Another type of electrochemical reduction for the synthesis of metal NPs was the electrodeposition of metal NPs into the surface of an electrode. In these cases, a metal salt was the electrolyte solution, which after the application of a current, was electrodeposited into the electrode. Rh nanocrystals supported into a glassy crystal electrode and Pt NPs into a gold electrolyte were obtained by this methodology.[65,66]

1.1.2.6.   SYNTHESIS OF PT, NI, AU AND RH NPS

After a brief review of the most common methods for the synthesis of metal NPs, we present a summary of the reported preparation methods for the metal NPs developed in this thesis.

a) Platinum nanoparticles:

Historically, supported Pt NPs were the firstly reported. In 1976 Turkevich applied successfully his own method (initially developed for the synthesis of gold NPs) to the preparation of platinum NPs.[67] In that first report, the Pt precursor (H_2PtCl_6) was reduced with sodium citrate and deposited into different solid supports. Pt NPs supported on metal oxides such SnO_2, synthesized though a pyrolytic method, were also reported.[68] In the first example of Pt colloidal solution published, Pt NPs were stabilized by poly-*N*-methylolacrylamide (PNMA). These NPs were obtained by the reduction of Pt(IV) species, simultaneously to the polymerization of corresponding monomers (methylacrylamide (MAA) or *N*-methylolacrylaminde (NMA)) via light irradiation.[69] Later, Henglein reported the synthesis of water soluble Pt NPs prepared by different methods (radiolysis, reduction with hydrogen or with sodium citrate). [70] In all cases, these first reports presented highly polydispersed Pt NPs.

After those first reports, the number of publications based in Pt NPs experienced a considerable growth. In the last years the synthesis of platinum nanoparticles has been mainly described through a chemical reduction of Pt(IV) or Pt(II) salts ($H_2Pt(OH)_6$, $Na_2Pt(OH)_6$, H_2PtCl_6, Na_2PtCl_6, K_2PtCl_4, $Pt(NH_3)_4(NO_3)_2$) with formic acid,[71] ascorbic acid,[72] ethanol,[73] ethyleneglycol (EG),[44d,74] carbon monoxide,[75,76] dihydrogen,[70,76] $NaBH_4$,[44b,73b,77]

[61] Huang, C.-J., Wang, Y.-H., Chiu, P.-H., Shih, M.-C., Meen, T.-H. *Mat. Lett.* **2006**, *60*, 1896.

[62] Rodríguez-Sánchez, L., Blanco, M. C., López-Quintela, M. A. *J. Phys. Chem. B* **2000**, *104*, 9683.

[63] Nasretdinova, G. R., Fazleeva, R. R., Mukhitova, R. K., Nizameev, I. R., Kadirov, M. K., Ziganshina, A. Y., Yanilkin, V. V. *Electrochem. Comm.* **2015**, *50*, 69.

[64] Cha, J.-H., Kim, K.-S., Choi, S., Yeon, S.-H., Lee, H., Lee, C.-S., Shim, J.-J. *Korean J. Chem. Eng.* **2007**, *24* (6), 1089.

[65] Yu, N.-F., Tian, N., Zhou, Z.-Y., Huang, L., Xiao, J., Wen, Y.-H., Sun, S.-G. *Angew. Chem. Int. Ed.* **2014**, *53*, 5097.

[66] Hirsch, T., Zharnikov, M., Shaporenko, A., Stahl, J., Weiss, D., Wolfbeis, O. S., Mirsky, V. M. *Angew. Chem. Int. Ed.* **2005**, *44*, 6775.

[67] Aika, K., Ban, L. L., Okura, I., Namba, S., Turkevich, J. *J. Res. Inst. Catal. Hokkaido Univ.* **1976**, *24* (1), 54.

[68] Labeau, M., Gautheron, B., Cellier, F., Vallet-Regi, M., Garcia, E., Gonzàlez Calbet, J. M. **1993**, *102*, 434.

[69] Rafaeloff, R., Haruvy, Y., Bienenboym, J., Baruch, G., Rajbenbach, L. A. *J. Mol. Catal.* **1983**, *22*, 219.

[70] Henglein, A., Ershov, B. G., Malow, M. *J. Phys. Chem.* **1995**, *99*, 14129.

[71] (a) Beier M. J., Andanson, J.-M., Mallat, T., Krumeich, F., Baiker, A. *ACS Catal.* **2012**, *2*, 337. (b) Beier, M. J., Andanson, J.-M., Baiker, A. *ACS Catal.* **2012**, *2*, 2587.

[72] Mohanty, A., Garg, N., Jin, R. *Angew. Chem. Int. Ed.* **2010**, *49*, 4962.

[73] (a) Mahmoud, M. A., Tabor, C. E., El-Sayed, M. A., Ding, Y., Wang, Z. L. *J. Am. Chem. Soc.* **2008**, *130*, 4590. (b) Mayer, A. B. R., Mark, J. E. *J. Polymer Sci. Part A Polymer Chem.* **1997**, *35*, 3151.

[74] Yuan, X., Yan, N., Xiao, C., Li, C., Fei, Z., Cai, Z., Kou, Y., Dyson, P. J. *Green Chem.* **2010**, *12*, 228.

[75] Maity, P., Basu, S., Bhaduri, S., Lahiti, G. K. *J. Mol. Catal. A Chem.* **2007**, *270*, 117.

[76] Maity, P., Gopinath, C. S., Bahduri, S., Lahiri, G. K. *Green Chem* **2009**, *11*, 554.

[77] (a) Li, X., Du, Y., Dai, J., Wang, X., Yang, P. *Catal. Lett.* **2007**, *118*, 151. (b) Kim, K.-S., Demberelnyamba, D., Lee, H. *Langmuir* **2004**, *20*, 556. (c) Zhang, H., Cui, H. *Langmuir* **2009**, *25*, 2604. (d) Yamamoto, D., Watanabe, S., Miyahara, M. T. *Langmuir* **2010**, *26* (4), 2339. (e) Salabat, A., Keshavarz, A., Torkzaban, S., Pureimani, R. *J. Iran. Chem. Soc.* **2019**, *16* (7), 1527.

$NaHCO_3$ under hydrothermal conditions,[78] or weak reductants such as potassium bitartrate.[79] Alternative synthetic methods such as electrochemical reduction,[66,80] microwave-assisted reduction,[81] reduction under visible light irradiation of a host-guest inclusion complex or gamma light irradiation have also been reported.[77e,82]

Other Pt(II) precursors, such as $Me_2Pt(COD)$, have been employed and reduced by dihydrogen,[83] or polymethylhydrosiloxane (PMHS) to obtain Pt NPs.[84] Water-soluble (NHC)Pt(II) dimethyl complexes have generated Pt NPs by thermal decomposition[85] or by treatment with carbon monoxide or dihydrogen.[86]

Alternatively, platinum zero-valent organometallic complexes, such as $Pt(dba)_2$,[46,87] $Pt_2(dba)_3$[88] or $Pt(NBE)_3$[89] (NBE: 2-norbornene) in the presence of different stabilizers, gave Pt NPs following the Chaudret's *organometallic approach*. Metal vapor synthesis of Pt NPs from bulk platinum has also been reported.[90]

b) *Nickel nanoparticles:*

Although the catalytic importance of Ni has been known since the initial stages of XX century,[91] it was not until the 90's when the first publications about Ni NPs appeared, by the Chakravorty group.[92,93] In the first report they synthesized Ni NPs supported on silica by a sol-gel process. The Ni(II) precursor was reduced under H_2 atmosphere at high temperature in the presence of the gel, obtaining particle sizes between 5 and 10 nm. Two years later, the same authors synthesized Ni NPs supported on potassium bromide powder. These NPs were obtained via thermal decomposition of $Ni(C_9H_6ON)_2 \cdot 2H_2O$ in the presence of the powder. During that decade other authors have reported Ni NPs supported in different materials.[94]

More recently, the synthesis of nickel nanoparticles has been described in the literature through a thermal[56] or chemical reduction of Ni(II) salts with $NaBH_4$, $LiEt_3BH$ or $NaEt_3BH$,[44a,95,96,97] dimethylaminoborane,[98]

[78] Patra, S. G., Sathiyan, K., Meistelman, M., Zidki, T. *Isr. J. Chem.* **2020**, *60*, 1.

[79] Tan, Y., Dai, X., Li, Y., Zhu, D. *J. Mater. Chem.* **2003**, *13*, 1069.

[80] Yu, P., Qian, Q., Wang, X., Cheng, H.,Ohsaka, T., Mao, L. *J. Mater. Chem.* **2010**, *20*, 5820.

[81] Yacou, C., Fontaine, M.-L., Ayral, A., Lacroix-Desmazes, P., Albouy, P.-A., Julbe, A. *J. Mater. Chem.* **2008**, *18*, 4274.

[82] Giuffrida, S., Ventimiglia, G., Petralia, S., Conoci, S., Sortino, S. *Inorg. Chem.* **2006**, *45*, 508.

[83] Debouttière, P.-J., Coppel, Y., Denicourt-Nowicki, A., Rocoux, A., Chaudret, B., Philippot, K. *Eur. J. Inorg. Chem.* **2012**, 1229.

[84] Chauhan, B. P. S., Sarkar, A. *Dalton Trans.* **2017**, *46*, 8709.

[85] Baquero, E. A., Tricard, S., Flores, J. C., de Jesús, E., Chaudret, B. *Angew. Chem. Int. Ed.* **2014**, *53*, 1.

[86] Baquero, E. A., Tricard, S., Coppel, Y., Flores, J. C., Chaudret, B., de Jesús, E. *Dalton Trans.* **2018**, *47*, 4093

[87] (a) Boualleg, M., Basset, J.-M., Candy, J.-P., Delichere, P., Pelzer, K., Veyre, L., Thieuleux, C. *Chem. Mater.* **2009**, *21*, 775. (b) Moraes, L. C., Figueiredo, R. C., Espinos, J. P., Vattier, F., Franconetti, A., Jaime, C., Lacroix, B, Rojo, J., Lara, P., Conejero, S. *Nanoscale* **2020**, *12*, 6821.

[88] Ramirez, E., Eradès, L., Philippot, K., Lecante, P., Chaudret, B. *Adv. Funct. Mater.* **2007**, *17*, 2219.

[89] Martínez-Prieto, L. M., Rakers, L., López-Vinasco, A. M., Cano, I., Coppel, Y., Philippot, K., Glorius, F., Chaudret, B., van Leeuwen, P. W. N. M. *Chem. Eur. J.* **2017**, *23*, 12779.

[90] Oberhauser, W., Evangelisti, C., Tiozzo, C., Bartoli, M., Frediani, M., Passaglia, E., Rosi, L. *Appl. Catal. A Gen.* **2017**, *537*, 50.

[91] Wisniak, J. *Educ. Quím.* **2010**, *21* (1), 60.

[92] Chatterhee, A., Chakravorty, D. *J. Phys. D: Appl. Phys.* **1990**, *23*, 1097.

[93] Chatterjee, A., Chakravorty, D. *Appl. Phys. Lett.* **1992**, *60* (1), 138.

[94] Roy, S., Chaterjee, A., Chakravorty, D. *J. Mat. Res.* **1993**, *8* (4), 689.

[95] (a) Kalbasi, R. J., Zamani, F. *RSC Adv.* **2014**, *4*, 7444. (b) Gawande, M. B., Rathi, A. K., Branco, P. S., Nogueira, I. D., Velhinho, A., Shrikhande, J. J., Indulkar, U. U., Jayaram, R. V., Ghumman, C. A. A., Bundaleski, N., Teodoro, O. M. N. D. *Chem. Eur. J.* **2012**, *18*, 12628. (c) Harrad, M. A., Boualy, B., Firdoussi, L. E., Mehdi, A., Santi, C., Giovagnoli, S., Nocchetti, M., Ali, M. A. *Catal. Commun.* **2013**, *32*, 92. (d) Rai, R. K., Mahata, A., Mukhopadhyay, S., Gupta, S., Li, P.-Z., Nguyen, K. T., Zhao, Y., Pathak, B., Singh, S. K. *Inorg. Chem.* **2014**, *53*, 2904. (e) Couto, G. G., Klein, J. J., Schreiner, W. H., Mosca, D. H., de Oliveira, A. J. A., Zarbin, A. J. G. *J. Colloid Interf. Sci.* **2007**, *311*, 461.

[96] Soulé, J.-F., Miyamura, H., Kobayashi, S. *J. Am. Chem. Soc.* **2013**, *135*, 10602.

[97] Knecht, M. R., Garcia-Martinez, J. C., Crooks, R. M. *Chem. Mater.* **2006**, *18*, 5039.

[98] Yamauchi, Y., Itagaki, T., Yokoshima, T., Kuroda, K. *Dalton Trans.* **2012**, *41*, 1210.

hydrazine,[44c,99] or ethylene glycol.[100] Some examples based in the thermal decomposition of Ni-oleylamine complexes for the synthesis of Ni NPs have also been reported.[101]

Moreover, dispersions of Ni NPs in different types of ionic-liquids have been obtained by auto-decomposition,[102] or microwave-induced decomposition [103] of Ni(COD)$_2$. This zero-valent organometallic complex has also been used as starting compound to produce Ni NPs following the *organometallic approach*.[47,104]

c) Gold nanoparticles:

As previously mentioned, the preparation of gold NPs described by Turkevich was the first reproducible method to obtain stable colloidal solutions.[7a] This method was based in the reduction of tetrachloroauric acid, HAuCl$_4$, with sodium citrate in aqueous medium. After that work, several authors published the synthesis of gold NPs based in that methodology.[105] Later on, different authors developed other procedures for the preparation of gold NPs, by using different reductants, or alternative methods, such as the vapour deposition.[106,107]

In recent years, the number of publications and the interest about gold NPs have experienced a huge increase. Although new top-down processes have been developed,[108] the bottom-up procedures are preferred for the formation of Au NPs.[109] Nowadays, the synthesis of gold NPs still consists mainly on chemical reducing methods.[2g] A modification of Turkevich method, reversing the order of addition of reactants, was reported for the preparation of sub-10 nm gold NPs.[110] Taking advantage of the strong Au-S bond, thiol stabilized gold NPs were reported by the reduction of AuCl$_4^-$ with NaBH$_4$ in a two phase system, using TOAB as a phase transfer.[21a] The use of other reducing agents such as 9-BBN , *tert*-butyl amine borane complex or thiol functionalized nanocrystalline cellulose, has also been reported.[111,112,113]

Alternative methods to the chemical reduction of gold salts have also been developed. Recently, the synthesis of gold NPs has been described through a thermal decomposition of Au(III) or Au(I) coordination

[99] (a) Xu, W., Liew, K. Y.,Liu, H., Huang, T., Sun, C., Zhao, Y. *Mater. Lett.* **2008**, *62*, 2571. (b) Hussain, N., Gogoi, P., Khare, P., Das, M. R. *RSC Adv.* **2015**, *5*, 103105. (c) Hu, Y., Yu, Y., Zhao, X., Yang, H., Feng, B., Li, H., Qiao, Y., Hua, L., Pan, Z., Hou, Z. *Sci. China Chem.* **2010**, *53*, 1541. (d) Vijayakrishna, K., Charan, K. T. P., Manojkumar, K., Venkatesh, S., Pothanagandhi, N., Sivaramakrishna, A., Mayuri, P., Kumar, A. S., Sreedhar, S. *ChemCatChem* **2016**, *8*, 1139. (e) Chen, D.-H., Wu, S.-H. *Chem. Mater.* **2000**, *12*, 1354. (f) Wu, Z. G., Munoz, M., Montero, O. *Adv. Powder Technol.* **2010**, *21*, 165.

[100] Blandez, J. F., Esteve-Adell, I., Primo, A., Alvaro, M., García, H. *J. Mol. Catal. A. Chem.* **2016**, *412*, 13.

[101] (a) Park, J., Kang, E., Son, S. U., Park, H. M. P., Lee, M. K., Kim, J., Kim, K. W., Noh, H.-J., Park, J.-H., Bae, C. J., Park, J.-G., Hyeon, T. *Adv. Mater.* **2005**, *17* (4), 429. (b) Carenco, S., Labouille, S., Bouchonnet, S., Boissière, C., Le Goff, X.-F., Sanchez, C., Mézailles, N. *Chem. Eur. J.* **2012**, *18*, 14165.

[102] (a) Konnerth, H., Prechtl, M. H. G. *New. J. Chem.* **2017**, *41*, 9594. (b) Prechtl, M. H. G., Campbell, P. S., Scholten, J. D., Fraser, G. B., Machado, G., Santini, C. C., Dupont, J., Chauvin, Y. *Nanoscale* **2010**, *2*, 2601.

[103] Wegner, S., Rutz, C., Schütte, K., Barthel, J., Bushmelev, A., Schmidt, A., Dilchert, K., Fischer, R. A., Janiak, C. *Chem. Eur. J.* **2017**, *23*, 6330.

[104] (a) Díaz de los Bernardos, M., Pérez-Rodríguez, S., Gual, A., Claver, C., Godard, C. *Chem. Commun.* **2017**, *53*, 7894. (b) Domínguez-Crespo, M. A., Ramírez-Meneses, E., Montiel-Palma, V., Torres Huerta, A. M., Dorantes Rosales, H. *Int. J. Hydrogen Energy* **2009**, *34*, 1664.

[105] (a) Frens, G. *Kolloid-Z. u. Z. Polymere* **1972**, *250*, 736. (b) Frens, G. *Nature Phys. Sci.* **1973**, *241*, 20. (c) Freund, P. L., Spiro, M. *J. Phys. Chem.* **1985**, *89*, 1074.

[106] (a) Horisberger, M., Rosset, J. *J. Histochem. Cytochem.* **1977**, *25*, 295. (b) Milligan, W. O., Morriss, R. H. *J. Am. Chem. Soc.* **1964**, *86*, 3461.

[107] (a) Lin, S.-T., Franklin, M. T., Klabunde, K. J. *Langmuir* **1986**, *2*, 259. (b) Satoh, N., Kimura, K. *Bull. Chem. Soc. Jpn.* **1989**, *62*, 1758.

[108] Ferlin, F., Giannoni, T., Zuliani, A., Piermatti, O., Luque, R., Vaccaro, L. *ChemSusChem* **2019**, *12*, 1.

[109] Zhao, P., Li, N., Astruc, D. *Coord. Chem. Rev.* **2013**, *257*, 638.

[110] Sivaraman, S. K., Kumar, S., Santhanam, V. *J. Colloid Interf. Sci.* **2011**, *361*, 543.

[111] Sardar, R., Shumaker-Parry, J. S. *Chem. Mater.* **2009**, *21* (7), 1167.

[112] MacLeod, M. J., Johnson, J. A. *J. Am. Chem. Soc.* **2015**, *137*, 7974.

[113] Huang, J.-L., Gray, D. G., Li, C.-J. *Beilstein J. Org. Chem.* **2013**, *9*, 1388.

complexes.[114,115] Moreover, *in situ* reduction of HAuCl₄ and immobilization of Au NPs on a graphene-silica nanocomposite was reported.[116] Biological structures (soil fungus) were also used for the preparation and stabilization of Au NPs.[117]

Imidazolium salts have been described as capping agents in the synthesis of Au NPs.[118] In order to enhance the stabilizing properties, very often coordinating groups (amino, thiol, ...) are introduced in the cationic moiety. Another option has been the use of polymers containing imidazolium moieties. NHC-protected gold nanoparticles have also been reported, which were obtained from organometallic NHC–Au(I) complexes[119] or by using NHC, *in situ* or previously formed from the corresponding imidazolium salts.[120] Alternativelly, gold NPs stabilized by *N*-heterocyclic thiones (NHT) bearing long hydrocarbon chains have been prepared from the reduction of the corresponding complexes.[121]

d) Rhodium NPs:

Although most of the articles based in Rh NPs were published in the XXI century, the first reports appeared during the 80s. These early publications were based in nanocomposites containing Rh NPs. Polymers,[122] metal oxides,[123] or pumice[124] were some of the reported supports for Rh NPs. To obtain these Rh colloids, the metal precursors were reduced with alcohols,[123] NaBH₄[124] or molecular hydrogen.[125]

Nowadays, chemical reduction of RhCl₃ is the most common methodology for the synthesis of Rh NPs.[125,126] Typical reductants of Rh(III) are: NaBH₄,[127] EG,[128] molecular hydrogen,[129] dimethylamine-borane[130] or lithium

[114] Aghahosseini, H., Rezaei, S. J. T., Tadayyon, M., Ramazani, A., Amani, V., Ahmadi, R., Abdolahanjadian, D. *Eur. J. Inorg. Chem.* **2018**, 2589.

[115] Crespo, J., Guari, Y., Ibarras, A., Larionova, J., Lasanta, T., Laurencin, D., Lopez-de-Luzuriaga, J. M., Monge, M., Olmos, M. E., Richeter, S. *Dalton Trans.* **2014**, *43*, 15713.

[116] Movahed, S. K., Shariatipour, M., Dabiri, M. *RSC Adv.* **2015**, *5*, 33423.

[117] Bhargava, A., Jain, N., Gangopadhyay, S., Panwar, J. *Process Biochem.* **2015**, *50*, 1293.

[118] (a) Itoh, H., Naka, K., Chujo, Y. *J. Am. Chem. Soc.* **2004**, *126*, 3026. (b) Dinda, E., Si, S., Kotal, A., Mandal, T. K. *Chem. Eur. J.* **2008**, *14*, 5528. (c) Wang, Z., Zhang, Q., Kuehner, D., Ivaska, A., Niu, L. *Green Chem.* **2008**, *10*, 907. (d) Buaki, M., Aprile, C., Dhakshinamoorthy, A., Alvaro, M., Garcia, H. *Chem. Eur. J.* **2009**, *15*, 13082. (e) Biondi, I., Laurenczy, G., Dyson, P. J. *Inorg. Chem.* **2011**, *50*, 8038. (f) Wender, H., Andreazza, M. L., Correia, R. R. B., Teixeira, S. R., Dupont, J. *Nanoscale* **2011**, *3*, 1240. (g) Casal-Dujat, L., Rodrigues, M., Yagüe, A., Calpena, A. C., Amabilino, D. B., González-Linares, J., Borràs, M., Pérez-García, L. *Langmuir* **2012**, *28*, 2368.

[119] (a) Salorinne, K., Man, R. W. Y., Li, C.-H., Taki, M., Nambo, M., Crudden, C. M. *Angew. Chem. Int. Ed.* **2017**, *56*, 6198. (b) Narouz, M. R., Li, C.-H., Nazemi, A., Crudden, C. M. *Langmuir* **2017**, *33*, 14211. (c) Young, A. J., Sauer, M., Rubio, G. M. D. M., Sato, A., Foelske, A., Serpell, C. J., Chin, J. M., Reithofer, M. R. *Nanoscale* **2019**, *11*, 8327.

[120] (a) Ling, X., Roland, S., Pileni, M.-P. *Chem. Mater.* **2015**, *27*, 414. (b) Ferry, A., Schaepe, K., Tegeder, P., Richter, C., Chepiga, K. M., Ravoo, B. J., Glorius, F. *ACS Catal.* **2015**, *5*, 5414. (c) Bridonneau, N., Hippolyte, L., Mercier, D., Portehault, D., Desage-El Murr, M., Marcus, P., Fensterbank, L., Chaneac, C., Ribot, F. *Dalton Trans.* **2018**, *47*, 6850.

[121] Moraes, L. C., Lacroix, B., Figuereido, R. C., Lara, P., Rojo, J., Conejero, S. *Dalton Trans.* **2017**, *46*, 8367.

[122] (a) Hirai, H. *J. Macromol. Sci.-Chem.* **1979**, *13* (5), 633. (b) Hirai, H., Nakao, Y., Toshima, N. *J. Macromol. Sci.-Chem.* **1979**, *13* (6), 727. (c) Hidefumi, H., Michitaka, O., Makoto, K. *Chem. Lett.* **1987**, *16*, 149.

[123] Nakao, Y., Kaeriyama, K. *Chem. Lett.* **1983**, *12*, 949.

[124] Boutonnet, M., Kizling, J., Mintsa-Eya, V., Choplin, A., Touroude, R., Maire, G., Stenius, P. *J. Catal.* **1987**, *103*, 95.

[125] *Co, Rh, and Ir Nanoparticles. Nanocatalysis in Ionic Liquids*; Scholten, J. D., Qadir, M. I. Ed.: Wiley-VCH, **2017**.

[126] Ramírez-Meneses, E., Philippot, K., Domínguez-Crespo, M. A., Ibrahim, M., Betancourt, I., Torres-Huerta, A. M., Ezeta-Mejia, A. J. *J. Mater. Sci.* **2018**, *53*, 8933.

[127] (a) Gacem, N., Diao, P. *Colloids Surf. A Physicochem. Eng. Aspects* **2013**, *417*, 32. (b) Chau, N. T. T., Menuel, S., Colombel-Rouen, S., Guerrero, M., Monflier, E., Philippot, K., Denicourt-Nowicki, A., Roucoux, A. *RSC Adv.* **2016**, *6*, 108125. (c) Barthe, L., Hemati, M., Philippot, K., Chaudret, B., Denicourt-Nowicki, A., Roucoux, A. *Chem. Engineer. J.* **2009**, *151*, 372. (d) Bilé, E. G., Sassine, Denicourt-Nowicki, A., Launay, F., Roucoux, A. *Dalton Trans.* **2011**, *40*, 6524. (e) Guha, N. R., Bhattacherjee, D., Das, P. *Tetrahedron Lett.* **2014**, *55*, 2912.

[128] (a) Zhang, Y., Grass, M. E., Kuhn, J. N., Tao, F., Habas, S. E., Huang, W., Yang, P., Somorjai, G. A. *J. Am. Chem. Soc.* **2008**, *130*, 5868. (b) Hoefelmeyer, J. D., Niesz, K., Somorjai, G. A., Tilley, T. D. *Nano Lett.* **2005**, *5* (3), 435.

[129] Srivastava, V. *Current Organocat.* **2017**, *4*, 209.

[130] Durap, F., Zahmakiran, M., Özkar, S. *Appl. Catal. A: Gen.* **2009**, *369*, 53.

triethylborohydride.[131] Other Rh sources were also reported, such as Na_3RhCl_6,[132] $(NH_4)_3RhCl_6$,[133] $Rh(acac)_3$,[134] $Rh(COCl)$,[135] $[Rh(\mu\text{-}Cl)(COD)]_2$,[136] $[Rh(O_2CC_7H_{15})_2]_2$.[137] The synthesis of supported Rh NPs via microwave assisted chemical reduction of $RhCl_3$ with EG has also been described.[138]

Despite the importance of the chemical reduction method, in the last years, alternative methods to obtain colloidal Rh have appeared. In that way, chemical vapour deposition,[139] thermal decomposition[140] or salt template heat treatment synthesis have been reported.[141] The *organometallic approach* has also been successfully applied for the preparation of Rh NPs. Thus, Philippot achieved the stabilization of Rh NPs with ferrocenyl phosphine ligands via H_2 decomposition of $[Rh(\eta^3\text{-}C_3H_5)_3]$,[22a] and $[Rh(\mu\text{-}OMe)(COD)]_2$ and $[Rh(acac)(1,5\text{-}C_8H_{12})]$ have been also been used as sources of Rh(0) species.[142,143]

1.1.3 CHARACTERIZATION OF METAL NANOPARTICLES

The characterization of metal NPs is a crucial step to know their morphology, size, composition and crystalline structure. Only the most common techniques for the general use in all types of metal NPs will be presented herein.

1.1.3.1. TRANSMISSION ELECTRON MICROSCOPY (TEM) AND HIGH RESOLUTION TRANSMISSION ELECTRON MICROSCOPY (HRTEM)

The size and shape of metal NPs can affect their properties, and future applications. The presence of active species in a nanomaterial is strongly dependent on the disposition of the forming atoms. For this reason, a precise knowledge of the morphology of the material is necessary.

In a simplified way, TEM operates as an optical microscopy but using electrons instead of light. As the electron wavelength is much smaller than the one offered by visible light, the reachable resolution of electron microscopy is several orders of magnitude better than the resolution obtained with the best optical microscopies. This technique consists in the passage of a beam of electrons though a fine layer of metal NPs deposited on a carbon supported copper grid. When the beam strikes the sample, the electrons are transmitted through the grid. The interaction between the electrons and the sample modifies the beam of electrons. When that beam hits the screen, forms an image revealing the morphologies of the NPs (**Figure 6 (A)**). As the transmission of the electrons is strongly dependent on the thickness of the deposited layer, a correct preparation of the sample is necessary. Generally, a diluted suspension of material in a volatile solvent is prepared. Then, the two main techniques used for placing the nanomaterial on the grid are: (i) dipping the grid into the solution and allow the solvent to evaporate; (ii) depositing a drop of suspension on the copper grid and allow the solvent to evaporate. For metal NPs the second technique is preferred because the distribution of the particles through the grid is more homogeneous.

[131] Marín-Almazo, M., Ascencio, J. A., Pérez-Álvarez, M., Gutiérrez-Wing, C., José-Yacamán, M. *Microchem. J.* **2005**, *81*, 133.

[132] Xie, S., Zhang, H., Lu, N., Jin, M., Wang, J., Kim, M. J., Xie, Z., Xia, Y. *Nano Lett.* **2013**, *13*, 6262.

[133] Yao, L., Zhao, J., Lee, J.-M. *ACS Sustainable Chem. Eng.* **2017**, *5*, 2056.

[134] Zhang, Y., Grass, M. E., Habas, S. E., Tao, F., Zhang, T., Yang, P., Somorjai, G. A. *J. Phys. Chem. C* **2007**, *111*, 12243.

[135] Sanchez-Dominguez, Boutonnet, M., Solans, C. *J. Nanopart. Res.* **2009**, *11*, 1823.

[136] Karahan, S., Zahmakiran, M., Özkar, S. *Chem. Commun.* **2012**, *48*, 1180.

[137] Ayvah, T., Zahmakiran, M., Özark, S. *Dalton Trans.* **2011**, *40*, 3584.

[138] Tzorbatzoglou, F., Brouzgou, A., Tsiakaras, P. *Appl. Catal. B: Enviromental* **2015**, *174-175*, 203.

[139] Khosravian, H., Liang, Z., Uhl, A., Trenary, M., Meyer, R. *J. Phys. Chem. C* **2012**, *116*, 11987.

[140] (a) Uribe-Godínez, J., García-Montalvo, V., Jiménez-Sandoval, O. *Int. J. Hydrogen Energ.* **2013**, *38*, 7680. (b) Li, Y., Yanagisawa, K., Ding, X., Li, X., Wei, Y.,Yan, X. *Chem. Eng. J.* **2013**, *228*, 45.

[141] Lin, C., Wu, G., Li, H., Geng, Y., Xie, G., Yang, J., Liu, B., Jin, J. *Nanoscale* **2017**, *9*, 1834.

[142] Axet, M. R., Castillón, S., Claver, C., Philippot, K., Lecante, P., Chaudret, B. *Eur. J. Inorg. Chem.* **2008**, 3460.

[143] Ramírez-Meneses, E., Philippot, K., Chaudret, B. *Ingeniería Investigación y Tecnología* **2015**, *16*, 225.

HRTEM is an imaging mode of TEM that enhances their resolution, even allowing atomic resolution in the best cases (**Figure 6 (B)**).[144] When an electron beam interacts with the sample, if it is thin enough, the incident electrons not only pass through of the sample, some of them are also scattered by the specimen (Bragg diffracted beam), changing the phase of the electron beam. In the HRTEM mode, these Bragg diffracted beams are included in the aperture of the objective lens. The high-resolution image generated in the plate is a result of the interaction between the scattered beams and the direct transmitted beams. For collecting all the Bragg diffracted beams is necessary to increase the objective aperture. However, a larger aperture of the objective leads to higher microscopy aberrations, which should be corrected with the lens focus.[145]
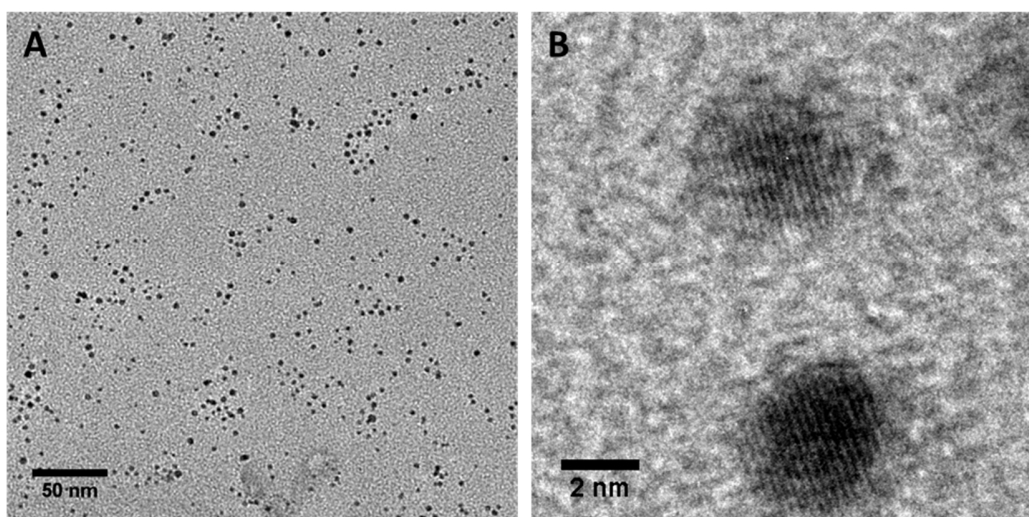
Figure 6 (A) TEM and **(B)** HRTEM images of Au NPs.

1.1.3.2. ELECTRON DIFFRACTION (ED)

ED is a technique commonly used to study the crystal structure of metal NPs, constituting an alternative to the X-Ray diffraction. The experiments are performed on a TEM instrument, focusing the generated electrons in a crystalline sample. The periodic structure of crystalline NPs scatters the incident electrons in a certain way depending on their structure. Adjusting the electron lenses, the diffraction spots are observed in the phosphorous screen (or in the microscope camera), as a diffraction pattern characteristic for each material. The analysis of the generated diffraction pattern permits the deduction of the crystalline structure of the sample. The NP composition can be confirmed by matching the obtained results with the known crystalline lattices reported in the literature.[146,147]

1.1.3.3. ENERGY-DISPERSIVE X-RAY SPECTROSCOPY (EDS)

This technique is also carried out on a TEM instrument, but in that case an X-ray detector is required. EDS provides an elemental analysis of a sample. It is based in the detection of the X-ray emitted in the de-excitation of an electron hole generated by a high energy electron beam in the surface of the sample. The falling of an electron, from a higher binding energy level to a lower energy hole, releases a certain amount of energy in

[144] (a) Kisielowski, C., Freitag, B., Bischoff, M., van Lin, H., Lazar, S., Knippels, G., Tiemeijer, P., van der Stam, M., von Harrach, S., Stekelenburg, M., Haider, M., Uhlemann, S., Müller, H., Hartel, P., Kabius, B., Miller, D., Petrov, I., Olson, E. A., Donchev, T., Kenik, E. A., Lupini, A. R., Bentley, J., Pennycook, S. J., Anderson, I. M., Minor, A. M., Schmid, A. K., Duden, T., Radmilovic, V., Ramasse, Q. M., Watanabe, M., Erni, R., Stach, E. A., Denes, P., Dahmen, U. *Microscop. Microanal.* **2008**, *14*, 469. (b) Aagaard, N. D., Azcárate, J. C., Zelaya, E. *Microsc. Microanal.* **2020**, *26*, 75.
[145] Wang, Z. L. *J. Phys. Chem. B* **2000**, *104*, 1153.
[146] Bendersky, L. A., Gayle, F. W. *J. Res. Natl. Inst. Stand. Technol.* **2001**, *106*, 997.
[147] Downs, R. T., Hall-Wallace, M. *American Mineralogist* **2003**, *88*, 247.

the form of X-ray. The quantized energy levels in the material emit characteristic X-ray energies for each element.[148]

1.1.3.4. X-RAY PHOTOELECTRON SPECTROSCOPY (XPS)

XPS is a powerful technique to have information about the chemical composition and the oxidation state of the elements present in the sample (**Figure 7**). It is based on the analysis of the emitted photoelectrons from the sample surface generated by irradiation with X-ray energy. Thus, by the analysis of the number of emitted electrons and their energy, the binding energy of the species present in the sample can be known. This binding energy is characteristic for each element, and it is dependent of its oxidation state. The number of detected electrons is directly related to the amount of the element in the sample. With these results the atomic percentage and the oxidation states of the species can be elucidated. The main drawback of XPS is that the energy of the incident X-ray beam only allows the emission of the surface electrons (less than 20 nm thick).[149]
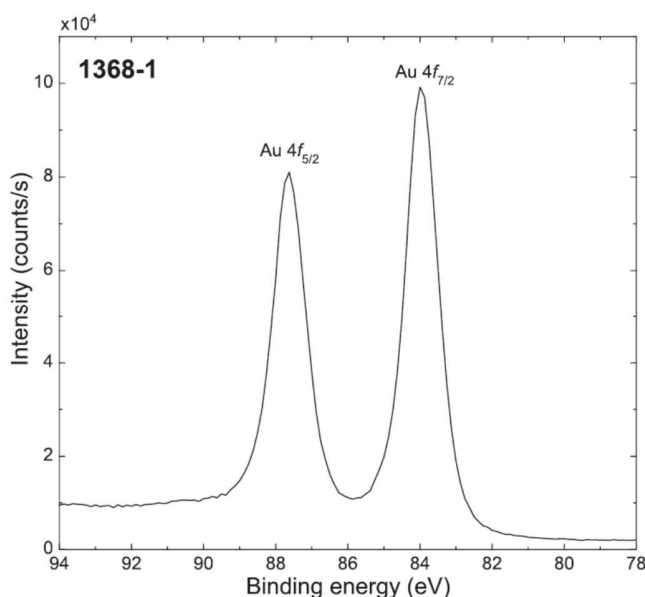
Figure 7 XPS spectrum at the Au 4f region of AgAu NPs (from [150]).

1.1.3.5. INDUCTIVELY COUPLED PLASMA – OPTICAL EMISSION SPECTROSCOPY (ICP-OES)

In catalysis, it is mandatory to know precisely the amount of active species present in the catalytic sample. In the case of metal NPs, these active species are the metal atoms. For this reason, it is very important to know the percentage of nanomaterial that is composed by metal atoms. Some techniques can be used for this purpose, but ICP-OES is, possibly, the most common. In that technique, the sample is nebulized into a plasma torch that breaks up the compounds into their respective atoms. When these atoms lose their electrons by interaction with the plasma, each element generates a characteristic wavelength that is directed to the optical chamber. There, the light is separated into different wavelengths and the light intensity of each wavelength is measured. These values provide quantitative information about the composition of the studied material.[151]

---

[148] *Physiscochemical characterization of nanofiber composites. Nanofiber Composites for Biomedical Aplications.* Polini, A., Yang, F. Ed.: Elsevier Ltd., **2017**.
[149] *Introduction and Outline. Auger- and X-Ray Photoelectron Spectroscopy in Materials Science*. Hofmann, S. Ed.: Sringer-Verlag, **2013**.
[150] Engelhard, M. H., Smith, J. N., Baer, D. R. *Surf. Sci. Spectra* **2016**, *23*, 29.
[151] *Inductively Coupled Plasma/Optical Emission Spectroscopy. Encyclopedia of Analytical Chemistry.* Hou, X., Jones, B. T. Ed.: John Wiley & Sons Ltd., **2000**.

1.2 CATALYSIS

The first use of species for the enhancement of the rate of different chemical processes appeared during the XVI-XVIII centuries, although initially the term catalysis was not employed and the nature of the processes that occurred was completely unknown. Jöns Jakob Berzelius was the first to introduce, in 1836, the term catalysis to describe this kind of processes. With the evolution of the chemistry, several reactions appeared using metal or metal oxides as catalysts for the preparation of different products.[91,152] In 1895, Ostwald introduced a more accurate definition of a catalyst, which is in accordance with the definition used today: *"Catalysts are substances which change the velocity of a reaction without modification of the energy factors of the reaction"*.[153] This author was awarded the Nobel Prize in chemistry in 1909 for his studies in catalysis, and his research based in chemical equilibrium and reaction rates.

After those initial advances, the presence of the catalysis in both academic and industrial chemical processes, experienced a notable growth. The development of new catalysts opened the possibility to use them in a huge amount of different applications: synthesis of basic chemicals, refining of petroleum to obtain fuel, polymer synthesis, synthesis of fine chemicals and drugs, environmental catalysis… Nowadays, 90% of the chemical processes involve some kind of catalysis.[154]

Unfortunately, the progress made by chemistry also has some drawbacks. The development of industry causes a notable increasing in the generated waste, affecting substantially to the environment. For this reason, concepts as green chemistry and atom economy have appeared. The term atom economy is defined as the ratio between the amount of the desired product to the total amount of products generated in a reaction, and it is expressed as a percentage. So, as much closer it is to 100%, more efficient is the reaction. Catalysts, especially those based on transition metals, play a crucial role in the enhancement of the reaction efficiency. The understanding of the reaction mechanism and the use of completely renewable sub-stoichiometric species, contribute to the improvement of the efficiency of the reactions.[155]

1.2.1 TRANSITION METAL CATALYSTS FOR ORGANIC REACTIONS

Two main factors that affect at the effectiveness of a catalyst are its activity and reusability. As introduced at the beginning of the chapter, the catalysts can be classified as heterogeneous or homogeneous, depending if they are present in the same phase or not respect to the reactants. The homogeneous catalysts are, in general, much more active than the heterogeneous ones because they bear more active sites and show higher miscibility with the reactants, which enhances their mutual contact. Nevertheless, in the industrial processes, the heterogeneous catalysts are preferred by their facile separation from the reaction medium. This enhances the recyclability of the catalyst and facilitates the purification of the products.

Soluble organometallic complexes are the most common form of homogeneous catalyst. A wide number of different complexes can be obtained by modifying the organic ligands or the oxidation state of the metal atoms. This variety allows a huge control of the selectivity of the reactions, besides high efficiency and yield. Although homogeneous catalysts are present mainly in academia, their industrial applications are limited by the difficult separation of the catalyst from the products.

As mentioned previously, the use of catalysts is extensive to a wide number of different processes. The synthesis of drugs could be one of the most important applications. An easy an affordable formation of new C-C bonds ins mandatory for the obtention of new compounds. In that way, the development of cross-coupling

---

[152] *Chapter 1 History of Catalysis. Catalysis, an Integrated Approach to Homogeneous, Heterogeneous and Industrial Catalysis.* Mouljin, J. A., van Leeuwen, P. W. N. M., van Santen, R. A. Ed.: Elsevier, **1993**.
[153] Roberts, M. W. *Catal. Lett.* **2000**, *67*, 1.
[154] Armor, J. N. *Catal. Today* **2011**, *163*, 3.
[155] Sheldon, R. A. *Chem. Soc. Rev.* **2012**, *41*, 1437.

reactions opened a lot of possibilities for the use of Pd complexes in catalysis.[156] After the first publications using $PdCl_2$ and $Pd(OAc)_2$ as catalysts in Mizoroky-Heck reactions,[157,158] the use of palladium was expanded to other C-C reactions. Other Pd complexes such as $[PdCl_2(PPh_3)_2]$ (Sonogashira;[159] Negishi[160]), $[Pd(PPh_3)_4]$ (Corriu-Kumada;[161] Suzuki-Miyaura[162]), $[\{Pd(allyl)Cl\}_2]$ (Hiyama[163]) and $[PhCH_2Pd(PPh_3)_2Cl]$ (Stille[164]) were also used as catalysts for carbon-carbon coupling. Recently, new palladium complexes with NHC or phosphine ligands have been reported for C-C catalysis.[165,166] Complexes based on other metals have also been reported for cross-coupling reactions.[167,168,169] Other examples of reactions catalyzed by transition metal complexes are the functionalization of C-H bond to obtain C-O, C-S, C-X, C-N… bonds.[170,171] Gold based organometallic species have been extensively studied and they have been found excellent catalysts in a broad type of reactions.[172]

So, the use of homogeneous catalysts in academia has become a powerful tool to obtain organic products. But, as mentioned previously, their use in industrial processes is limited due to the difficult separation of the catalyst once the reaction is finished. To solve these problems, different strategies have been developed such as the formation of complexes inside dendrimers, which will act as a solid support. In that case the active site will be completely accessible to the reagents, and the catalyst could be removed from the media by microfiltration. Another option is the use of a biphasic medium reactions, where the catalyst and the reagents appear in different liquid phases. These reactions require a strong stirring to ensure a complete interaction between the species.[173]

Heterogeneous catalysts, although less active and selective, are preferred than homogeneous catalysts for industrial applications. Their recyclability, facile separation from the final products and robustness makes them the perfect catalysts for large scalable processes. The most common heterogeneous catalysts are based on metals or metal oxide surfaces. These catalysts were extensively used in industry for the obtention of "commodity chemicals" in a large scale.[174,175,176,177] Heterogenized organometallic species, prepared by anchoring them into a surface (bulk metal, polymer, silica or metal oxide), constitute heterogeneous catalysts with an activity close to that of an homogeneous catalyst. In order to obtain stable catalysts, anchoring the catalyst via covalent bonds seems the best option. However, in general, these catalysts present lower activity in front of the corresponding metal complex in solution.[178] Recently metal organic frameworks (MOFs) have

[156] Seechurn, C. C. C. J., Kitching, M. O., Colacot, T. J., Snieckus, V. *Angew. Chem. Int. Ed.* **2012**, *51*, 5062.

[157] Mori, K., Mizoroki, T., Ozaki, A. *Bull. Chem. Soc. Japan.* **1973**, *46*, 1505.

[158] Dieck, H. A., Heck, R. F. *J. Am. Chem. Soc.* **1974**, *96* (4), 1133.

[159] Sonogashira, K., Tohda, Y., Hagihara, N. *Tetrahedron Lett.* **1975**, *50*, 4467.

[160] Negishi, E.-i., King, A. O., Okukado, N. *J. Org. Chem.* **1977**, *42* (10), 1821.

[161] Murahashi, S.-I., Yamamura, M., Yanagisawa, K.-i., Mita, N., Kondo, K. *J. Org. Chem.* **1979**, *44* (14), 2408.

[162] Miyaura, N., Suzuki, A. *J. Chem. Soc. Commun.* **1979**, *19*, 866.

[163] Hatanaka, Y., Hiyama, T. *J. Org. Chem.* **1988**, *53*, 920.

[164] Milstein, D., Stille, J. K. *J. Am. Chem. Soc.* **1978**, *100* (11), 3636.

[165] Fortman, G. C., Nolan, S. P. *Chem. Soc. Rev.* **2011**, *40*, 5151.

[166] Mannepalli, L. K., Gadipelly, C., Deshmukh, G., Likhar, P., Pottabathula, S. *Bull. Chem. Soc. Japan* **2020**, *93* (3), 355.

[167] Sherry, B. D., Fürstner, A. *Acc. Chem. Res.* **2008**, *41* (11), 1500.

[168] (a) Phapale, V. B., Cárdenas, D. J. *Chem. Soc. Rev.* **2009**, *38*, 1598. (b) Han, F.-S. *Chem. Soc. Rev.* **2013**, *42*, 5270. (c) Tasker, S. Z., Standley, E. A., Jamison T. F. *Nature* **2014**, *509*, 299.

[169] Beletskaya, I. P., Cheprakov, A. V. *Coord. Chem. Rev.* **2004**, *248*, 2337.

[170] Lyons, T. W., Sanford, M. S. *Chem. Rev.* **2010**, *110*, 1147.

[171] Song, G., Wang, F., Li, X. *Chem. Soc. Rev.* **2012**, *41*, 3651.

[172] (a) Gorin, D. J., Sherry, B. D., Toste, F. D. *Chem. Rev.* **2008**, *108*, 3351. (b) Gorin, D. J., Toste, F. D. *Nature* **2007**, *446* (22), 395. (c) Hashmi A. S. K. *Chem. Rev.* **2007**, *107*, 3180. (d) Corma, A., Leyva-Pérez, A., Sabater, M. J. *Chem. Rev.* **2011**, *111*, 1657.

[173] Cole-Hamilton, D. J. *Science* **2003**, *299*, 1702.

[174] (a) Subramanu, V., Gangwal, S. K. *Energy & Fuels* **2008**, *22*, 814.

[175] (a) Helwani, Z., Othman, M. R., Aziz, N., Fernando, W. J. N., Kim, J. *Fuel Process. Technol.* **2009**, *90*, 1502. (b) Zabeti, M., Daud, W. M. A. W., Aroua, M. K. *Fuel Process. Technol.* **2009**, *90*, 770.

[176] Guil-López, R., Mota, N., Llorente, J., Millán, E., Pawelec, B., Fierro, J. L. G., Navarro, R. M. *Materials* **2019**, *12*, 3902.

[177] Ren, Z., Lyu, Y., Song, X., Ding, Y. *Appl. Cat. A Gen.* **2020**, *595*, 117488.

[178] (a) McMorn, P., Hutchings, G. J. *Chem. Soc. Rev.* **2004**, *33*, 108. (b) Copéret, C., Chabanas, M., Aint.Arroman, R. P., Basset, J.-M. *Angew. Chem. Int. Ed.* **2003**, *42* (2), 156.

gained popularity in their use as a support for the anchoring of different organometallic catalysts. MOFs present high porosity that guarantee a high interaction between the solution and the anchored metal species.[179]

1.2.2 METAL NANOPARTICLES AS CATALYSTS FOR ORGANIC REACTIONS

The catalytic properties of metal NPs have gained much interest in the chemical community as alternative to heterogenized metal complexes, principally by their versatility, selectivity and high surface area to volume ratio. Due to their morphological characteristics, metal NPs present high activities under mild conditions. As mentioned earlier in this chapter, bottom-up approaches are preferred for the synthesis of metal NPs, allowing almost a complete control in terms of the structure of the catalyst. In an ideal stage, this could give a specific active site for a concrete type of reaction, which could increase much more the selectivity respect to a classical heterogeneous catalyst. The formation of suspensions of metal NPs, in the same phase as the reagents, increases considerably their contact, in a similar way than in the homogeneous catalysis. These suspended species can also be easily removed from the reaction medium by changing the solvent, or by precipitation depending on their nature (for example with the use of a magnet in magnetic NPs). So, their recyclability is, in most cases, much easier than for a pure homogeneous catalyst. For these characteristics, some authors consider metal NPs as "semi-heterogeneous" catalysts, with properties in between homo and heterogeneous species. Metal NPs can also be supported on a solid surface, obtaining heterogeneous catalyst containing highly active metal NPs.

Metal NPs have been used in a wide range of organic reactions (hydrogenations, C-C bond formation reactions, oxidations, hydrosilylations, ….).[125, 180] Depending on the functionalization of the particles and their composition, their properties can be modulated, even in some cases catalysing enantioselective processes.[181]

1.2.2.1.   HYDROGENATION REACTIONS

Possibly, the hydrogenations of different chemical groups are the most studied reactions, being Pt and Pd NPs the most frequently used. However, several examples with other metals (Rh, Ru, Au) have also been reported[182,183,184]

A lot of examples have been published on the use of different Pt NPs for hydrogenation reactions. In that way, the reduction of different functional groups (olefins,[73b,83,85] nitroarenes,[46,74,77e] carbonyl groups,[75,77a]) was investigated. Molecular hydrogen has been the typical reducing agent for these transformations, but the use of other reductants have also been reported. These Pt catalysts tend to be highly selective.[71,74]

Other metal NPs, such as Pd,[27c] Rh,[22,127b,e,128a,134,141] Ru[185] or Au,[31a,119e,121] have also been reported to catalyze different hydrogenation reactions. The use of cheaper transition metals for these transformations was studied using Ni or Co.[95a,d,99c,d,102a,103,104a,186]

1.2.2.2.   OXIDATION REACTIONS

Oxidation of certain functional groups via catalysis by metal NPs has also been extensively studied.[25,187] These oxidative processes have been mainly described with noble metals (Pt,[44d,76] Pd,[27a] Rh[133] and Au[37,118d]) which

[179] (a) Lee, J. Y., Farha, O. K., Roberts, J., Scheidt, K. A., Nguyen, S.T., Hupp, J. T. *Chem. Soc. Rev.* **2009**, *38*, 1450. (b) Zhao, M., Ou, S., Wu, C.-D. *Acc. Chem. Res.* **2014**, *47*, 1199.

[180] Mikami, Y., Dhakshinamoorthy, A., Alvaro, M., García, H. *Catal. Sci. Technol.* **2013**, *3*, 58.

[181] Chng, L. L., Erathodiyil, N., Ying, J. Y. *Acc. Chem. Res.* **2013**, *46* (8), 1825.

[182] Zang, W., Li, G., Wang, L., Zhang, X. *Catal. Sci. Technol.* **2015**, *5*, 2532.

[183] Shultz, L. R., Hu, L., Preradovic, K., Beazley, M. J., Feng, X., Jurca, T. *ChemCatChem* **2019**, *11*, 2590.

[184] *Hydrogenation with Nanoparticles Using Supported Ionic Liquids. Supported Ionic Liquids: Fundamentals and Applications*. Scholten, J. D., Dupont, J. Ed.: Wiley-VCH, **2014**.

[185] Tschan, M. J.-L., Diebolt, O., van Leeuwen, P. W. N. M. *Top. Catal.* **2014**, *57*, 1054.

[186] Alonso, F., Riente, P., Yus, M. *Acc. Chem. Res.* **2011**, *44* (5), 379.

[187] Parmeggiani, C., Cardona, F. *Green Chem.* **2012**, *14*, 547.

are the most resistant to the oxidation conditions, being gold the most used. A great number of examples have been reported with supported and soluble Au NPs for the oxidation of alcohols, although some publications have described the oxidation of other compounds such as alkanes or alkenes.[188,189]

1.2.2.3. CARBON-CARBON BOND FORMING REACTIONS

The formation of new C-C bonds has become a key step to obtain useful building blocks in organic synthesis.

As mentioned previously, Pd complexes have resulted the most effective catalysts in the formation of C-C bonds via Suzuki, Heck, Sonogashira and other coupling reactions. For this reason, with the growth of the importance of nanocatalysts, Pd NPs became the most studied catalysts for this transformation. Among all the different types of nanomaterials based in Pd, supported Pd NPs possibly will offer the best future perspectives for the industrial application of these reactions due their high stability, durability and recyclability.[27b,31b,190] Pd-based bimetallic species have also been reported, being, in some cases more active than pure Pd NPs. These nanostructures maximise the amount of Pd atoms in the surface that, in general, are the active species in the catalyst.[58, 191] These structures can reduce the cost of the catalyst with the construction of a core composed by a cheaper material. Also, some core materials can provide novel properties to the nanoparticles by, for example, using magnetic species in the core of the particles. In that way Rothenberg et al.[192] reported the high activity of a bimetallic NiPd NPs for Hiyama coupling. These NPs are composed by an inner core of Ni (cheaper than Pd) surrounded by a thin layer of Pd atoms. With this NiPd nanostructure, the efficiency of the Pd species is enhanced by location of more proportion of Pd atoms on the surface, being these bimetallic NPs more active than pure Pd NPs.

Corma et al. published two of the first studies about the catalysis of Sonogashira coupling with supported Au NPs on ceria.[193,194] In these works, the authors describe that Au(I) species present in the particles play a key role in the reaction. Interestingly, they do not observe conversion for the Sonogashira reaction with the use of Au(0) NPs. In a subsequent DFT study focused on a Au^0/Au^+ catalyst for Sonogashira reaction, these authors showed that the formation of the product is promoted if the catalyst contains both species.[195] Later on, other authors reported the successful catalysis of other coupling reactions by different kinds of Au nanoparticles.[196,197,198]

The formation of carbon-carbon bonds catalyzed by Ni and Pt NP has also been investigated.[72] Different types of Ni NPs have catalyzed successfully cross-coupling reactions such as Suzuki-Miyaura,[44a,101a] Sonogashira[99b] or Corriu-Kumada.[96]

In recent years, multicomponent reactions for the obtention of diverse organic molecules have gained interest. One of the best examples of this kind of reactions was the synthesis of propargylamines via A^3-coupling reaction between aldehydes, amines and terminal alkynes catalyzed by Au NPs.[196,199] Au(I) and Au(III)

---

[188] Li, G., Jin, R. *Acc. Chem. Res.* **2013**, *46* (8), 1749.

[189] Liu, Y., Tsunoyama, H., Akita, T., Xie, S., Tsukuda, T. *ACS Catal.* **2011**, *1*, 2.

[190] (a) Hong, K., Sajjadi, M., Suh, J. M., Zhang, K., Nasrollahzadeh, M., Jang, H. W., Varma, R. S., Shokouhimehr, M. *ACS Appl. Nano Mater.* **2020**, *3*, 2070. (b) Jin, M., Zhang, H., Xie, Z., Xia, Y. *Angew. Chem. Int. Ed.* **2011**, *50*, 7850.

[191] Shylesh, S., Schünemann, V., Thiel, W. R. *Angew. Chem. Int. Ed.* **2010**, *49*, 3428.

[192] Pachón, L. D., Thathagar, M. B., Hartl, F., Rothenberg, G. *Phys. Chem. Chem. Phys.* **2006**, *8*, 151.

[193] González-Arellano, C., Abad, A., Corma, A., García, H., Iglesias, M., Sánchez, F. *Angew. Chem. Int. Ed.* **2007**, *46*, 1536.

[194] Corma, A., Juárez, R., Boronat, M., Sánchez, F., Iglesias, M., García, H. *Chem. Commun.* **2011**, *47*, 1446.

[195] Boronat, M., Combita, D., Concepción, P., Corma, A., García, H., Juárez, R., Laursen, S., López-Castro, J. D. *J. Phys. Chem. C* **2012**, *116*, 24855.

[196] Li, G., Jin, R. *Nanotechnol. Rev.* **2013**, *2*, 529.

[197] Raheem, A. A., Thangasamy, P., Sthish, M., Praveen, C. *Nanoscale Adv.* **2019**, *1*, 3177.

[198] Candu, N., Dhakshinamoorthy, A., Apostol, N., Teodorescu, C., Corma, A., Garcia, H., Parvulescu, V. I. *J. Catal.* **2017**, *352*, 59.

[199] Lauder, K., Toscani, A., Scalacci, N., Castagnolo, D. *Chem. Rev.* **2017**, *117*, 14091.

catalysts have been typically used for this transformation,[200,201,202] in some cases with the generation *in situ* of Au(0)[203] or Au(I)[204] NPs. Corma and Zhang[205] described Au NPs supported on ceria or zirconia containing Au(III)/Au(I), which were the actives sites for the A[3]-coupling. Au(0) NPs immobilized in MOFs that contains Au(III) species presented high catalytic activity for the synthesis of propargylamines.[206] Other authors have reported zerovalent gold nanoparticles supported on different heterogeneous catalysts for this reaction.[113,116,207] Publications involving unsupported Au NPs were unusual compared with the amount of reports based in heterogeneous gold nanocatalysts.[117] Silver[208] and copper[209] nanoparticles have also been reported for the A[3]-coupling reaction (**Scheme 3**).
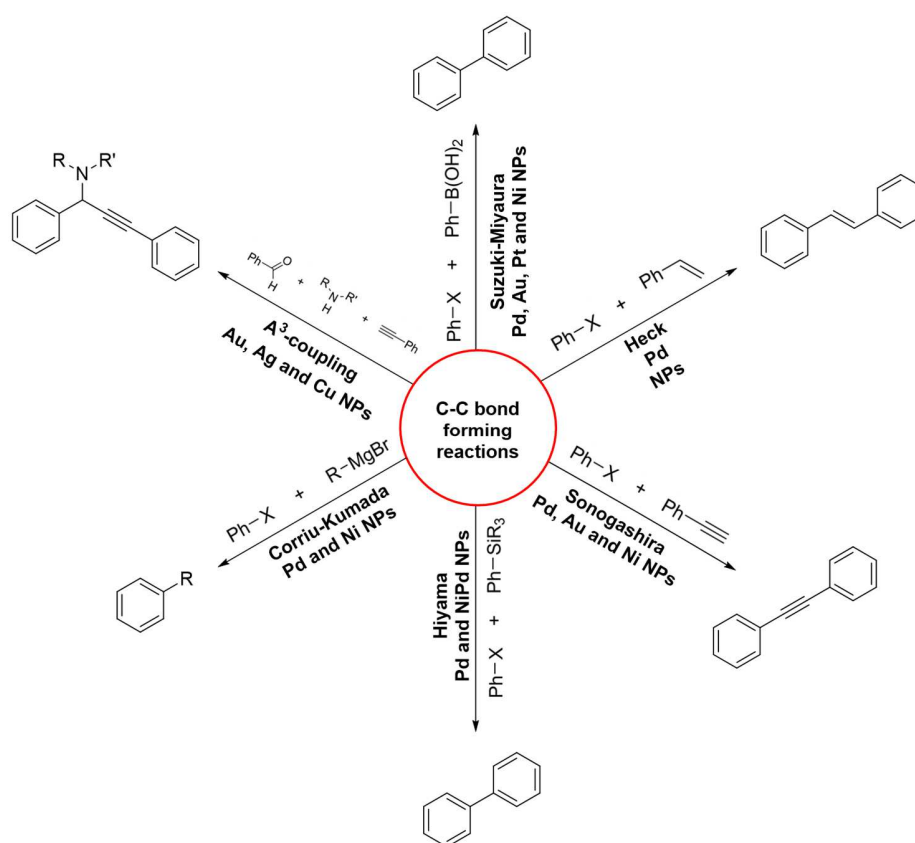
Scheme 3 Summary of carbon-carbon bond forming reactions catalyzed by metal NPs.

1.2.2.4.   HYDROSILYLATION REACTIONS OF ALKYNES

The transition-metal catalyzed hydrosilylation of alkynes and alkenes are a straightforward, convenient and atom-efficient method for the synthesis of alkenylsilanes and akylsilanes, respectively, which are versatile building blocks in the synthesis of different organic compounds. Traditionally Pt complexes have been used

[200] (a) Peshkov, V. A., Pereshivko, O. P., Van der Eycken, E. V. *Chem Soc. Rev.* **2012**, *41*, 3790. (b) Jesin, I., Nandi, G. C. *Eur. J Org. Chem.* **2019**, 2704.

[201] Wei, C., Li, C.-J. *J. Am. Chem. Soc.* **2003**, *125*, 9584.

[202] Price, G. A., Brisdon, A. K., Flower, K. R., Pritchard, R. G., Quayle, P. *Tetrahedron Lett.* **2014**, *55*, 151.

[203] Soengas, R., Navarro, Y., Iglesias, M. J., López-Ortiz, F. *Molecules* **2018**, *23*, 2975.

[204] Sánchez, E. B., Iglesias, M. J., Hajjouji, H., Roces, L., García-Granada, S., Villuendas, P., Urriolabeitia, E. P., Ortiz, F. L. *Organometallics* **2017**, *36*, 1962.

[205] Zhang, X., Corma, A. *Angew. Chem. Int. Ed.* **2008**, *47*, 4358.

[206] Lili, L., Xin, Z., Jinsen, G., Chunming, X. *Green Chem.* **2012**, *14*, 1710.

[207] Borah, B. J., Borah, S. J., Saikia, K., Dutta, D. K. *Catal. Sci. Technol.* **2014**, *4*, 4001.

[208] Cao, J., Tian, H. *Chem. Asian J.* **2018**, *13*, 1561.

[209] Albaladejo, M. J., Alonso, F., Moglie, Y., Yus, M. *Eur. J. Org. Chem.* **2012**, 3093.

for these reactions,[210] although catalysts based on other metals such as Ru, Rh, Pd or Co have also been reported.[211] During the last years, some articles describing the use of metal based nanocatalysts for the preparation of alkenylsilanes appeared, Pt and Pt oxides NPs being the most frequently employed for this transformation, especially those immobilized on solid supports. [212 , 213] However, besides the Pt NPs, nanomaterials based on other metals (Pd, Rh, Au) have also been described to catalyze these hydrosilylation reactions.[214,215]

[210] (a) Stein, J., Lewis, L. N., Gao, Y., Scott, R. A. *J. Am. Chem. Soc.* **1999**, *121*, 3693. (b) Silbestri, G. F., Flores, J. C., de Jesús, E. *Organometallics* **2012**, *31*, 3355. (c) Chay, R. S., Rocha, B. G. M., Pombeiro, A. J. L., Kukushkin, V. Y., Luzyanin, K. V. *ACS Omega* **2018**, *3*, 863.

[211] (a) Maifeld, S. V., Tran, M. N., Lee, D. *Tetrahedron Lett.* **2005**, *46*, 105 (b) Naganawa, Y., Inomata, K., Sato, K., Nakajima, Y. *Tetrahedron Lett.* **2020**, *61*, 151513. (c) Gutiérrez-Tarriño, S., Concepción, P., Oña-Burgos, P. *Eur. J. Inorg. Chem.* **2018**, 4867. (d) Morales-Cerón, J. P., Lara, P., López-Serrano, J., Santos, L. L., Salazar, V., Álvarez, E., Suárez, A. *Organometallics* **2017**, *36*, 2460.

[212] (a) Alonso, F., Buitrago, R., Moglie, Y., Ruiz-Martínez, J., Sepúlveda-Escribano, A., Yus, M. *J. Organometallic Chem.* **2011**, *696*, 368. (b) Alonso, F., Buitrago, R., Moglie, Y., Sepúlveda-Escribano, A., Yus, M. *Organometallics* **2012**, *31*, 2336. (c) Hu, W., Xie, H., Yue, H., Prinsen, P., Luque, R. *Catal. Commun.* **2017**, *97*, 51. (d) Duke, B. J., Akeroyd, E. N., Bhatt, S. V., Onyeagusi, C. I., Bhatt, S. V., Adolph, B. R., Fotie, J. *New J. Chem.* **2018**, *42*, 11782. (e) Fang, H., Chen, J., Xiao, Y., Zhang, J. *Appl. Catal. A Gen.* **2019**, *585*, 117186. (f) Dobó, D. G., Sipos, D., Sápi, A., London, G., Juhász, K. L., Kukovecz, A., Kónya, Z. *Catal.* **2018**, *8*, 22.

[213] Cano, R., Yus, M., Ramon, D. J. *ACS Catal.* **2012**, *2* (6), 1070.

[214] *For Pd and PdAu NPs in hydrosilylations see:* (a) Planellas, M., Guo, W., Alonso, F., Yus, M., Shafir, A., Pleixats, R., Parella, T. *Adv. Synth. Catal.* **2014**, *356*, 179. (b) Reddy, C. B., Shil, A. K., Guha, N. R., Sharma, D., Das, P. *Catal. Lett.* **2014**, *144*, 1530. (c) Miura, H., Endo, K., Ogawa, R., Shishido, T. *ACS Catal.* **2017**, *7* (3), 1543; *For Au NPs in hydrosilylations see:* (d) Psyllaki, A., Lykakis, I. N., Stratakis, M. *Tetrahedron* **2012**, *68*, 8724; *For Rh NPs in hydrosilylations see:* (e) Guo, W., Pleixats, R., Shafir, A., Parella, T. *Adv. Synth. Catal.* **2015**, *357*, 89.

[215] Pascu, O., Liautard, V., Vaultier, M., Pucheault, M., Aymonier, C. *RSC Adv.* **2014**, *4*, 59953.

1.3   PRECEDENTS IN OUR RESEARCH GROUP

Our research group has been interested in the preparation of metal NPs (Pd, Pt, Au, Rh and Ru) stabilized with different organic species. These nanomaterials were used as catalysts in some organic reactions.[216]

1.3.1   METAL NANOPARTICLES STABILIZED BY FLUORINATED COMPOUNDS

The initial research in that field started in 2000 when, trying to obtain a fluorinated analogous of Pd(dba)$_2$, Pd NPs were obtained instead of the corresponding complex. These Pd NPs were soluble in fluorinated solvents and catalytically active in Heck and Suzuki couplings.[217] These preliminary results encouraged our group to expand the research to other fluorinated nanomaterials. Thus, other organic molecules bearing polyfluorinated chains (**Figure 8**) were tested as stabilizers for Pd,[218] Au,[219] Ru[220] and Pt NPs.[221] These Pd nanoparticles resulted active as catalysts in cross-coupling reactions. [222]
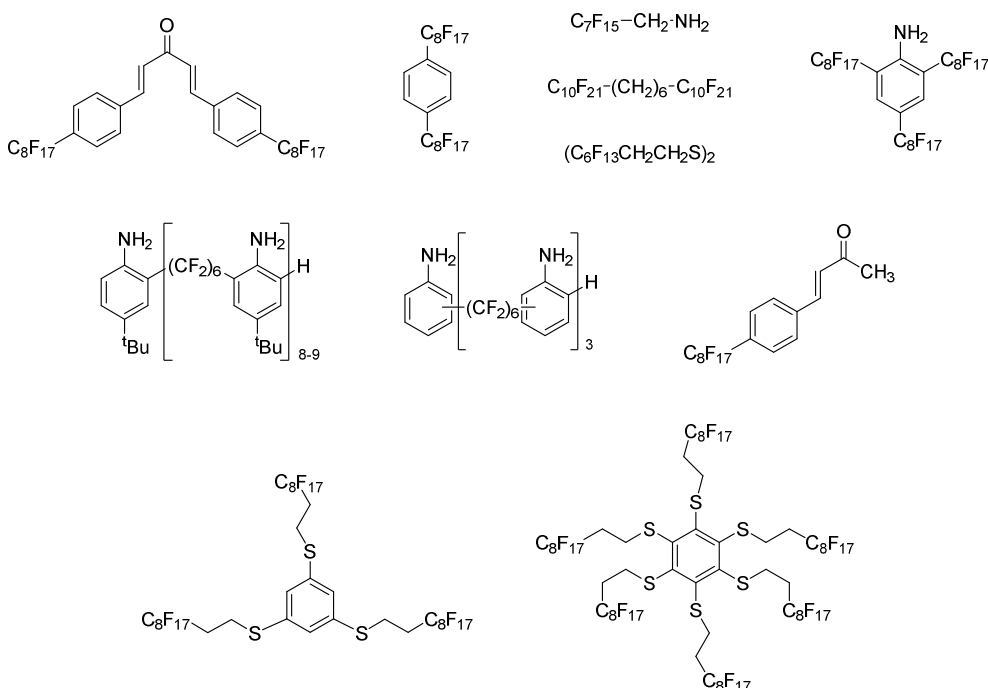
Figure 8 Heavily fluorinated stabilizers developed in our group for the preparation of metal NPs.

In order to obtain more stable and easily recyclable nanomaterials, our group also prepared metal NPs supported on silica. This immobilization was performed by two different methods. The first method developed was based on the treatment of Pd and Au NPs, stabilized with fluorinated compounds, with fluorous silica gel.[223] These Pd nanomaterials were active for Heck,[223a] Suzuki[223e] and Sonogashira[223c] reactions and the gold

[216] Pleixats, R., Shafir, A. *An. Quím.* **2017**, *113* (2), 92.

[217] (a) Moreno-Mañas, M., Pleixats, R., Villarroya, S. *Organometallics* **2001**, *20*, 4524. (b) Moreno-Mañas, M., Pleixats, R., Villarroya, S. *Chem. Commun.* **2002**, 60. (c) Villarroya, S. *Doctoral thesis*, Universitat Autònoma de Barcelona, **2002**.

[218] (a) Tristany, M., Courmarcel, J., Dieudonné, P., Moreno-Mañas, M., Pleixats, R., Rimola, A., Sodupe, M., Villaroya, S. *Chem. Mater.* **2006**, *18*, 716. (b) Niembro, S., Vallribera, A., Moreno-Mañas, M. *New. J. Chem.* **2008**, *32*, 94.

[219] Moreno-Mañas, M., Pleixats, R., Tristany, M. *J. Fluorine Chem.* **2005**, *126*, 1435.

[220] Tristany, M., Chaudret, B., Dieudonné, P., Guari, Y., Lecante, P., Matsura, V., Moreno-Mañas, M., Philippot, K., Pleixats, R. *Adv. Funct. Mater.* **2006**, *16*, 2008.

[221] (a) Tristany, M., Moreno-Mañas, M., Pleixats, R., Chaudret, B., Philippot, K., Dieudonné, P., Lecante, P. *J. Mater. Chem.* **2008**, *18*, 660. (b) Tristany, M., Moreno-Mañas, M., Pleixats, R., Chaudret, B., Philippot, K., Guari, Y., Matsura, V., Lecante, P. *New. J. Chem.* **2009**, *33*, 1529.

[222] (a) Tristany, M. *Doctoral thesis*, Universitat Autònoma de Barcelona, **2005**. (b) Niembro, S. *Doctoral thesis*, Universitat Autònoma de Barcelona, **2010**.

[223] (a) Bernini, R., Cacchi, S., Fabrizi, G., Forte, G., Niembro, S., Petrucci, F., Pleixats, R., Prastaro, A., Sebastián, R. M., Soler, R., Tristany, M., Vallribera, A. *Org. Lett.* **2008**, *10* (4), 561. (b) Bernini, R., Cacchi, S., Fabrizi, G., Niembro, S., Prastaro, A.,

NPs were successfully used in the oxidation of alcohols.[223b] Although, in some cases these materials could be reused without loss of the activity, an exhaustive analysis revealed degradation of the catalysts and leaching of metal NPs on the supernatant. To solve this problem, the fluorinated stabilizer was covalently anchored to the silica matrix. This approach gave nanomaterials with better results of recovery and reusability.[222b]

1.3.2 METAL NANOPARTICLES STABILIZED BY PEG-TAGGED COMPOUNDS AND TRIS-IMIDAZOLIUM SALTS

Our group had observed that the introduction of polyoxyethylenated or polyfluorinated chains into triolefinic fifteen-membered azamacrocycles lead to the formation of Pd(0) NPs,[224] instead of the previously reported Pd(0) complexes.[225] These PEG-tagged stabilizers provide solubility in water and insolubility in diethyl ether to the Pd NPs. These solubility properties allowed to perform the reaction in water and then the nanocatalyst could be easily recycled by addition of diethyl ether.

After this first publication the group was interested in the synthesis of water-soluble metal NPs stabilized with these PEG-tagged macrocyclic ligands (with and without double bonds, **Figure 9**). Thus, Pd, Pt and Ru NPs were obtained by decomposition of the corresponding zerovalent complexes, Pd(dba)$_2$, Pt$_2$(dba)$_3$ and Ru(COD)(COT), with hydrogen in the presence of the stabilizers following the *organometallic approach*. Rh and Au NPs were also obtained by chemical reduction method.[226] But the low nanoparticle yields obtained with these macrocyclic stabilizers, prompted us to design new polyoxyethylenated ligands, with better stabilizing properties and which could be easily synthesized. With this objective in mind, a star-shaped stabilizer with a benzene core and three triazole rings was synthesized through a [3+2] cycloaddition between a trialkyne and a PEG-tagged azide (**Figure 9**). The ligand containing coordinating nitrogen atoms was successfully applied as stabilizer for the preparation of Pd NPS by the decomposition of Pd(dba)$_2$ with hydrogen following the *organometallic approach*. The obtained Pd NPs catalyzed the Suzuki reaction in aqueous media.[227]

Shafir, A., Vallribera, A. *ChemSusChem* **2009**, *2*, 1036. (c) Bernini, R., Cacchi, S., Fabrizi, G., Forte, G., Petrucci, F., Prastaro, A., Niembro, S., Shafir, A., Vallribera, A. *Org. Biomol. Chem.* **2009**, *7*, 2270. (d) Niembro, S., Shafir, A., Vallribera, A., Alibés, R. *Org. Lett.* **2008**, *10* (15), 3215. (e) Bernini, R., Cacchi, S., Fabrizi, G., Forte, G., Petrucci, F., Prastaro, A., Niembro, S., Shafir, A., Vallribera, A. *Green Chem.* **2010**, *12*, 150.

[224] Serra-Muns, A., Soler, R., Badetti, E., de Mendoza, P., Moreno-Mañas, M., Pleixats, R., Sebastián, R. M., Vallribera, A. *New J. Chem.* **2006**, *30*, 1584.

[225] Moreno-Mañas, M., Pleixats, R., Sebastián, R. M., Vallribera, A., Roglans, A. *J. Organomet. Chem.* **2004**, *689*, 3669.

[226] (a) Serra-Muns, A. *Doctoral thesis*, Universitat Autónoma de Barcelona, **2008**. (b) Mejías, N., Serra-Muns, A., Pleixats, R., Shafir, A., Tristany, M. *Dalton Trans.* **2009**, 7748.

[227] (a) Mejías, N. *Doctoral thesis*, Universitat Autònoma de Barcelona, **2011**. (b) Mejías, N., Pleixats, R., Shafir, A., Medio-Simón, M., Asensio, G. *Eur. J. Org. Chem.* **2010**, 5090.
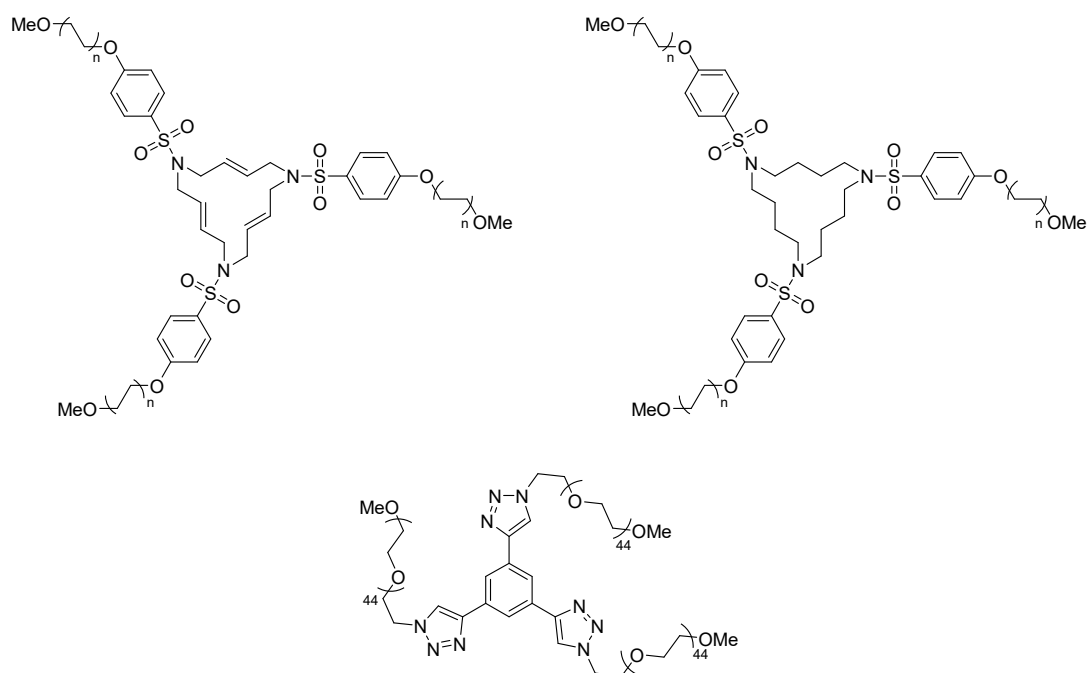
Figure 9 PEG-tagged stabilizers developed by our group.

Despite of the good results obtained with the formation of Pd NPs, the efforts to apply this PEG-tagged ligand for the stabilization of Au NPs did not give satisfactory and reproducible results. For this reason, a stabilizer with a higher number of coordinating nitrogen atoms was designed (**Scheme 4**). This star-shaped stabilizer with a triazine core and three PEG-tagged chains, containing each one a secondary amine and a triazole moiety, was synthesized through a CuAAC reaction between the corresponding trialkyne and the PEG-tagged azide (**Scheme 4**). With this stabilizer, Rh[214e] and Au NPs[228] were prepared from RhCl₃ and HAuCl₄, respectively, by chemical reduction method. These NPs were found catalytically active for the hydrosilylation of internal alkynes (Rh NPs) and for the reduction of nitroarenes (Au NPs).[229]
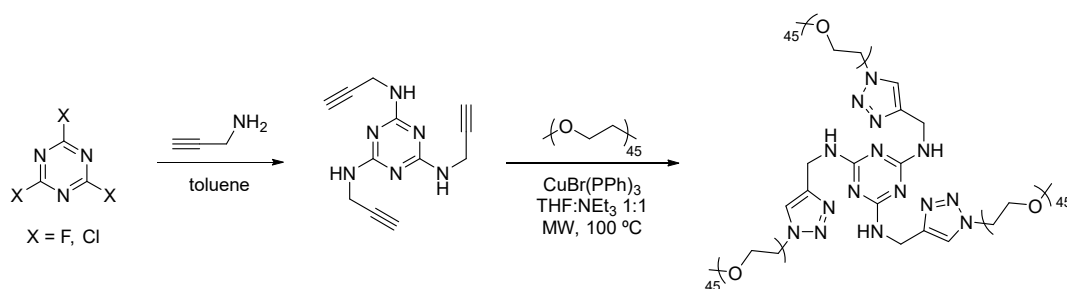
Scheme 4 Preparation of PEG-tagged N-rich stabilizer developed by Dr. Guo.

On the other hand, our group had described in 2008 the synthesis of tris-imidazolium salts (with iodide and tetrafluoroborate as counter anions) containing a mesitylene core and hexadecyl chains (**Figure 10**), which were then considered suitable for the preparation of metal NPs soluble in organic media. Dr. M. Planellas obtained Pd NPs stabilized by these tris-imidazolium salts in a reproducible way by using the *organometallic approach.* The Pd NPs resulting from the iodide salt were very effective catalysts for several cross-coupling reactions (Suzuki, Heck, Sonogashira, Hiyama) with a wide range of substrates bearing different functional groups.[230] The Pd NPs stabilized by the tetrafluoroborate salt presented much lower catalytic activity for these

[228] Guo, W., Pleixats, R., Shafir, A. *Chem. Asian J.* **2015**, *10*, 2437.

[229] Guo, W. *Doctoral thesis*, Universitat Autònoma de Barcelona, **2014**.

[230] (a) Planellas, M., Pleixats, R., Shafir, A. *Adv. Synth. Catal.* **2012**, *354*, 651. (b) Planellas, M., Moglie, Y., Alonso, F., Yus, M., Pleixats, R., Shafir, A. *Eur. J. Org. Chem.* **2014**, 3001.

reactions with challenging aryl chlorides, which showed the importance of the anion effect in the catalytic activity of the nanomaterials. Conversely, the Pd NPs derived from the tetrafluoroborate salt presented good catalytic activity in the hydrosilylation of internal alkynes, although the process was very sensitive to the presence of water.[214a,231]
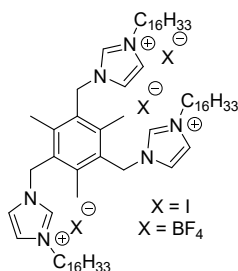
Figure 10 Tris-imidazolium salt-based stabilizers for Pd NPs developed by Dr. Planellas.

---

[231] Planellas, M. *Doctoral thesis*, Universitat Autònoma de Barcelona, **2012**.

Chapter 2.   OBJECTIVES

According to the precedents previously exposed, the main goals of this thesis were the preparation and characterization of novel metal NPs stabilized by imidazolium salts soluble either in organic solvents or in water, and the evaluation of their catalytic activity in different organic reactions.

Thus, in the present thesis, we planned the following specific objectives:

a) Design and preparation of a new type of stabilizers based on imidazolium salts bearing PEG-tagged chains through triazole-containing linkers (see **S2A, S2B** and **S3** in **Figure 11**). The imidazolium moieties would provide electrostatic interactions and the coordinating nitrogen atoms of triazole rings would enhance the stabilizing properties. The hydrophilic PEGylated fragments would contribute to the electrosteric stabilization and to the tuning of the solubility of the substrates and the resulting metal nanoparticles (solubility in water, insolubility in diethyl ether). In all cases, the synthesis involves a [2+3] cycloaddition reaction between azides and alkynes.
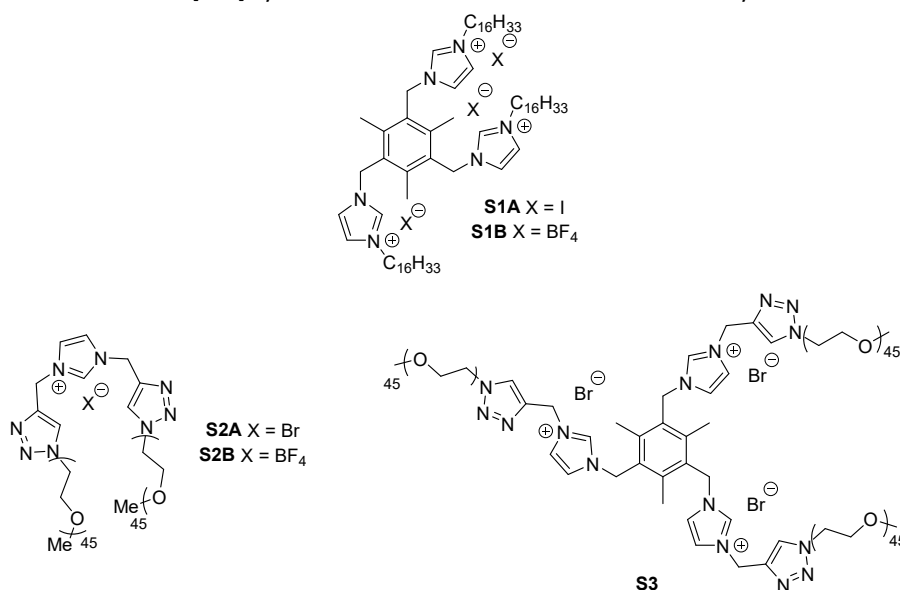
Figure 11 Imidazolium salts developed for the stabilization of metal NPs.

b) Preparation of Pt and Ni NPs soluble in organic media stabilized by the tris-imidazolium salts previously developed in our group (see **S1A** and **S1B** in **Figure 11**). Complete characterization of the nanomaterials by HRTEM, ED, EDS, ICP-OES, ^{1}H NMR and XPS. Magnetic characterization in the case of Ni NPs.

c) Preparation and characterization (HRTEM, ED, EDS, ICP-OES, ^{1}H NMR and XPS) of new water-soluble Au and Rh NPs stabilized by the previously obtained PEG-tagged imidazolium salts **S2A**, **S2B** and **S3**.

d) Evaluation of the catalytic activity of the obtained metal NPs in cross-coupling reactions (Ni and Rh NPs), hydrosilylation of internal alkynes (Pt, Rh and Ni NPs), three component A^3 coupling between aldehydes, amines and terminal alkynes (Au NPs), cycloisomerization of γ-alkynoic acids (Au NPs), reduction of nitroarenes (Ni and Rh NPs). We were interested in the comparison of the activity of Ni and Pt/**S1A-B** NPs in cross-coupling and/or hydrosilylation reactions with respect to the activity of Pd/ **S1A-B** NPs in the same type of reactions, a study previously performed in our group. On the other hand, the solubility in water of metal NPs stabilized by **S2A-B** and **S3** would allow us to carry out organic reactions in sustainable aqueous medium. Moreover, we aimed to the recycling of the different nanocatalysts taking advantage of the solubility properties of the corresponding stabilizers.

Chapter 3. SYNTHESIS AND CHARACTERIZATION OF METAL NANOPARTICLES STABILIZED BY IMIDAZOLIUM SALTS CONTAINING HEXADECYL OR POLYOXYETHYLENATED CHAINS

3.1 INTRODUCTION

As we have mentioned in the objectives, and based on the previous research of the group, we decided to continue our investigations on the synthesis of metal NPs stabilized by differently substituted imidazolium salts, soluble in organic or aqueous media, for catalytic applications. First we have undertaken the preparation of Pt and Ni NPs stabilized by tris-imidazolium salts bearing hydrocarbon chains (**S1A-B**) used previously in our group for the synthesis of Pd NPs by Dr. M. Planellas.[214a,230] Then we have developed two new kinds of PEG-tagged imidazolium salts (**S2A-B**, **S3**) for the stabilization of Au and Rh NPs.

3.1.1 OVERVIEW OF COPPER-CATALYZED AZIDE-ALKYNE CYCLOADDITION (CuAAC)

Thermal 1,3-dipolar cycloaddition between an azide and an alkyne was firstly introduced by Huisgen in 1963.[232] However, this process provided a mixture of two regioisomeric 1,4- and 1,5-disubstituted triazoles. It was in 2002 when this reaction gained special attention when, in an independent way, Meldal[233] and Sharpless[234] described the cycloaddition between organic azides and alkynes catalyzed by Cu(I) species, introducing the concept of "click chemistry" (**Scheme 5**). These conditions resulted in a major improvement of regioselectivity (selective formation of 1,4-disubstituted triazoles) involving milder conditions.
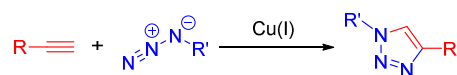
Scheme 5 Cu-catalyzed Azide Alkyne Cycloaddition (CuAAC).

In the last years CuAAC reactions have become a powerful synthetic tool due to their high selectivity, quantitative yields, robust and mild conditions, that allow the possibility to be applied *in vivo*.[235] These advantages open the use of this type of reaction in a wide kind of different areas such as drug development, polymers, medicine, etc..[236,237,238,239] Despite copper(II) sulphate is the most common source of copper for this transformation, using sodium ascorbate as a reducing agent to generate the required Cu(I) species,[234] other copper sources have been reported recently.[240]

The mechanistic details of the reaction and the role of copper into the catalytic cycle have been the subject of debate since the discovery of the reaction. After a DFT study, Sharpless and collaborators[241] proposed a mechanism involving a single Cu(I) species in the catalytic cycle (**Scheme 6**). The cycle starts with the coordination of the alkyne **a** with the Cu(I) displacing one of the ligands L and generating the copper(I) acetylide **b**. Then the azide **c** displaces another of the copper coordinating ligands L generating the intermediate **d**. At this point the distant nitrogen of the azide moiety attacks the C2 of the acetylide forming a six membered Cu(III) metallacycle **e** and subsequently a copper metallated triazole **f**. Upon protonation, the target triazole **g** is released and the copper(I) complex is regenerated for another cycle.

[232] a) Huisgen, R. *Angew. Chem. Int. Ed.* **1963**, *11*, 565. b) Huisgen, R. *Angew. Chem. Int. Ed.* **1963**, *10*, 633.

[233] Tornøe, C. W., Christensen, C., Meldal, M. *J. Org. Chem.* **2002**, *67*, 3057.

[234] Rostovtsev, V. V., Green, L. G., Fokin, V. V., Sharpless, K. B. *Angew. Chem. Int. Ed.* **2002**, *41*, 2596.

[235] Singh, M. S., Chowdhury, S., Koley, S. *Tetrahedron*, **2016**, *72*, 5257.

[236] Jiang, X., Hao, X., Jing, L., Wu, G., Kang, D., Liu, X., Zhan, P. *Exp. Opinion Drug Discover.* **2019**, *14* (8), 779.

[237] Arslan, M., Acik, G., Tasdelen, M. A. *Polym. Chem.* **2019**, *10*, 3806.

[238] a) Gopinathan, J., Noh, I. *Tissue Eng. Regen. Med.* **2018**, *15*, 531. b) Lee, S., Jung, S., Koo, H., Na, J. H., Yoon, H. Y., Shim, M. K., Park, J., Kim, J.-H., Lee, S., Pomper, M. G., Kwon, I. C., Ahn, C.-H, Kim, K. *Biomaterials* **2017**, *148*, 1.

[239] Meldal, M., Tornøe, C. W. *Chem. Rev.* **2008**, *108*, 2952.

[240] a) Sirion, U., Bae, Y. J., Lee, B. S., Chi, D. Y. *Synlett* **2008**, *15*, 2326. b) Seus, N., Saravia, M. T., Alberto, E. E., Savegnago, L., Alves, D. *Tetrahedron* **2012**, *68*, 10419. c) Sau, S. C., Roy, S. R., Sen, T. K., Mullangi, D., Mandal, S. K. *Adv. Synth. Catal.* **2013**, *355*, 2982. d) Alonso, F., Moglie, Y., Radivoy, G., Yus, M. *Eur. J. Org. Chem.* **2010**, 1875.

[241] Himo, F., Lovell, T., Hilgraf, R., Rostovtsev, V. V., Noodleman, L., Sharpless, K. B., Fokin, V. V. *J. Am. Chem. Soc.* **2005**, *127* (1), 210.
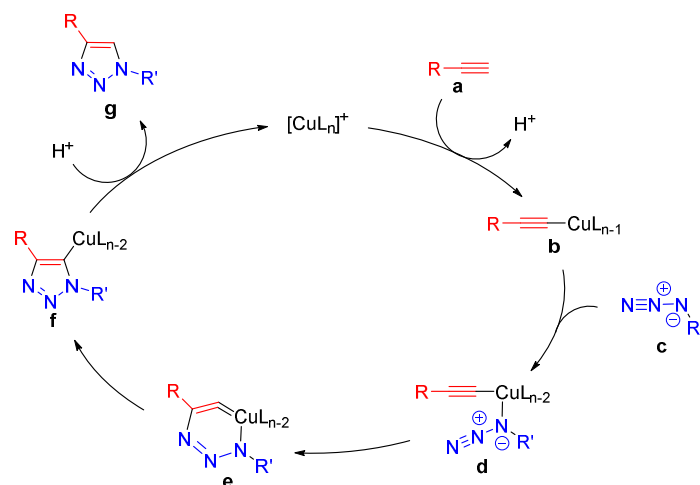
Scheme 6 Sharpless's proposed mechanism for the CuAAC.[241]

However, recent studies suggested a transition state with more than one copper species involved[242]. This new proposal (**Scheme 7**) starts with the formation of the π-complex **h** that after the deprotonation of the terminal H coordinates to another Cu(I) species generating a copper acetylide intermediate **i**. Then the π-Cu complex coordinates to the azide giving the complex **j** in which one Cu is coordinated with the acetylide and the other is coordinated with the azide. After this step a nucleophilic attack at the terminal N of the azide by the β-carbon of the acetylide forms a covalent bond producing intermediate **k**. At this point cyclization takes place to form **l**, which after protonation generates the target triazole **g** and the copper catalyst is recovered for subsequent cycles.
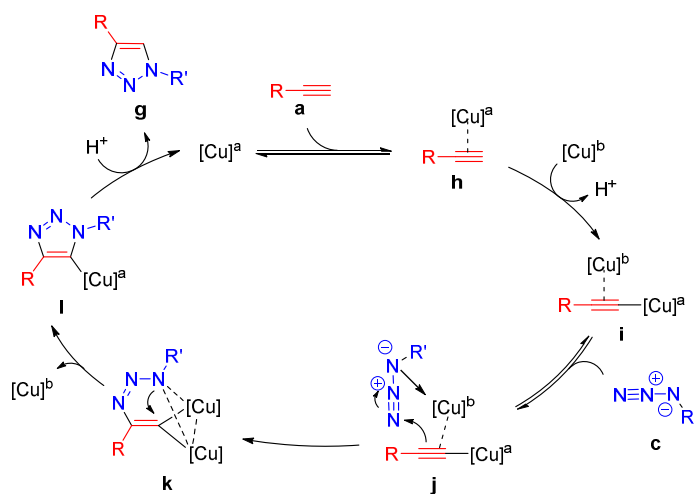
Scheme 7 Revised proposal for CuAAC.[242]

---

[242] Worrell, B. T., Malik, J. A., Fokin, J. J. *Science* **2013**, *340*, 457.

3.2 SYNTHESIS OF IMIDAZOLIUM SALTS AS STABILIZERS

3.2.1 SYNTHESIS OF TRIS-IMIDAZOLIUM SALTS CONTAINING HEXADECYL CHAINS **S1A-B**

The synthesis of the stabilizers **S1A-B** is summarized in **Scheme 8**. This synthetic procedure was previously developed in our group by Montserrat Trilla in 2007[243] for the synthesis of liquid crystals and then improved by Marc Planellas.[214a,230]
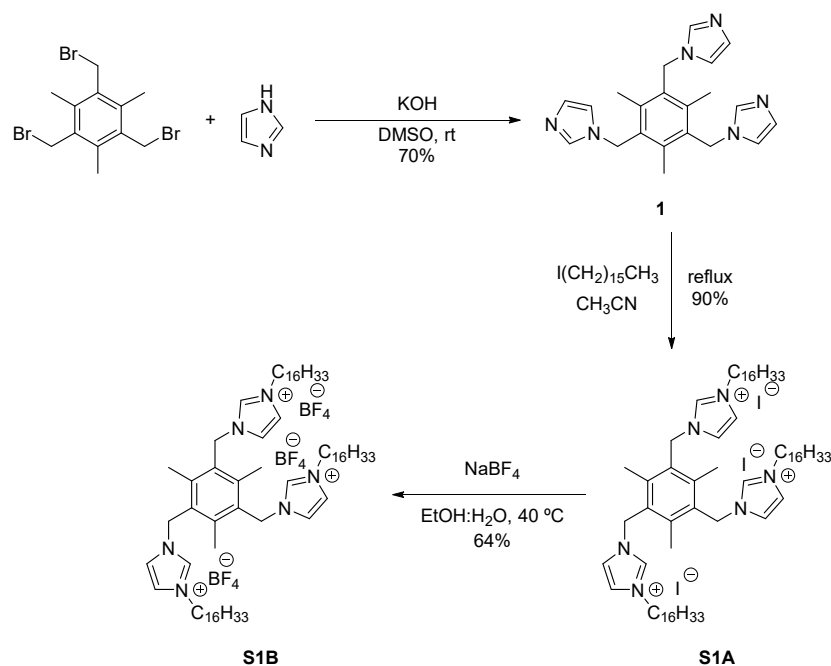
Scheme 8 Synthesis of tris-imidazolium salts **S1A** and **S1B**.

The star-shaped product **1** was obtained, in 70% yield, by the reaction of commercially available 2,4,6-tris(bromomethyl)mesitylene and imidazole in DMSO at room temperature using KOH as base.[244] The alkylation of imidazole rings of compound **1** with 1-iodohexadecane in refluxing CH_3CN overnight gave the tris-imidazolium salt **S1A** in 90% yield. Treating **S1A** with an excess of $NaBF_4$ in $EtOH:H_2O$ mixture at 40 ºC produced the anion exchange and tris-imidazolium salt **S1B** precipitated as a white solid. To ensure the complete exchange of the three anions is a key factor for the posterior efficiency of the imidazolium salt in the NPs stabilization. For this reason, this exchange process was repeated 3 times (64% yield of **S1B**). As described previously,[231] the anion exchange modifies the ^1H NMR chemical shift of the protons of the imidazolium rings. As observed in **Figure 12** the chemical shifts decrease by gradual exchange of iodide by tetrafluoroborate obtaining values of 8.97, 7.75 and 7.24 ppm for pure **S1B**.

We should consider for all the imidazolium salts described in section 3.2 that different samples of the same product in the same solvent can display some differences in the chemical shifts due to different concentration. Indeed, chemical shift variations in imidazolium salts with changing concentrations have been previously reported.[245]

[243] Trilla, M., Pleixts, R., Parella, T., Blanc, C., Dieudonné, P., Guari, Y., Chi Man, M. W. *Langmuir* **2008**, *24*, 259.

[244] Liu, H.-K., Sun, W.-Y., Zhu, H.-L., Yu, K.-B., Tang, W.-X. *Inorg. Chim. Act.* **1999**, *295*, 129.

[245] Marekha, B. A., Kalugin, O. N., Bria, M., Idrissi, A. *Phys. Chem. Chem. Phys.* **2015**, *17*, 23183
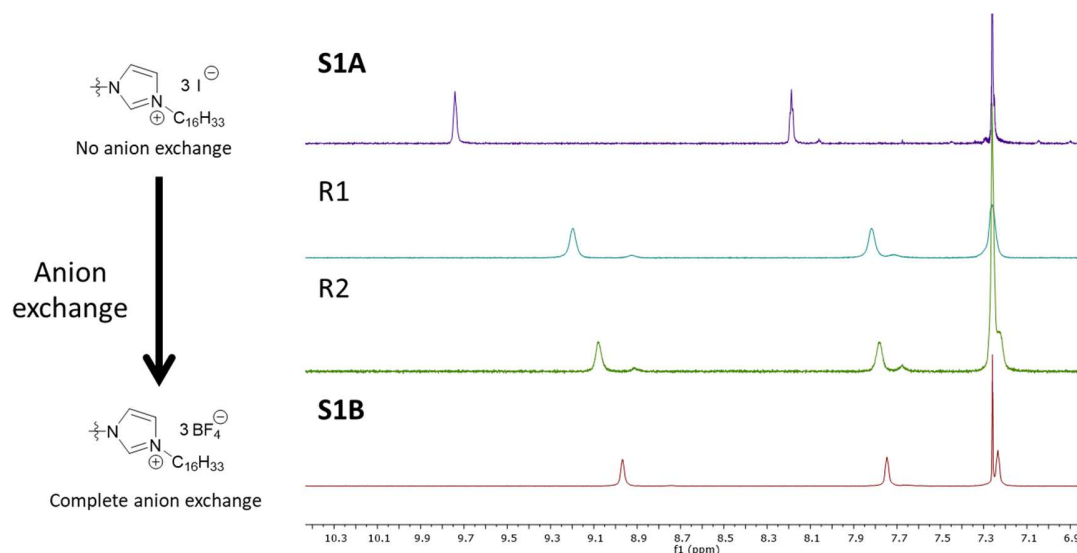
Figure 12 Chemical shifts of imidazolium protons before and after anion exchanging.

Finally, **S1A** and **S1B** were obtained in 63% and 40% overall yield, respectively. We synthesized these stabilizers in order to find an effective and reproducible procedure to prepare Pt and Ni NPs and to investigate the effect of the nature of counteranion.

3.2.2 SYNTHESIS OF PEG-TAGGED IMIDAZOLIUM SALTS **S2A-B**

As previously mentioned in the introduction, in our group some PEG-tagged stabilizers had been prepared using CuAAC chemistry for the obtention of water soluble NPs.[214e,226b,227b,228] Inspired by these results and our experience, imidazolium salts containing polyoxyethylenated chains have been developed in this thesis. As shown in **Scheme 9**, the reaction of *N*-(trimethylsilyl)imidazole with an excess of propargyl bromide in toluene at 50 ºC afforded the imidazolium salt **2a** in 94% of yield as an hygroscopic solid.[246] Treatment of this imidazolium bromide **2a** with an excess of sodium tetrafluoroborate in acetone at room temperature gave the imidazolium tetrafluoroborate **2b** in high yield.[246]

For the preparation of PEG-tagged azide **4** a two-step process from commercial polyethylene glycol ($n_{average}$ = 45) was performed. The previously dried substrate was treated with methanesulfonyl chloride in the presence of Et_3N as base in anhydrous CH_2Cl_2 to obtain PEG-tagged mesylate **3** in 97% yield. The subsequent reaction with NaN_3 in DMF at 60 ºC gave azide **4** in 96% yield.[214e,227b]

---

[246] Fei, Z., Zhao, D., Scopelliti, R., Dyson, P. J. *Organometallics* **2004**, *23* (7), 1622.
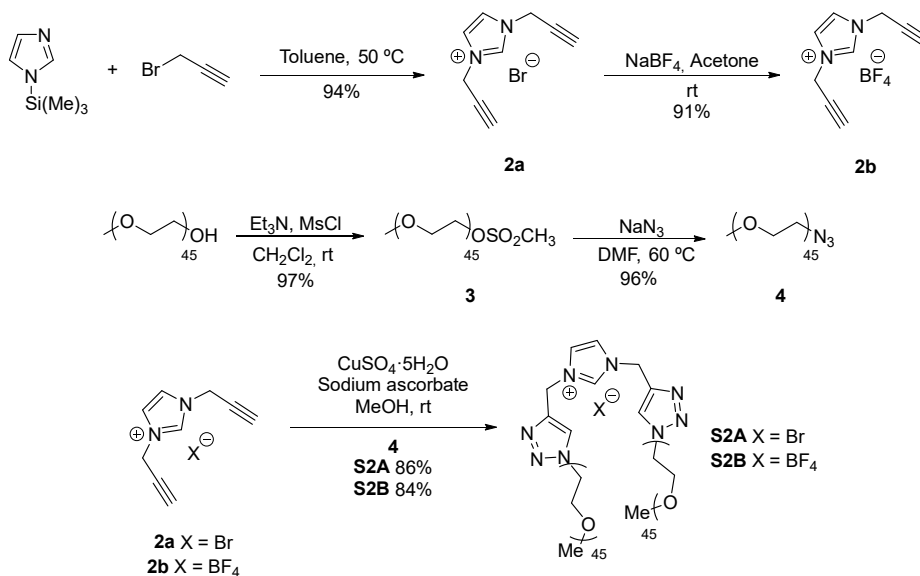
Scheme 9 Synthesis of PEG-tagged imidazolium salts **S2A** and **S2B**.

Finally, **S2A-B** were obtained through a CuAAC[234,239] reaction between the corresponding alkyne-derivatized imidazolium salts **2a-b** and the PEGylated azide **4** in methanol at room temperature by a modification of a described procedure.[112] The stabilizers **S2A** and **S2B** were obtained in 86% and 84% yields, respectively (**Scheme 9**).

Both stabilizers were characterized by ^{1}H NMR, ESI-TOF-MS and IR. The broad signal around 3.60 ppm in the ^{1}H NMR spectrum confirms the presence of PEG-tagged chains. As in the case of **S1A-B** stabilizers, the chemical shifts of the imidazolium protons are modified after the anion exchange from bromide to tetrafluoroborate (**Figure 13**). According to the ESI-TOF-MS, the polyoxyetylenated chains were confirmed by the most intense [M]$^+$ peaks corresponding to 4047.7 (86 CH_2CH_2O units) for **S1A** and 3870.4 (82 CH_2CH_2O units) for **S1B** (**Figure 14**). The absence of the starting azide in the final products **S2A** and **S2B** was ensured by the non-appearance of the azide peak (at 2098 cm^{-1}) in the IR spectrum (**Figure 15**).
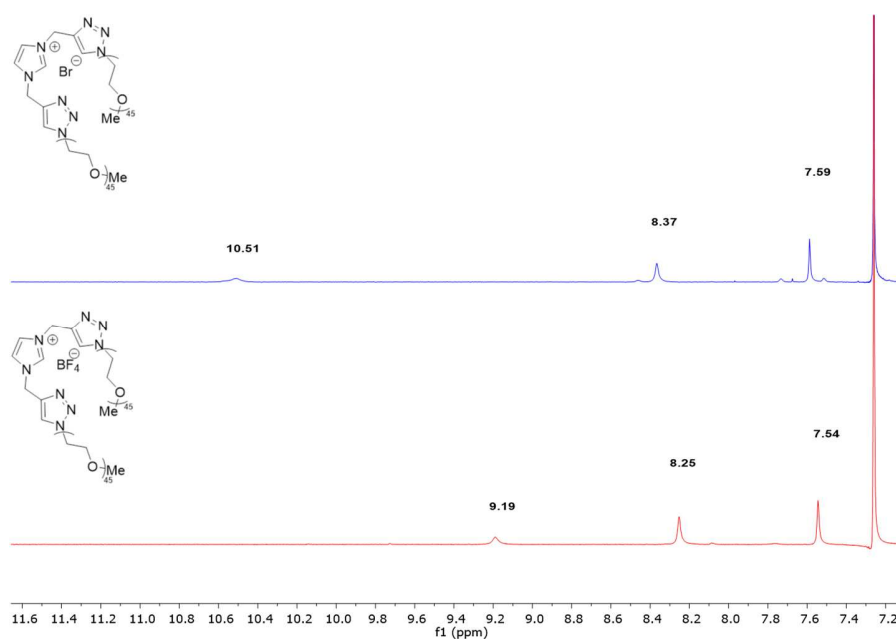
Figure 13 ^{1}H NMR spectra of **S2A** and **S2B** (only imidazolium protons).
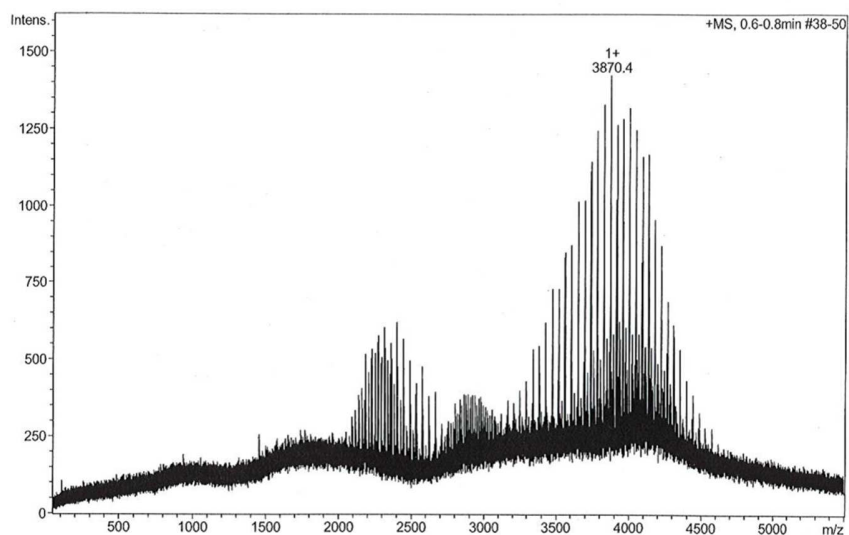
Figure 14 ESI-TOF-MS spectrum of **S2B**.
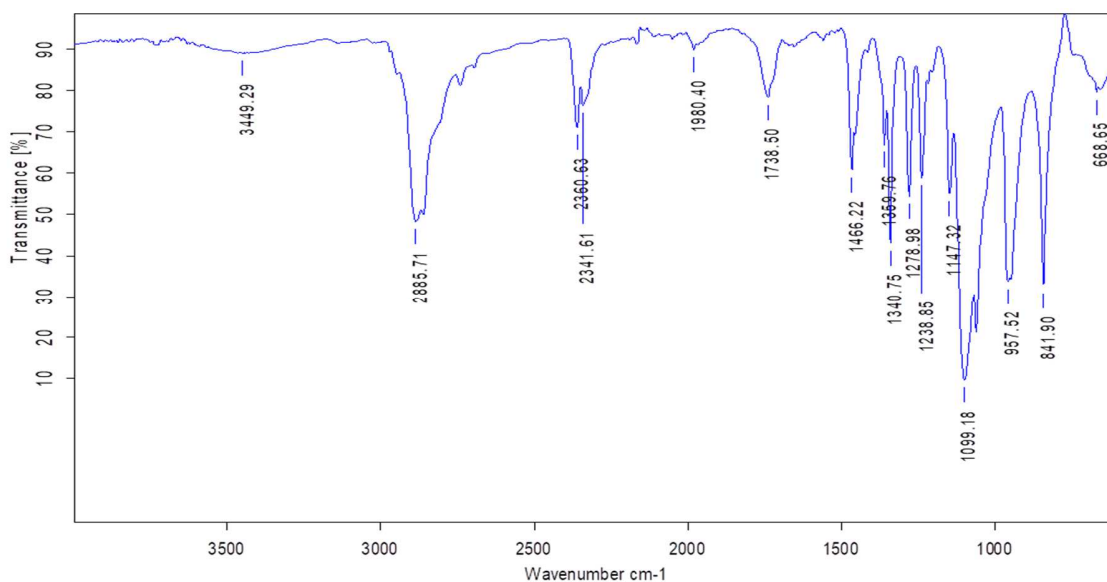
Figure 15 IR spectrum of **S2A**.

3.2.3 SYNTHESIS OF PEG-TAGGED TRIS-IMIDAZOLIUM SALT **S3**

The synthesis of the PEG-tagged tris-imidazolium salt **S3** was accomplished as outlined in **Scheme 10**.
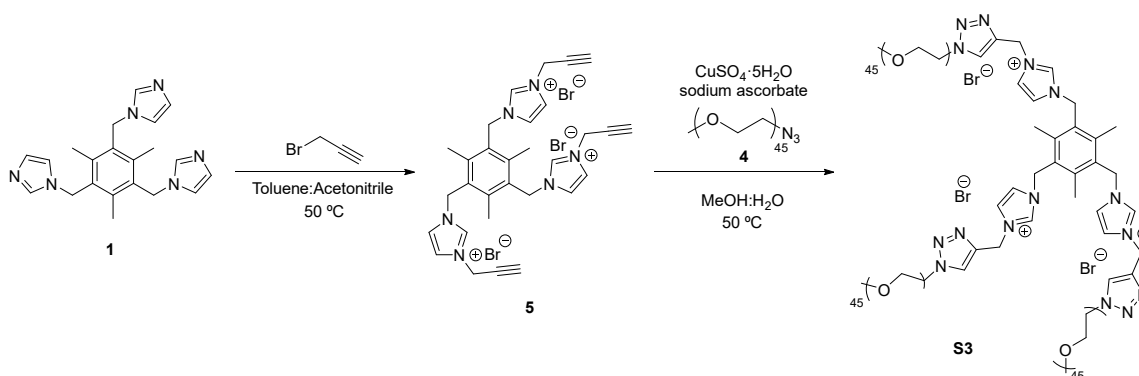
Scheme 10 Synthesis of PEG-tagged tris-imidazolium salt **S3**.

42

The reaction of the C^3-symmetric tris-imidazole **1**[230a,244] with excess of propargyl bromide in a 2:1 mixture of toluene:acetonitrile at 50 ºC afforded the tris-imidazolium salt **5** as an hygroscopic solid in 63% yield. It was insoluble in dichloromethane, chloroform, acetone, diethyl ether and acetonitrile, slightly soluble in ethanol and methanol, and very soluble in water and dimethyl sulfoxide. A three-fold CuAAC reaction between the trialkyne **5** and the azide **4** in methanol:water (1:1) at 50 ºC was performed to give the desired stabilizer **S3** in 79% isolated yield.

The final product was characterized by ^{1}H NMR, MALDI-TOF-MS and IR. As in the case of **S2A-B** a broad and intense absorption at 3.6 ppm due to methylene groups of PEG chains is observed in the ^{1}H NMR spectrum. Also the presence of polyoxyethylenated chains is confirmed by the MALDI-TOF-MS spectrum, showing peaks between 1685.650 (33 CH_2CH_2O units + $C_{30}H_{33}N_{15}$ nitrogen-rich core + 3 CH_3) and 2253.907 (46 CH_2CH_2O units + $C_{30}H_{33}N_{15}$ nitrogen-rich core + 3 CH_3) corresponding to $[M]^{3+}$ separated by 44 D (CH_2CH_2O unit); the most intense peak at 1903.742 (38 CH_2CH_2O units + $C_{30}H_{33}N_{15}$ nitrogen-rich core + 3 CH_3) (**Figure 16**). From the IR spectrum the complete absence of free azide in **S3** is deduced.
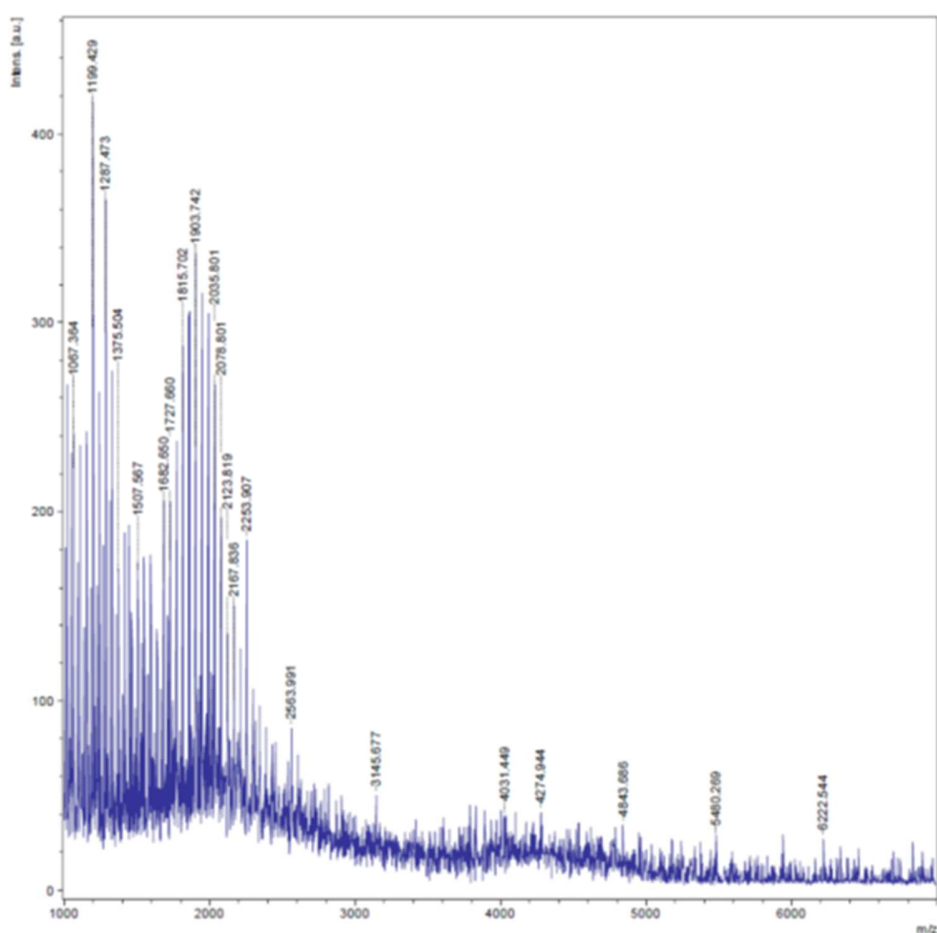
Figure 16 MALDI-TOF-MS spectrum of **S3**.

3.3 Preparation and characterization of transition metal nanoparticles stabilized by imidazolium salts

3.3.1 Preparation and characterization of platinum nanoparticles stabilized by imidazolium salts containing hexadecyl chains S1A-B

A variety of procedures have been reported for the obtention of platinum NPs, as mentioned in the introduction. In this work the synthesis of Pt NPs stabilized by **S1A-B** was performed in a two-step process.[247] As summarized in **Scheme 11**, we first prepared a solution of Pt NPs stabilized by EG and then we carried out an exchange of the stabilizer to obtain the final nanomaterials. We have adapted a method described by the group of Wang[248] for the preparation of unprotected metal nanoparticles (Pt, Ru, Rh) involving the heating of metal salts in ethylene glycol containing NaOH at high temperature. Then, different polymers or ligands were added by the authors to the solution of metal NPs in EG, such as poly(N-vinyl-2-pyrrolidone) or triphenylphosphine, to obtain the corresponding protected metal nanoparticles.
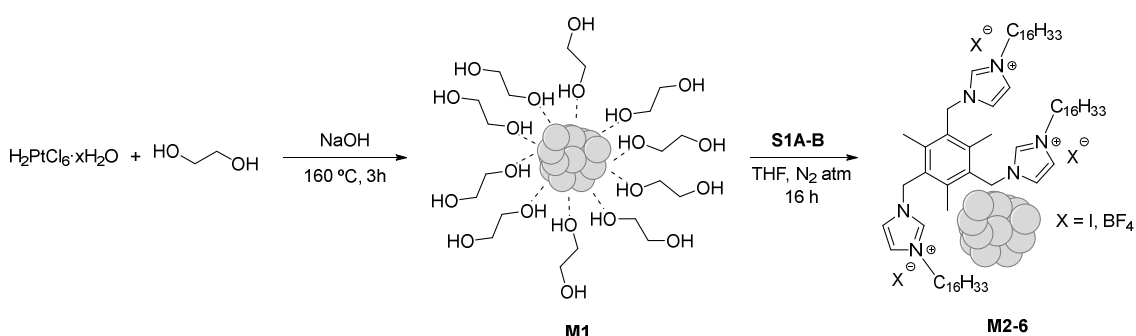
Scheme 11 Synthesis of Pt NPs stabilized by **S1A** and **S1B**.

In the first step, a solution of the hexachloroplatinic(IV) acid hydrate and NaOH in ethylene glycol was heated at 160 ºC for 3 h obtaining a brown colloidal solution of Pt NPs **M1**. The ethylene glycol in the presence of a base, such as NaOH, acts as reductant of the Pt(IV) salt and, at the same time, as stabilizer of the NPs. As is observed in the TEM image of **Figure 17**, small Pt NPs were obtained with an average size of 1.9 ± 0.5 nm with a face-centered cubic (FCC) structure, according to the ED analysis.
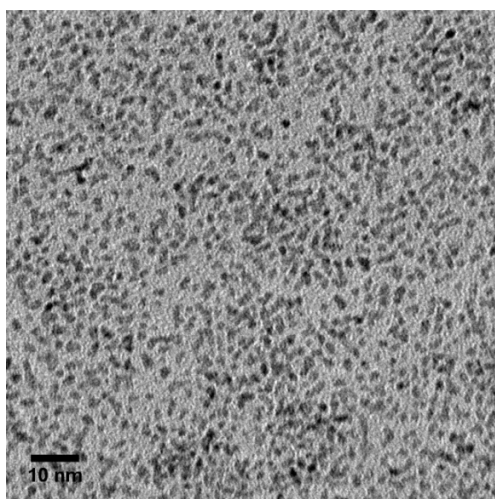
Figure 17 TEM image of Pt NPs **M1** stabilized by ethylene glycol.

247 Fernández, G., Pleixats, R. *ChemistrySelect* **2018**, *3*, 11486.
248 Wang, Y., Ren, J., Deng, K., Gui, L., Tang, Y. *Chem. Mater.* **2000**, *12*, 1622.

Then the stabilizer **S1A** or **S1B** dissolved in dry and degassed THF was added to the colloidal solution of **M1** to exchange the stabilizer. The mixture was stirred at room temperature under N_2 atmosphere overnight. Once the reaction was over, water was added to the mixture and the Pt NPs were extracted with CH_2Cl_2. The dark brown organic phase was washed several times with water in order to get rid of most of the EG. The organic layer was then filtered through a nylon membrane filter (Milli-pore, 0.2 μm) to eliminate possible traces of bulk Pt. After evaporation of the solvent, the resultant solid was washed with methanol and hexane to remove residues of ethylene glycol and free ligand unreacted. The final nanomaterials were obtained after centrifugation and decantation of supernatant. Pt NPs were obtained as a black powder soluble in toluene, THF, dichloromethane and chloroform and insoluble in pentane, diethyl ether, ethyl acetate, methanol and water. Different reaction conditions for the synthesis of the Pt NPs were tested (**Table 1**).

Table 1 Preparation of Pt NPs stabilized by **S1A** and **S1B**.

Ent.	Stabilizer	S1: Pt[a]	mmol Pt	mmol NaOH	mL EG[b]	mL THF[b]	Diameter (nm)[c]	% Pt Theor.	% Pt Exp.[d]	Yield[e] (%)	Nanomaterial
1	**S1A**	2.5:1	0.04	0.5	20	5	bulk	5.2	11.8	10.8	**M2**
2	**S1A**	1:1	0.2	2.5	100	25	2.4 ± 0.7	12.1	10.0	2.7	**M3**
3	**S1B**	1:1	0.04	0.5	20	5	3.7 ± 1.5	13.1	24.2	90	**M4**
4	**S1B**	1:1	0.2	2.5	100	25	1.6 ± 0.6	13.1	30.3	85	**M5**
5	**S1B**	0.5:1	0.2	2.5	100	25	1.8 ± 0.6	23	43.3	55	**M6**

[a] Molar ratio. [b] Volume of solvent in the final mixture. See experimental section. [c] Determined by TEM (500 - 1000 particles measured). [d] Determined by ICP-OES. [e] Based on $H_2PtCl_6 \cdot xH_2O$ (40% wt Pt) used.

The first experiment with stabilizer **S1A** was performed in a small scale with 0.04 mmol of Pt and a molar ratio **S1A**:Pt of 2.5:1 (**Table 1**, entry 1). The obtained material **M2**, although was a soluble dark solid, consisted mainly in a mixture of aggregates of Pt and stabilizer, according to the TEM analysis (**Figure 18 (A)**). In order to prevent an excess of organic species in the final material a second run was performed with an equimolar **S1A**:Pt ratio and using 0.2 mmol of Pt (**Table 1**, entry 2) obtaining the nanomaterial **M3**. As observed in the TEM images (**Figure 18 (B)**), **M3** consists in small Pt NPs well dispersed with an average size of 2.4 nm. Even small particles were obtained, the yield was too low which was an indication that most of the initial metal precipitated as bulk platinum and was removed in the filtration step. According to the obtained results we concluded that the tris-imidazolium iodide **S1A** was not a good candidate for the stabilization of Pt NPs.
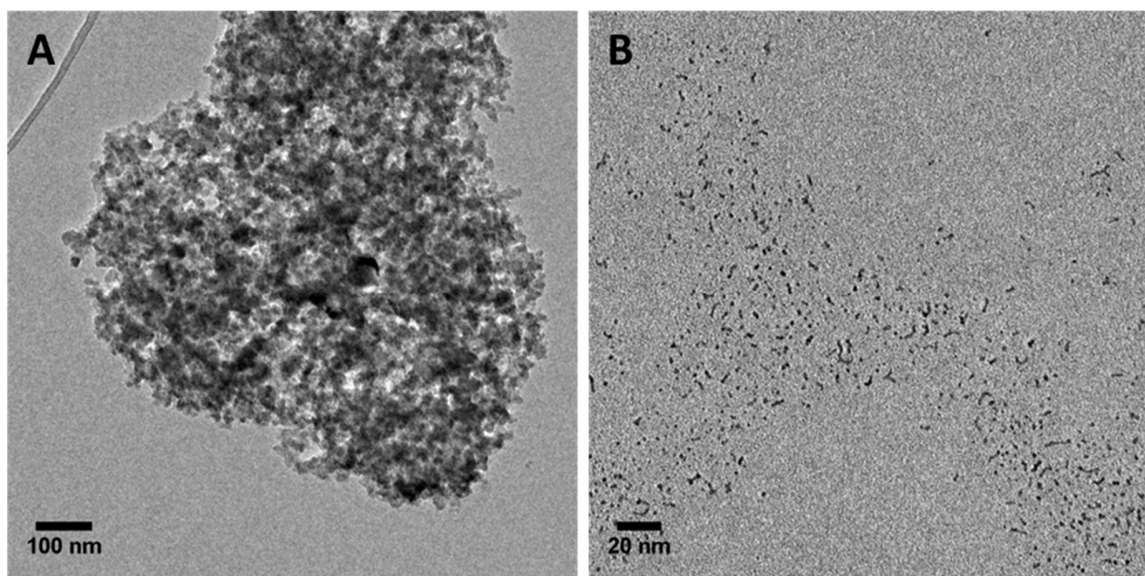
Figure 18 TEM images of **(A) M2** and **(B) M3**.

Conversely, the tetrafluoroborate salt **S1B** was much more efficient as a stabilizer for Pt NPs, giving good results under all the conditions tested (**Table 1**, entries 3-5). Due to the bad results observed in entry 1, the

first experiment with **S1B** was performed in a small scale (0.04 mol of Pt) but with an equimolar proportion of **S1B**:Pt (**Table 1**, entry 3). TEM images of the obtained material **M4** revealed the presence of small NPs with an average size of 3.7 nm and the obtained yield was 90%. Increasing the scale to 0.2 mmol of Pt with two different molar ratios **S1B**:Pt (1:1 and 0.5:1) was explored to afford nanomaterials **M5** and **M6** (**Table 1**, entries 4 and 5 respectively). These materials consisted in small, well dispersed and spherical NPs with sizes of 1.6 and 1.8 nm respectively (**Figure 19**). According to the elemental analysis of the materials (obtained by ICP-OES, 30.3% for **M5** and 40.3% for **M6**) the yield with respect to the initial Pt was calculated as 85 and 55%, respectively. Thus, a reduction in the amount of stabilizer does not affect significantly to the size of the particles but results in a lower yield. These results indicated that tris-imidazolium tetrafluoroborate **S1B** was a much better stabilizer for Pt NPs than the iodide **S1A**, highlighting the importance of the counter-anion on the stabilizing properties.
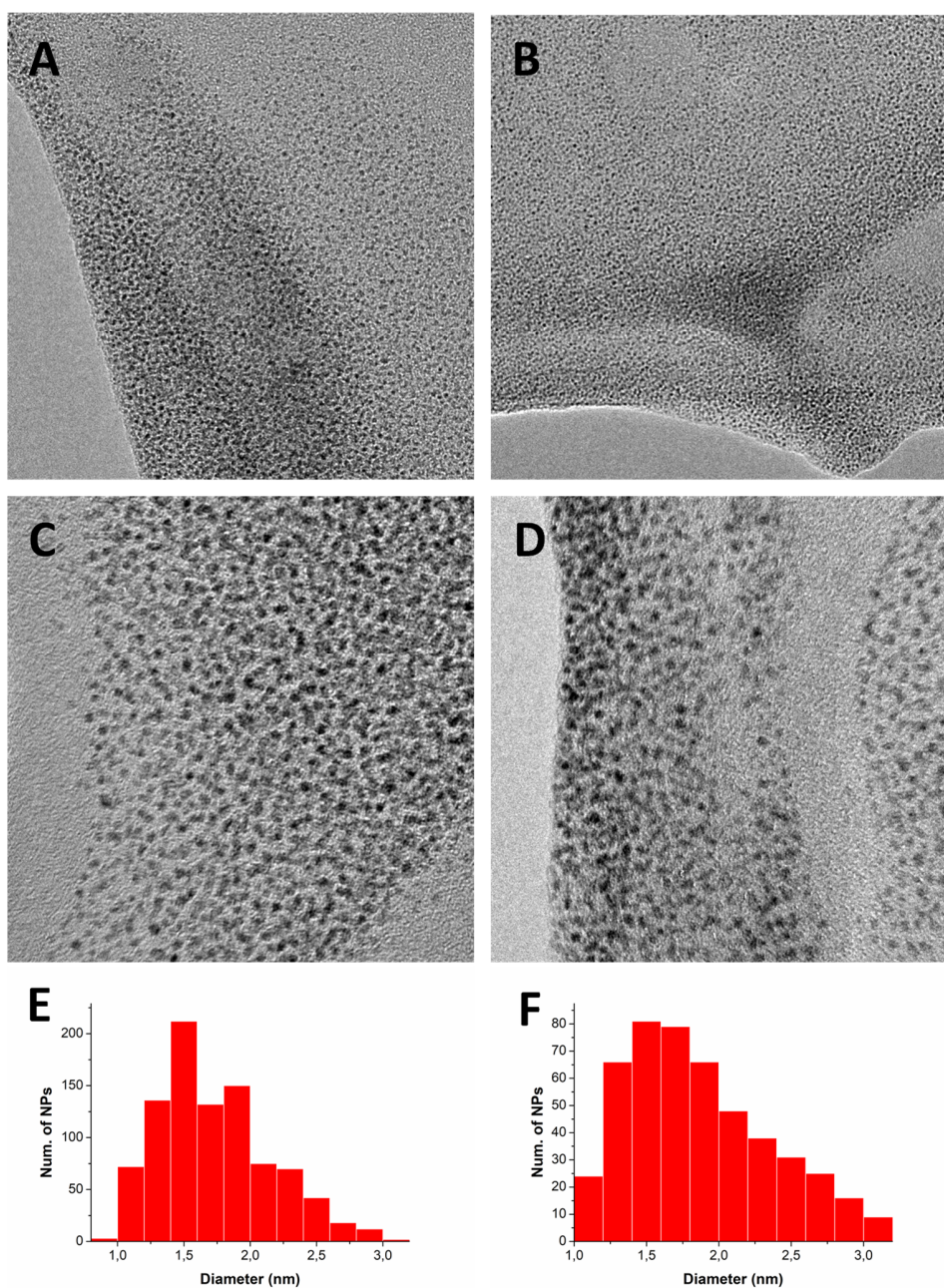
Figure 19 TEM images and particle size distribution of **M5 (A, C, E)** and **M6 (B, D, F)**.

The presence of platinum and the complete absence of traces of other metals in the samples was confirmed by EDS of **M5** (**Figure 20**). As in the case of the Pt NPs stabilized by ethylene glycol **M1**, the experimental interplanar distances measured by electron diffraction (ED) were in accordance with FCC Pt(0) lattice for all the Pt NPs obtained (**Table 2**).
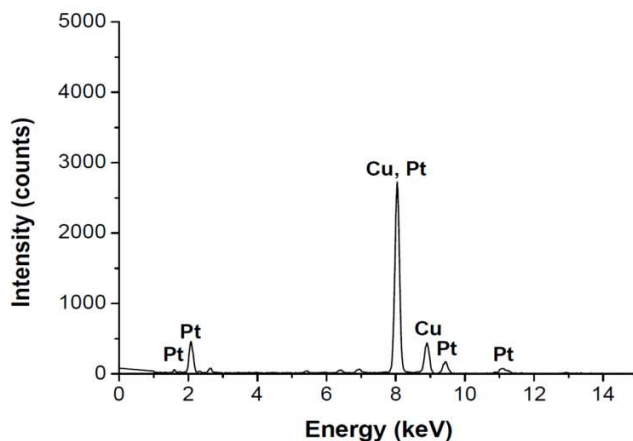
Figure 20 EDS spectrum of **M5.**

Table 2 Electron diffraction pattern of **M5**.

h l k	d_{hlk} (nm)	
	Exper.	Theor.[a]
(111)	0.2200	0.2265
(200)	0.1923	0.1962
(220)	0.1354	0.1387

[a] Data according to American Mineralogist Crystal Structure Database.[249]

3.3.2 PREPARATION AND CHARACTERIZATION OF NICKEL NANOPARTICLES STABILIZED BY IMIDAZOLIUM SALTS CONTAINING HEXADECYL CHAINS **S1A-B**

The chemical reduction of Ni(II) salts with different reducing agents such as $NaBH_4$, $LiEt_3BH$, dimethylaminoborane, hydrazine, etc. is the most commonly reported method for the synthesis of Ni NPs.[44a,95b,96,98,99b] Moreover, Ni NPs can alternatively be obtained by decomposition of $Ni(COD)_2$ in the presence of ionic liquids.[102b,103] This Ni(0) complex has also been used for the obtention of NPs following the *organometallic approach* (Chaudret's method).[45a,104]

---

[249] Downs, R. T., Bartelmehs, K. L., Gibbs, G. V. *American Mineralogist* **1993**, *78*, 1104.

3.3.2.1   ATTEMPTED SYNTHESIS OF NICKEL NANOPARTICLES STABILIZED BY **S1A-B** USING THE BRUST'S METHOD (APPROACH 1)

The Brust's method is a typical procedure for the synthesis of Au NPs stabilized by thiol based ligands in a biphasic medium in the presence of a phase-transfer agent.[21a] We applied first a similar approach for the obtention of Ni NPs as summarized in **Scheme 12**.
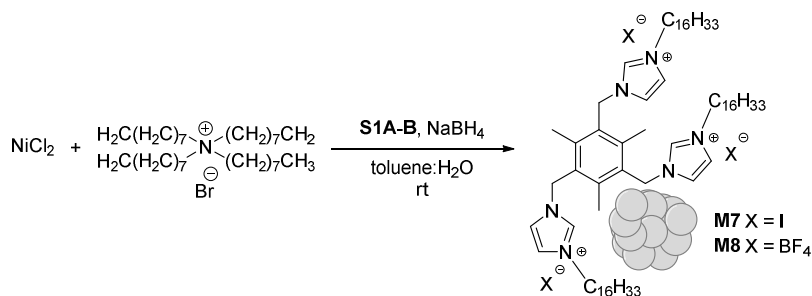
Scheme 12 Modification of Brust's method for the synthesis of Ni NPs.

For the preparation of Ni NPs, the reaction was performed in a biphasic medium consisting in a mixture of toluene (in which the stabilizers where soluble) and water (where the nickel source was soluble). An aqueous solution of $NiCl_2$ was mixed vigorously with a solution of TOAB, as a phase transfer agent, in toluene. Once the two phases have been completely mixed the stabilizer **S1A** or **S1B** was added. Then an aqueous solution of $NaBH_4$ was added dropwise to reduce the Ni(II) species. The reaction mixture became black and was stirred for 3 h at room temperature. After that, the solution was filtered through a nylon membrane (0.46 μm, Millipore) and the aqueous phase was extracted with dichloromethane. After removing the solvent, nanomaterials **M7** and **M8** were obtained as black solids.

Although the obtained solids could be redispersed in organic solvents such as dichloromethane or THF, TEM images showed that the obtained materials consisted in Ni aggregates (> 200 nm of size) (**Figure 21**). Perhaps the phase transfer agent enters in competition with our imidazolium salts as stabilizer. In any case, this method was discarded.
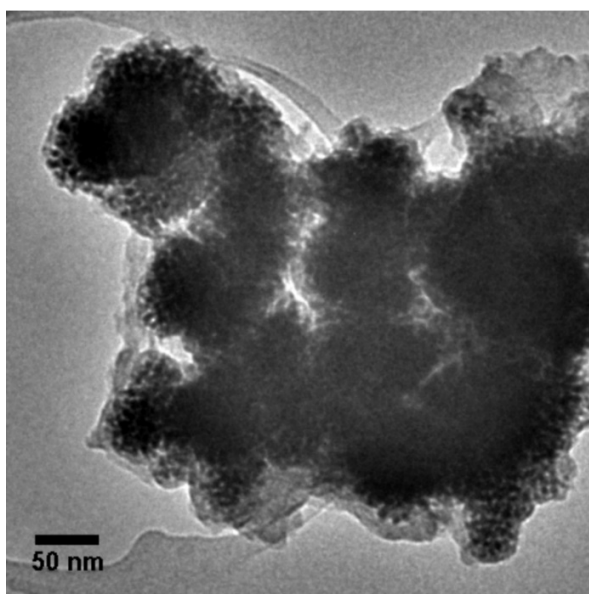
Figure 21 TEM image of material **M7**.

3.3.2.2 ATTEMPTED SYNTHESIS OF NICKEL NANOPARTICLES STABILIZED BY **S1A** FROM NICKEL(II) CHLORIDE IN THF:H$_2$O (APPROACH 2)

In the second approach THF (where the stabilizers are soluble) was used as cosolvent of water in order to avoid the requirement of the phase transfer agent in the reduction of NiCl$_2$ by NaBH$_4$. As a preliminary test in that case only **S1A** was used (**Scheme 13**).
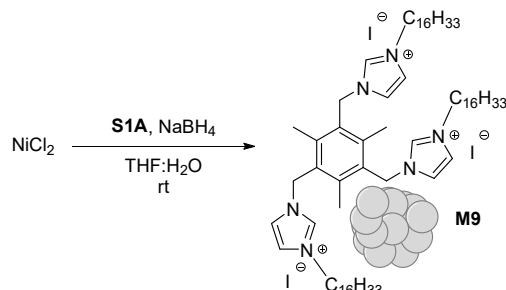
Scheme 13 Second attempted approach for the synthesis of Ni NPs.

In that second approach the nickel precursor, NiCl$_2$, and the stabilizer **S1A** were dissolved in a THF:H$_2$O mixture. Then an aqueous solution of NaBH$_4$ was added dropwise and the reaction mixture became dark. The solution was stirred at room temperature for 3 h. A black precipitate of bulk nickel (**M9**) appeared, remaining the solution colourless.

The low solubility of the stabilizer in water seems to prevent a good interaction between nickel(0) and **S1A** , and, consequently, the formation of stable clusters of Ni NPs.

3.3.2.3 ATTEMPTED SYNTHESIS OF NICKEL NANOPARTICLES STABILIZED BY **S1A** FROM NICKEL(II) ACETYLACETONATE IN THF (APPROACH 3)

The high insolubility of **S1A** and **S1B** in water causes a bad dispersion in the reaction mixture which leads to the precipitation of Ni(0) species as a bulk material. For this reason, a third approach for the synthesis of Ni NPs was attempted in organic medium. Ni(II) acetylacetonate (Ni(acac)$_2$) was used as a nickel source due to its solubility in THF (**Scheme 14**).
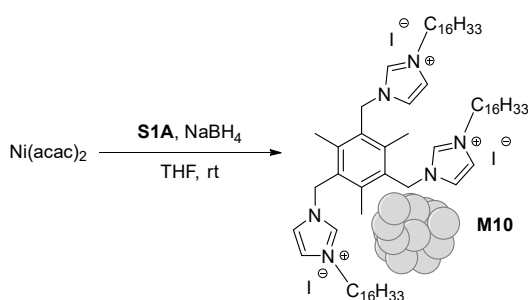
Scheme 14 Third attempted approach for the synthesis of Ni NPs.

A solution of Ni(acac)$_2$ and **S1A** in THF was prepared. A solution of NaBH$_4$ in the minimum amount of water was added dropwise under a vigorous stirring. After the addition of the reductant the solution became black and was stirred at room temperature for one hour. Then a black precipitate of metallic Ni appeared (**M10**), indicating that this was not a suitable procedure for the synthesis of Pt NPs stabilized by **S1A-B**.

3.3.2.4 Synthesis and characterization of nickel nanoparticles stabilized by **S1A** by the organometallic approach or Chaudret's method (approach 4)

After the unsuccessful attempts using $NaBH_4$ as reductant, and inspired by the results previously obtained by our group in the synthesis of Pd NPs with the same ligands,[214a,230] we considered the application of Chaudret's method for the synthesis of Ni NPs.[102b,103, 250] As described previously, that methodology consist in the reduction and subsequent displacement of a ligand from a zerovalent organometallic precursor in the presence of a suitable stabilizer forming the final nanomaterial. In our case, $Ni(COD)_2$ was the Ni(0) precursor chosen for the formation of Ni NPs. The preparation of Ni NPs is summarized in **Scheme 15**.
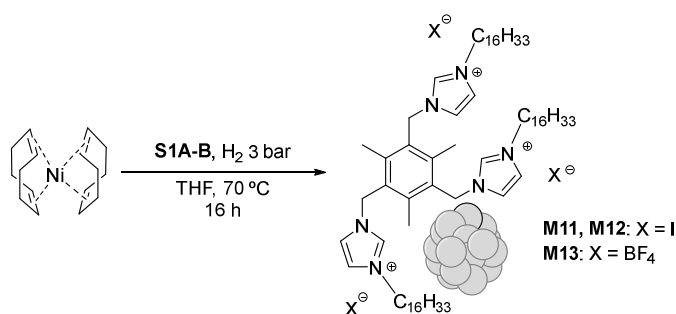
Scheme 15 Synthesis of Ni NPs by Chaudret's method.

A Fischer-Porter apparatus was charged with a solution of $Ni(COD)_2$ and stabilizer **S1A** or **S1B** in THF and a three evacuate-refill process of hydrogen was performed. The resultant solution was stirred overnight at 70 ºC under dihydrogen pressure (3 atm). The reaction mixture underwent a colour change from yellow to black. After that, the solvent was evaporated and the resulting black solid was washed with anhydrous and degassed pentane and then with methanol to remove cyclooctane residues and unreacted free ligand. A magnet was used for the separation of the Ni NPs from the solvent in the process of decantation. Both the isolation and storage process were performed under inert Ar atmosphere in order to prevent the oxidation of Ni(0) species. Finally, Ni NPs were obtained as a magnetic black powder. These NPs were soluble in toluene, THF, dichloromethane and chloroform and insoluble in pentane, diethyl ether, ethyl acetate, methanol and water. Different molar ratios **S1A-B**:$Ni(COD)_2$ used for the synthesis of Ni NPs and the corresponding results are summarized in **Table 3**.

Table 3 Preparation of Ni NPs stabilized by **S1A-B** from the reaction of $Ni(COD)2$ with dihydrogen.[a]

Entry	Stabilizer	S1:Ni[b]	Diameter (nm)[c]	% Ni		Yield[e] (%)	Nanomaterial
				Theoretical	Experimental[d]		
1	**S1A**	0.1:1	10.1 ± 5	30.1	30.7	82	**M11**
2	**S1A**	0.05:1	17.0 ± 6	50.4	48.5	78	**M12**
3	**S1B**	0.1:1	17.2 ± 7	30.9	17.8	36	**M13**

[a] 1.8 mmol $Ni(COD)_2$ in 80 mL THF. [b] Molar ratio. [c] Determined by TEM (500 - 1000 particles measured). [d] Determined by ICP-OES. [e] Based on $Ni(COD)_2$ used.

In contrast to what we had previously observed with Pt NPs, the iodide **S1A** was found to be a more efficient stabilizer than tetrafluoroborate **S1B** for Ni NPs. However, in that case dispersed NPs were obtained with both stabilizers. In the case of **S1A**, two different molar ratios **S1A**:Ni were explored (0.1:1 and 0.05:1) to afford **M11** and **M12,** respectively. When less amount of stabilizer was used (entry 2 of **Table 3**), the particle size and the percentage of Ni in the final material increased. As observed in the TEM images (**Figure 22 (A)**, **(C)**), **M11** and **M12** present well dispersed particles, but with a high variety of shapes and a wide size distribution (**Figure 22 (B)**, **(D)**). For **S1B**, due the worse results, only 0.1:1 **S**:Ni ratio was explored. In that case, the size of particles of the obtained **M13** nanomaterial was 17.2 ± 7 (entry 3 of **Table 3**), a higher value compared with **M11** obtained under the same conditions with **S1A**. TEM images of **M13** (**Figure 22 (E)**, **(F)**) showed some agglomeration of particles in accordance with the lower stabilizing ability of **S1B**. Both the amount of Ni and

250 Fernández, G., Sort, J., Pleixats, R. *ChemistrySelect* **2018**, *3*, 8597.

the yield were lower for that material, a clear indication that some of the metal has been removed in the filtration step (bulk Ni).
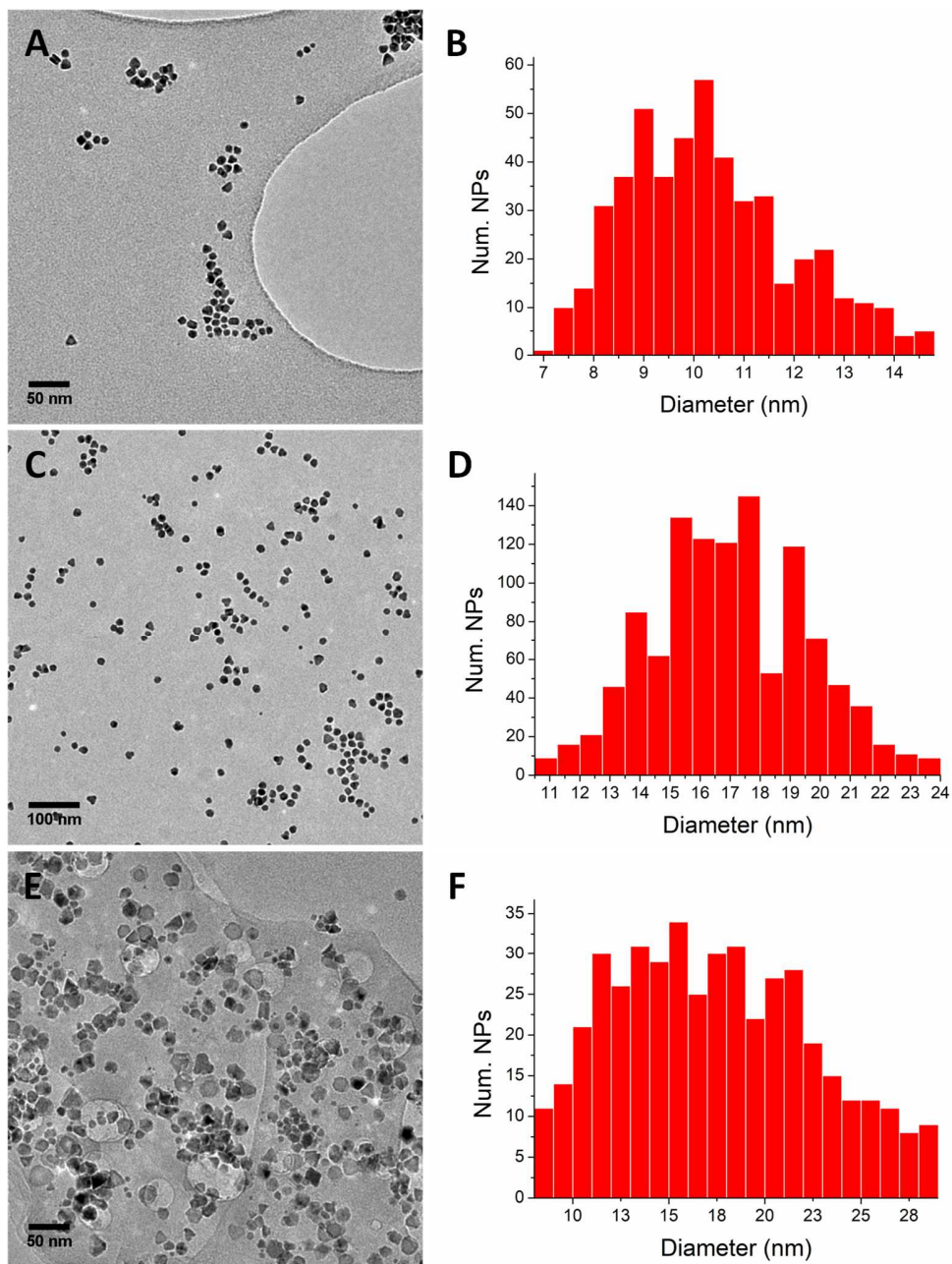
Figure 22 TEM images and particle size distribution of **M11 (A, B)**, **M12 (C, D)** and **M13 (E, F)**.

According to the HRTEM images (**Figure 23**) the obtained Ni NPs presented a high crystallinity. This was also confirmed by the ED analysis for **M11** that showed interplanar distances very close to those expected for an FCC nickel lattice (**Table 4**).
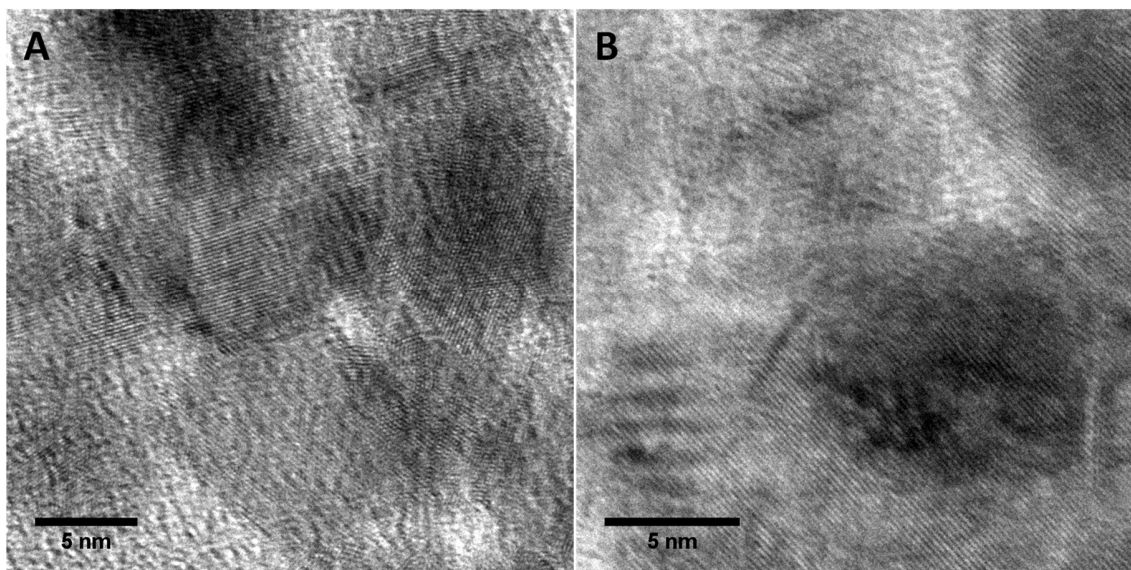
Figure 23 Detail of the crystalline planes observed in HRTEM of **M11 (A)** and **M13 (B)**.

Table 4 Electron diffraction pattern of **M11**.

h l k	d_{hlk} (nm)	
	Exper.	Theor.[a]
(111)	0.2055	0.2035
(200)	0.1741	0.1762
(220)	0.1246	0.1246

[a] Data according to American Mineralogist Crystal Structure Database.[249]

Nickel oxides or hydroxides could be easily formed by the interaction of zerovalent nickel with air atmosphere. However, EDS data of **M12** indicated the presence of nickel but not oxygen in the material (**Figure 24**). This was confirmed by the XPS spectrum of **M12** (**Figure 25**), which presented two main peaks at 852.6 eV (Ni $2p_{3/2}$) and 871.3 eV (Ni $2p_{1/2}$) attributed to Ni(0) species.[251] Additionally, we did not observe relevant signals around 853.7 and 855.6 eV, which would be due to oxide and hydroxide species. All the analyses revealed that no oxides or hydroxide were formed.

[251] a) Jie, Y., Fan, H., You, W. *Colloids Surf A. Physicochem. Eng. Aspects* **2013**, *434*, 194. b) Furstenau, R. P., McDougall, G., Langell, M. A. *Surface Science* **1985**, *150*, 55. c) Metin, O., Özkar, S. *J. Mol. Catal. A: Chem.* **2008**, *295*, 39.
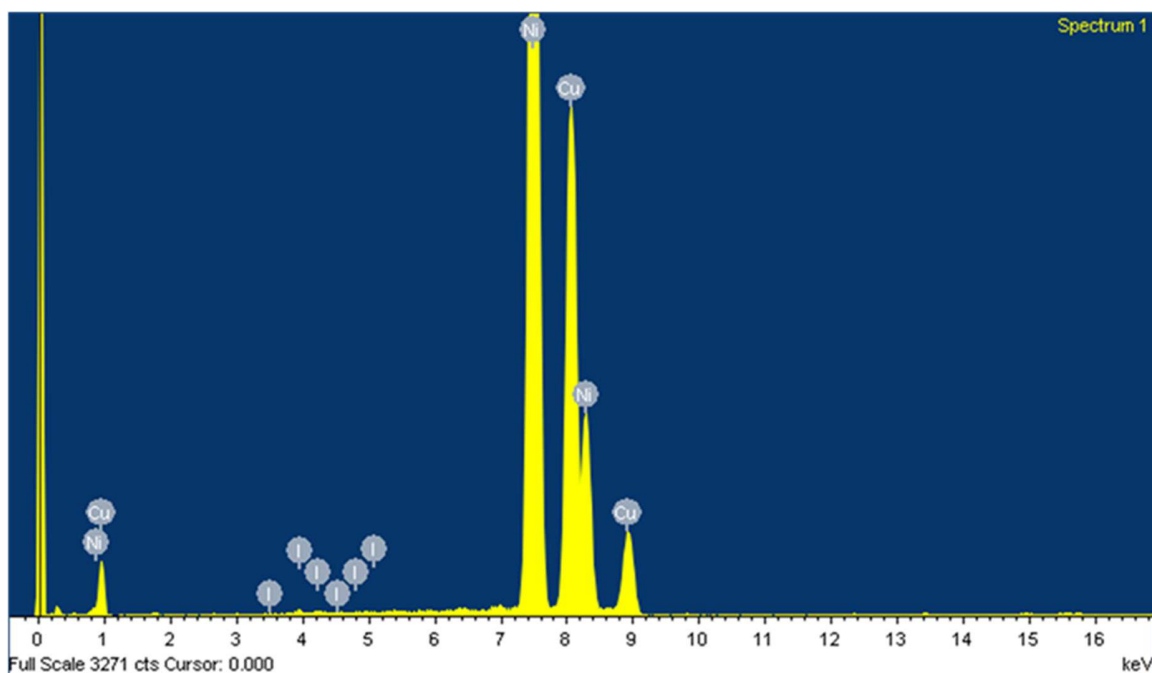
Figure 24 EDS spectrum of **M12**.
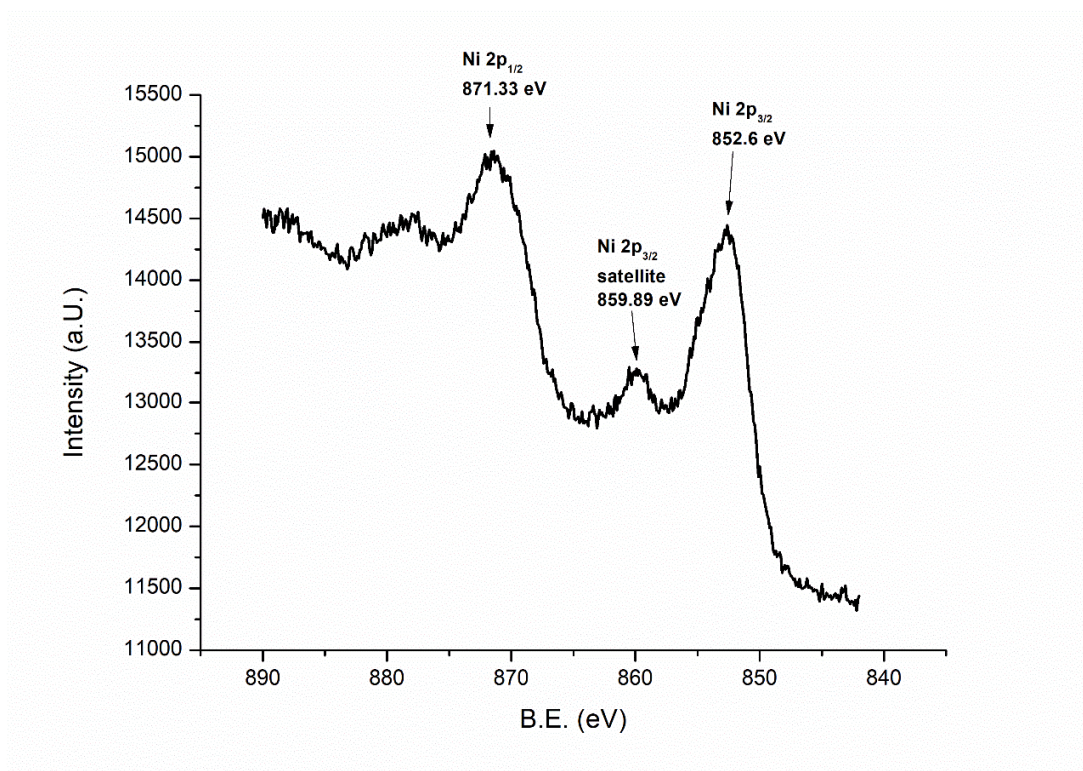
Figure 25 XPS spectrum of **M12** in the Ni 2p region.

Nickel is one of the few elements that present ferromagnetism at room temperature. For this reason, a study of the magnetic properties of the obtained NPs was performed. These properties are depending of the characteristics of the NPs, such as size, morphology, synthetic procedure and support or stabilizer used. The temperature at which the experiments are performed could also affect to the magnetism of the particles.

Chapter 3. Synthesis and Characterization of Metal Nanoparticles

According to the magnetic properties, the NPs can be classified as ferromagnetic, paramagnetic or superparamagnetic.[252]

Two types of measurements were performed for the synthesized NPs, in collaboration with Dr Jordi Sort (Department of Physics, UAB): (i) hysteresis loops at 100 K and 300 K and (ii) zero-field cooled/field cooled (ZFC/FC) curves using an applied field of 50 Oe (**Figure 26**).

Magnetic hysteresis loops consist in the application of an external magnetic field over a sample aligning their atomic dipoles themselves with the external field. An application of an opposite magnetic field will generate a hysteresis loop of the sample. Ferromagnetic materials, such as bulk Ni, maintain a remanent magnetization and coercivity (intensity of a magnetic field necessary to reduce the magnetization of a material to 0) even when the external field was not applied. ZFC/FC curves consist in a change of the temperature over the sample maintaining constant the applied magnetic field. This experiment shows the blocking temperature of the sample. The blocking temperature, which is characteristic of each sample, is the limit temperature at which the material exhibits ferromagnetic behaviour with a remaining magnetization.

The hysteresis loops at 300 K (**Figure 26 (A-C)**) reveal a virtually superparamagnetic behaviour at room temperature, with no coercivity and no remanent magnetization. Conversely, a small but finite coercivity is observed at 100 K for all samples, indicating that they become ferromagnetic upon cooling. The saturation magnetization (M_s) of these NPs (in the range 12 emu/g – 25 emu/g) is lower than the value expected for bulk Ni (where M_s = 55 emu/g at 300 K and 58.6 emu/g at 0 K). Such a decrease of M_s in Ni NPs (compared to the bulk) has been reported[252d] and might be related to the high surface-to-volume ratio of the NPs. The ZFC/FC measurements (**Figure 26 (D-F)**) show that the blocking temperature (T_B) for sample **M11** is around 200 K (as determined from the maximum in M *versus* T in the ZFC curve), whereas for samples **M12** and **M13** is close to room temperature. This is expectable bearing in mind that T_B is defined by $K \cdot Vol = 25 \cdot k_B \cdot T_B$ (where K, k_B and Vol are the anisotropy constant for Ni, the Boltzmann constant and the average volume of the nanoparticles, respectively) and the volume of nanoparticles **M11** is smaller than for nanoparticles **M12** and **M13** (**Table 3**). Remarkably, the superparamagnetic behaviour of these NPs at room temperature is desirable since, due to their negligible remanent magnetization, they do not aggregate once the magnetic field is removed. This is advantageous for the catalytic performance of these particles since interparticle aggregation would cause a decrease of the effective surface area-to-volume ratio.

---

[252] For Ni NPs with ferromagnetic behaviour, see: a) Paredes-García, V., Cruz, C., Toledo, N., Denardin, J., Venegas-Yazigi, D., Castillo, C., Spodine, E., Luo, Z. *New J. Chem.* **2014**, *38*, 837. b) Castillo, C., Seguin, K., Aguirre, P., Venegas-Yazigi, D., Viegas, A. D. C., Spodine, E., Paredes-García, V. *RSC Adv.* **2015**, *5*, 63073. Also ref. 56,97,99b. For Ni Nps with paramagnetic behaviour, see: c) Carenco, S., Noissière, C., Nicole, L., Sánchez, C., Le Floch, P., Mézailles, N. *Chem. Mater.* **2010**, *22*, 1340. Also ref. 95e,103. For Ni NPs with superparamagnetic behaviour, see: d) Chen, D.-H., Hsieh, C.-H. *J. Mater. Chem.* **2002**, *12*, 2412. e) Migowski, P., Teixeira, S. R., Machado, G., Alves, M. C. M., Geshev, J., Dupont, J. *J. Electron Spectrosc. Relat. Phenom* **2007**, *156-158*, 195.
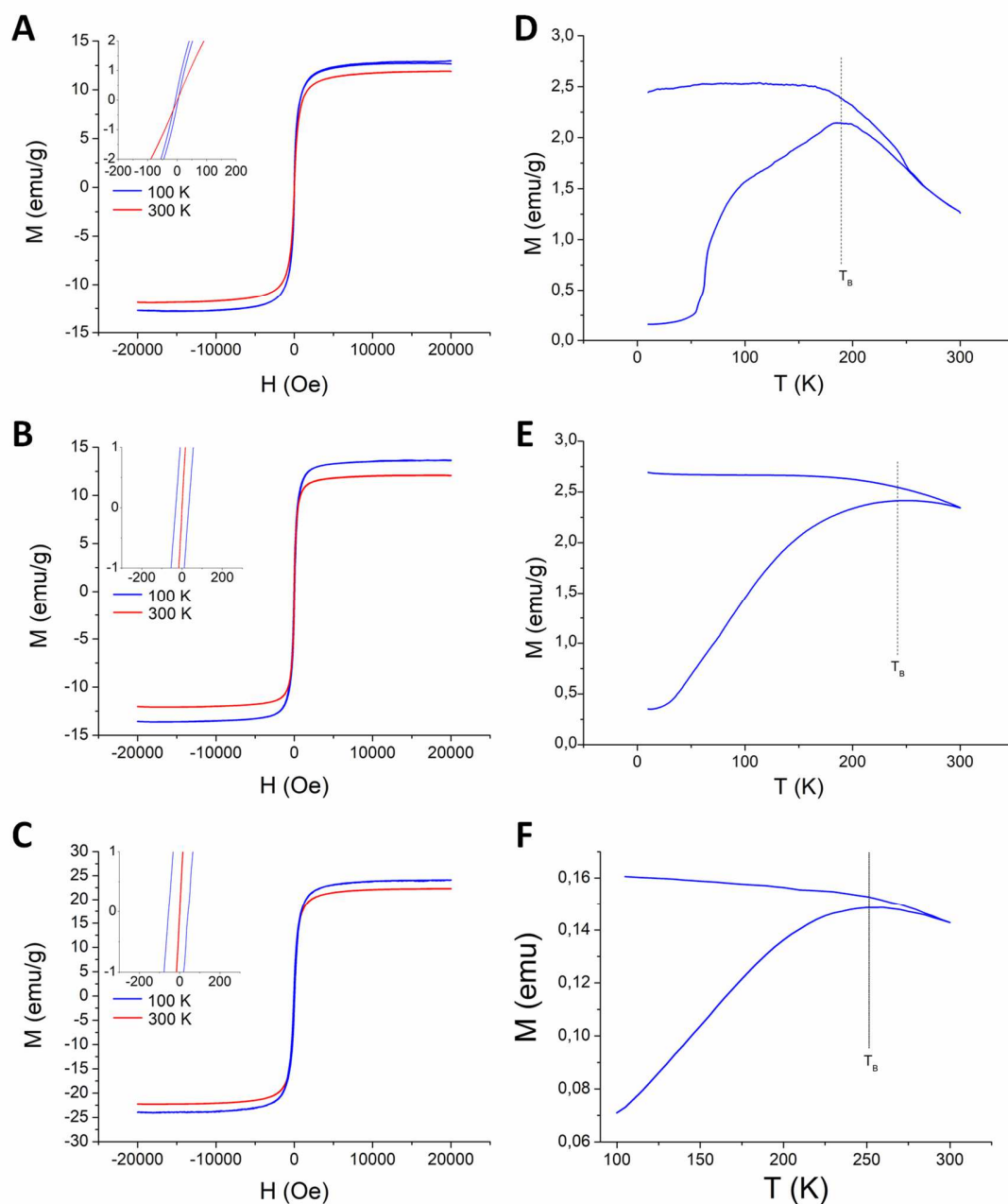
Figure 26 Hysteresis loops at 100 K and 300 K of Ni NPs **(M11-M13) (A-C)** and zero-field cooled/field cooled (ZFC/FC) curves of Ni NPs **(M11-M13) (D-F)**.

3.3.3 PREPARATION AND CHARACTERIZATION OF GOLD NANOPARTICLES STABILIZED BY PEG-TAGGED IMIDAZOLIUM SALTS **S2A-B** AND **S3**

Inspired by the previous results in the group concerning the stabilization of Au NPs by N-rich PEG-tagged ligands,[228] the PEG-tagged imidazolium salts **S2A-B** and **S3** were also designed and prepared for this purpose. Some imidazolium salts had been reported as good stabilizers for Au NPs.[118a,d,g,253] The synthesis of Au NPs stabilized by **S2A-B** and **S3** are summarized in **Scheme 16**.[254]

[253] Thawarkar, S., Thombare, B., Khupse, N. D. *New. J. Chem.* **2017**, *41*, 12989.
[254] Fernández, G., Bernardo López, L., Villanueva, A., Pleixats, R. *New J. Chem.* **2020**, *44*, 6130.
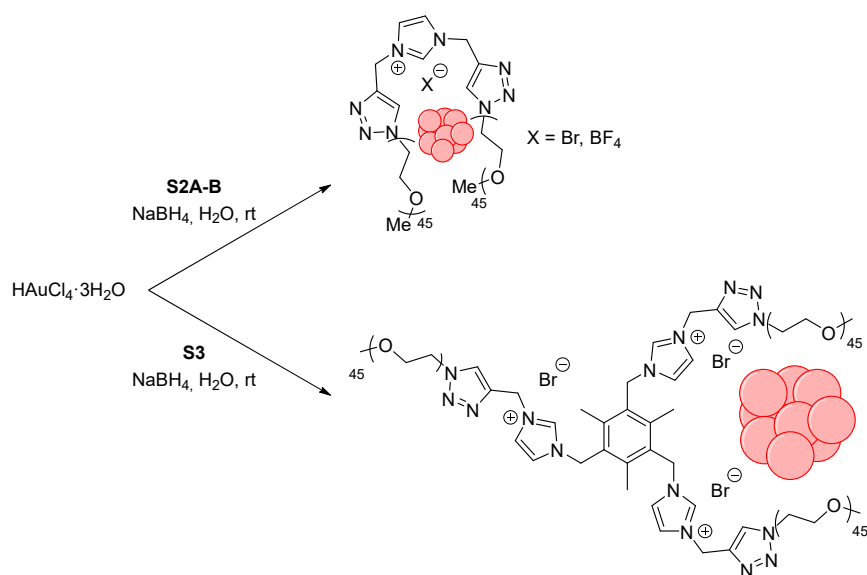
Scheme 16 Synthesis of Au NPs stabilized by **S2A-B** and **S3**.

Gold NPs were prepared by a chemical reduction of tetrachloroauric acid trihydrate with NaBH₄ in water at room temperature in the presence of the corresponding stabilizer. A solution of tetrachloroauric acid and the stabilizer (an **S**:Au molar ratio of 0.3:1 was used, which had been found convenient for other type of PEG-tagged ligands) [228] in degassed water was prepared under a N₂ flow. Upon addition of an excess of NaBH₄ the reaction mixture underwent a colour change from light yellow to dark red. The solution was stirred overnight at room temperature. After filtration of the reaction mixture through a nylon membrane filter (0.45 µm, Millipore), the filtrate was extracted with dichloromethane. Upon removal of the solvent the corresponding nanomaterial was obtained as a dark maroon solid. The obtained NPs were soluble in water, THF, dichloromethane and chloroform and insoluble in diethyl ether and hexane. The results for all the nanomaterials obtained are summarized in **Table 5**.

Table 5 Preparation of Au NPs stabilized by **S2A-B** and **S3**.[a]

Entry	Stabilizer	Diameter (nm)[b]	% Au		Yield[d] (%)	Nanomaterial
			Theoretical	Experimental[c]		
1	**S2A**	5.2 ± 3	11.6	10.9	79	**M14**
2	**S2B**	4.5 ± 2	11.6	9.5	69	**M15**
3	**S3**	5.6 ± 1.5	7.5	6.9	69	**M16**
4[e]	**S3**	3.3 ± 1.4	7.5	8.2	74	**M17**

[a] Molar ratio Au:**S**:NaBH₄ = 1:0.3:6.7; [Au] = 0.6 mM. [b] Determined by TEM (500 - 1000 particles measured). [c] Determined by ICP-OES. [d] Based on amount of HAuCl₄ used. [e] Au:**S**:NaBH₄ = 1:0.3:20.

For Au NPs good results were achieved with the three types of stabilizers. In all cases spherical and well dispersed NPs were obtained in good yield. The presence of gold in the final materials was confirmed by the EDS spectroscopy. As an example, the EDS spectrum for **M15** is given in **Figure 27**. The amount of Au in each nanomaterial was determined by ICP-OES. For materials **M14**, **M15** and **M16** (**Table 5**, entries 1-3) a molar ratio Au:NaBH₄ of 1:6.7 was used and the corresponding TEM images (**Figure 28 (A-F)**) showed the presence of NPs of sizes ranging from 4.5 to 5.6 nm. For material **M17** (**Table 5**, entry 4) a larger excess of reducing agent was used (Au:**S3**:NaBH₄ = 1:0.3:20).
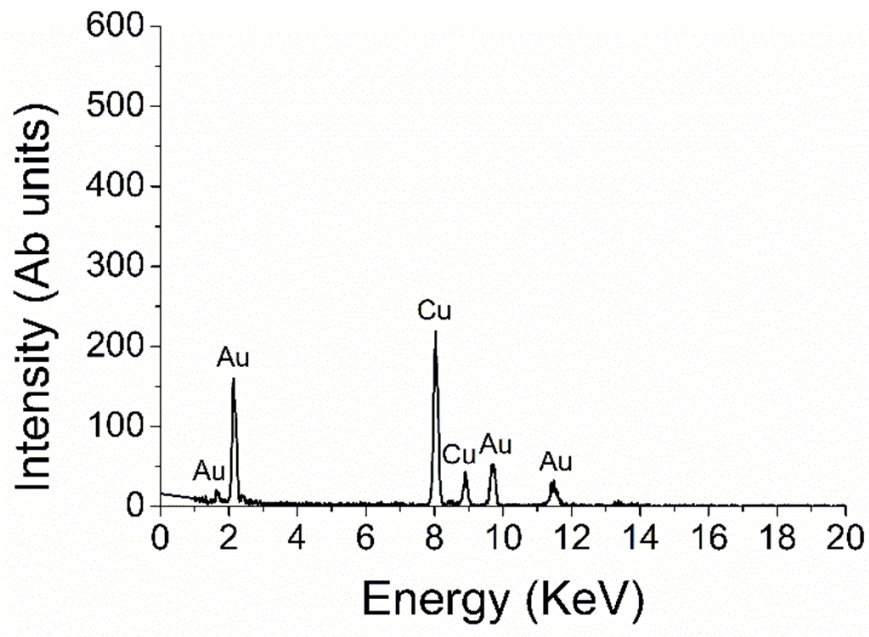
Figure 27 EDS spectrum of **M15**.
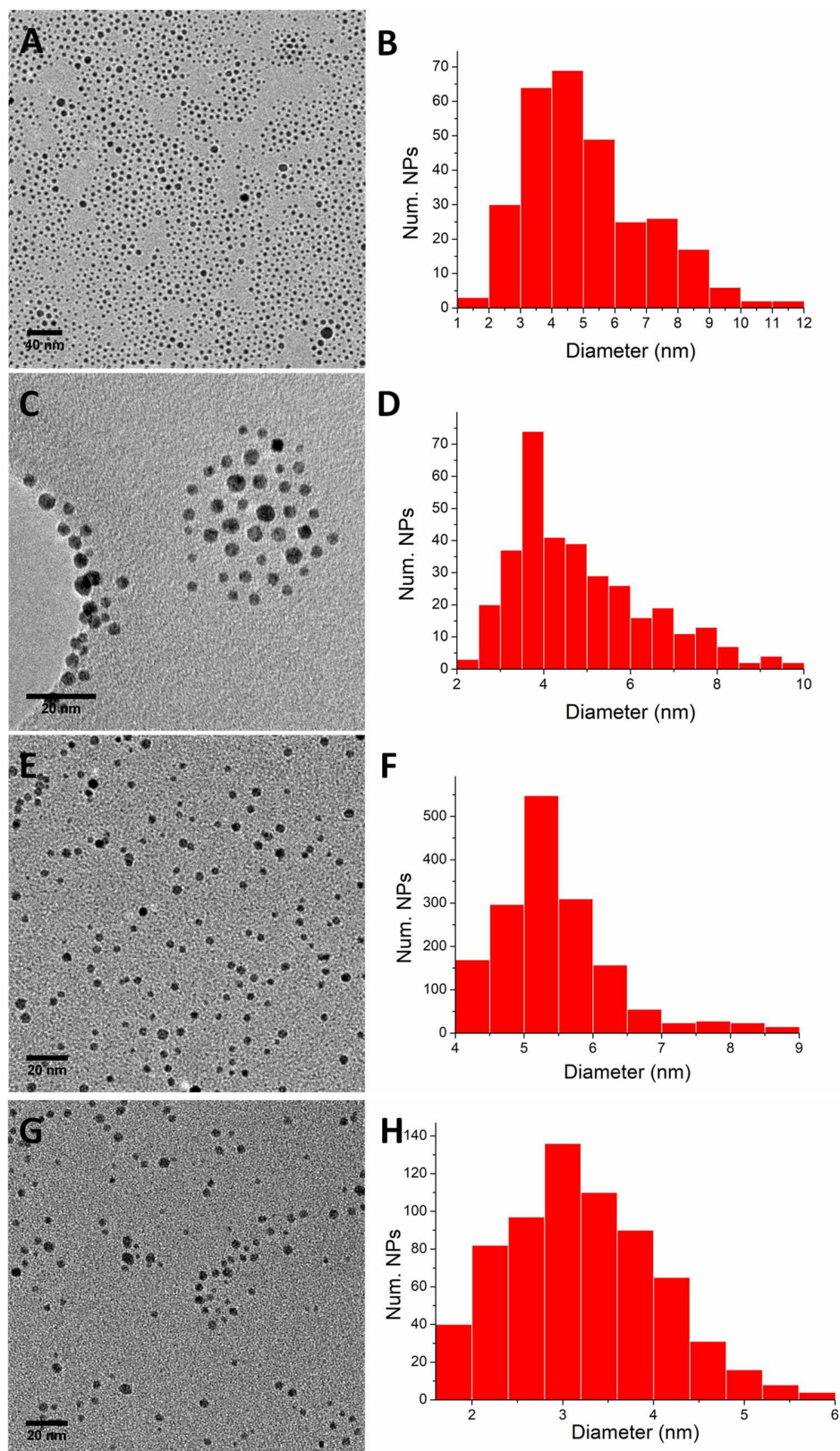
Figure 28 TEM images and particle size distributions of **M14 (A, B)**, **M15 (C, D)**, **M16 (E, F)** and **M17 (G, H)**.

The obtained Au NPs presented a crystalline structure according to the HRTEM images of **M17** (**Figure 29**) in which can be clearly distinguished the crystalline planes. Moreover, the ED for **M15** showed interplanar distances close to those expected for FCC gold lattice (**Table 6**).
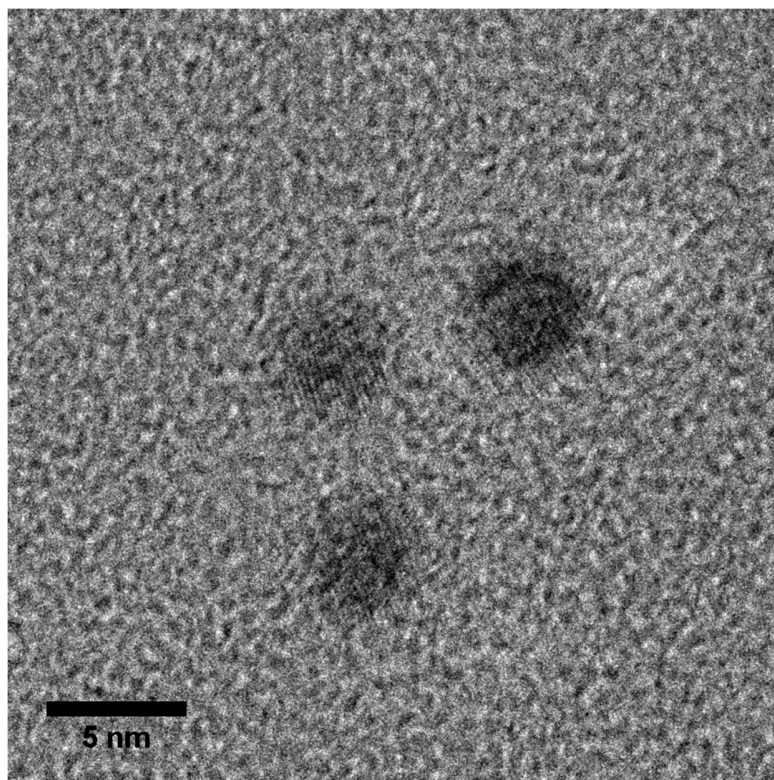
Figure 29 HRTEM image of **M17**.

Table 6 Electron diffraction pattern of **M15**.

h l k	d_{hlk} (nm)	
	Exper.	Theor.[a]
(111)	0.2293	0.2355
(200)	0.2040	0.2040
(220)	0.1426	0.1442
(311)	0.1203	0.1230

[a] Data according to American Mineralogist Crystal Structure Database.[249]

All those results suggested the formation of crystalline Au(0) NPs. However, the XPS of the materials (**M14** - **16**) in the Au 4f region indicated a mixture of two valence states of gold. Taking **M16** as an example, the spectrum exhibited a doublet at 83.8 and 87.5 eV for the Au $4f_{7/2}$ and Au $4f_{5/2}$ respectively, corresponding to Au(0).[77,117,204,255] Additionally, another doublet was observed at 85.1 and 88.8 eV attributed to $4f_{7/2}$ and $4f_{5/2}$ of Au(I) species.[204] We considered the possibility that all of the Au(III) species from $HAuCl_4$ were not completely reduced, although an excess of $NaBH_4$ was used. For this reason, a similar experiment, but adding a much higher amount of reductant, was performed, as mentioned before, to obtain **M17** (**Table 5**, entry 4).[118g] This experiment gave smaller crystalline Au NPs, according to TEM and HRTEM images (**Figure 28 (G**, **H)** and **Figure 29**) with a slightly higher percentage of Au in the final material. Unfortunately, XPS spectrum of **M17** (**Figure 30 (D)**) was similar to that of **M16** (**Figure 30 (C)**) and displayed signals of Au(0) and Au(I) species. Even, a slightly higher intensity of Au(I) doublet with respect to Au(0) doublet was observed. In contrast, according to

[255] Panwar, V., Jain, S. L. *Mater. Sci. Eng. C* **2019**, *99*, 191.

XPS spectra of **M14** and **M15** (**Figure 30 (A**, **B)**) both Au species were present, but Au(0) predominated for these materials.
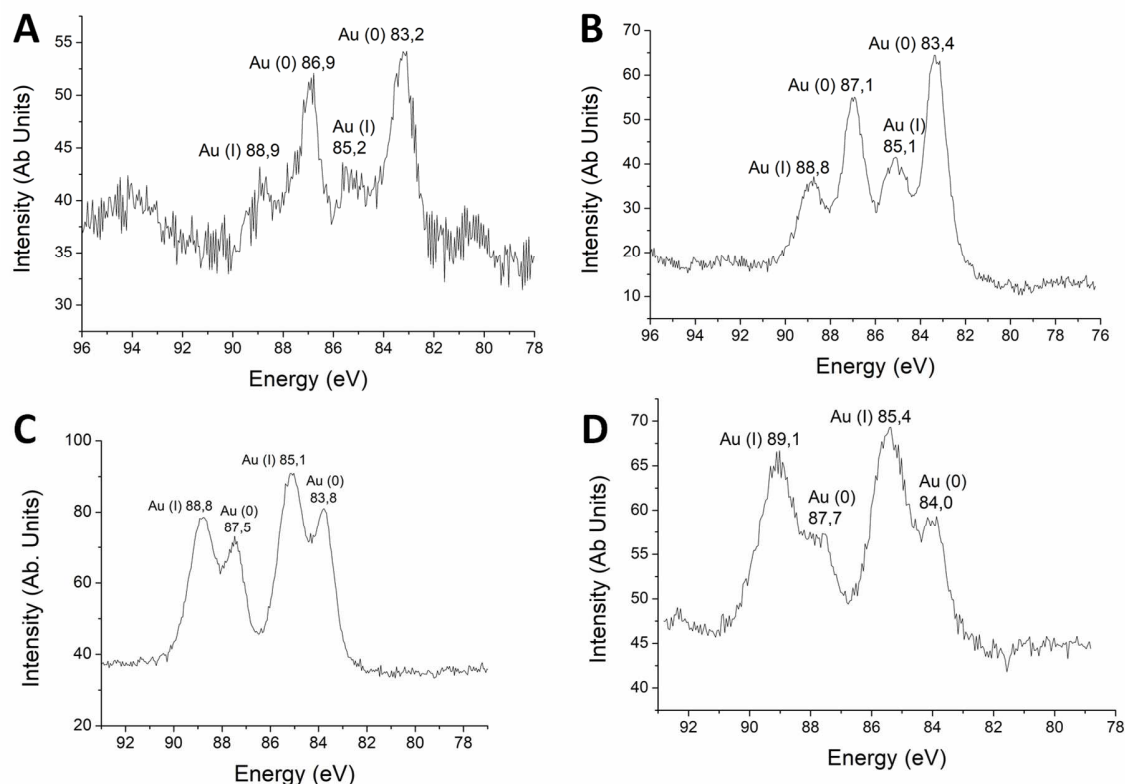
Figure 30 XPS spectra in the Au 4f region of **M14 (A)**, **M15 (B)**, **M16 (C)** and **M17 (D)**.

After the surprising observation of Au(I) species in the XPS spectra alternative explanations should arise. The first possible option is the formation of an oxidized layer in the surface of the Au NPs. It has been described that the surface of some metal NPs stabilized by imidazolium ionic liquids is more susceptible to oxidation in air rather than the bulk material, enhancing the stability of the particles.[256] Another option is the formation of Au(I) NPs, species which have been described to be formed *in situ* from Au(III) complex in a catalytic A[3] coupling reaction.[204] Another possibility is the generation of a Au(I) complex NHC-Au-X through deprotonation of the acidic hydrogen at the C2 position of the imidazolium moiety by a hydride anion of the reducing agent used in excess. The resulting NHC ligand would coordinate to Au(I) intermediate derived from partial reduction of the Au(III) present in the HAuCl$_4$ precursor. Although NaBH$_4$ has been reported by some authors to reduce NHC-Au(I) complexes to the corresponding NHC-stabilized Au NP,[119a,b] a recent article[119c] describes the presence of Au(0) and Au(I) species by XPS after treatment of an NHC-Au-Cl complex with excess of this reducing agent (20 mol-equiv.). In that case, the values of Au 4f signals for the NHC-Au-Cl complex and the formed NHC-Au(I) NPs do not differ significantly. However, as they could not detect a significant amount of Cl by XPS, they discard the presence of the complex. Finally, even though the exact nature of the material remains unsolved, they postulate a structure consisting in an Au(0) core surrounded by a layer of Au(I) species

At that point, we decided to perform additional XPS measurements (Cl, Br and N) of the stabilizers and the final materials. In that way Cl signals were detected in **M16** (**Figure 31 (A)**) possibly coming from the tetrachloroauric acid precursor. Notably, for **M17** we did not observe the presence of Cl (**Figure 31 (B)**). The presence of Br could not be clearly identified by XPS neither in the nanomaterials **M14-17** nor in the stabilizers **S1A-B** and **S3**, probably due to the low percentage of this element in the high molecular weight stabilizers. On the other hand, XPS of the N 1s has been claimed to evidence the formation of NHC-capped Au(0)

---

[256] a) Migowski, P., Dupont, J. *Chem. Eur. J.* **2007**, *13*, 32. b) Ott, L. S., Finke, R. G. *Inorg. Chem.* **2006**, *45*, 8382.

nanoparticles from the reduction of imidazolium-AuX$_4$ salts with NaBH$_4$ (a shift from 401.6 eV for imidazolium bromide to 400.2 eV for the Au NPs capped by NHC).[120c] In our case, the N 1s photopeaks were very weak and the smaller differences in the positions of the signals makes it difficult to draw conclusions.
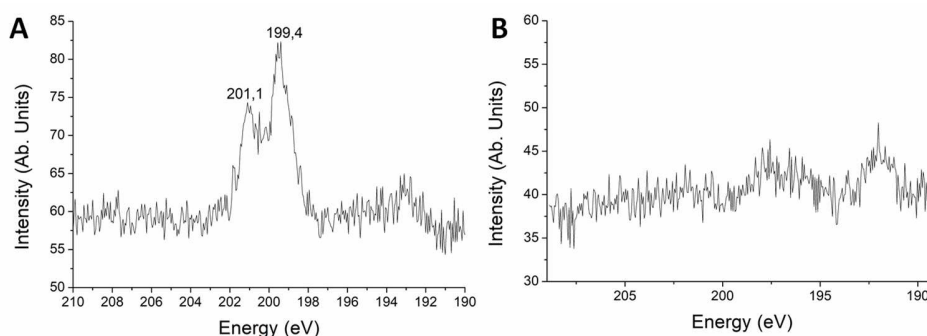
Figure 31 XPS spectra in the Cl 2p region for **M16 (A)** and **M17 (B)**.

On the other hand, the effect of the counter-anion was evident in the appearance of the ^{1}H NMR spectra of the gold nanoparticles. Thus, for **M14**, **M16** and **M17** (in which the counter-anion of the stabilizer is Br) only the signals from the methyl and methylene groups of the PEGylated chains were clearly observed. In contrast, the ^{1}H NMR spectrum of **M15** (with the tetrafluoroborate salt as stabilizer, **Figure 32 (A)**) presented all the absorptions of the free stabilizer (**Figure 32 (B)**), including the proton at C2 of the imidazolium ring at 9.12 ppm, but the other signals of imidazole, triazole and the methylene group between both rings were splitted. The broadening and disappearance of absorptions of some protons would be in line with a stronger stabilizer-metal surface interaction in the case of bromide salts.[257] This indicates that the heterocycle is close to the surface of the metal. Although it seems clear that for the tetrafluoroborate **S2B** the imidazolium salt is the responsible of the stabilization, for the bromides **S2A** and **S3** the two possibilities of coordination between the stabilizers and metal, carbene or imidazolium, remain open. A similar phenomenon of counter-anion effect was previously observed in the group for Pd NPs stabilized with **S1A-B**.[214a]
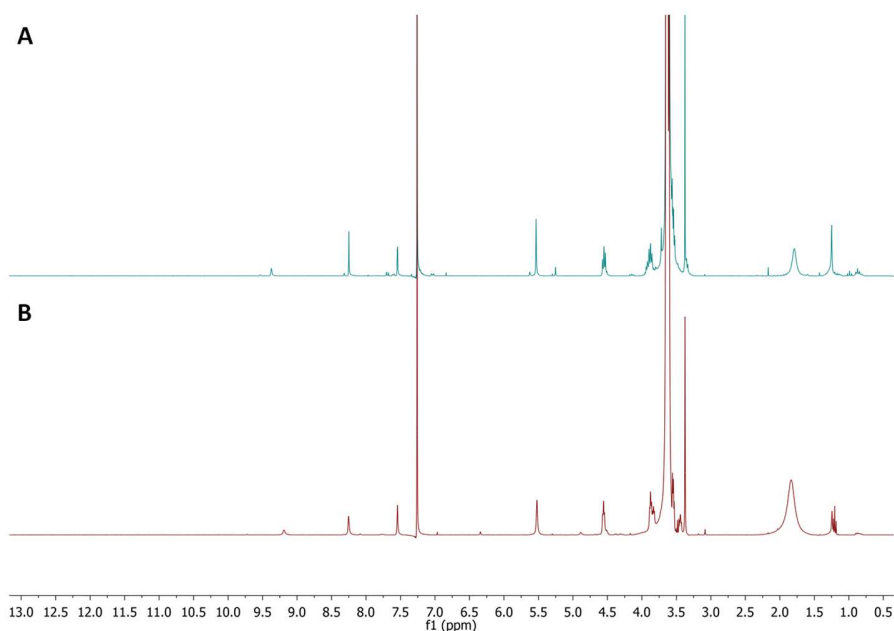
Figure 32 Comparison of ^{1}H NMR spectra of **M15 (A)** and **S2B (B)**.

---

[257] Pan, C., Pelzer, K., Philippot, K., Chaudret, B., Dassenoy, F., Lecante, P., Casanove, M.-J. *J Am. Chem. Soc.* **2001**, *123*, 7584.

Chapter 3. Synthesis and Characterization of Metal Nanoparticles

In the UV-Vis spectra of all the Au NPs, we observed the appearance of a broad shoulder (centered at 526, 519 and 519 nm for **M14**, **M15** and **M16**, respectively) representing the localized surface plasmon resonance (LSPR) band (**Figure 33**).

Thus, after the analysis of all the characterization data, the formation of a mixture of Au(I) and Au(0) NPs seems more likely in our case, but we cannot rule out the presence of a certain amount of Au-NHC-Cl complex in **M16** (observation of Cl in the XPS spectrum, **Figure 31**).
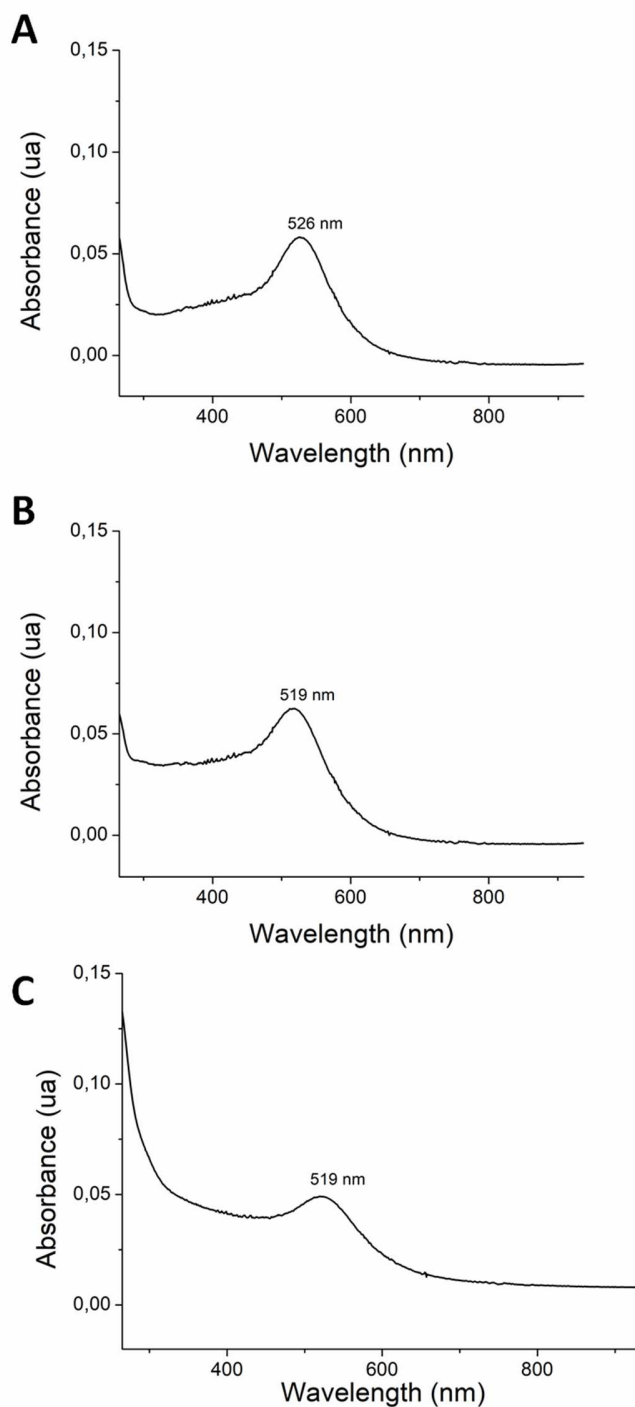
Figure 33 LSPR band in the UV-Vis spectra of **M14 (A)**, **M15 (B)** and **M16 (C)**.

3.3.4 PREPARATION AND CHARACTERIZATION OF RHODIUM NANOPARTICLES STABILIZED BY PEG-TAGGED IMIDAZOLIUM SALTS **S2A-B** AND **S3**

Inspired by the previous results in the group concerning the stabilization of Rh NPs by N-rich PEG-tagged ligands,[214e] the PEG-tagged imidazolium salts **S2A-B** and **S3** were also used for that purpose. Most of the few cases of Rh NPs stabilized by imidazolium salts reported in the literature consist in suspensions of Rh(0) nanoparticles in imidazolium ionic liquids.[258] We performed the synthesis of Rh NPs stabilized by **S2A-B** and **S3** as summarized in **Scheme 17**.
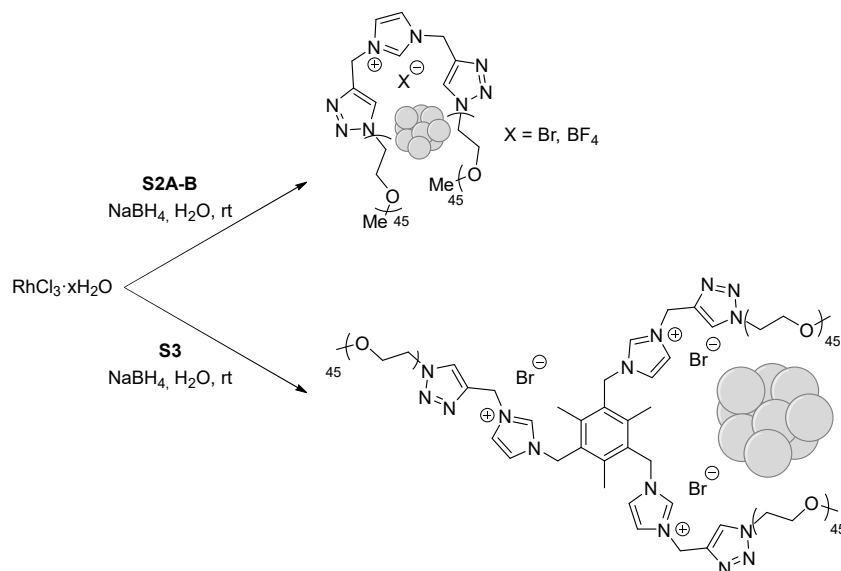
Scheme 17 Synthesis of Rh NPs stabilized by **S2A-B** and **S3**.

As for the synthesis of gold nanoparticles, we also used the chemical reduction method for the obtention of Rh NPs. In that case, the Rh(III) source was hydrated rhodium trichloride and the reductant was $NaBH_4$ in water at room temperature. Thus, a solution of $RhCl_3 \cdot 3H_2O$ and the corresponding stabilizer (**S**:Rh molar ratio of 0.02:1, which was found convenient for other type of PEG-tagged ligands[214e]) in degassed water was prepared under a N_2 flow. Upon addition of an excess of $NaBH_4$ the reaction mixture underwent a colour change from orange to blackish. The solution was stirred overnight at room temperature. After filtration of the reaction mixture through a nylon membrane filter (0.45 µm, Millipore), the filtrate was extracted with dichloromethane. Upon removal of the solvent the corresponding nanomaterial was obtained as a black solid that was stored under inert atmosphere to prevent the oxidation. The obtained NPs were soluble in water, THF, dichloromethane and chloroform and insoluble in diethyl ether and hexane. The results of the different experiments are summarized in **Table 7**. An excess of sodium borohydride was employed (from 14 to 18 mmol per mmol of Rh).

Table 7 Preparation of Rh NPs stabilized by **S2A-B** and **S3**.

Entry	Stabilizer	**S**:Rh:NaBH$_4$	[Rh] (mM)	Diameter (nm)[a,b]	% Rh Theoretical	% Rh Experimental[c]	Yield[d] (%)	Nanomaterial
1	**S2A**	0.019:1:14	1	2.9 ± 3	30.3	31.7	40	**M18**
2	**S2B**	0.019:1:14	1	3.3 ± 2	30.3	29.9	27	**M19**
3	**S3**	0.025:1:18	0.8	5.6 ± 3	24.2	27.4	41	**M20**

[a] Determined by TEM (500 - 1000 particles measured). [b] Bigger aggregates of small particles were also formed in entries 2 and 3. See text and **Figure 34**. [c] Determined by ICP-OES. [d] Based on $RhCl_3 \cdot xH_2O$ (40% wt Rh) used.

Previous work developed in our group showed the tendency of small Rh NPs to form flower-like aggregates.[214e] This was also the result observed for **M19** and **M20**. These materials presented well dispersed small Rh

[258] a) Mu, X.-d., Meng, J.-q., Li, Z.-C., Kou, Y. *J. Am. Chem. Soc.* **2005**, *127*, 9694. b) Stratton, S. A., Luska, K. L., Moores, A. *Catal. Today* **2012**, *183*, 96. c) Serrano-Maldonado, A., Rozenel, S. S., Jimenez-Santiago, J. L., Guerrero-Ríos, I., Martin, E. *Catal. Sci. Technol.* **2018**, *8*, 4373. d) Jiang, H.-y., Cheng, H.-m., Bian, F.-x. *Catal. Lett.* **2019**, *149*, 1975.

Chapter 3. Synthesis and Characterization of Metal Nanoparticles

NPs of 3.3 and 5.6 nm together with flower-like aggregates around 33 and 21 nm, respectively (entries 2 and 3 of **Table 7**, **Figure 34 (C**, **E)**). Surprisingly, these aggregates were much smaller (around 14 nm) and less abundant for **M18** which principally presented small particles of 2.9 ± 3 nm (entry 1 of **Table 7**, **Figure 34 (A)**). The yields for Rh NPs based on the amount of initial rhodium were moderate (from 27% for the tetrafluoroborate **S2B** to 40 and 41% for the bromides **S2A** and **S3**), showing that the stabilizing ability of these PEG-tagged imidazolium salts for rhodium nanoparticles was lower than in the case of gold. The presence of Rh in the materials was confirmed by the EDS spectra (**Figure 35**) and the amount of Rh was determined by ICP-OES (**Table 7**).
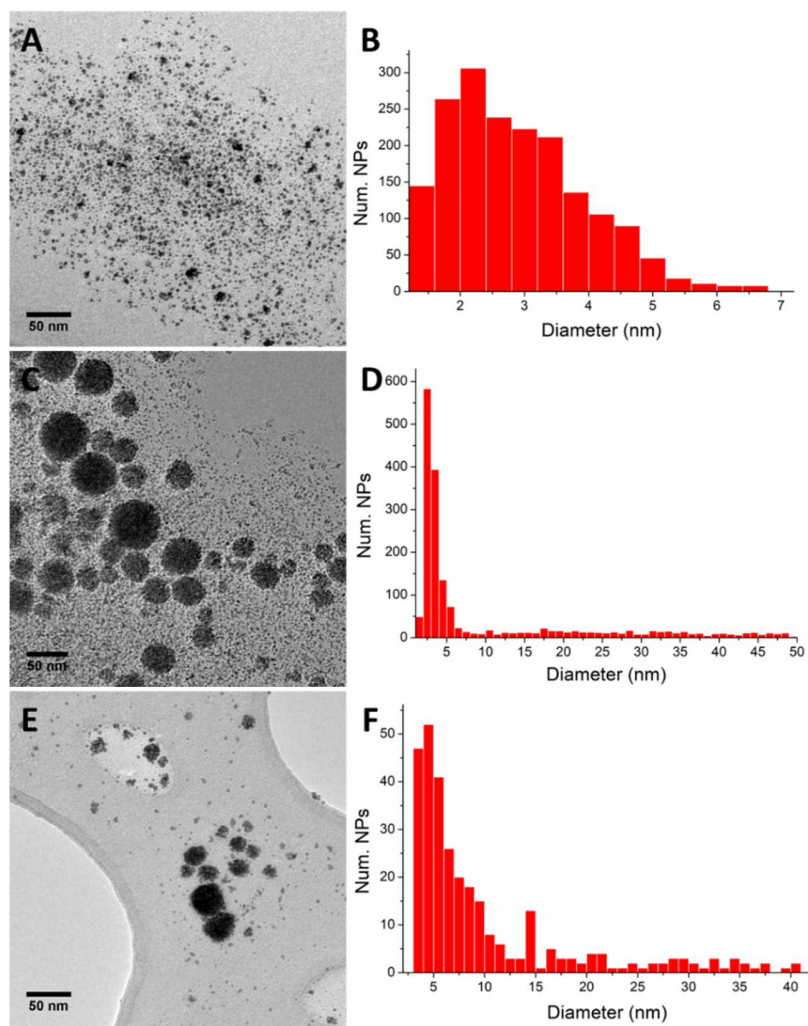
Figure 34 TEM images and particle size distributions of **M18 (A, B)**, **M19 (C, D)** and **M20 (E, F)**.
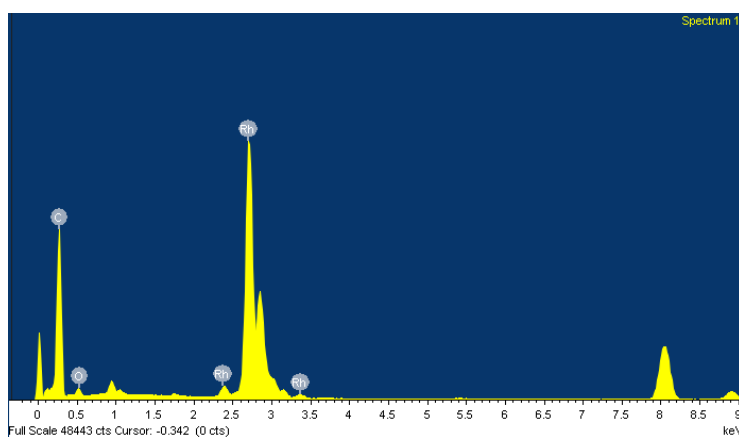
Figure 35 EDS spectrum of **M20**.

HRTEM images of **M20** (**Figure 36**) showed clearly the crystalline planes of the Rh NPs. This was consistent with the ED analysis (**Table 8**) which confirmed interplanar distances in accordance with FCC Rh(0) lattice.
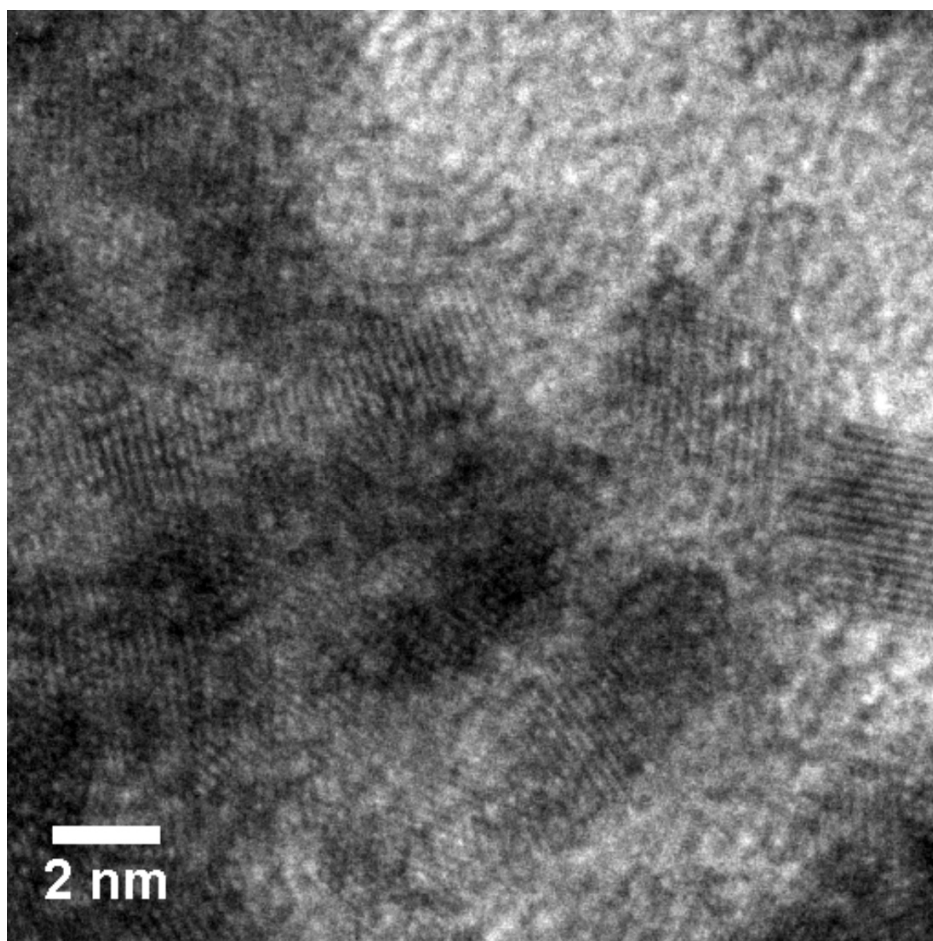
Figure 36 HRTEM image of **M20**.

Table 8 Electron diffraction pattern of **M20**.

h l k	d_{hlk} (nm)	
	Exper.	Theor.[a]
(111)	0.2186	0.2196
(200)	0.1907	0.1902
(220)	0.1340	0.1345
(311)	0.1157	0.1147

[a] Data according to American Mineralogist Crystal Structure Database.[249]

In order to discard the presence of oxidized rhodium species, the nanoparticulated materials **M18-20** were analysed by XPS spectroscopy (**Figure 37**). The doublet at 307.7 and 312.5 eV for Rh $3d_{5/2}$ and Rh $3d_{3/2}$ in **M19**

(**Figure 37 (B)**) corresponded clearly to Rh(0) species[259] We did not observe any peak at 308.8 eV that could be attributed to rhodium oxide binding energy.[260]
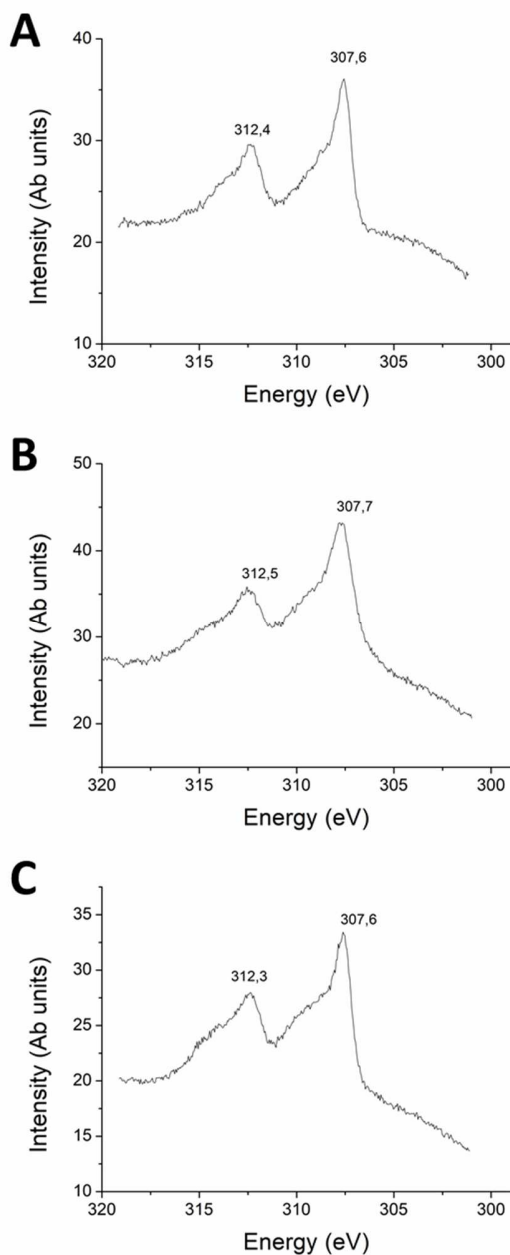
Figure 37 XPS spectra in the Rh 3d region of **M18 (A)**, **M19 (B)** and **M20 (C)**.

[259] Yao, Q., Lu, Z.-H., Jia, Y., Chen, X., Liu, X. *Int. J. Hydrogen Energy* **2015**, *40*, 2207. b) Gopiraman, M., Saravanamoorthy, S., Ullah, S., Ilangovan, A., Kim, I. S., Chung, I. M. *RSC Adv.* **2020**, *10*, 2545.
[260] Liu, C., Zhang, J., Liu, H., Qiu, J., Zhang, X. *Ind. Eng. Chem. Res.* **2019**, *58*, 21285.

3.4   CONCLUSIONS

New water-soluble imidazolium salts (bromide **S2A**, tetrafluoroborate **S2B**, and bromide **S3**) bearing long polyoxyethylenated chains have been synthesized. Imidazolium moieties and PEG chains were linked via a triazole ring obtained by a copper-catalyzed [2+3] cycloaddition between alkynes and azides (CuAAC reaction).

Platinum(0) NPs (1.6 nm) stabilized by tris-imidazolium tetrafluoroborate **S1B** containing hexadecyl chains have been successfully obtained in a two-step process involving the reduction of chloroplatinic acid with EG/NaOH at 160°C and subsequent treatment with a THF solution of **S1B** at room temperature. They have been fully characterized by TEM, HRTEM, ED, EDS and ICP-OES. Tris-imidazolium iodide **S1A** containing hexadecyl chains failed as stabilizer in the preparation of Pt NPs using an analogous procedure.

On the other hand, magnetic nickel(0) nanoparticles stabilized by tris-imidazolium iodide **S1A** and tetrafluoroborate **S1B** have been prepared by the hydrogenation (3 bar H_2) of $Ni(COD)_2$ at 70°C (*organometallic approach* or Chaudret's method) in the presence of these salts. The iodide **S1A** was found to be better stabilizer than the tetrafluoroborate **S1B**. Ni NPs have been characterized by TEM, HRTEM, ED, EDS, XPS, ICP-OES. A study of their magnetic properties was performed (hysteresis loops and ZFC/FC). Remarkably, they presented superparamagnetic behaviour at room temperature. This is a desirable property since, due to their negligible remanent magnetization, they do not aggregate once the magnetic field is removed. This is advantageous for the catalytic performance of these particles since interparticle aggregation would cause a decrease of the effective surface area-to-volume ratio.

Both Pt and Ni NPs are soluble in toluene, THF, dichloromethane and chloroform, and insoluble in pentane, diethyl ether, methanol and ethyl acetate.

Gold and rhodium NPs stabilized by PEG-tagged imidazolium salts (bromide **S2A,** tetrafluoroborate **S2B** and bromide **S3**) have been prepared. All these nanoparticles are soluble in water and insoluble in diethyl ether.

Gold NPs have been obtained by reduction of tetrachloroauric acid with $NaBH_4$ in the presence of the stabilizer in water at room temperature. Gold nanomaterials have been characterized by TEM, HRTEM, EDS, ED, XPS, UV-Vis and ICP-OES. XPS spectra showed the presence of two valence states of gold corresponding to Au(0) and Au(I) species, being the oxidized form the major one in the nanomaterials derived from **S3**. A stronger interaction between the imidazolium ring and the metal surface in the case of bromides **S2A** and **S3** was suggested according to the ^{1}H NMR spectra of the corresponding gold nanoparticles.

Rhodium(0) NPs have been prepared by reduction of Rh(III) chloride with $NaBH_4$ in water at room temperature in the presence of the corresponding stabilizer. Rh nanomaterials have been completely characterized by TEM, HRTEM, EDS, ED, XPS and ICP-OES.

3.5 EXPERIMENTAL SECTION

3.5.1 GENERAL REMARKS

Commercial reagents were used directly as received. Milli-Q water and HPLC grade solvents were used in the preparation and purification of products. All NMR spectra were recorded with Bruker Avance DRX-250 (250 MHz for ^{1}H), Bruker Avance DPX-360 MHz (360 MHz for ^{1}H) and Bruker Avance III 400SB (400 MHz for ^{1}H) spectrometers. ICP-OES measurements of metal content were carried out at the Servei d'Anàlisi Química of the Universitat Autònoma de Barcelona with a Perkin-Elmer instrument, model Optima 4300DV. TEM, ED and EDS analyses were performed at the Servei de Microscòpia of the Universitat Autònoma de Barcelona, with a JEOL JEM-2011 model instrument operating at 200 kV. The nanoparticle sizes were determined by measuring 500-1000 particles using ImageJ (Fiji) program and were subsequently averaged to produce the mean NP diameter. High resolution mass spectra were performed at the Servei d'Anàlisi Química of the Universitat Autònoma de Barcelona using a Bruker Daltoniks MicroTOFQ spectrometer (Bremen, Germany) equipped with an ESI inlet. Absorption spectra were recorded on an Agilent 8453 spectrophotometer by using 1 cm thick quartz cuvettes. XPS measurements were performed with a Phoibos 150 analyzer (SPECS GmbH, Berlin, Germany)) in ultra-high vacuum conditions (base pressure 5E-10 mbar) with a monochromatic aluminium Kalpha x-ray source (1486.74 eV); the energy resolution as measured by the FWHM of the Ag $3d_{5/2}$ peak for a sputtered silver foil was 0.58 eV. Hysteresis loops were recorded at T = 100 K and 300 K in a SQUID magnetometer (Quantum Design MPMS-XL7) with a maximum applied magnetic field of 20 kOe. Zero-field-cooled/field-cooled (ZFC/FC) curves were also recorded in the SQUID magnetometer in the temperature range 5 K – 300 K applying a magnetic field of 50 Oe.

3.5.2 SYNTHESIS OF 1,3,5-TRIS(IMIDAZOLE-1-YLMETHYL)-2,4,6-TRIMETHYLBENZENE **1**[244]

1
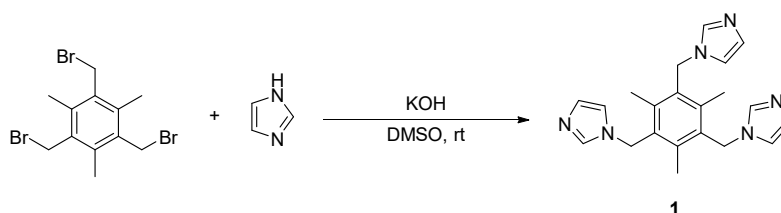
1H-imidazole (1.09 g, 16.1 mmol) and KOH (3.67 g, 65.17 mmol) were dissolved in 40 mL of DMSO and the solution was stirred for 2h at room temperature. Then 1,3,5-tris(bromomethyl)-2,4,6-trimethylbenzene (2.00 g, 5.01 mmol) was added. After stirring for another 3 h at room temperature, an equivalent volume of water was added, and the mixture was extracted with $CHCl_3$ (4 x 30 mL), dried over anhydrous Na_2SO_4 and filtered. Solvent was partially removed under vacuum and diethyl ether was added to the residue. A white powder precipitated, which was filtered and washed with diethyl ether. The solid was then recrystalized from dichloromethane-diethyl ether, affording compound **1** as a white solid, (1.26 g; 70%). ^{1}H NMR (250 MHz, $CDCl_3$) δ (ppm): 7.31 (s, 3H), 7.06 (s, 3H), 6.74 (s, 3H), 5.24 (s, 6H), 2.32 (s, 9H).

3.5.3 Synthesis of 3,3',3''-hexadecyl-1,1',1''-(1,3,5-mesitylene)tris(methylene)imidazolium iodide S1A[243]

1 → **S1A**
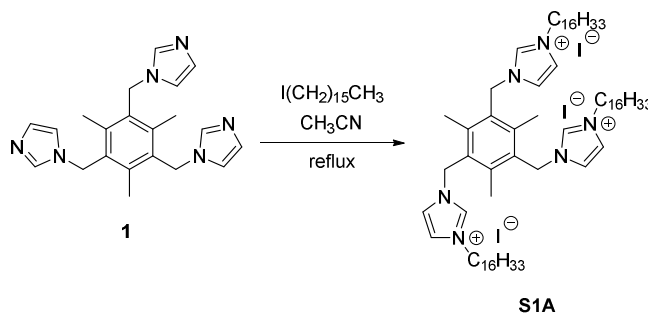
A stirred solution of 1,3,5-tris(imidazole-1-ylmethyl)-2,4,6-trimethylbenzene **1** (1.0 g, 2.774 mmol) and 1-iodohexadecane (2.93 g, 8.323 mmol) in 40 mL of acetonitrile was heated at reflux temperature overnight. The solvent was partially evaporated, and a precipitate appeared upon addition of diethyl ether. The resulting solid was filtered and washed with diethyl ether to afford **S1A** as a white powder. (3.642 g; 93%). ^{1}H NMR (250 MHz, CDCl$_3$) δ (ppm): 9.74 (s, 3H), 8.19 (s, 3H), 7.26 (s, 3H under CDCl$_3$ peak), 5.76 (s, 6H), 4.35 (t, J = 7.44 Hz, 6H), 2.41 (s, 9H), 1.85 (m, 6H), 1.23 (m, 78H), 0.84 (t, J = 7.0 Hz, 9H).

3.5.4 Synthesis of 3,3',3''-hexadecyl-1,1',1''-(1,3,5-mesitylene)tris(methylene)imidazolium tetrafluoroborate S1B[243]

S1A → **S1B**
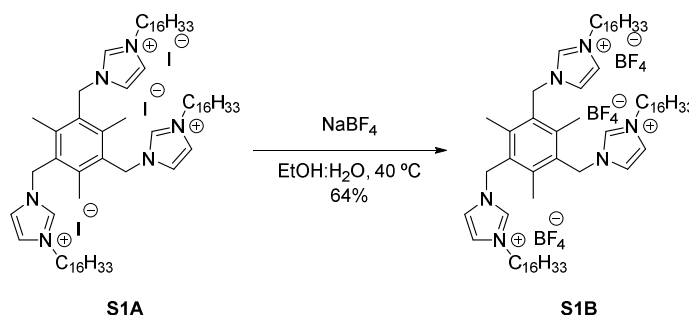
A solution of sodium tetrafluoroborate (0.69 g, 6.35 mmol) in 25 mL of water was added dropwise to a solution of **S1A** (1.5 g, 1.06 mmol) in 50 mL of ethanol. The mixture was stirred at room temperature for 3 h. A white solid precipitated and was filtered off. The process was repeated three times to ensure the complete anion exchange, which was confirmed by ^{1}H NMR. The white solid was dissolved in dichloromethane. The organic layer was washed with water (3 x 25 mL) and dried with anhydrous sodium sulphate. The product was recrystallized in dichloromethane-diethyl ether to give **S1B** as a white solid. (0.884 g; 64%). ^{1}H NMR (360 MHz, CDCl$_3$) δ (ppm): 8.67 (s, 3H), 7.67 (s, 3H), 7.21 (s, 3H), 5.49 (s, 6H), 4.13 (t, J = 7.4 Hz, 6H), 2.23 (s, 9H), 1.81 (m, 6H), 1.23 (m, 78H), 0.88 (t, J = 7.0 Hz, 9H).

3.5.5 Synthesis of 1,3-di(2-propyn-1-yl)imidazolium bromide 2a[246]

2a
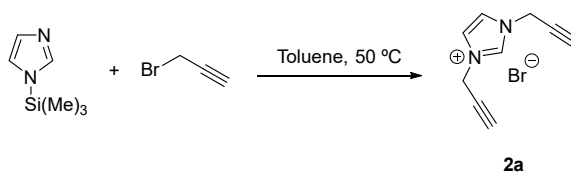
Propargyl bromide (17.8 mL; 80 wt% in toluene; ρ = 1.335 g/mL; 160 mmol) was added into a round bottom flask containing N-(trimethylsilyl)imidazole (7.34 mL; 7.013 g; 50 mmol) under inert atmosphere. The mixture was heated under stirring at 50 ºC. Upon completion of the reaction (24 h) the solid obtained was filtered, washed with Et$_2$O (3 x 30 mL) and dried under vacuum. The product **2a** was obtained as a white hygroscopic

solid (10.59 g; 94%; mp = 123-125 ºC). ^{1}H NMR (250 MHz, CD$_3$CN) δ (ppm): 9.49 (s, 1H, NCHN), 7.60 (s, 2H, NCH=CHN), 5.17 (d, J = 2.5 Hz, 4H; 2 x CH$_2$C≡CH), 3.06 (t, J = 2.5 Hz, 2H, 2 x CH$_2$C≡CH). ^{13}C NMR (62.5 MHz, CD$_3$CN) δ (ppm): 123.4 (NCHN), 118.3 (NCH=CHN) (masked by solvent), 78.4 (CH$_2$C≡CH), 75.5 (CH$_2$C≡CH), 40.2 (NCH$_2$C≡CH). ESI-HRMS (m/z) calculated for C$_9$H$_9$N$_2$[+]: 145.0760; found: 145.0761.

3.5.6 Synthesis of 1,3-di(2-propyn-1-yl)imidazolium tetrafluoroborate 2b[246]
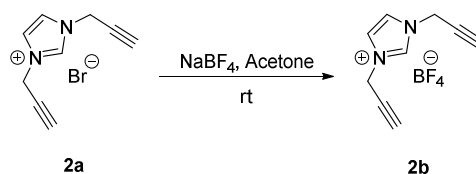
A mixture of **2a** (2.88 g, 12.8 mmol) and NaBF$_4$ (1.41 g, 12.84 mmol) in acetone (30 mL) was stirred at room temperature. After 24 h of reaction the mixture was filtered and the resultant solid was washed with Et$_2$O (2 x 50 mL). The combined organic layers were dried with anhydrous sodium sulphate and the solvent was evaporated under reduced pressure. The product **2b** was obtained as a pale yellow solid (2.71 g, 91%, mp = 66-68 ºC). ^{1}H NMR (250 MHz, CD$_3$CN) δ (ppm): 8.81 (s, 1H, NCHN), 7.55 (s, 2H, NCH=CHN), 5.03 (d, J = 2.5 Hz, 4H; 2 x CH$_2$C≡CH), 3.05 (t, J = 2.5 Hz, 2H, 2 x CH$_2$C≡CH). ^{13}C NMR (62.5 MHz, CD$_3$CN) δ (ppm): 136.6 (NCHN), 123.5 (NCH=CHN), 78.5 (CH$_2$C≡CH), 75.2 (CH$_2$C≡CH), 40.3 (NCH$_2$C≡CH).

3.5.7 Synthesis of polyethylene glycol monomethyl ether mesylate 3[214E,227B]
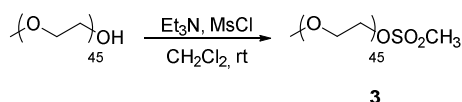
Commercial MeO-PEG-OH (n = 45; 10.08 g; 5.04 mmol), previously dried at 80 ºC overnight, and anhydrous triethylamine (2.1 mL, 1.53 g, 15.1 mmol) were dissolved in anhydrous CH$_2$Cl$_2$ (140 mL). The mixture was cooled at 0 ºC and methanesulfonyl chloride (0.8 mL, 1.184 g, 10.2 mmol) was added dropwise (15 min) under magnetic stirring. The reaction mixture was stirred at 0 ºC during 15 min and then 5 h more at room temperature. After that point the reaction mixture was filtered throw a plug of silica gel and washed with CH$_2$Cl$_2$. The solvent was evaporated under reduced pressure and the oily product was treated with Et$_2$O to obtain a white solid. The resultant solid was filtered, washed with Et$_2$O and dried under vacuum obtaining compound **3** as a white solid. (10.47 g; 97%; mp = 50-52 ºC). ^{1}H NMR (360 MHz, CDCl$_3$) δ (ppm): 4.34-4.37 (m, 2H, CH$_2$), 3.80-3.82 (m, 1H, CH$_2$), 3.73-3.75 (m, 2H, CH$_2$), 3.67-3.53 (m, 198H, CH$_2$), 3.51-3.53 (m, PEG chains), 3.35 (s, 3H, OCH$_3$), 3.06 (s, 3H, SO$_2$CH$_3$).

3.5.8 Synthesis of polyethylene glycol monomethyl ether azide 4[214E,227B]
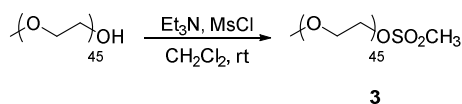
Mesylate **3** (6.56 g, 3.14 mmol) was dissolved in DMF (230 mL). Then NaN$_3$ (2.07 g, 31.8 mmol) was added and the resulting solution was heated at 60 ºC during 24 h. At that point the solvent was evaporated under reduced pressure and the resultant solid was dissolved in CH$_2$Cl$_2$. The organic layer was washed with water (3 x 30 mL), dried over anhydrous Na$_2$SO$_4$ and the solvent was evaporated. Et$_2$O was added to the oily product and a white solid was formed. The solid was filtrated and washed with Et$_2$O obtaining the azide **4** as a white solid. (6.1 g; 96%; mp = 48-50 ºC). ^{1}H NMR (360 MHz, CDCl$_3$) δ (ppm): 3.63 (m, 249H, CH$_2$), 3.37 (s, 5H, CH$_2$OCH$_3$), 3.06 (s, 3H, SO$_2$CH$_3$).

3.5.9 SYNTHESIS OF PEG-TAGGED STABILIZER **S2A**
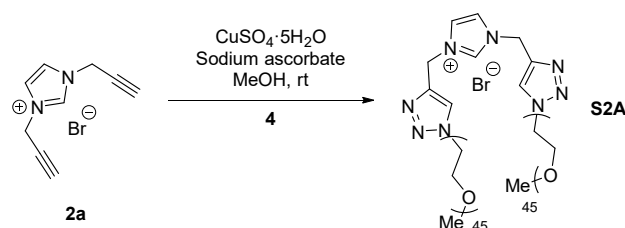
Imidazolium salt **2a** (0.30 g, 1.33 mmol), azide **4** (3.63 g, 1.78 mmol), sodium ascorbate (0.14 g, 0.76 mmol) and copper(II) sulphate pentahydrate (0.089 g, 0.35 mmol) were dissolved in methanol (10 mL), previously degassed, and the solution was purged with N_2 flow for 10 min. The mixture was stirred in the dark, at room temperature, for 24 h under inert atmosphere. Then the solvent was evaporated under reduced pressure and the solid residue was dissolved in water. The aqueous layer was extracted with CH_2Cl_2 (4 x 20 mL) and the organic phase was washed with water (4 x 20 mL), dried with anhydrous Na_2SO_4 and filtered. The solvent was evaporated under reduced pressure obtaining **S2A** as a pale brown solid. (3.13 g; 86%). ^1H NMR (250 MHz, $CDCl_3$) δ (ppm): 10.51 (s, 1H, NCHN), 8.37 (s, 2H, NCH=CHN), 7.59 (s, 2H, 2 x triazole-H), 5.67 (s, 4H, 2 x NCH_2-triazole), 4.55 (t, J = 5 Hz, 4H, 2 x NCH_2-PEG), 3.94-3.65 (m, 2 x CH_2 PEG chains), 3.40 (m, 6H, 2 x OCH_3). ESI-TOF-MS (m/z): peaks between 3519.3 and 4445.0 corresponding to $[M]^+$ separated by 44 D (CH_2CH_2O); the most intense peak at 4047.7 (86 CH_2CH_2O units + $C_9H_9N_8$ nitrogen-rich core + 2 CH_3).

3.5.10 SYNTHESIS OF PEG-TAGGED STABILIZER **S2B**
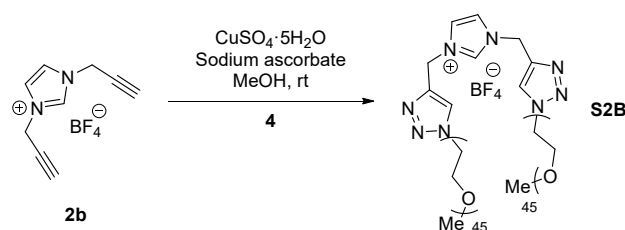
Imidazolium salt **2b** (55 mg, 0.22 mmol), azide **4** (883 mg, 0.43 mmol), sodium ascorbate (34.9 mg, 0.18 mmol) and copper(II) sulphate pentahydrate (21.5 mg, 0.09 mmol) were dissolved in methanol (10 mL), previously degassed, and the solution was purged with N_2 flow for 10 min. The mixture was stirred in the dark, at room temperature, for 3 days under inert atmosphere. Then the mixture was filtered through Celite and washed with MeOH (20 mL) and CH_2Cl_2 (20 mL). The organic phase was dried with anhydrous Na_2SO_4, filtered and the solvent was evaporated under reduced pressure. The obtained residue was washed with Et_2O and dried under vacuum obtaining **S2B** as a pale yellow solid. (783 mg; 84%). ^1H NMR (360 MHz, $CDCl_3$) δ (ppm): 9.19 (s, 1H, NCHN), 8.25 (s, 2H, NCH=CHN), 7.54 (s, 2H, 2 x triazole-H), 5.52 (s, 4H, 2 x NCH_2-triazole), 4.56 (t, J = 5 Hz, 4H, 2 x NCH_2-PEG), 3.87 – 3.44 (m, 2 x CH_2 PEG chains), 3.37 (m, 6H, 2 x OCH_3). ESI-TOF-MS (m/z): peaks between 3474.3 and 4267.1 corresponding to $[M]^+$ separated by 44 D (CH_2CH_2O); the most intense peak at 3870.4 (82 CH_2CH_2O units + $C_9H_9N_8$ nitrogen-rich core + 2 CH_3).

3.5.11 Synthesis of 1,1′,1′′-[(2,4,6-trimethylbenzene-1,3,5-triyl)tris(methylene)]tris(3-propargyl-1*H*-imidazol-3-ium) bromide **5**
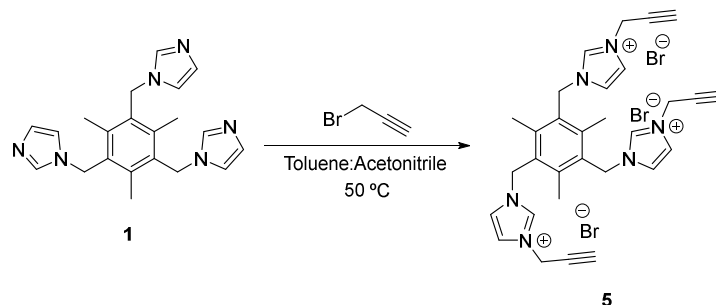
Propargyl bromide (1.4 mL; 80% wt in toluene; ρ = 1.335 g/mL; 15.7 mmol) was added to a solution of **1** (0.452 g; 1.25 mmol) in a 2:1 toluene:acetonitrile mixture (9 mL). The reaction mixture was stirred at 50 ºC under inert atmosphere for 24 h. Then Et$_2$O was added until a fine solid precipitated which was separated by decantation, washed with Et$_2$O and dried to obtain **5**. (0.77 g; 63%). ^{1}H NMR (360 MHz, (CD$_3$)$_2$SO) δ (ppm): 9.28 (s, 3H, N=CHN), 7.88 (s, 3H, C=CHN), 7.81 (s, 3H, C=CHN), 5.59 (s, 6H, CH$_2$), 5.24 (s, 6H, CH$_2$), 3.82 (s, 3H, ≡CH), 2.30 (s, 9H, CH$_3$). ^{13}C NMR (360 MHz, (CD$_3$)$_2$SO) δ (ppm): 141.2 (Ph), 135.7 (N=CN), 129.3 (Ph), 122.9 (NCH=), 122.3 (NCH=), 78.7 (-C≡), 76.3 (≡CH), 48.0 (CH$_2$), 16.4 (CH$_3$). ESI-TOF-HRMS (m/z) calculated for C$_{30}$H$_{33}$Br$_2$N$_6$$^+$: 635.1128; found: 635.1115.

3.5.12 Synthesis of PEG-tagged stabilizer **S3**
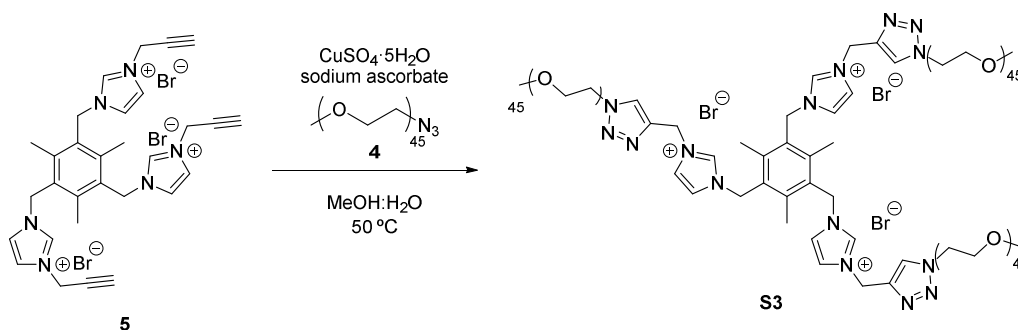
Tris-imidazolium salt **5** (0.201 g, 0.28 mmol), azide **4** (1.883 g, 0.92 mmol), sodium ascorbate (0.131 g, 0.663 mmol) and copper(II) sulphate pentahydrate (0.077 g, 0.308 mmol) were dissolved in a previously degassed 1:1 MeOH:water mixture (3.2 mL). The solution was purged with a N$_2$ flow for 10 min and then it was stirred in the dark at 50 ºC for 24 h under inert atmosphere. The mixture was centrifuged and the methanol from the supernatant was evaporated at reduced pressure. The aqueous residue was extracted with CH$_2$Cl$_2$ (4 x 20 mL) and the organic phase was washed with water (3 x 20 mL). Then, the organic layer was dried over anhydrous Na$_2$SO$_4$, filtered and the solvent was evaporated to obtain a brownish oily residue. Then, Et$_2$O was added until a solid precipitated, which was filtered and washed with Et$_2$O to obtain **S3** (1.504 g, 79%, mp = 52-53 ºC). ^{1}H NMR (360 MHz, CDCl$_3$) δ (ppm): 10.21 (br s, 3H, N=CHN), 8.29 (br s, 3H, NCH=), 7.89 (br s, 3H, C=CHN), 7.56 (br s, 3H, C=CHN), 5.75 (br s, 6H, CH$_2$), 5.62 (br s, 6H, CH$_2$), 4.54 (m, 6H), 3.90-3.38 (m, CH$_2$ of PEG chains), 3.38 (s, 9H, -OCH$_3$), 2.43 (br s, 9H, -CH$_3$). MALDI-TOF-MS (m/z): peaks between 1685.650 (33 CH$_2$CH$_2$O units + C$_{30}$H$_{33}$N$_{15}$ nitrogen-rich core + 3 CH$_3$) and 2253.907 (46 CH$_2$CH$_2$O units + C$_{30}$H$_{33}$N$_{15}$ nitrogen-rich core + 3 CH$_3$) corresponding to [M]$^{3+}$ separated by 44 D (CH$_2$CH$_2$O unit); the most intense peak at 1903.742 (38 CH$_2$CH$_2$O units + C$_{30}$H$_{33}$N$_{15}$ nitrogen-rich core + 3 CH$_3$).

3.5.13 GENERAL PROCEDURE FOR THE PREPARATION OF PT NPS (**M5**, **TABLE 1**, ENTRY 4)

A 0.5 M solution of NaOH in ethylene glycol (5 ml, 2.5 mmol NaOH) was added to a stirred solution of $H_2PtCl_6 \cdot xH_2O$ (40% wt Pt, 94.1 mg; 0.19 mmol Pt) in ethylene glycol (5 mL) under N_2 atmosphere. The mixture was heated at 160 ºC under N_2 atmosphere for 3 hours. Then, it was cooled down at room temperature and ethylene glycol was added to reach 100 mL of a black colloidal solution of Pt NPs in ethylene glycol. A solution of stabilizer **S1B** (246.8 mg; 0.19 mmol) in anhydrous THF (25 mL) was added. The resulting solution was stirred overnight (18 h) at room temperature under inert atmosphere. Then, water (10 mL) was added and the crude mixture was extracted with dichloromethane (10 mL). The black organic phase was washed with water (5x10 mL) and dried with anhydrous sodium sulphate. The resulting organic layer was filtered through a Millipore filter (0.46 μm). The solvent was removed under vacuum and the residue was washed successively with MeOH (20 mL) and hexane (20 mL). **M5** was obtained as a black powder after centrifugation and decantation of the supernatant in each washing. (95 mg; 30.3% Pt (ICP-OES); 85% yield with respect to the Pt used).

3.5.14 GENERAL PROCEDURE FOR THE PREPARATION OF NI NPS (**M12**, **TABLE 3**, ENTRY 2)

A well dried Fischer-Porter apparatus equipped with a magnetic stir bar was charged with $Ni(COD)_2$ (480 mg, 1.7 mmol) in a glove box and closed by a septum. A solution of **S1A** (98 mg, 0.07 mmol) in anhydrous and degassed THF (80 mL) was prepared in a schlenk and then transferred by cannula to the Fischer-Porter maintained at -116 ºC in an ethanol/N_2 liquid bath (consistency of a gel). The septum was changed by a connector under argon atmosphere, and the contents of the Fischer-Porter were subjected to three evacuate-refill cycles with H_2, bringing the pressure of H_2 to 3 atm. Then the mixture was stirred at 70 ºC overnight (16 h). The solution darkened and became black. The hydrogen was removed by three evacuate-refill cycles with N_2. The solvent was evaporated in the vacuum line. The black solid residue was washed twice with anhydrous and degassed pentane (80 mL) and then twice with anhydrous and degassed methanol (20 mL) under inert atmosphere, using a magnet to separate the magnetic nanoparticles from the solvent by decantation. The solid was redissolved in anhydrous and degassed CH_2Cl_2, and the solution transferred to a vial under nitrogen atmosphere. After removal of the solvent, Ni NPs were obtained as a black powder. (171 mg; 48.5% Ni (ICP-OES); 78% yield with respect to the Ni used).

3.5.15 GENERAL PROCEDURE FOR THE PREPARATION OF AU NPS (**M16**, **TABLE 5**, ENTRY 3)

Stabilizer **S3** (133.6 mg; 0.02 mmol) and tetrachloroauric acid trihydrate (23.6 mg; 0.06 mmol) were dissolved in distilled water (100 mL) under inert atmosphere to afford a yellow solution. Then, 4 mL of 0.1 M $NaBH_4$ solution (0.4 mmol) were added dropwise for 2 min. The reaction mixture turned deep red and was stirred at room temperature overnight. After this time, the mixture was filtered through a Milli-Pore filter (0.2 μm, nylon) and then extracted with CH_2Cl_2 (6 x 30 mL). The organic phase was dried over anhydrous Na_2SO_4, filtered and then the solvent was evaporated to obtain the Au NPs **M16** as a dark red powder. (117.9 mg; 6.9% Au (ICP-OES); 68.8% yield according to the starting Au).

3.5.16 GENERAL PROCEDURE FOR THE PREPARATION OF RH NPS (**M18**, **TABLE 7**, ENTRY 1)

Stabilizer **S2A** (43 mg; 0.01 mmol) and rhodium(III) chloride hydrate (135 mg; 0.52 mmol) were dissolved in distilled water (450 mL) under inert atmosphere to afford an orange solution. Then, 50 mL of 0.15 M $NaBH_4$ solution (7.5 mmol) were added dropwise for 10 min and the mixture turned black. The solution was stirred at room temperature overnight. After this time the mixture was filtered through a Milli-Pore filter (0.45 μm, nylon) and then extracted with CH_2Cl_2 (6 x 30 mL). The organic phase was dried over anhydrous Na_2SO_4, filtered and then the solvent was evaporated to obtain the Rh NPs **M18** as a black powder. (68.2 mg; 31.7% Rh (ICP-OES); 40% yield according to the starting Rh.

Chapter 4. CATALYTIC ACTIVITY OF METAL NANOPARTICLES

4.1 INTRODUCTION

Metal NPs have been extensively used as catalysts in the last 15 years. However, the mechanism of the catalysis under metal NPs is still a source of discussion. Initially, metal NPs were considered heterogeneous catalysts, but presenting a higher surface area compared with bulk metals. More recent studies have proposed that, in some cases, homogeneous species are released from metal NPs, which are the active ones. The leaching of metal atoms from the surface of the NPs may cause that the catalytic cycle occurs as an homogeneous process. If this leaching involves a significant proportion of atoms, the morphology of the catalysts could change, losing their catalytic activity in subsequent cycles. In these cases the NPs would act as a carrier of the active species, instead of being the catalyst itself.[261]

Nowadays, three possibilities are considered for the mechanism of these catalytic processes. The first one is that the reaction occurs on the surface of the particle as in a pure heterogeneous catalyst. This would be, in general, the preferred one because the particles remain unaltered during the catalytic cycles. Nevertheless, other factors (temperature of the media, secondary reactions, etc.) could cause the agglomeration of the NPs.

The second possibility is what is known as "local leaching". In that case, the released metal atoms remain close to the particles. Both kind of species, free atoms and surface atoms, could take part in the catalytic cycle. In that mechanism, the close distance between the free atoms and the particles facilitates the reincorporation of these atoms in the structure of the NPs, maintaining the initial morphology.

The last option is the loss of metal atoms from the surface of the particles, which will be the active species. In that case the metal NPs would act as a precursor or reservoir of the true catalytically active species, instead of the catalyst itself. Normally this process causes the degradation of the catalyst due to the loss of the active species.

Different methodologies have been reported in the literature for the elucidation of the nature of the processes that take place in each case. Garcia-Antón, Philippot and collaborators studied the chemoselectivity of molecular Pd complexes with hybrid pyrazole ligands and Pd NPs stabilized by the same type of ligands. The different reactivity of both kind of catalysts support that the Pd NPs catalyze the reaction through an heterogeneous mechanism in contrast to the homogeneous process observed with the palladium complexes.[262] Besides the study of the reaction patterns, alternative methods to understand the pathway of the catalytic process have been reported, such as catalyst poisoning (generally mercury poisoning) or kinetic studies of the mechanism, among others.[263]

---

[261] Eremin, D. B., Ananikov, V. P. *Coord. Chem. Rev.* **2017**, *346*, 2.
[262] Peral, D., Gómez-Villarraga, F., Sala, X., Pons, J., Bayón, J. C., Ros, J., Guerrero, M., Vendier, L., Lecante, P., García-Antón, J., Philippot, K. *Catal. Sci. Technol.* **2013**, *3*, 475.
[263] Widergren, J. A., Finke, R. G. *J. Mol. Catal. A Chem.* **2013**, *198*, 317.

4.2   Ni and Rh nanoparticles as catalysts for cross-coupling reactions

4.2.1   Introduction to cross-coupling reactions

As mentioned in the introduction, metal NPs have been extensively studied as catalysts in C-C bond forming reactions. Suzuki, Sonogashira and Heck reactions have been typically used for testing the catalytic activity of these nanomaterials.[157,158,159,162]

Since the discovery of these reactions, Pd species have been the most used catalysts for these transformations, mainly Pd(0) complexes.[156] Sometimes these species can be generated *in situ* from Pd(II) salts. However, other kind of catalysts (NPs) or other transition metals, have also been studied.[99b,101a,190,192,193]

The catalytic cycle of Suzuki and other cross-coupling reactions (Kumada, Negishi, Stille, Hiyama) (**Scheme 18**), involves an oxidative addition into the metallic centre **a** to form the intermediate **b**. Then a transmetallation step occurs to form the intermediate **c** that, through a reductive elimination, gives the desired product and regenerates the catalyst in the initial stage **a**. Group 10 transition metals (Pd, Ni) have been found highly active as catalysts in these transformations, but other transition metal-based catalysts have also been explored. A broad variety of organometallic reagents R-m can be employed, which permits the use of different reaction conditions to obtain a wide number of different products.[264]
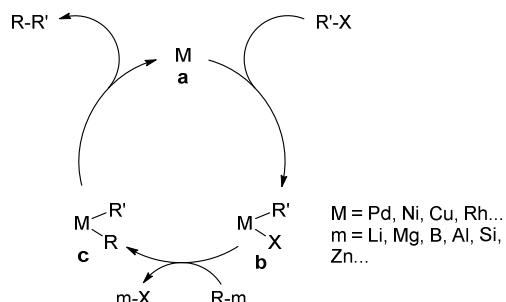
Scheme 18 General catalytic cycle for cross-coupling reactions.

As mentioned previously, our group has reported that nanosized Pd(0) particles stabilized by tris-imidazolium salts present high activity for cross-coupling reactions. In that way, excellent yields were obtained for the Suzuki cross-coupling between different aryl halides and arylboronic acids.[230a] Interestingly, depending on the counteranion (iodide or tetrafluoroborate) present in the tris-imidazolium salts, the reactivity in front of the more challenging aryl chlorides differs, being the Pd NPs stabilized by the tris-imidazolium iodides the most active. Moreover, the Pd NPs stabilized by tris-imidazolium iodides presented high activity as catalysts in Heck reactions with different substrates and in the Sonogashira coupling in the absence of Cu co-catalysts and phosphine ligands.[230b]

In the present work we have tested Ni NPs as catalysts for Suzuki and Sonogashira couplings and Rh NPs for a Heck-type coupling between arylboronic acids and *n*-butyl acrylate.

4.2.2   Suzuki-Miyaura cross-coupling

4.2.2.1   Introduction to Suzuki-Miyaura reaction

Cross-coupling of haloarenes with aryl boronic acids, generally named Suzuki-Miyaura reaction, has become a powerful tool for the formation of Ar-Ar structures, in both academia and industrial field. This importance is based in the characteristics of that reaction, which involves mild conditions, commercially available

---

[264] *C-C Bond Formation by Cross-Coupling*; Nolan, S. P., Navarro, O. Ed.: Elsevier Inc., **2013**.

reagents, easy purification of the products and the possibility of using water as solvent (or co-solvent). An equivalent of base is required.

The initial mechanism proposed by Suzuki and Miyaura was based in the palladium catalyzed reaction of 1-alkenylboranes with bromoalkenes for the formation of conjugated alkadienes (**Scheme 19**).[162] In that initial paper, the authors propose an initial step of oxidative addition of organic halide to the coordinatively unsaturated Pd(0) complex PdL$_2$ **A** (step **a**) to form the intermediate **B**. Then, the halide ligand is displaced by the alkoxide used as base to form complex **C** (step **b**). This intermediate reacts with an alkenylborane (step **c**) to generate the diorganopalladium complex **D**. Finally, reductive elimination from **D** (step **d**) gives the corresponding cross-coupling product and regenerates the catalyst for the next cycle.

After this initial proposal several publications based in that methodology were published, which expanded the scope of the reaction using different types of reagents such as haloarenes and aryl boronic acids. These compounds have become the most typical precursors for Suzuki reaction nowadays.[265]
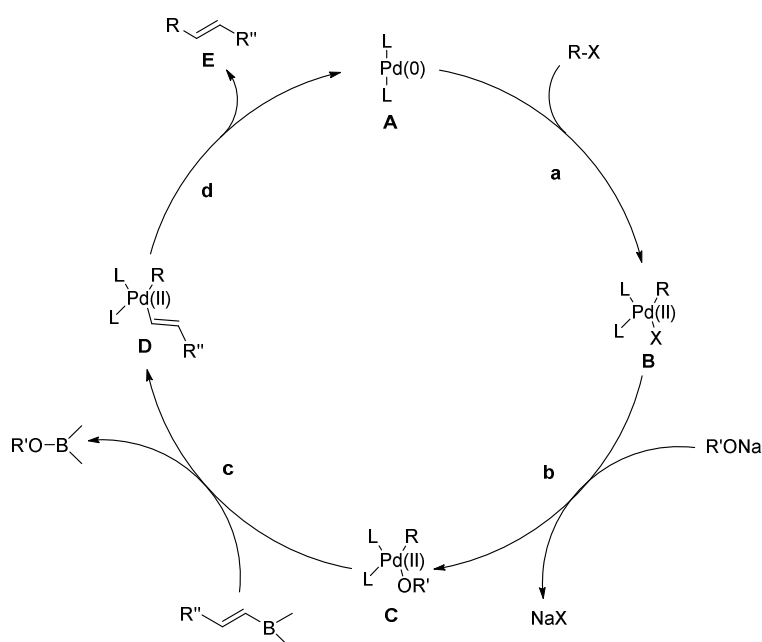
Scheme 19 Catalytic cycle initially proposed by Suzuki and Miyaura for the coupling of organic halides (haloalkenes and haloarenes) with alkenylboranes.

In spite of good results achieved with Pd based catalysts, the high cost of this metal motivated the search of more economical species. In that way, the use of first row transition metals as catalysts is much more appealing, due their cheapness and higher abundance than precious metals. In the last years, the number of publications based in nickel-catalyzed Suzuki-Miyaura reactions have experienced a notable growth. Different Ni(0) complexes have been found highly active for the formation of C-C bonds via Suzuki reaction.[168c,266]

Concerning to the reaction mechanism of Ni-catalyzed Suzuki-Miyaura coupling, a catalytic cycle analogous to that proposed for Pd (involving Ni(0) and Ni(II) species) is the most commonly accepted.[168b] However, alternative suggestions have appeared, such as the Ni(I)/Ni(III) cycle proposed by Louie and collaborators, in which the *in situ* generated Ni(I) has been found catalytically active.[267]

The development of Ni based nanomaterials opens the door to use it as catalysts for the Suzuki cross-coupling reaction. Some examples have been reported recently. The problem that present the Ni NPs is the easily

[265] Suzuki, A. *J. Organometal. Chem.* **1999**, *576*, 147.
[266] Mesganaw, T., Grag, N. K. *Org. Proc. Res. Develop.* **2013**, *17*, 29.
[267] Zhang, K., Conda-Sheridan, M., Cooke, S. R., Louie, J. *Organometallics* **2011**, *30*, 2546.

oxidable surface that can lead to the loss of efficiency after the catalytic cycle. In order to maintain the efficiency of the catalyst in successive cycles a robust nanomaterial is required, in which the Ni surface is hardly oxidable. Thus, Hyeon and collaborators reported soluble Ni NPs which present high catalytic activity for the Suzuki in the first run, but, the easily oxidation of the metal prevented the recycling of the catalyst.[101a] Instead, other authors reported Ni NPs stabilized by dendrimers which result much more robust and resistant through the oxidation. These NPs have been recycled for various cycles without loss of activity.[44a]

4.2.2.2   SUZUKI-MIYAURA REACTION CATALYZED BY NI NPS

We undertook a preliminary study to test the ability of the synthesized Ni NPs stabilized by **S1A** (**M12**) as catalyst (1 mol%) for the Suzuki reactions between *p*-iodoacetophenone and two organoboron compounds, namely *p*-methylphenylboronic acid and phenylboronic acid (**Table 9**).

Table 9 Suzuki cross-coupling between *p*-iodoacetophenone and arylboronic acid catalyzed by Ni NPs (**M12**).

Entry[a]	Arylborane	Solvent	Base	T (ºC)	Time (h)	Conv. (%)[b]
1	7	Toluene:^{t}BuOH (10:1)	K_2PO_4	110	40	14
2	7	Toluene:^{t}BuOH (10:1)	Na_2CO_3	110	20	-
3	7	Toluene:^{t}BuOH (10:1)	K_2CO_3	110	20	-
4	7	Toluene:^{t}BuOH (10:1)	DBU	110	40	45
5	7	Toluene:^{t}BuOH (10:1)	$NaHCO_3$	110	20	-
6	7	Toluene:^{t}BuOH (10:1)	NEt_3	110	20	-
7	8	Toluene	K_2PO_4	130	24	-
8	8	Toluene	DBU	130	24	-

[a] Reaction conditions: *p*-iodoacetophenone: 0.4 mmol; arylboronic acid: 0.6 mmol; solvent: 2 mL; Base: 3 equiv.; Ni NPs (**M12**): 1 mol %; reaction performed in a closed vessel. [b] Conversion of *p*-iodoacetophenone determined by GC-MS.

For the coupling reaction of *p*-iodoacetophenone **6** with (*p*-methylphenyl)boronic acid **7**, different bases were tested using a mixture of toluene:^{t}BuOH (10:1) as solvent at 110 ºC (entries 1-6 of **Table 9**). In this medium

both catalyst and reagents were soluble. All the reactions were performed in a sealed tube under inert atmosphere to prevent the oxidation of the Ni NPs. Only low or moderate conversion of *p*-iodoacetophenone was found (GC-MS) by using K_2PO_4 and DBU as bases (entries 1 and 4 of **Table 9**) and the final coupling product was not observed in the presence of DBU and only traces in the case of using K_2PO_4 as base. In both cases the precipitation of bulk nickel was observed after 40 h of reaction. With the aim to prevent the precipitation of the metal, the reaction of *p*-iodoacetophenone **6** with phenylboronic acid **8** was tested at 130 ºC using only toluene as solvent, in which the Ni NPs were much more soluble. Unfortunately, in these two cases there was no conversion of *p*-iodoacetophenone **6** after one day of reaction.

Due to the poor results obtained in these preliminary tests, the Suzuki-Miyaura coupling catalyzed with **M12** was not further investigated. However, we must note that to conclude that these NPs are completely inactive in this model reaction, a broader screening of different reaction conditions would be necessary.

4.2.3 SONOGASHIRA CROSS-COUPLING

4.2.3.1   INTRODUCTION TO SONOGASHIRA REACTION

The Pd catalyzed coupling between aryl halides and terminal alkynes was firstly reported independently by Heck and Cassar.[268,269] The problem was that the described protocols required high temperatures. The same year, Sonogashira reported that when CuI was added as a cocatalyst the reaction takes place at room temperature.[159] But the addition of copper has also some drawbacks. The main problem that present the addition of Cu(I) species was the generation of homocoupling side products between the terminal alkynes. Nevertheless, the methodology proposed by Sonogashira became more popular due to the mild reaction conditions.

A precise description of the mechanism of the Sonogashira reaction cocatalized by copper is still a source of discussion.[270] However, the most accepted catalytic pathway involves two independent cycles (**Scheme 20**). The accepted mechanism for the Pd cycle was based in the typical procedure for cross-coupling reactions, involving Pd(0) and Pd(II) species. The first step **a** involves a fast oxidative addition of aryl halide to the Pd catalyst, generating the Pd(II) complex **B**. The step **b** connects the Pd cycle with the Cu cycle by the transmetallation from the Cu acetylide to the Pd complex, generating the intermediate **C**. Normally, that would be the rate-determining step of the reaction. Finally, the reductive elimination (step **c**) of the complex gives the desired cross-coupling product **G** and regenerates the catalyst.

The secondary Cu cycle remains unclear. The commonly used amines are normally not basic enough to deprotonate the alkyne to form the copper acetylide. For that reason, the π-alkyne-Cu complex **E** is generated, making the terminal proton of the alkyne more acidic. Although it is assumed that the *in situ* generation of the copper acetylide **F** is necessary for the formation of the intermediate **C**, the formation of **F** has been never proved.

[268] Dieck, H. A., Heck, F. R., *J. Organometal. Chem.* **1975**, *93*, 259.
[269] Cassar, L. *J. Organometal. Chem.* **1975**, *93*, 253.
[270] Chinchilla, R., Nájera, C. *Chem. Rev.* **2007**, *107*, 874.
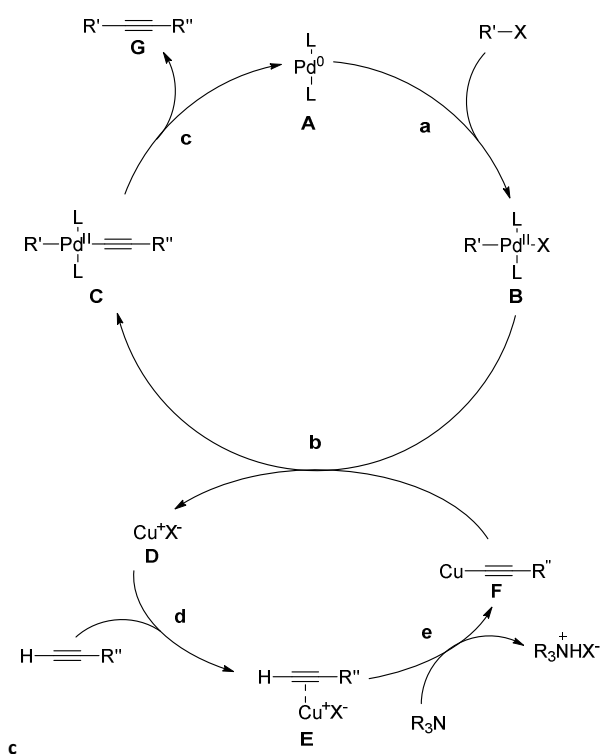
Scheme 20 Mechanism proposed for the Pd-Cu cocatalyzed Sonogashira cross-coupling.

A copper-free Sonogashira cross-coupling has also been reported (**Scheme 21**).[271] As in the case of Cu-cocatalyzed reaction, the mechanism is also unclear. The first step **a** is, as in the case of Suzuki reaction, the oxidative addition of the organic halide to the Pd(0) complex **A** to generate **B**. However, the second step is controversial. As it has been mentioned previously, the employed amines generally cannot deprotonate the alkyne for the transmetallation step **c**. Hence, the most accepted idea is the generation of the intermediate complex **C** with the displacement of one ligand from **B**. Then the transmetallation step **c** can take place and the following reductive elimination **d** gives the desired product and regenerates the catalyst **A** for subsequent cycles.
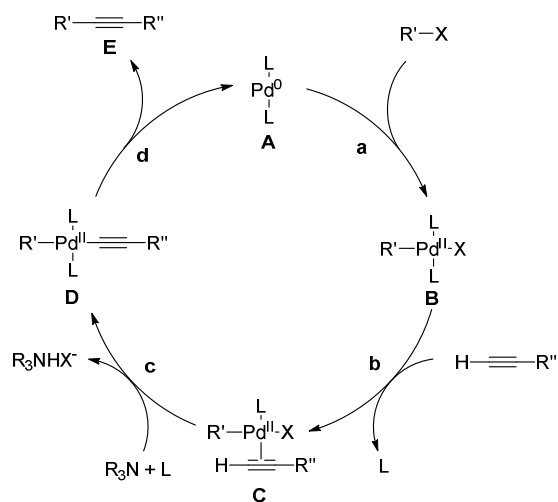
Scheme 21 Commonly proposed mechanism for the copper-free Pd-catalyzed Sonogashira cross-coupling.
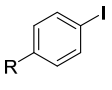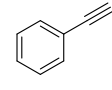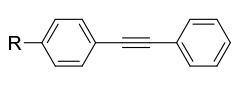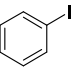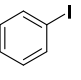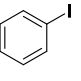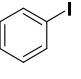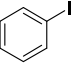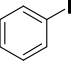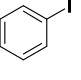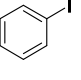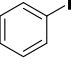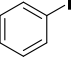
[271] Soheli, A., Albaneze-Walker, J., Murry, J. A., Dormer, P. G., Hughes, D. L. *Org. Lett.* **2003**, *5* (22), 4191.

Even though Pd complexes were the most used catalysts for Sonogashira couplings, alternative options have been described. Different Pd and other transition metal based nanocatalysts have been also employed for that reaction.[58,190a,191,193,99b]
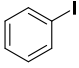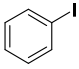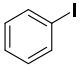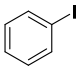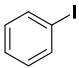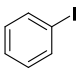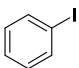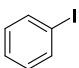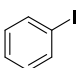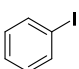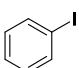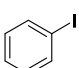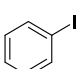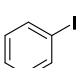
4.2.3.2 SONOGASHIRA REACTION CATALYZED BY NI NPS

In order to test the catalytic activity of the prepared Ni NPs stabilized by **S1A** (**M12**) (1 mol%), the coupling reactions of iodobenzene **11** and *p*-iodoacetophenone **6** with phenylacetylene **12a** under different conditions were tried (**Table 10**). All the experiments were performed into a sealed tube under inert atmosphere, and the conversion of aryl iodide and the formation of products were monitored by GC-MS.

Table 10 Sonogashira reaction between aryl iodides and phenyl acetylene catalyzed by Ni NPs (**M12**).

Entry[a]	Catalyst	R	Solvent	Base	T (ºC)	Time (h)	Conv. (%)[b]
1[c]	M12	11	NMP	K$_2$CO$_3$	120	24	-
2[c],[d]	M12	11	NMP	K$_2$CO$_3$	120	24	-
3[c],[d]	M12	11	NMP	Na$_2$CO$_3$	120	24	-
4[c],[d]	M12	11	NMP	KOH	120	16	-
5[c],[d]	M12	11	NMP	NaOH	120	16	-
6	M12	11	NMP	KOH	120	16	-
7	M12	11	NMP	K$_2$CO$_3$	120	16	-
8	M12	11	NMP	Na$_2$CO$_3$	120	16	-
9	M12	11	NMP	NaOH	120	16	-
10	M12	11	NMP	NaOAc	120	16	-

11	**M12**	![11](iodobenzene 11)	DMF	K_2CO_3	130	16	-
12	**M12**	11	DMF	Na_2CO_3	130	16	-
13	**M12**	11	DMF	KOH	130	16	-
14	**M12**	11	DMF	NaOH	130	16	-
15	**M12**	11	DMF	NaOAc	130	16	-
16	**M12**	11	DMF	NEt_3	130	16	-
17	**M12**	11	DMF	piperidine	130	16	15
18	**M12**	11	DMF	$iPrNH_2$	130	16	-
19	**M12**	11	DMF	pyrrolidine	130	16	14
20	**M12**	11	DMF	Na_2PO_4	130	16	-
21	**M12**	11	CH_3CN	K_2CO_3	120	16	-
22	**M12**	11	CH_3CN	Na_2CO_3	120	16	-
23	**M12**	11	CH_3CN	KOH	120	16	-
24	**M12**	11	CH_3CN	NaOH	120	16	-

25	**M12**	**11**	CH₃CN	NaOAc	120	16	-
26	**M12**	**11**	CH₃CN	NEt₃	120	16	-
27	**M12**	**6**	CH₃CN	piperidine	120	35	36
28	**M11**	**6**	CH₃CN	piperidine	120	24	15
29	**M12**	**6**	CH₃CN	pyrrolidine	120	35	32
30	**M11**	**6**	CH₃CN	pyrrolidine	120	24	35
31	**M12**	**6**	CH₃CN	NEt₃	120	16	-
32	**M12**	**6**	CH₃CN	iPrNH₂	120	16	-
33	**M12**	**6**	CH₃CN	Na₃PO₄	120	16	-

[a] Reaction conditions: Aryl iodide: 0.4 mmol; phenylacetylene: 0.6 mmol; solvent: 2.5 mL; Base: 3 equiv.; Ni NPs (**M12**): 1 mol %; reaction performed in a closed vessel. [b] Conversion of aryl iodide determined by GC-MS with mesitylene as internal standard. [c] heating in a reactor open to air. [d] Adding CuI (2 mol%) as cocatalyst.

The initial tests were performed with iodobenzene, heating the reaction mixture in *N*-methylpyrrolidone (NMP) at 120 ºC in an open reactor in the presence of different bases (entries 1-5 of **Table 10**) and CuI (2 mol%) was added as cocatalyst (entries 2-5 of **Table 10**), but small amounts of the homocoupling product of the alkyne were observed. For that reason, in the following reactions we maintained the solvent and temperature, but we decided to avoid the use of the cocatalyst to prevent the formation of undesired side-products and the reactions were performed in a closed vessel (entries 6-10 of **Table 10**). As no conversion was detected, we changed to dimethylformamide (DMF) at 130 ºC (entries 11-20 of **Table 10**) and acetonitrile at 120 ºC (entries 21-26 of **Table 10**), in both cases in the presence of different bases. Among all the conditions tested, the desired aryl alkynes where only produced in small amounts when secondary amines were used as base. These results were consistent with the fact that often secondary amines proved to be very efficient,

especially for copper-free Sonogashira reaction under Pd catalysis.[272] When piperidine and pyrrolidine were used the results were similar. With DMF as solvent (entries 17 and 19 of **Table 10**) a conversion around 15% was achieved after 16 h of reaction, without any further evolution of the reaction by increasing the reaction time and the formation of side-products.

Then we moved to *p*-iodoacetophenone as substrate in acetonitrile at 120 ºC in the presence of different bases (entries 27-33 of **Table 10**). Again, only secondary amines provided the corresponding final product, obtaining conversions up to 30% (**Table 10** entries 27 and 28 for piperidine and 29 and 30 for pyrrolidine). Also, **M11** was tested as catalyst (entries 28 and 30 of **Table 10**). In these cases all the reactant conversion yielded the desired product **14** (**Table 10** entry 28, **14** 36% GC-MS yield for **M12**; **Table 10** entry 29, **14** 15% GC-MS yield for **M11**; **Table 10** entry 30, **14** 32% GC-MS yield for **M12**; **Table 10** entry 31, **14** 35% GC-MS yield for **M11**), with only traces of some undesired side-products. However, no further evolution of the reaction was observed after 35 h.

Despite the last promising results with secondary amines, the yields obtained were low and the Sonogashira reaction catalyzed by Ni NPs was not further investigated.

4.2.4 HECK-TYPE REACTION

4.2.4.1 INTRODUCTION TO HECK-TYPE REACTION BETWEEN ARYLBORONIC ACIDS AND ALKENES

The Heck (or Mizoroki-Heck) reaction was discovered at the early seventies independently by Heck and Mizoroki.[158] This reaction was then developed by Heck during the following years and became one of the most general method for the formation of Csp^2-Csp^2 bonds. Roughly, Heck reaction was defined as the coupling between an aryl (heteroaryl) or vinyl halide with an alkene catalyzed by Pd(0) in the presence of a base.[273]

In the last years, other Heck-type based reactions have been developed for the preparation of new Csp^2-Csp^2 bonds, using different reagents and with alternative catalysts. Several reports have been published using Rh species as catalyst for coupling reactions between arylboronic acids or silanediols and olefinic compounds.[274,275]

Lautens has proposed a mechanism for the coupling of arylboronic acids with activated alkenes catalyzed by Rh(I) complexes (**Scheme 22**).[276] Initially the presence of water was needed for the generation of the Rh(I)-OH intermediate **A** which was the catalytically active species.[277] This intermediate transmetallate (step **a**) with the boronic acid generating the intermediate **B**. Then, the addition of the alkene (step **b**) gives the organorhodium complex **C**, which through a β-hydride elimination (step **c**) affords the Heck-type product **D** and the rhodium hydride **E**. From this point, the initial Rh complex could be regenerated by two ways. Herrmann's group observed that the rhodium hydride species were in equilibrium with the equivalent hydroxorhodium complexes **A** in the presence of water (step **d**).[278] On the other hand, an excess of alkene act as hydride donor in the step **e** and regenerate **A** for a subsequent cycle. Alternatively, complex **C** could demetalate (step **f**) in presence of water to give product **F** and regenerate **A** for a following cycle. As reported by some authors, the

[272] Jutand, A., Négri, S., Principaud, A. *Eur. J. Inorg. Chem.* **2005**, 631.
[273] Beletskaya, I. P., Cheprakov, A. V. *Chem. Rev.* **2000**, *100*, 3009.
[274] (a) Lautens, M., Roy, A., Fukuoka, K., Fagnou, K., Martín-Matute, B. *J. Am. Chem. Soc.* **2001**, *123*, 5358. (b) Fujita, N., Motokura, K., Mori, K., Mizugaki, T., Ebitani, K., Jitsukawa, K., Kaneda, K. *Tetrahedron Lett.* **2006**, *47*, 5083.
[275] Mori, A., Danda, Y., Fujii, T., Hirabayashi, K., Osakada, K. *J. Am. Chem. Soc.* **2001**, *123*, 10774.
[276] Lautens, M., Mancuso, J., Grover, H. *Synthesis* **2004**, *12*, 2006.
[277] Hayashi, T., Takahashi, M., Takaya, Y., Ogasawara, M. *J. Am. Chem. Soc.* **2002**, *124*, 5052.
[278] Herrmann, W. A., Kulpe, J. A., Kellner, J., Riepl, H., Bahrmann, H., Konkol, W. *Angew. Ghem. Int. Ed. Engl.* **1990**, *29* (4), 391.

addition of a certain amount of base increases the selectivity through the β-elimination to form as a major product the Heck-type product **D**.[279]
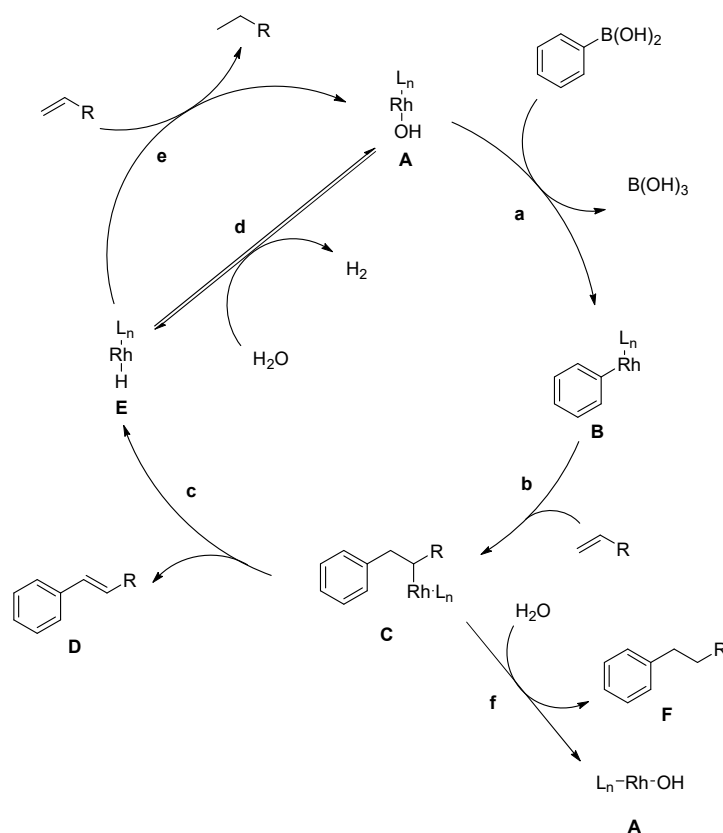
Scheme 22 General mechanism proposed for the Heck-type coupling between arylboronic acids and alkenes catalyzed by Rh(I) complexes.

4.2.4.2   HECK-TYPE REACTION OF ARYLBORONIC ACIDS WITH ALKENES CATALYZED BY RH NPS

Based in the examples using Rh complexes present in the literature, the Rh NPs stabilized with PEG-tagged tris-imidazolium salt (**M20**) were tested as catalysts for the Heck-type reaction between differently substituted arylboronic acids and *n*-butyl acrylate (**Table 11**). The reactions were performed in a closed vessel with 0.5 mol% of catalyst, an excess of the olefin and in the presence of an additive, monitoring the consumption of phenylboronic acid and the formation of the coupling products by TLC and ^{1}H NMR.
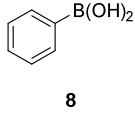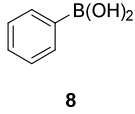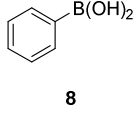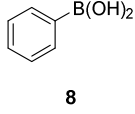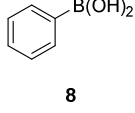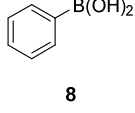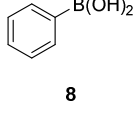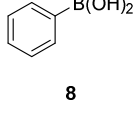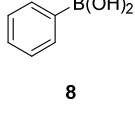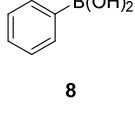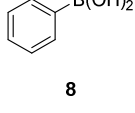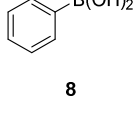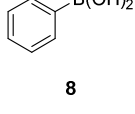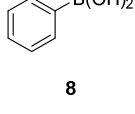
Table 11 Heck-type reaction between aryllboronic acids and *n*-butyl acrylate catalyzed by Rh NPs (**M20**).

Entry[a]	Phenylboronic acid	Solvent	Additive	T (ºC)	Time (h)	Yield. (%)[b]
1	8	Toluene:H₂O (3:1)	K₂CO₃	100	24	12

[279] (a) Zou, G., Guo, J., Wang, Z., Huang, W., Tang, J. *Dalton Trans.* **2007**, 3055. (b) Kuuloja, N., Vaismaa, M., Franzén, R. *Tetrahedron* **2012**, *68*, 2313.

Entry	Substrate	Solvent	Base	Temp	Time	Yield
2	B(OH)$_2$ **8**	H$_2$O	K$_2$CO$_3$	100	24	-
3	B(OH)$_2$ **8**	H$_2$O	Na$_2$CO$_3$	100	24	-
4	B(OH)$_2$ **8**	H$_2$O	NH$_4$Cl	100	24	-
5	B(OH)$_2$ **8**	EtOH:H$_2$O (5:1)	K$_2$CO$_3$	100	42	-
6	B(OH)$_2$ **8**	EtOH:H$_2$O (5:1)	Na$_2$CO$_3$	100	42	-
7	B(OH)$_2$ **8**	Dioxane:H$_2$O (10:1)	K$_2$CO$_3$	100	24	-
8	B(OH)$_2$ **8**	Dioxane:H$_2$O (10:1)	Na$_2$CO$_3$	100	24	-
9	B(OH)$_2$ **8**	Dioxane:H$_2$O (10:1)	KOH (0.3 equiv.)	120	24	-
10	B(OH)$_2$ **8**	Dioxane:H$_2$O (10:1)	K$_2$CO$_3$ (0.3 equiv.)	120	24	-
11	B(OH)$_2$ **8**	Toluene:H$_2$O (1:1)	K$_2$CO$_3$	100	42	27
12	B(OH)$_2$ **8**	Toluene:H$_2$O (5:1)	Na$_2$CO$_3$	100	42	9
13	B(OH)$_2$ **8**	Toluene:H$_2$O (5:1)	K$_2$CO$_3$ (0.3 equiv.)	100	48	21
14	B(OH)$_2$ **8**	Toluene:H$_2$O (5:1)	KOH (0.3 equiv.)	100	48	27
15	B(OH)$_2$ **8**	Toluene:H$_2$O (5:1)	K$_2$CO$_3$ (0.3 equiv.)	120	24	10[c]

16	B(OH)$_2$ **8**	Toluene:H$_2$O (5:1)	K$_2$CO$_3$ (1 equiv.)	120	24	-
17	B(OH)$_2$ **8**	Toluene:H$_2$O (5:1)	KOH (1 equiv.)	120	24	15
18	B(OH)$_2$ **8**	Toluene:H$_2$O (10:1)	K$_2$CO$_3$ (0.3 equiv.)	120	24	-
19	B(OH)$_2$ **8**	Toluene:H$_2$O (10:1)	KOH (0.3 equiv.)	120	24	-
20	MeO—C$_6$H$_4$—B(OH)$_2$ **15**	Toluene:H$_2$O (5:1)	K$_2$CO$_3$ (0.3 equiv.)	100	24	13
21	F$_3$C—C$_6$H$_4$—B(OH)$_2$ **16**	Toluene:H$_2$O (5:1)	K$_2$CO$_3$ (0.3 equiv.)	100	24	-

[a] Reaction conditions: phenylboronic acid: 1 mmol; *n*-butyl acrylate: 3 mmol; solvent: 3 mL; additive: 3 equiv. unless otherwise stated; Rh NPs (**M12**): 0.5 mol %; reaction performed in a closed vessel. [b] Yield by ^{1}H NMR. [c] isolated yield.

Initially phenylboronic acid was tested as substrate in a mixture of toluene:water (3:1) as solvent using K$_2$CO$_3$ as base. Under these conditions just a low conversion was observed (entry 1 of **Table 11**, 12% ^{1}H NMR yield). No reaction occurred when the solvent was changed to water (entries 2-4 of **Table 11**), EtOH:H$_2$O (5:1) (entries 5-6 of **Table 11**) or dioxane:H$_2$O (10:1) (entries 7-10 of **Table 11**) in the presence of different additives and at 100 or 120 ºC. Using toluene:H$_2$O (1:1) and potassium carbonate at 100 ºC for longer reaction times some conversion was obtained (entry 11 of **Table 11**, 27% ^{1}H NMR yield). When the amount of base was reduced to 0.3 equiv. and the solvent was toluene:water (5:1) similar results were achieved (entry 13 of **Table 11**, 21% ^{1}H NMR yield with K$_2$CO$_3$; entry 14, 27% ^{1}H NMR yield with KOH). Interestingly, increasing the temperature to 120 ºC resulted in the same conversion in lower reaction time. Under these conditions (entry 15 of **Table 11**), the product was isolated in 10% yield. Finally, two differently substituted arylboronic acids were used as substrates using the following conditions: potassium carbonate (0.3 equiv.), toluene:water (5:1), 100 ºC for 24 h. When an electron donor group was present (**15**, -OMe), a 13% ^{1}H NMR yield was found (entry 20 of **Table 11**). Conversely, when the boronic acid contains an electron withdrawing substituent (**16**, -CF$_3$) no evolution of the reaction was observed (entry 21 of **Table 11**).

Thus, after obtaining the desired product in just a 10% isolated yield in the best case, this type of reaction was not further investigated with Rh NPs.

4.3 SYNTHESIS OF PROPARGYLAMINES VIA A³ COUPLING BETWEEN CARBONYLIC COMPOUNDS, AMINES AND TERMINAL ALKYNES CATALYZED BY AU NPS

4.3.1 INTRODUCTION

The development of multicomponent reactions has experienced a notable growth in the last years.[280] They consist in the combination of three or more initial reagents in a one pot procedure to obtain diverse organic molecules. Among the multicomponent reactions, the synthesis of propargylamines from aldehydes or ketones, secondary amines and terminal acetylenes, performed under metal catalysis, is of particular interest.

Propargylamines are versatile building blocks for the preparation of *N*-heterocyclic compounds and for the synthesis of drugs and natural products.[199,200a] The typical synthetic method involves the nucleophilic attack of lithium acetylides (or Grignard reagents) to an imine. In that way, Rodriques *et al*. published an early report describing the addition of aryllithium compounds to oximes for the preparation of alkoxyamines (**Scheme 23 (A)**).[281] Later, Collum reported the synthesis of propargylamines via coupling of lithium phenylacetylide to inactivated imines (**Scheme 23 (B)**).[282] Noteworthy, these methods needed low temperatures and a stoichiometrically amount of BF₃·Et₂O. Other authors have reported the synthesis of this kind of compounds with similar methodologies.[283]
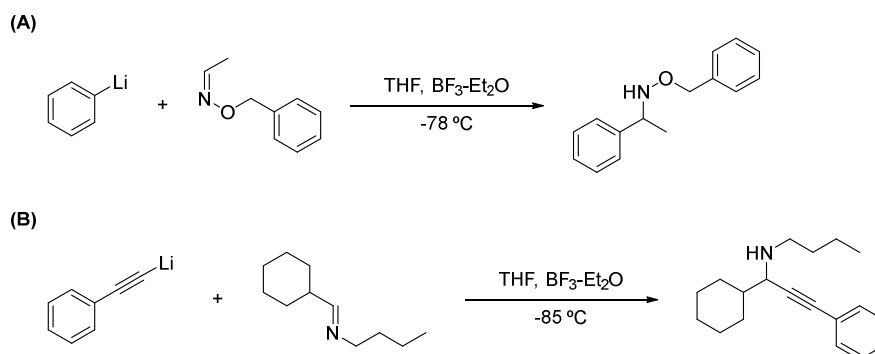
Scheme 23 Typical synthetic method for the coupling between aryllithium compounds with: **(A)** oximes; **(B)** imines.

These procedures have some drawbacks such as the need of stoichiometric amount of reagents, moisture-free conditions and the protection of sensitive functional groups. For these reasons, a more atom-economical alternative based on a metal-catalyzed three-component reaction between aldehydes, amines and terminal alkynes has been developed (**Scheme 24**).[284]
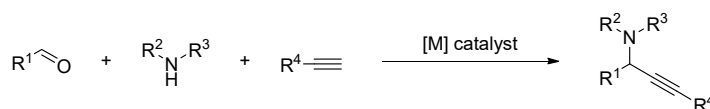
Scheme 24 General approach for the metal-catalyzed synthesis of propargylamines via A³ coupling of aldehydes, amines and alkynes.

Several examples with different metals (Au, Ag, Cu...) under mild conditions have been reported.[208,209] Herein we will focus in Au catalyzed three-component synthesis of propargylamines. The ability of gold to coordinate with triple carbon-carbon bonds opens the possibility for its use in a variety of reactions. Wei and Li published the first gold catalyzed synthesis of propargylamines via A³ coupling.[201] The authors observed that the desired

---

[280] Syamala, M. *Org. Preparations Proced. Int.* **2009**, *41*, 1.

[281] Rodriques, K. E., Basha, A., Summers, J. B., Brooks, D. W. *Tetrahedron Lett.* **1988**, *29* (28), 3455.

[282] Aubrecht, K. B., Winemiller, M. D., Collum, D. B. *J. Am. Chem. Soc.* **2000**, *122*, 11084.

[283] (a) Wee, A. G. H., Zhang, B. *Tetrahedron Lett.* **2007**, 4135. (b) Huang, P.-Q., Huang, Y.-H., Xiao, K.-J., Wang, Y., Xia, X.-E. *J. Org. Chem.* **2015**, *80*, 2861.

[284] (a) Aliaga, M. J., Ramón, D. J., Yus, M. *Org. Biomol. Chem.* **2010**, *8*, 43. (b) Zhu, F.-Q., Wang, W., Li, H.-X. *J. Am. Chem. Soc.* **2011**, *133*, 11632. (c) Dindulkar, S. D., Kwan, B., Lim, K. T., Jeong, Y. T. *J. Chem. Sci.* **2013**, *125*, 101.

product was obtained in a high yield when Au^{3+} or Au$^+$ salts were used as catalysts, although they proposed that the alkyne was only activated by Au(I) species. In the case of catalysts based in Au^{3+} species, the active Au(I) was generated *in situ* by the reduction of gold with the alkyne. Interestingly, Au^0 did not present any activity for this reaction. Other authors reported similar behaviour with different kinds of Au(I) and Au(III) catalysts.[199]

In order to facilitate the recyclability of the gold catalyst some authors reported the application of heterogeneous or nanosized gold species for this reaction.[285] As mentioned in 1.2.2.3 section, different types of Au NPs have been employed for that transformation, from *in situ* generated Au(0) and Au(I) NPs to supported Au NPs.[195,203,204,205,207] With these nanosized Au catalysts, the nature of the real catalytic species is still a source of discussion. Some authors, especially with supported NPs, suggested that Au(I)/Au(III)species stabilized by the support were the active catalytic sites, [195,205] which seems consistent with what is observed under catalysis by gold complexes. However, other authors have confirmed a zerovalent state for the Au NPs.[113,116,207]

Both with gold complexes or gold NPs, the most accepted mechanism starts with the coordination of the catalyst **A** with the alkyne, leading to the formation of a π-metal-alkyne complex **B**, which makes more acidic the terminal proton (step **a**). This would be followed by the abstraction of this proton and subsequent formation of the σ-metal complex **C** (step **b**), which would react with the iminium cation to form the final product **D**. The catalytic cycle would end with the recovery of the catalyst for the next cycle (step **c**) (**Scheme 25**).[286]
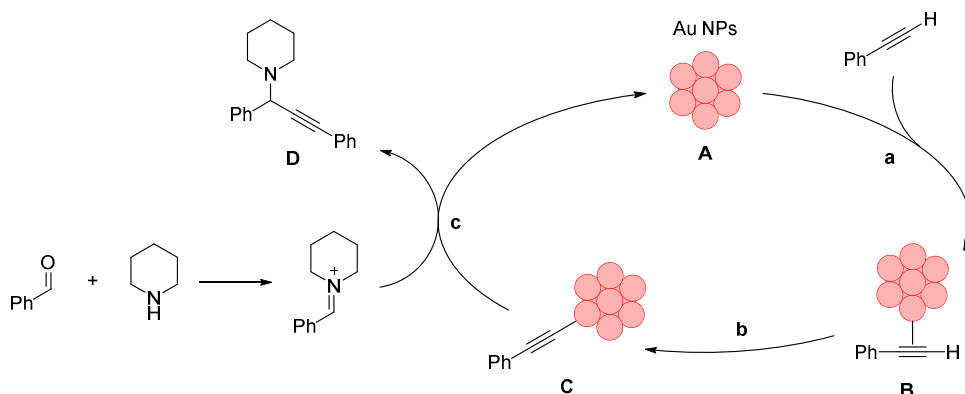
Scheme 25 Commonly proposed mechanism for the A^3 coupling between aldehydes, amines and alkynes catalyzed by Au NPs.

4.3.2 A^3 COUPLING CATALYZED BY AU NPS STABILIZED BY PEG-TAGGED IMIDAZOLIUM SALTS

In order to test the catalytic activity of the synthesised Au NPs, their application in the synthesis of propargylamines was considered. As starting point, the A^3 coupling between benzaldehyde **21a**, morpholine **22a** and phenylacetylene **12a** was planned in order to find the optimal conditions (**Table 12**). All the reactions were monitored by TLC and then the yield was determined by ^{1}H NMR using 4-methoxyphenol as internal standard. As previously mentioned in the objectives, we were interested in the use of aqueous medium with our water-soluble gold NPs.

[285] Kantam, M. L., Prakash, B. V., Reddy, C. R. V., Sreedhar, B. *Synlett* **2015**, *15*, 2329.
[286] Kidwai, M., Bansal, V., Kumar, A., Mozumdar, S. *Green Chem.* **2007**, *9*, 742.

Table 12 Optimization of the synthesis of propargylamines via A[3] coupling between benzaldehyde, morpholine and phenylacetylene catalyzed by Au NPs (**M14**, **M15** or **M16**).

Entry[a]	Catalyst	Solvent	Temperature (º C)	Reactor	Yield (%)[b]
1[c]	**M16**	H_2O (3 mL)	reflux	open to air	-
2	**M16**	H_2O (3 mL)	reflux	open to air	traces
3	**M15**	H_2O (3 mL)	reflux	open to air	-
4	**M16**	-	100	open to air	93
5	**M16**	-	100	Closed vessel	96
6[d]	**M16**	H_2O (1 mL)	100	Closed vessel	95
7	**M14**	H_2O (1 mL)	100	Closed vessel	-
8	**M16**	-	120	Closed vessel	95
9	**M14**	-	100	Closed vessel	80

[a] Reaction conditions: **21a**: 0.5 mmol; **22a**: 0.65 mmol; **12a**: 0.7 mmol; 0.5 mol% of Au, 24 h [b] Yield by ^{1}H NMR. [c] Benzyl alcohol as substrate (see text). [d] 48 h.

As a preliminary experiment and taking into account some reports on the use of Au NPs as catalyst in oxidation reactions,[287] we tried to obtain the benzaldehyde *in situ* by the oxidation of benzyl alcohol under an air flux (entry 1 of **Table 12**). The reaction was performed with **M16** (0.5 mol%), in refluxing water. Unfortunately, the formation of benzaldehyde was not observed after 24 h of reaction and, consequently, the propargylamine **23aaa** was not formed. For this reason, in the following experiments benzaldehyde, freshly distilled, was used as starting material.

When the reaction was tried with a slight excess of the amine and the alkyne, using **M15** and **M16** as catalysts (0.5 mol%) in boiling water in an open-air round bottom flask, the desired product was not obtained in significant amount (entries 2 and 3 of **Table 12**). An alternative green option would be to perform the reaction in the absence of solvent. Under neat conditions the reactivity was undoubtedly improved obtaining the product **23aaa** (93%) after 24 hours of reaction (entry 4 of **Table 12**). With the aim to increase the reactivity and to simplify the experimental procedure, we decided to carry out the reaction in a closed vessel, obtaining similar results (entry 5 of **Table 12**, **23aaa** 96%). When a small amount of water was added, the reaction time required for a good conversion of the reagents increased substantially (**Table 12** Entry 6, **23aaa** 95% after 48 h) and **M14** failed to react under these conditions (entry 7 of **Table 12**) Finally, no improvement was found by increasing the temperature to 120 ºC (entry 8 of **Table 12**) and **M14** was less active than **M16** (compare entries 5 and 9 of **Table 12**).
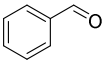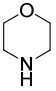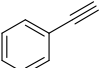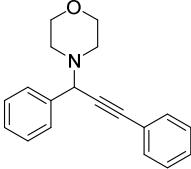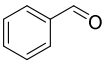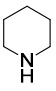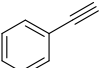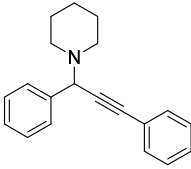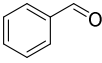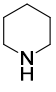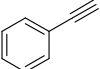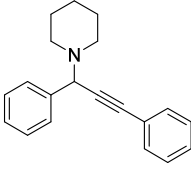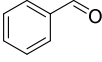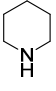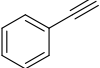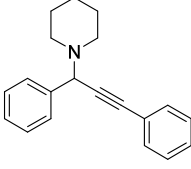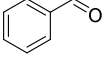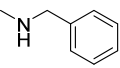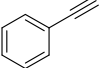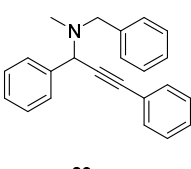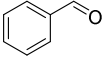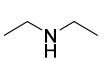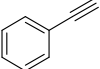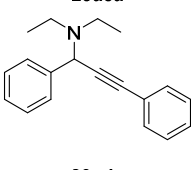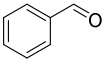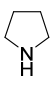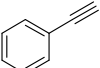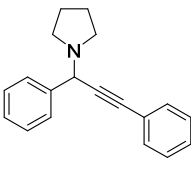
So, we concluded that the best conditions for this reaction were: neat, in a closed vessel at 100 ºC. Also, we observed that the Au NP **M16** stabilized by PEG-tagged tris-imidazolium salt **S3** present better catalytic activity for this reaction than Au NPs **M14** and **M15** stabilized by PEG tagged imidazolium salts **S1A-B**.

Next, we examined the scope of the reaction with different aldehydes, amines and terminal alkynes and the results are summarized in **Table 13**.

---
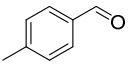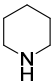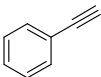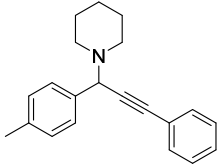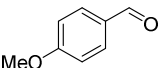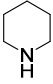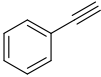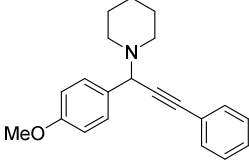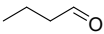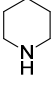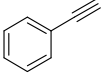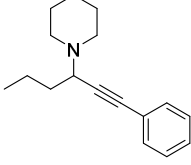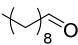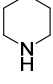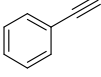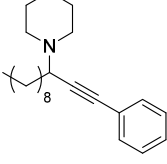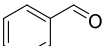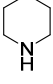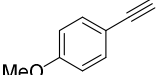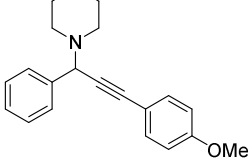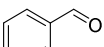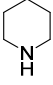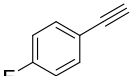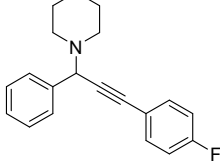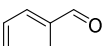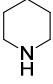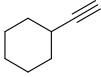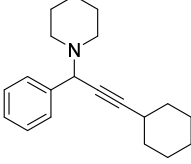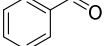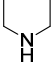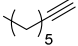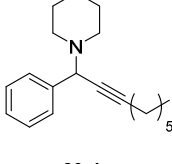
[287] Corma, A., Navas, J., Sabater, M. J. *Chem. Eur. J.* **2012**, *18*, 14150.

92

Table 13 A[3] coupling between aldehydes, amines and terminal alkynes catalyzed by Au NPs (**M14**, **M15** or **M16**).

Entry[a]	Catalyst	Aldehyde	Amine	Alkyne	Product	Yield (%)[b]
1	**M16**	21a	22a	12a	23aaa	84
2	**M16**	21a	22b	12a	23aba	96
3	**M14**	21a	22b	12a	23aba	58
4	**M15**	21a	22b	12a	23aba	36
5	**M16**	21a	22c	12a	23aca	97
6	**M16**	21a	22d	12a	23ada	87
7[c]	**M16**	21a	22e	12a	23aea	35

8	**M16**	21b	22b	12a	23bba	98
9	**M16**	21c	22b	12a	23cba	85[d]
10	**M16**	21d	22b	12a	23dba	89
11	**M16**	21e	22b	12a	23eba	83
12	**M16**	21a	22b	12b	23abb	94
13	**M16**	21a	22b	12c	23abc	54
14[e]	**M16**	21a	22b	12d	23abd	20
15	**M16**	21a	22b	12e	23abe	-

[a] Reaction conditions: **21**: 0.5 mmol; **22**: 0.65 mmol; **12**: 0.7 mmol; in a closed vessel of 4 mL [b] yield determined by ^{1}H NMR using 4-methoxyphenol as internal standard. [c] **21a**: 1 mmol; **22e**: 2 mmol; **12a**: 1.25 mmol; in a closed vessel of 15 mL. [d] Isolated yield. [e] **21a**: 1 mmol; **22b**: 1.25 mmol; **12d**: 2 mmol; in a closed vessel of 15 mL.

Under the optimized conditions, the reaction of benzaldehyde and phenylacetylene under catalysis by **M16** yielded the desired product using cyclic secondary amines, such as morpholine **22a** and piperidine **22b** in excellent yields (**Table 13** entry 1, **23aaa** 84% ^{1}H NMR yield; **Table 13** entry 2, **23aba** 96% ^{1}H NMR yield). Nanomaterials **M14** and **M15** were found much less active than **M16** giving, under the same conditions, the product **23aba** in a 56 and 36% yield for **M14** and **M15** respectively (**Table 13** entries 3 and 4, **Table 4-5**). This could be explained by the highest amount of Au(I) species that present **M16** in front of **M14** and **M15**. As it has been mentioned previously, in the literature most of the authors have observed that oxidized gold species take a crucial role in the catalytic activity for that reaction, being the Au(0) based catalysts inactive in most cases. This is in agreement with our results in which the nanocatalyst with higher amount of oxidized gold species becomes the most active. Acyclic secondary amines such as *N*-benzylmethylamine **22c** and diethylamine **22d** performed very well for this reaction under **M16** catalysis (**Table 13** entry 5, **23aca** 97% ^{1}H NMR yield; **Table 13** entry 6, **23ada** 87% ^{1}H NMR yield). However, with pyrrolidine **22e** the yield of product was much lower reaching just a 35 % (entry 7 of **Table 13**).

Other substituted aromatic aldehydes and aliphatic aldehydes gave also good results in the reaction with piperidine and phenylacetylene (entries 8-11 of **Table 13**). Taking into account the proposed mechanism for this reaction (**Scheme 25**), it seems that the nature of the terminal alkyne has an effect in the yield of the reaction. In that way, strong electron donor groups, such as methoxy (alkyne **12b**, could facilitate the formation of metal-alkyne complex, which results into a higher yield of final product (**Table 13** entry 12, **23abb** 94% ^{1}H NMR yield). When fluorine is the substituent of the alkyne, the yield drops considerably reaching just a 54% of **23abc** (entry 13 of **Table 13**). Noteworthy, poor yields were achieved when nonaromatic terminal alkynes were used, obtaining just a 20% of product **23abd** with cyclohexylacetylene **12d** (entry 14 of **Table 13**) and without formation of product **23abe** with 1-octyne **12e** (Entry 15 of **Table 13**).

A few authors reported the application of this reaction to ketones instead of aldehydes.[288] After the good results obtained with aldehydes, the application of the A^3 coupling of ketones, secondary amines and phenylacetylene catalyzed by Au NPs was investigated (**Table 14**).
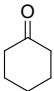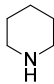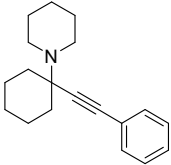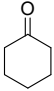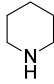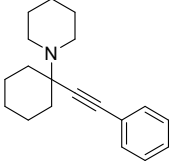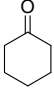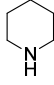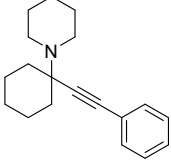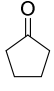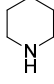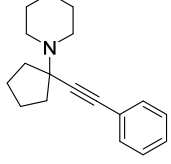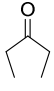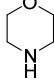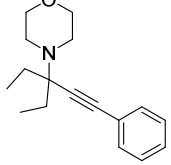
Table 14 A^3 coupling between ketones, amines and terminal alkynes catalyzed by Au NPs (**M14**, **M15** or **M16**).

Entry[a]	Catalyst	Ketone	Amine	Product	Yield (%)[b]
1	**M16**	**24a**	**22a**	**25aaa**	96

---

[288] (a) Cheng, M., Zhang, Q., Hu, X.-Y., Li, B.-G., Ji, J.-X., Chan, A. S. C. *Adv. Synth. Catal.* **2011**, *353*, 1274. (b) Hosseini-Sarvari, M., Moeini, F. *New J. Chem.* **2014**, *38*, 624.

2	**M16**	24a	22b	25aba	97
3	**M14**	24a	22b	25aba	70
4	**M15**	24a	22b	25aba	30
5	**M16**	24b	22b	25bba	80
6	**M16**	24c	22a	25caa	33

[a] Reaction conditions: **24**: 0.65 mmol; **22**: 0.5 mmol; **12a**: 0.7 mmol; in a closed vessel of 4 mL [b] yield determined by ^{1}H NMR using 4-methoxyphenol as internal standard.

Cyclic ketones (cyclohexanone **24a** and cyclopentanone **24b**) were coupled with cyclic secondary amines (morpholine **22a** and piperidine **22b**) and phenylacetylene **12a**, giving the correspondent propargylamines in high yield when catalyzed by **M16** (**Table 14** entry 1, **25aaa** 96% ^{1}H NMR yield; **Table 14** entry 2, **25aba** 97% ^{1}H NMR yield; **Table 14** entry 5, **25bba** 80% ^{1}H NMR yield). As was previously observed with aldehydes, **M14** and **M15** exhibit less activity than **M16** obtaining the corresponding product **25aba** only with 70 and 30% yield respectively (entries 3 and 4 of **Table 14**). The use of an acyclic ketone **24c** resulted in a much lower yield of product **25caa** compared with cyclic ketones (**Table 14** entry 6, **25caa** 33% ^{1}H NMR yield).

In general, **M16** present a high activity as catalyst in the A[3] coupling processes, both with aldehydes and ketones as substrates. Conversely, **M14** and **M15** present a much lower performance, which could be attributed to different factors. The first one, which was already mentioned, is the lower proportion of Au(I) species. Moreover, an influence related with the structural features of the stabilizers could be found. Comparing the results obtained with **M14** and **M15** for the synthesis of **23aba** and **25aba** (**Table 13**, entries 3 and 4 and **Table 14**, entries 3 and 4) with the results under **M16** catalysis (**Table 13**, entry 2 and **Table 14**, entry 2), we observed that the nanoparticles that contained three imidazolium units in the stabilizer (**M16**) were much more active than the NPs that only contained one imidazolium unit in the stabilizer (**M14** and **M15**). Also, the counter anion present in the imidazolium salt may exert an influence in the activity of the catalyst. In that way, **M14** with bromide anion was better as catalyst for the A[3] coupling than **M15** with

tetrafluoroborate anion. That anion effect in the catalytic activity was previously observed in our group using Pd NPs stabilized with tris-imidazolium salts as catalyst in Suzuki cross-coupling reactions.[230a]

So, the final catalytic performance of the materials must be a sum of the three factors: the amount of oxidized gold species, the number of imidazolium cations and the counter-anions present in the stabilizer of the NPs.

4.3.3 RECYCLABILITY OF THE AU NPS IN THE A^3 COUPLING BETWEEN BENZALDEHYDE, *N*-BENZYLMETHYLAMINE AND PHENYLACETYLENE

The reusability of the catalyst was tested in the coupling reaction between benzaldehyde **21a**, *N*-benzylmethylamine **22c** and phenyacetylene **12a** catalyzed by **M16** (**Table 15**).

Table 15 Recycling of the Au NPs (**M16**) in the A^3 coupling between benzaldehyde, *N*-benzylmethylamine and phenylacetylene.

Cycle[a]	Yield (%)[b]
1	96
2	97
3	93
4	89

[a] Reaction conditions: **21a**: 0.5 mmol; **22c**: 0.65 mmol; **12a**: 0.7 mmol; in a closed vessel of 4 mL. [b] Yield determined by ^{1}HRMN using 4-methoxyphenol as internal standard.

The work-up employed for the recovery of the Au NPs started with the addition of diethyl ether in order to precipitate the catalyst. Then the NPs were centrifuged, and the supernatant was removed by decantation. The NPs were washed again with diethyl ether and the process of centrifugation-decantation was repeated. Then, after drying the particles, they were ready for another run. This methodology was applied for 4 consecutive runs (96, 97, 93 and 89% yield), observing just a slightly decrease in the yield in the last cycles.

In order to check the stability of the Au NPs after the reaction, **M16** was analysed by XPS after the last cycle (**Figure 38**). Unexpectedly, the XPS of the recycled NPs (**Figure 38 (B)**) shows a much less proportion of Au(I) species compared with the fresh Au NPs (**Figure 38 (A)**). This fact could explain the decrease in the activity of the catalyst upon reuse. This was consistent with the lower activity observed with **M14** and **M15** catalysts which present lower amounts of Au(I) species.
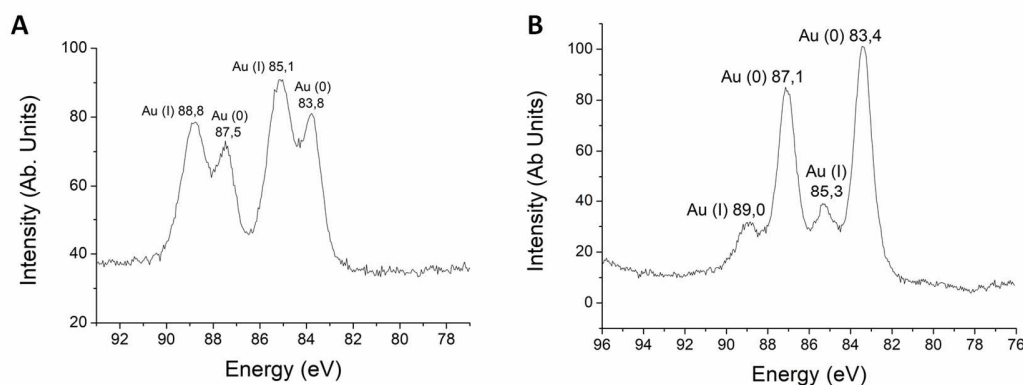
Figure 38 XPS spectra of **M16** (A) before the catalysis and (B) after the catalysis of the A^3 coupling reaction.

4.4 CYCLOISOMERIZATION OF ALKYNOIC ACIDS INTO ENOL-LACTONES CATALYZED BY AU NPs.

4.4.1 INTRODUCTION TO CYCLOISOMERIZATION OF ALKYNOIC ACIDS

Catalytic cycloisomerization of γ-alkynoic acids has become one interesting and atom-economical method for the synthesis of enol-lactones. Exo-cyclic enol-lactones are present in many natural organic molecules and in synthetic key intermediates of interest.[289,290,291]

Typically, this reaction has been accomplished under catalysis by metal species, generally complexes. Au(I) and Au(III)-NHC complexes have been extensively reported for cycloisomerization reactions.[292] Michelet and collaborators have described an heterogeneous gold catalyst for this reaction by precipitation of AuCl$_3$ into different solid supports.[293] In that way the authors found that cationic gold species supported on zeolite beta-NH$_4^+$ exhibit high activity for that transformation. Recently, various cycloisomerization processes have been reported under supported Au(0) NPs catalysis.[294,295,296] However, we have not found evidence of the use of soluble Au NPs for this kind of reactions.

Previously, our group has applied silica supported NHC-AuCl complexes as catalysts for the cycloisomerization of internal alkynes (**Scheme 26 (A)**). The reaction was performed in a biphasic system under stirring by a wrist type shaker. Different enol-lactones have been obtained by this method, in all cases with excellent conversions.[297]

The proposed general mechanism for the intramolecular addition of a nucleophile to an alkyne under Au(I) catalysis is outlined in **Scheme 26 (B)**.[298a] Importantly, it is worth to remind that in this reaction, apart from obtaining the desired 5-membered ring enol-lactone coming from a *5-exo-dig* cyclization, it can be generated a 6-membered ring derived from the corresponding *6-endo-dig* cyclization according to the Baldwin rules (**Scheme 26 (C)**).[298b] Usually the *5-exo-dig* cyclization is favoured for terminal alkynes.

[289] Mellor, J. M., Mohammed, S. *Tetrahedron* **1993**, *49* (34), 7547.

[290] Haga, Y., Okazaki, Shuto, Y. *Biosci. Biotechnol. Biochem.* **2003**, *67* (10), 2215.

[291] Zheng, Y., Liu, J., Lei, X. *Org. Chem. Front.* **2020**, *7*, 660.

[292] (a) Tomás-Mendivil, E., Toullec, P. Y., Borge, J., Conejero, S., Michelet, V., Cadierno, V. *ACS Catal.* **2013**, 3086. (b) Belger, K., Krause, N. *Org. Biomol. Chem.* **2015**, *13*, 8556. (c) Gasperini, D., Maggi, L., Dupuy, S., Veenboer, R. M. P., Cordes, D. B., Slawin, A. M. Z., Nolan, S. P. *Adv. Synth. Catal.* **2016**, *358*, 3857.

[293] Neatu, F., Li, Z., Richards, R., Toullec, P. Y., Genêt, J.-P., Dumbuya, K., Gottfried, J. M., Steinrück, H.-P., Pârvulescu, V. I., Michelet, V. *Chem. Eur. J.* **2008**, *14*, 9412.

[294] Eriksson, K., Verho, O., Nyholm, L., Oscarsson, S., Bäckvall, J.-E. *Eur. J. Org. Chem.* **2015**, 2250.

[295] Zorba, L., Kidonakis, M., Saridakis, I., Stratakis, M. *Org. Lett.* **2019**, *21*, 5552.

[296] Schröder, F., Erdmann, N., Noël, T., Luque, R., Van der Eycken, E. V. *Adv. Synth. Catal.* **2015**, *357*, 3141.

[297] (a) Ferré, M., Cattoën, X., Wong Chi Man, M., Pleixats, R. *ChemCatChem* **2016**, *8*, 2824. (b) Ferré, M. *Doctoral thesis*, Universitat Autònoma de Barcelona, **2015**.

[298] (a) Loh, C. C. J., Enders, D. *Chem. Eur. J.* **2012**, *18*, 10212. (b) Baldwin, J. E. *J. Chem. Soc., Chem. Commun.* **1976**, 734.

(A)

Cat.

(B)

(C)
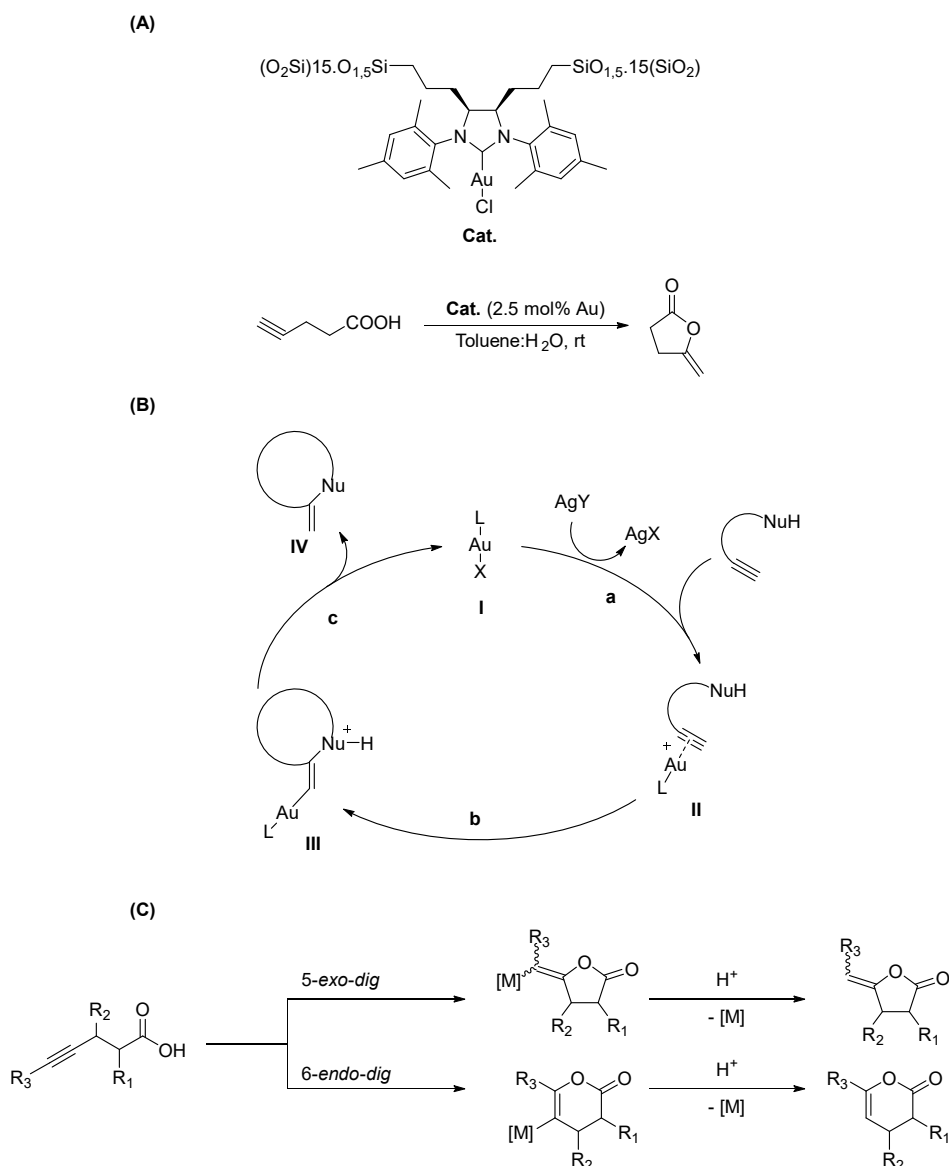
Scheme 26 (A) Silica supported NHC-AuCl developed by our group for the cycloisomeriztion of γ-alkynoic acids into enol-lactones;[297] **(B)** general mechanism for the intramolecular addition of a nucleophile to an alkyne under Au(I) catalysis;[298a] **(C)** Cycloisomerization products according to the Baldwin rules.[298b]
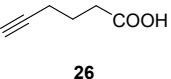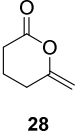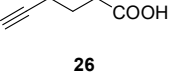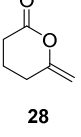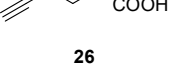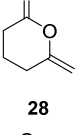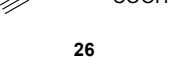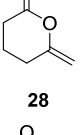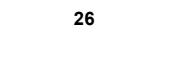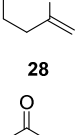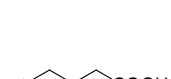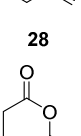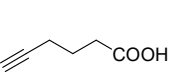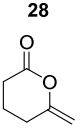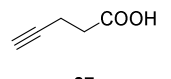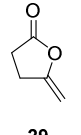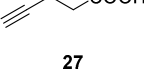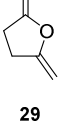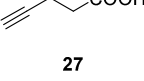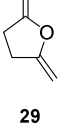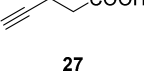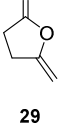
4.4.2 CYCLOISOMERIZATION OF Γ-ALKYNOIC ACIDS INTO ENOL-LACTONES CATALYZED BY AU NPS STABILIZED BY PEG-TAGGED IMIDAZOLIUM SALTS

After the good results achieved in our group on the cycloisomerization of alkynoic acids catalyzed by supported NHC-AuCl complexes, we planned the use of the water-soluble Au NPs for this transformation. Initial experiments were undertaken with 1 mol% of Au in order to optimize the reaction conditions (solvent, temperature, reaction time, type of stirring), which are summarized in **Table 16**.

Table 16 Optimization of the cycloisomerization of γ-alkynoic acids into enol-lactones catalyzed by Au NPs (**M14**, **M15** or **M16**).

Entry[a]	Catalyst	Solvent	γ-Alkynoic acid	Enol-lactone	T (º C)	Time (h)	Stirring	Yield (%)[b]

Entry	Catalyst	Solvent	Substrate	Product	Temp	Time	Method	Yield
1	M15	Toluene:H₂O (1:1)	26	28	rt	24	Magnetic stirring	18
2	M15	Toluene:H₂O (1:1)	26	28	40	40	Magnetic stirring	60
3	M14	Toluene:H₂O (1:1)	26	28	40	40	Magnetic stirring	43
4	M14	H₂O	26	28	40	18	Magnetic stirring	12
5	M16	H₂O	26	28	100	24	Magnetic stirring	-
6	M16	Toluene:H₂O (1:1)	26	28	rt	40	shaker	57
7	M15	Toluene:H₂O (1:1)	26	28	rt		Shaker	31
8	M14	Toluene:H₂O (1:1)	26	28	rt	24	Shaker	traces
9	M14	Toluene:H₂O (1:1)	27	29	rt	24	Shaker	>99
10	M15	Toluene:H₂O (1:1)	27	29	rt	24	Shaker	>99
11	M16	Toluene:H₂O (1:1)	27	29	rt	24	Shaker	>99

[a] Reaction conditions: γ-Alkynoic acid: 0.3 mmol; solvent: 2 mL; in a closed vessel of 4 mL. [b] Yield of enol-lactone determined by ^{1}H NMR.

Initially, we tested the more challenging cycloisomerization of 5-hexynoic acid **26** catalyzed by Au NPs **M14** and **M15** stabilized by PEG-tagged imidazolium salts **S2A** and **S2B**. For these first reactions a biphasic system

of toluene:water (1:1) was used as solvent, in which the Au NPs will remain in the aqueous phase and the reactant and product in the organic phase (**Figure 39 (B)**). To ensure the complete mixing of the biphasic system the solution was vigorously magnetically stirred at room temperature. Unfortunately, the six-membered ring cyclic lactone **28** was only obtained in 18% yield after 24 h (entry 1 of **Table 16**). For that reason, the temperature was increased to 40 ºC, performing the reaction in a sealed tube. In that case, we achieved a 60% yield of **28** after 40 h (entry 2 of **Table 16**), although the nanoparticles precipitated and they could not be reused. Then, the catalyst **M14** was tested under these conditions, but lower yield was observed (43%, entry 3 of **Table 16**). By changing the biphasic mixture of solvents to only water a deleterious effect on the activity was found (**Table 16** entry 4, 12% of **28** with **M14**). Then, Au NPs **M16** were used in the reaction with water as solvent and at 100 ºC, but the NPs precipitated quickly and the lactone was not formed (entry 5 of **Table 16**).

The previous results in our group showed that the stirring method plays a crucial role in the outcome of this reaction. For this reason, after these preliminary experiments, a change in the stirring method was planned. So, the use of a wrist type shaker (**Figure 39 (A)**) was tried to ensure a complete mixing of the immiscible phases. Thus, the reaction was tested in toluene:water (1:1) at room temperature under this kind of stirring. Under these conditions the conversion of the alkynoic acid to the product **28** was improved for **M16** and **M15** (**Table 16** entry 6, 57% for **M16**; **Table 16** entry 7, 31% for **M15**). However, no conversion was obtained with **M14** as catalyst (entry 8 of **Table 16**). Under these conditions the cycloisomerization of 4-pentynoic acid **27** was tried with the three catalysts. For this substrate the results were excellent, obtaining an almost complete conversion to the five-membered ring enol-lactone **29** with the three catalysts (entries 9, 10 and 11 of **Table 16**).

Figure 39 (A) wrist type shaker; **(B)** biphasic system of toluene-water used for this reaction.

Finally, the optimized conditions for the cycloisomerization of 4-pentynoic acid were stablished as follows: biphasic medium of toluene:water (1:1) at room temperature under stirring with a wrist type shaker. Noteworthy, the biphasic medium facilitates the isolation of the final product, a simple decantation is required to separate the catalyst from the products.

With the optimized conditions in hand, the reaction was performed with other alkynoic acids. With the aim to increase the number of different substrates, the hydrolysis of 2,2-di(prop-2-yn-1-yl)malonate **30** was performed to prepare the corresponding substituted terminal alkynes: 2-(methoxycarbonyl)-2-(prop-2-yn-1-yl)pent-4-ynoic acid **31** and 2,2-di(prop-2-ynyl)malonic acid **32**, following previously described procedures.[294,299] In **Table 17** we summarize the results with **M14**, **M15** and **M16** for the cycloisomerization reaction of the mentioned substrates.

---

[299] Alemán, J., Solar, V., Navarro-Ranninger, C. *Chem. Commun.* **2010**, *46*, 454.

Table 17 Cycloisomerization of γ-alkynoic acids into enol-lactones catalyzed by Au NPs (**M14**, **M15** or **M16**).

Entry[a]	Catalyst	γ-alkynoic acid	*Enol*-lactone	Time (h)	Yield (%)[b]
1	**M16**	27	29	50 min	99
2	**M14**	27	29	2	99
3	**M15**	27	29	3	97
4	**M16**	31	33	24	92
5	**M14**	31	33	24	65
6	**M15**	31	33	24	53
7	**M16**	32	34	48	95

[a] Reaction conditions: γ-alkynoic acid: 0.3 mmol; toluene:H₂O 1:1, 2 mL; in a closed vessel of 4 mL; under wrist type stirring. [b] Yield determined by ¹H NMR using 4-methoxyphenol as internal standard.

As it can be observed, with the three Au catalysts the desired 5-methylene-dihydrofuran-2-one **29** was obtained with almost quantitative yield. However, with **M16** the reaction was much faster (**Table 17** entry 1, **29** 99% ¹H NMR yield for **M16** in 50 min) than with **M14** and **M15** (**Table 17** entry 2, **29** 99% ¹H NMR yield for **M14** in 2 h; **Table 17** entry 3, **29** 97% ¹H NMR yield for **M15** in 3h). The higher activity of **M16** was also evident in the case of the α-disubstituted lactone **33** which was obtained in a 92% yield after 24 h of reaction (entry 4 of **Table 17**) instead of the 65 and 53% achieved with **M14** and **M15** after the same reaction time (**Table 17** entries 5 and 6, respectively). Finally, the spiranic dilactone **34** was afforded by a double cycloisomerization process catalyzed by **M16** with a 95% yield after 48 h (entry 7 of **Table 17**).

These results were consistent with the activity observed with the three catalysts in the A³ coupling reactions. Also in this case, the catalyst **M16**, with a higher amount of Au(I) species, present higher activity than **M14**

and **M15**. As it has been previously mentioned, generally the reported Au based catalysts for this reaction contained oxidized gold species as the active catalyst.

4.4.3 RECYCLABILITY OF THE AU NPS IN THE CYCLOISOMERIZATION OF 4-PENTYNOIC ACID

Noteworthy, the biphasic system greatly facilitates the recyclability of the catalyst by having the products and the catalyst in two different and immiscible phases. As can be observed in **Figure 39 (B),** the Au NPs remained in the aqueous phase (reddish colour) and the product in the organic phase (colourless). Thus, a simple decantation allowed the separation of the product. Then the aqueous layer can be directly reused in the subsequent cycle. With this methodology, the catalyst **M16** was reused successfully up to 6 times with excellent yields in the cycloisomerization of 4-pentynoic acid (**Table 18**). A slight decrease in the obtained yield was observed after a few cycles. This can be caused by some degradation of the active species of the Au NPs and by some losses of the catalyst during the decantation process.

Table 18 Recyclability of the Au NPs (**M16**) for the cycloisomerization of 4-pentynoic acid.
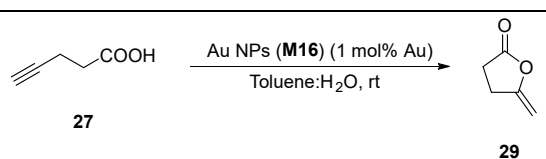
Cycle[a]	Time (h)	Yield (%)[b]
1	1	99
2	1	96
3	1	92
4	1	95
5	1	90
6	1	88

[a] Reaction conditions: γ-alkynoic acid: 0.3 mmol; toluene:H_2O 1:1, 2 mL; in a closed vessel of 4 mL; under wrist type stirring. [b] Yield determined by ^{1}H NMR using 4-methoxyphenol as internal standard.

4.5 HYDROSILYLATION OF INTERNAL ALKYNES CATALYZED BY PT AND RH NPS

4.5.1 INTRODUCTION TO HYDROSILYLATION OF INTERNAL ALKYNES

The hydrosilylation reaction consists in the addition of silanes to unsaturated chemical bonds. Thus, a wide number of different molecules can be obtained. The hydrosilylation reactions were discovered in 1947, when Sommer et al. described the reaction between trichlorosilane and 1-octene in the presence of diacetyl peroxide to give *n*-octylchlorosilane.[300] Later, other authors applied similar methodologies to different types of organic compounds containing unsaturated bonds (**Scheme 27**).
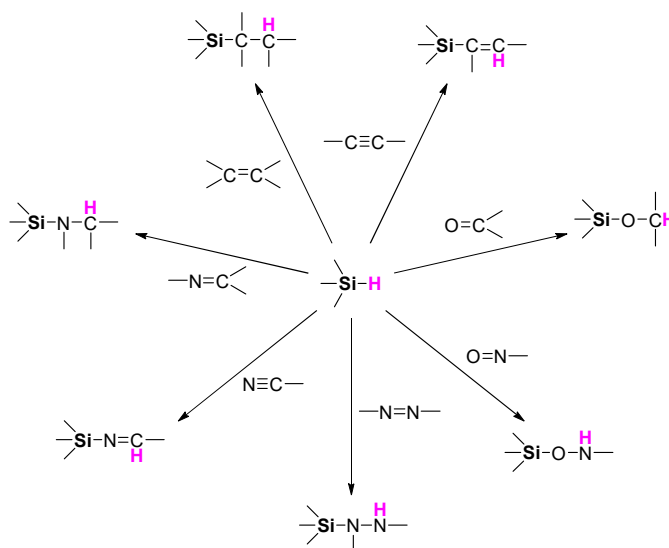
Scheme 27 Hydrosilylation of different kinds of unsaturated bonds.

The organosilicon compounds obtained with these processes have gained a huge importance. Specifically, vinylsilanes are widely used as building blocks in modern organic synthesis. In general, this kind of compounds provide advantages in terms of cost, low molecular weight, chemical stability and low toxicity. One of the most important applications of vinylsilanes is their use in the Hiyama coupling with aryl halides.[301] Moreover, they are also employed in the formation of vinyl iodides[302] or in the Tamao-Fleming oxidation.[303,304]

Nowadays, transition-metal catalyzed hydrosilylation of alkynes represents the most straightforward, powerful, convenient and atom-efficient method for the preparation of alkenylsilanes.[305] Notwithstanding, the main drawback of these reactions is their performing in a regio- and stereoselective way. As summarized in **Scheme 28**, depending on the alkyne used, several different isomeric vinyl silanes can be obtained. In the case of terminal alkynes (**Scheme 28 (a)**), in general the most affordable substrates, three different products can be achieved. In the case of internal alkynes, two different products can be formed when the alkyne is symmetric (**Scheme 28 (b)**) and four different products when the alkyne is asymmetrically substituted (**Scheme 28 (c)**).

[300] Sommer, L. H., Pieteusza, E. W., Whitmore, F. C. *J. Am. Chem. Soc.* **1947**, *69*, 188.

[301] Hiyama, T., Nakao, Y. *Chem. Soc. Rev.* **2011**, *40*, 4893.

[302] May, T. L., Dabrowski, J. A., Hoveyda, A. H. *J. Am. Chem. Soc.* **2011**, *133*, 736.

[303] (a) Tamao, K., Ishida, N., Tanaka, T., Kumada, M. *Organomet.* **1983**, *2*, 1964. (b) Fleming, I., Sanderson, P. E. J. *Tetrahedron Lett.* **1987**, *28* (36), 4229.

[304] Jones, G. R., Landais, Y., *Tetrahedron* **1996**, *52* (22), 7599.

[305] *Hydrosilylation: A Comprehensive Review on Recent Advances, Advances in Silicon Science Series*, Marciniec, B., Maciejewski, H., Pietraszuk, C., Pawluc, P. Ed.: Springer Verlag: Berlin, Heidelberg, **2009**, Vol1, Chapter 2.
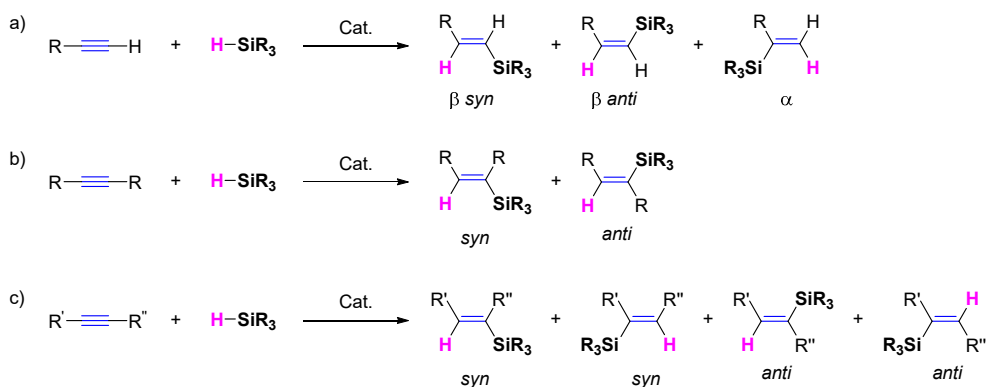
Scheme 28 Possible isomers formed in the hydrosilylation of **(a)** terminal, **(b)** symmetric or **(c)** asymmetric alkynes.

Platinum-based catalysts are the most commonly used for the hydrosilylation of unsaturated bonds. Traditionally, Speier's (H_2PtCl_6) and Karstedt's ($Pt_2[Me_2SiCH=CH_2)_2O]_3$ catalysts, have been the choice for these transformations (**Figure 40**).[306,307] Speier's catalyst needs an induction time to reduce the Pt(IV) species to Pt(0) to make it catalytically active. Instead, Karstedt's catalyst is active without that induction time and, additionaly, offers better results of reactivity and regioselectivity. Generally, this catalyst has been used with terminal alkynes, giving mainly the product of the *syn* addition to the β position of the corresponding alkynes.
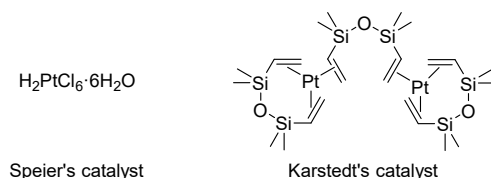
Figure 40 Traditional Pt catalysts used in the hydrosilylation of alkynes.

To overcome the limitations of these traditional Pt-based catalysts, recently, alternative Pt complexes containing N-heterocyclic carbenes, chelating acyclic aminocarbenes or bulky phosphine ligands have been investigated for the hydrosilylation of olefins and acetylenes.[210c,308,309]

Other transition-metal based complexes have been studied. Ruthenium based catalysts, have gained importance due their high stereoselectivity, although generally presented lower reactivity. In the **Figure 41** the most common ruthenium catalysts are shown, such as [RuCl$_2$(*p*-cymene)]$_2$ developed by Chang,[310] the Grubbs catalysts[211a,311] or the Trost's catalyst.[312] Notably, Trost's catalyst works well with internal alkynes, which are typically more challenging substrates. Moreover, some reports have been published on the use of Rh(I) and Pd complexes as catalysts for different hydrosilylation reactions.[313,314]

---

[306] Speier, J. L., Webster, J. A., Barnes, G. H. *J. Am. Chem. Soc.* **1957**, *79*, 974.

[307] (a) Karstedt, B. D. U.S. Patent 3 775 452, **1973**. (b) Chandra, G., Lo, P. Y., Hitchcock, P. B., Lappert, M. F. *Organometal.* **1987**, *6*, 191. See also ref. 210a

[308] (a) Zak, P., Bolt, M., Kubicki, M., Pietraszuk, C. *Dalton Trans.* **2018**, *47*, 1903. (b) Dierick, S., Vercruysse, E., Berthon-Gelloz, G., Markó, I. *Chem. Eur. J.* **2015**, *21*, 17073.

[309] Ortega-Moreno, L., Peloso, R., Maya, C., Suárez, A., Carmona, E. *Chem. Commun.* **2015**, *51*, 17008.

[310] Na, Y., Chang, S. *Org. Lett.* **2000**, *2* (13), 1887.

[311] (a) Menozzi, C., Dalko, P. I., Cossy, J. *J. Org. Chem.* **2005**, *70*, 10717. (b) Aricó, C. S., Cox, L. R. *Org. Biomol. Chem.* **2004**, *2*, 2558.

[312] (a) Trost, B. M., Ball, Z. T. *J. Am. Chem. Soc.* **2001**, *123*, 12726. (b) Trost, B. M., Ball, Z. T. *J. Am. Chem. Soc.* **2005**, *127*, 17644.

[313] (a) Sanada, T., Kato, T., Mitani, M., Mori, A. *Adv. Synth. Catal.* **2006**, *348*, 51. (b) Monney, A., Albrecht, M. *Chem. Commun.* **2012**, *48*, 10960.

[314] Zhou, H., Moberg, C. *Org. Lett.* **2013**, *15* (7), 1444.

[RuCl₂(*p*-cymene)]₂ Grubbs 1st generation Grubbs 2nd generation

Grubbs-Hoveyda 2nd generation Trost's catalyst
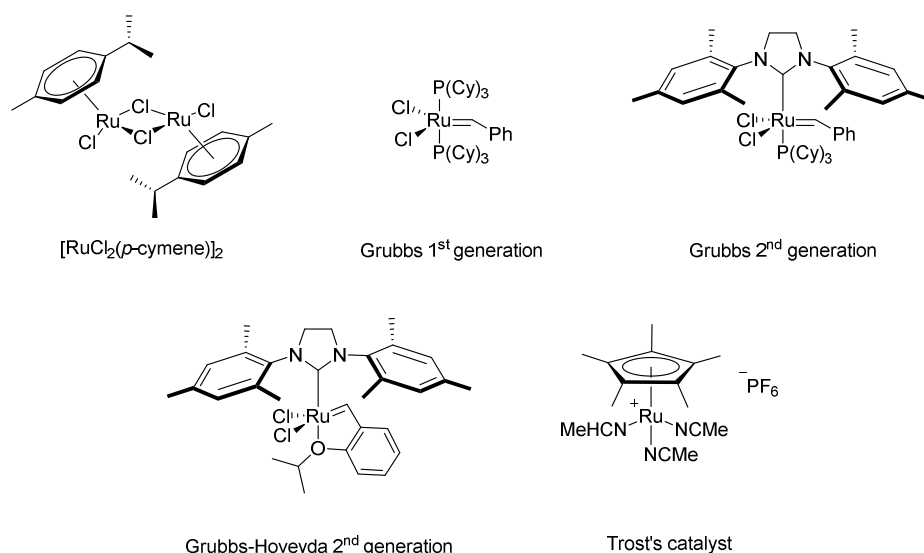
Figure 41 Ruthenium complexes applied for the hydrosilylation of alkynes.

Unfortunately, these kinds of complexes are, in general, difficult to recycle. For this reason, some supported Pt catalysts have been developed. However, some examples using organic polymers, carbon, magnesium oxide or alumina as a support, did not offer good results of recycling. Recently, the use of titania or silica supported Pt NPs has also been reported. These catalysts seem to give better results, although after some catalytic runs the yield decreases considerably.[212] Pt NPs impregnated into magnetite have been reused several times without loss of activity.[213] Other metal NPs have also been reported for hydrosilylation of different unsaturated bonds.[214]

The mechanism for the hydrosilylation of alkynes has become a topic of discussion in several publications. Nowadays, the mechanism commonly accepted is the one proposed by Chalk and Harrod for the first Pt catalysts, and later modified by Crabtree and Ojima.[315,316] This mechanism is often known as the Crabtree-Ojima cycle.

Khlobystov et al. have prepared Rh species confined into carbon nanotubes for the hydrosilylation of phenylacetylene.[317] These authors found that the selectivity of the reaction was affected by the confinement effects of the catalyst. So, they use the mechanism shown in **Scheme 29** to explain the number of different products obtained during the reaction with terminal alkynes.

The cycle starts with the oxidative addition of the silane (Si-H bond) to the metal centre (step **a**), followed by an *syn*-addition (step **b**) of the M-Si bond to the alkyne to form the intermediate **B**. A reductive elimination (step **c**) leads to the thermodynamically favourable, β-(*E*) vinylsilane **C** and the consequent recovery of the catalyst. Alternatively, the double bond of intermediate **B** can isomerize, relieving the steric repulsion, to form the intermediate **D**. Again, the reductive elimination (step **e**) of this intermediate, releases the β-(*Z*) product **E**. Besides, both η¹-vinylmetal intermediates (**B** or **D**) could be converted into an η² form (step **f**) that after a rearrangement gives the new η¹-vinylsilanes intermediates **F**, which will give the α addition product **G**. Also, the intermediate **B** can undergo metal hydride β-elimination (step **i**) giving the dehydrogenative product **H** along with metal hydride species, which can give rise to the alkene **I** by further reaction with the acetylenic substrate.

[315] Chalk, A. J., Harrod, J. F. *J. Am. Chem. Soc.* **1965**, *87* (1), 16.
[316] (a) Tanke, R. S., Crabtree, R. H. *J. Am. Chem. Soc.* **1990**, *112* (20), 7984. (b) Ojima, I., Clos, N., Donovan, R. J., Ingallina, P. *Organometal.* **1990**, *9*, 3127.
[317] Solomonsz, W. A., Rance, G. A., Suyetin, M., Torre, A. L., Bichoutskaia, E., Khlobystov, A. N. *Chem. Eur. J.* **2012**, *18*, 13180.

$H-SiR_3$

ML_n

a

L_nM-H
SiR_3
A

b

$R'-\!\!\!\equiv$

H SiR_3

R'   β-(E)
C

c

i

$H-ML_n$ SiR_3

R'   **B**

d

f

MH_2L_n + $R'-\!\!\!\equiv-SiR_3$
H

R'
$\|$

j

ML_n

R'
I

$H-ML_n$

R' SiR_3
D

f

ML_n

e

H SiR_3
L_nM
R'

H
L_nM
R' SiR_3

R'
G   α addition

h

ML_n

R'
$H-ML_n$ SiR_3

and/or

$H-ML_n$ R'
SiR_3

F

g

H
R' SiR_3

β-(Z)
E
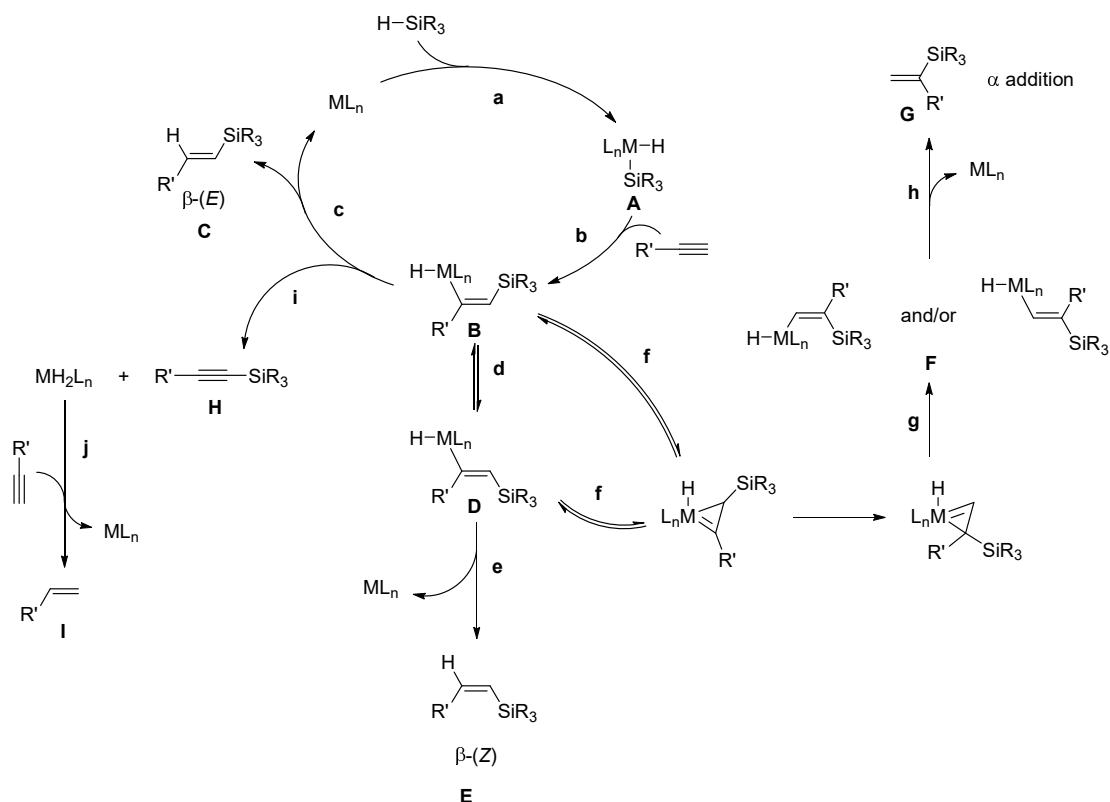
Scheme 29 Mechanism proposed for the metal-catalyzed hydrosilylation of alkynes.

Recently, our group has been interested in the hydrosilylaton of internal alkynes catalyzed by Pd and Rh NPs. In 2014, Dr. M. Planellas described an efficient and stereoselective *syn* addition of silanes to internal alkynes catalyzed by Pd NPs stabilized by tris-imidazolium tetrafluoroborates. The system requires complete anhydrous conditions and in presence of water a competitive transfer hydrogenation gives the corresponding alkenes or alkanes.[214a,231] Later, Dr. W. Guo prepared Rh nanoflowers stabilized by a N-rich PEG-tagged substrate for the hydrosilylation of internal alkynes. In that case the reaction proceeded well even in the presence of traces of water, without the formation of the reduction side-products.[214e,229]

4.5.2 PREPARATION OF INTERNAL ALKYNES AS STARTING SUBSTRATES
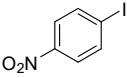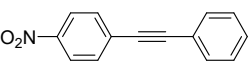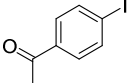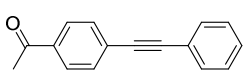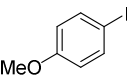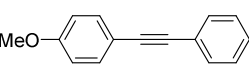
As mentioned previously in this chapter, Sonogashira reactions are commonly used for the preparation of diaryl internal alkynes.[159] As we have shown in **Scheme 20**, the classical conditions for this reaction involve a palladium/copper catalyst to form the C-C bond between a terminal alkyne and an aryl halide. However, in some cases, the copper cocatalyst can also lead to the homocoupling product of the terminal alkynes, reducing the yield of the desired internal alkyne. For this reason, alternative protocols of copper-free Sonogashira have been developed (see previous **Scheme 21**).[270]

To expand the range of internal alkynes as substrates for the hydrosilylation reaction, some asymmetric diaryl alkynes were prepared by the Sonogashira coupling between different aryl iodides and phenylacetylene. For these reactions we employed the conditions described by Zhang.[231,318] These conditions consist in the use of Pd(II) acetate as precatalyst, sodium hydroxide as base in a mixture of acetone-water at 60 ºC (**Table 19**).

---

[318] Shi, S., Zhang, Y. *Synlett* **2007**, *12*, 1843.

Table 19 Sonogashira cross-coupling reaction catalyzed by Pd(OAc)₂ for the preparation of asymmetric diaryl alkynes.

Entry[a]	Aryl iodide	Product	Yield (%)[b]
1	35	37	51
2	6	14	52
3[c]	36	38	77

[a] Reaction conditions: aryl iodide: 3 mmol; phenylacetylene: 3.9 mmol; Pd(OAc)₂ 0.06 mmol; NaOH: 6 mmol; acetone:H₂O 1.3:1, 21 mL; in a closed vessel. [b] isolated yield. [c] Reaction conditions: *p*-iodoanisole: 5.1 mmol; phenylacetylene: 6.6 mmol; Pd(OAc)₂ 0.102 mmol; NaOH: 10.2 mmol; acetone:H₂O 1.3:1: 42 mL; in a closed vessel.

4.5.3 HYDROSILYLATION OF SYMMETRIC INTERNAL ALKYNES CATALYZED BY PT NPS STABILIZED BY TRIS-IMIDAZOLIUM SALTS AND BY RH NPS STABILIZED BY PEG-TAGGED IMIDAZOLIUM SALTS

After the good previous results obtained by our group,[214a,e] the hydrosilylation of internal alkynes catalyzed by the synthesized Pt and Rh NPs was investigated. In that way, the first option was to apply the same conditions that have been successfully used by Dr. M. Planellas and Dr. W. Guo with Pd and Rh NPs. Firstly, mixtures of the nanocatalyst (**M5** for Pt; **M18**, **M19** or **M20** for Rh) and the corresponding acetylenic substrate in the presence of an excess of neat silane were heated at 90 ºC into a closed vessel (method A) (**Table 20**).

Table 20 Hydrosilylation of diphenylacetylene catalyzed by Pt (**M5**) or Rh (**M18**, **M19** or **M20**) NPs (method A).

Entry[a]	Metal	Catalyst	Time (h)	Conversion (%)[b]	Yield (%)[c]
1	Pt	**M5**	0.75	>99	89
2		**M18**	16	>99	76
3	Rh	**M19**	16	>99	84
4		**M20**	20	>99	68

[a] Reaction conditions: diphenylacetylene: 0.5 mmol; triethylsilane: 2 mmol; in a closed vessel. [b] Conversion of diphenylacetylene by GC. [c] isolated yield.

To our delight, complete conversion of the alkyne was reached in the reaction of diphenylacetylene with triethylsilane, being completely stereoselective for the formation of the *syn*-addition product **40**, with both kind of catalysts Pt (entry 1 of **Table 20**) and Rh NPs (entries 2, 3 and 4 of **Table 20**). Noteworthy, the reaction with Pt nanocatalyst **M5** was much faster than with Rh nanocatalysts **M18-M20**. Longer reaction times were also needed with the Pd (17 h of reaction) and Rh (6-40 h of reaction) NPs previously described in the group. Furthermore, inert and anhydrous conditions were not necessary with either Pt or Rh nanocatalysts.

However, with the aim to reduce the excess of silane, a suitable solvent for the reaction was sought. Indeed, the use of a minimum amount of Si-H reagent is desirable when using solid or more expensive silanes. In **table 21** we summarize the conditions tested with both Pt and Rh NPs.

Table 21 Hydrosilylation of diphenylacetylene catalyzed by Pt (**M5**) or Rh (**M18**, **M19** or **M20**) NPs (method B).

Entry[a]	Metal	Catalyst	Solvent	Conversion (%)[b]	Yield (%)[c]
1	Pt	**M5**	EtOH	25	-
2		**M5**	THF	>99	82
3	Rh	**M18**	EtOH	65	-
4		**M18**	THF	>99	86
5		**M19**	EtOH	73	-

[a] Reaction conditions: diphenylacetylene: 0.5 mmol; triphenylsilane: 0.6 mmol; solvent: 1 mL; in a closed vessel. [b] Conversion of diphenylacetylene by GC. [c] isolated yield.

The use of EtOH as solvent at 90 ºC in a closed vessel in the reaction of diphenylacetylene with triphenylsilane did not give the expected results (entries 1, 3 and 5 of **Table 21**) and some of the triphenylsilane **41** was oxidized to the corresponding silanol. Then, anhydrous THF was used as solvent at the same temperature for the reaction with **M5** and **M18** as catalysts. To our delight, complete conversion was achieved in both cases and silanol species were not detected in the final crude mixtures. Upon purification by flash chromatography the products were obtained in high yields (**Table 21** entry 2, **42** 82% isolated yield under **M5** catalysis; **Table 21** entry 4, **42** 86% isolated yield under **M18** catalysis).
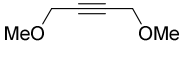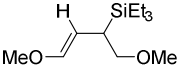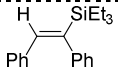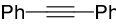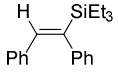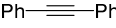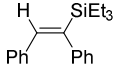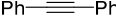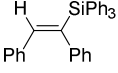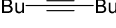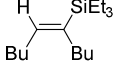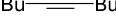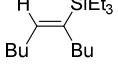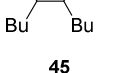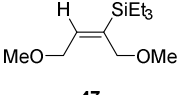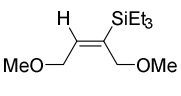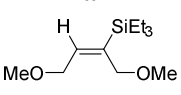
After these preliminary experiments, the reaction was performed with both Pt and Rh NPs with different symmetrically substituted internal alkynes. The results under neat conditions (method A) and using THF as solvent (Method B) are summarized in **Table 22**.

Table 22 Hydrosilylation of internal alkynes catalyzed by Pt (**M5**) or Rh (**M18**, **M19** or **M20**) NPs.

Entry	Metal	Catalyst	Alkyne	Product	Method A[a] Time (h)	Method A[a] Yield (%)[c]	Method B[b] Time (h)	Method B[b] Yield (%)[c]
1		**M5**	Ph—≡—Ph **13**	**40**	0.75	84	24	89
2	Pt	**M5**	Ph—≡—Ph **13**	**42**	_[d]	_[d]	24	82
3		**M5**	Bu—≡—Bu **43**	**45**	2	82	_[d]	_[d]

Entry	Catalyst	Substrate	Product	[a]	[b]	[c]	[d]
4	**M5**	MeO—≡—OMe **44**	H SiEt₃ vinylsilane **46**	1	79	24	83
5	**M18**	Ph—≡—Ph **13**	H SiEt₃ vinylsilane **40**	16	76	24	79
6	**M19**	Ph—≡—Ph **13**	H SiEt₃ vinylsilane **40**	16	84	_[d]	_[d]
7	**M20**	Ph—≡—Ph **13**	H SiEt₃ vinylsilane **40**	20	68	_[d]	_[d]
8	**M18**	Ph—≡—Ph **13**	H SiPh₃ vinylsilane **42**	_[d]	_[d]	24	86
9	**M18**	Bu—≡—Bu **43**	H SiEt₃ vinylsilane **45**	16	84	_[d]	_[d]
10	**M19**	Bu—≡—Bu **43**	H SiEt₃ vinylsilane **45**	16	66	_[d]	_[d]
11	**M20**	Bu—≡—Bu **43**	H SiEt₃ vinylsilane **45**	16	78	_[d]	_[d]
12	**M18**	MeO—≡—OMe **44**	H SiEt₃ vinylsilane **47**	16	68	24	97
13	**M19**	MeO—≡—OMe **44**	H SiEt₃ vinylsilane **47**	16	56	_[d]	_[d]
14	**M20**	MeO—≡—OMe **44**	H SiEt₃ vinylsilane **47**	_[d]	_[d]	24	90

Rh

[a] Reaction conditions: alkyne: 0.5 mmol; silane: 2 mmol; at 90 ºC in a closed vessel. [b] Reaction conditions: alkyne: 0.5 mmol; silane: 0.6 mmol; THF: 1 mL, at 90ºC in a closed vessel. [c] Full conversion in all cases; isolated yield of the mixture. [d] Not performed.

The vinylsilane **40** was obtained in high yield in a stereoselective manner under method A with both Pt and Rh NPs (**Table 22** entry 1, 84% under **M5** catalysis; **Table 22** entry 5, 76% under **M18** catalysis; entry 6, 84% under **M19** catalysis; **Table 22** entry 7, 68% under **M20** catalysis). Interestingly, Pt NPs have been found to be much more active obtaining the product after 45 min of reaction. With the three different Rh NPs, the reaction had to be left overnight for full conversion. When method B was applied, the reaction time increased considerably for both kinds of nanocatalysts (24 h for full conversion in all cases); nevertheless, the product was also obtained in high yields. In the reaction of diphenylacetylene with triphenylsilane under method B, the full conversion was also achieved after 24 h obtaining the product **42** in 82 and 86% of isolated yield with **M5** (entry 2 of **Table 22**) and **M18** (entry 8 of **Table 22**), respectively. Under method A, the non-aromatic substrate 5-decyne **43** yielded the corresponding vinylsilane **45** after 2 h with Pt NPs **M5** (**Table 22** entry 3, 82%) and after 16 h with Rh NPs **M18** (**Table 22** entry 9, 84%), **M19** (**Table 22** entry 10, 66%) and **M20** (**Table 22** entry 11, 78%).

The reaction of 1,4-dimethoxy-2-butyne **44** with triethylsilane catalyzed by Rh NPs gave the desired product **47** after 16 h under method A and after 24 h under method B (**Table 22** entry 12, A: 68% B: 97% with **M18**; **Table 22** entry 13, A: 56% with **M19**; **Table 22** entry 14, B: 90% with **M20**). Surprisingly, with Pt NPs **M5** this vinylsilane was not formed. In this case, the enol ether (*E*)-(1,4-dimethoxy-3-buten-2-yl)triethylsilane **46** was achieved in 79 and 83% yield with method A and B, respectively (entry 4 of **Table 22**). The product was completely characterized by NMR and HR-MS. The *trans* configuration of the olefinic bond was determined by NOE selective experiments. As can be observed in **Figure 42** a positive NOE effect was found between the selected olefinic proton (at 6.2 ppm) and the proton **H₄**. This effect is only possible if the double bond has a *trans* configuration. In the case of the *cis* isomer these two protons are too far away to present NOE effect.
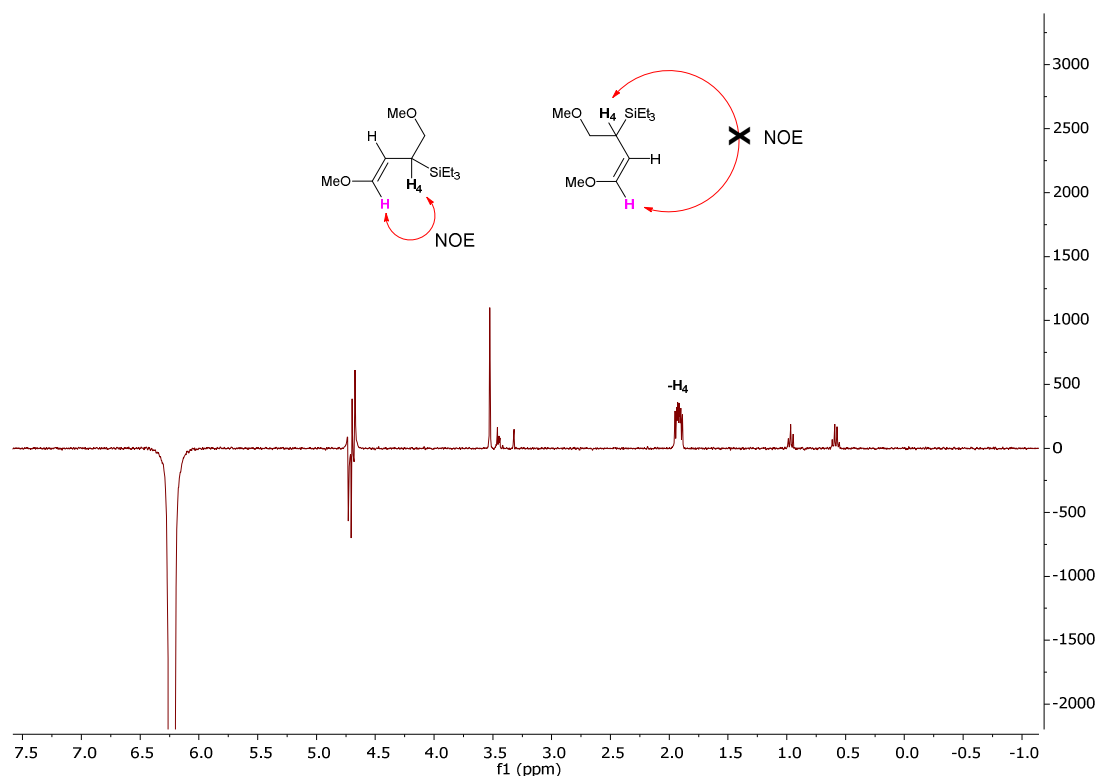
Figure 42 Selective NOE experiments to confirm the *trans* configuration of compound **46**.

In order to explain the formation of this product, an isomerization of the double bond after the addition of silane to the alkyne was postulated. In order to confirm this hypothesis, the (*E*)-(1,4-dimethoxy-2-buten-2-yl)triethylsilane **47** (prepared under Rh NPs catalysis) was submitted to the conditions of method A under Pt NPs **M5** catalysis. However, the starting vinylsilane was recovered unaltered (**Scheme 30**).
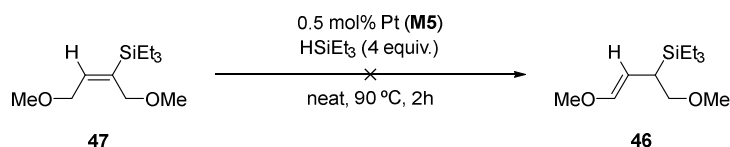
Scheme 30 The enol-ether **46** is not formed by isomerization of the vinylsilane **47**.

Consequently, this hypothesis was discarded. If we assume that the Chalk-Harrod (or a modified Chalk-Harrod) mechanism is operating (see previous **Scheme 29**), an isomerization or rearrangement should take place in the intermediate formed after alkyne insertion on Pt-Si (or Pt-H) bond, previously to the final reductive elimination.

It is worth to note the different behaviour of the alkyne **44** in the hydrosilylation reaction in front of different nanocatalysts (Pt, Rh, Pd), as the hydrosilylation of 1,4-dimethoxy-2-butyne **44** failed with the Pd NPs stabilized by tris imidazolium salt **S1B**, as Marc Planellas reported in his doctoral thesis.

111

4.5.4 HYDROSILYLATION OF ASYMMETRIC INTERNAL ALKYNES CATALYZED BY PT NPS STABILIZED BY TRIS-IMIDAZOLIUM SALTS AND BY RH NPS STABILIZED BY PEG-TAGGED IMIDAZOLIUM SALTS

The addition of triethylsilane to internal diaryl alkynes bearing two different aryl groups was also performed with both Pt and Rh NPs. In these cases, up to four possible vinylsilanes could be envisaged with two stereoisomers (*syn* and *anti*-addition) for each of the two regioisomeric forms. However, we have found that in most of the cases the reactions afforded only the regioisomers derived from the *syn* addition.

The hydrosilylation reactions of unsymmetric diaryl alkynes were carried out under the conditions of method A and the results with Pt (**M5**) and Rh (**M18**, **M19** and **M20**) NPs are summarized in **Table 23**.

Table 23 Hydrosilylation of unsymmetric diaryl alkynes under catalysis by Pt (**M5**) or Rh (**M18**, **M19** or **M20**) NPs.

Entry[a]	Metal	Catalyst	R	Product		Time (h)	Yield (%)[b]
1		**M5**	$-NO_2$ **37**	(*E*)-48a	(*E*)-48b	30	71 (68:32)[c]
2	Pt	**M5**	**14**	(*E*)-49a	(*E*)-49b	7	88 (58:42)[c]
3		**M5**	$-OMe$ **38**	(*E*)-50a	(*E*)-50b	4	99 (47:53)[c]
4		**M18**	**14**	(*E*)-49a	(*E*)-49b	16	98 (65:35)[c]
5	Rh	**M19**	**14**	(*E*)-49a	(*E*)-49b	16	73 (68:32)[c]

6	**M20**	**14**	(*E*)-49a	(*E*)-49b	16	85 (64:36)[c]
7	**M18**	**38**	(*E*)-50a	(*E*)-50b	48	85 (43:57)[c]
8	**M19**	**38**	(*E*)-50a	(*E*)-50b	24	97 (44:56)[c]
9	**M20**	**38**	(*E*)-50a	(*E*)-50b	24	92 (36:64)[c]

[a] Reaction conditions: alkyne: 0.5 mmol; triethylsilane: 2 mmol; at 90ºC in a closed vessel. [b] Full conversion in all cases; isolated yield of the mixture. [c] Molar ratio of the regioisomers determined by NMR techniques.

As mentioned, in all cases a complete selectivity for the *syn* addition was observed. The regioselectivity was from low to moderate, depending on the substituent present in the aryl ring and on the catalyst used. In general, the favoured isomer was the one with the triethylsilyl group closest to the more electron-deficient aryl ring, in accordance with the previous experience of the group in the hydrosilylation of this kind of substrates with Pd NPs.[214a,231] A report by Ferreira relates the electronic effect of the substituents with the regioselectivities obtained in the final vinylsilanes.[319]

In that way, under Pt NPs catalysis (**M5**) the presence of electron-withdrawing groups (nitro and acetyl) in the aryl moiety favours the regioisomers (*E*)-**48a** and (*E*)-**49a** (**Table 23** entry 1, (*E*)-**48a**:(*E*)-**48b** 68:32, 71% isolated yield; **Table 23** entry 2, (*E*)-**49a**:(*E*)-**49b** 58:42, 88% isolated yield). Consequently, the presence of an electron-donating group (methoxy) in the aryl moiety gives a slight selectivity for the position close to the unsubstituted aryl (**Table 23** entry 3, (*E*)-**50a**:(*E*)-**50b** 47:53, 99% isolated yield).
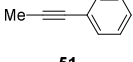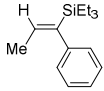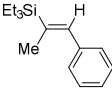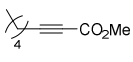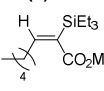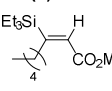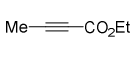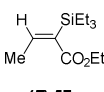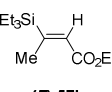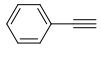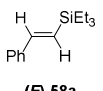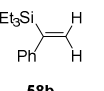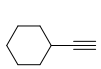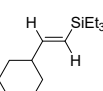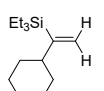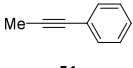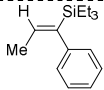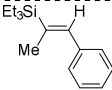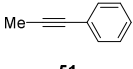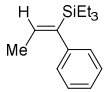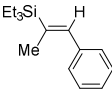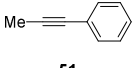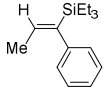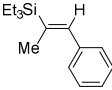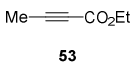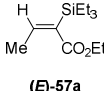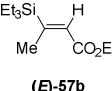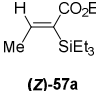
In the case of Rh NPs (**M18**, **M19** and **M20**) stabilized by PEG-tagged imidazolium salts **S2A-B** and **S3** longer reaction times were needed for full conversion, which is in accordance with the results obtained with symmetric alkynes. However, under Rh catalysis the regioselectivity was higher. Thus, with the electron-withdrawing substituent (acetyl group) in one aryl ring, better selectivity for the (*E*)-**49a** vinylsilane was observed (**Table 23** entry 4, (*E*)-**49a**:(*E*)-**49b** 65:35, 98% isolated yield for **M18**; **Table 23** entry 5, (*E*)-**49a**:(*E*)-**49b** 68:32, 73% isolated yield for **M19**; **Table 23** entry 6, (*E*)-**49a**:(*E*)-**49b** 64:36, 85% isolated yield for **M20**), compared with the reaction under Pt catalysis for the same substrate. With an electron-donating substituent in the aryl ring, low regioselectivities were observed with the Rh NPs stabilized by **S2A-B** (**Table 23** entry 7, (*E*)-**50a**:(*E*)-**50b** 43:57, 85% isolated yield for **M18**; **Table 23** entry 8, (*E*)-**50a**:(*E*)-**50b** 44:56, 97% isolated yield for **M19**). In contrast, Rh NPs stabilized by **S3** provided higher selectivity (**Table 23** entry 9, (*E*)-**50a**:(*E*)-**50b** 36:64, 92% isolated yield for **M20**).

[319] Rooke, D. A., Ferreira, E. M. *Angew. Chem. Int. Ed.* **2012**, *124*, 3279.
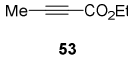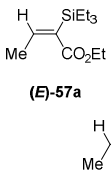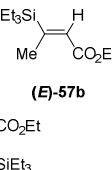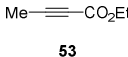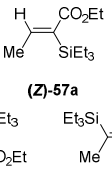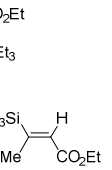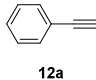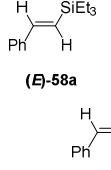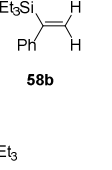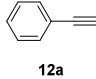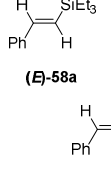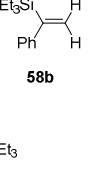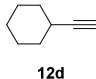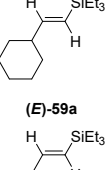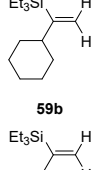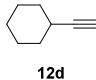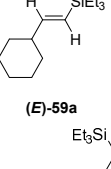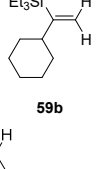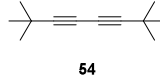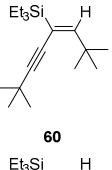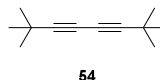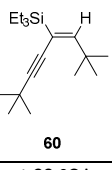
Chapter 4. Catalytic Activity of Metal Nanoparticles

After the experiments with unsymmetric diaryl alkynes, the hydrosilylation of unsymmetric internal alkynes bearing significantly different groups in each side was undertaken. Some terminal alkynes were also tested. The results with Pt (**M5**) and Rh (**M18**, **M19** or **M20**) catalysts are summarized in **Table 24**.

Table 24 Hydrosilylation of differentiated unsymmetric internal alkynes and terminal alkynes under catalysis by Pt (**M5**) or Rh (**M18**, **M19** or **M20**) NPs.

R—≡—R' + HSiEt₃ (**39**) → (0.5 mol% Pt (**M5**) or 0.5 mol% Rh (**M18, M19 or M20**); Method A: neat, 90 ºC; Method B: THF, Δ, Ar) → vinylsilane products

Ent.	Metal	Cat.	Alkyne	Product	Method A[a] t (h)	Method A[a] Yield (%)[c]	Method B[b] t (h)	Method B[b] Yield (%)[c]
1		**M5**	**51** (Me—≡—Ph)	(E)-55a / (E)-55b	1.3	84 (58:42) [e]	24	90 (59:41)[e]
2		**M5**	**52**	(E)-56a / (E)-56b	1	72 (85:15) [e]	–[f]	–[f]
3	Pt	**M5**	**53** (Me—≡—CO₂Et)	(E)-57a / (E)-57b	1	81 (64:36) [e]	24	98 (67:33) [e],[g]
4		**M5**	**12a**	(E)-58a / 58b	1.3	82 (83:17) [e]	24	94 (90:10) [e],[h]
5		**M5**	**12d**	(E)-59a / 59b	1.5	80 (62:38) [e]	–[f]	–[f]
6		**M18**	**51** (Me—≡—Ph)	(E)-55a / (E)-55b	15	69 (76:24) [e]	24	98 (76:24) [e]
7		**M19**	**51** (Me—≡—Ph)	(E)-55a / (E)-55b	16	75 (77:23) [e]	24	94 (77:23) [e]
8	Rh	**M20**	**51** (Me—≡—Ph)	(E)-55a / (E)-55b	–[f]	–[f]	24	99 (78:22) [e]
9		**M18**	**53** (Me—≡—CO₂Et)	(E)-57a / (E)-57b / (Z)-57a	–[f]	–[f]	24	80 (11:14:74)[e]

Entry	Catalyst	Substrate	Products				
10	**M19**	Me—≡—CO₂Et **53**	(*E*)-57a, (*E*)-57b, (*Z*)-57a	_[f]	_[f]	24	85 (10:19:71)[e]
11	**M20**	Me—≡—CO₂Et **53**	(*E*)-57a, (*E*)-57b, (*Z*)-57a	_[f]	_[f]	24	79 (14:15:71)[e]
12	**M18**	**12a**	(*E*)-58a, 58b, (*Z*)-58a	20	85 (65:25:10)[e]	_[f]	_[f]
13	**M19**	**12a**	(*E*)-58a, 58b, (*Z*)-58a	20	79 (59:30:11)[e]	_[f]	_[f]
14	**M18**	**12d**	(*E*)-59a, 59b	23	36 (80:20)[e]	_[f]	_[f]
15	**M19**	**12d**	(*E*)-59a, 59b	23	47 (80:20)[e]	_[f]	_[f]
16	**M18**	**54**	**60**	16	99	_[f]	_[f]
17	**M19**	**54**	**60**	16	64	_[f]	_[f]

[a] Reaction conditions: alkyne: 0.5 mmol; triethylsilane: 2 mmol; at 90 ºC in a closed vessel. [b] Reaction conditions: alkyne: 0.5 mmol; triphenylsilane: 0.6 mmol; THF: 1 mL; at 90 ºC in a closed vessel. [c] Full conversion in all cases; isolated yield of the mixture. [e] Molar ratio of the regioisomers determined by NMR techniques. [f] Not performed. [g] Reaction at 60 ºC: (*E*)-57a:(*E*)-57b (74:26) 78% isolated yield. [h] Reaction performed at 60 ºC.

Under Pt catalysis (**M5**) only (*E*)-vinylsilanes derived from the *syn*-addition were obtained, with different regioselectivities depending on the substrate. The reaction of triethylsilane with prop-1-yn-1-ylbenzene **51** under both conditions gave moderate regioselectivity favoring the isomer with the silyl moiety attached to the carbon close to the phenyl group (**Table 24** entry 1, A: (*E*)-55a:(*E*)-55b 58:42, 84% isolated yield, B: (*E*)-55a:(*E*)-55b 59:41, 90% isolated yield). In the case of alkynoic esters, the regioselectivity increased in favour of the isomer with the triethysilyl moiety close to the ester group, as expected due its electron-withdrawing nature. Higher selectivity was observed in the case of methyl 2-octynoate **52** (**Table 24** entry 2, A: (*E*)-56a:(*E*)-56b 85:15, 72% isolated yield) compared with ethyl 2-butynoate **53** (**Table 24** entry 3, A: (*E*)-57a:(*E*)-57b 64:36,

81% isolated yield, B: (**E**)-**57a**:(**E**)-**57b** 67:33, 98% isolated yield). This difference may be caused by steric effects derived from the size of the pentyl chain. Interestingly, when the hydrosilylation of ethyl 2-butynoate **53** was performed at lower temperature under method B, a slight increase of selectivity was found (**Table 24** entry 3, (**E**)-**57a**:(**E**)-**57b** 74:26, 78% isolated yield). Two terminal alkynes, which did not react under catalysis by Pd NPs, were also tested. In the case of phenylacetylene **12a**, the vinylsilane derived from *beta syn*-addition was the major regioisomer (**Table 24** entry 4, A: (**E**)-**58a**:**58b** 83:17, 82% isolated yield, B (at 60ºC): (**E**)-**58a**:**58b** 90:10, 94% isolated yield). Similar results, but with lower regioselectivities, were found with ethynylcyclohexane **12d** (**Table 24** entry 5, A: (**E**)-**59a**:**59b** 62:38, 80% isolated yield).

As in the case of the hydrosilylation of diaryl alkynes, Rh NPs present higher regioselectivity with prop-1-yn-1-ylbenzene **51** as substrate than under Pt catalysis (**Table 24** entry 6 with **M18**, A: (**E**)-**55a**:(**E**)-**55b** 76:24, 69% isolated yield, B: (**E**)-**55a**:(**E**)-**55b** 76:24, 98% isolated yield; **Table 24** entry 7 with **M19**, A: (**E**)-**55a**:(**E**)-**55b** 77:23, 75% isolated yield, B: (**E**)-**55a**:(**E**)-**55b** 77:23, 94% isolated yield; **Table 24** entry 8 with **M20**, B: (**E**)-**55a**:(**E**)-**55b** 78:22, 99% isolated yield). For ethyl 2-butynoate **53**, higher regioselectivity was also observed in favour of the isomer with the silyl moiety close to the ester group. Unexpectedly, in that case the major isomer was that derived from the *anti*-addition (**Table 24** entry 9 with **M18**, B: (**E**)-**57a**:(**E**)-**57b**:(**Z**)-**57a** 11:14:74, 80% isolated yield; **Table 24** entry 10 with **M19**, B: (**E**)-**57a**:(**E**)-**57b**:(**Z**)-**57a** 10:19:71, 85% isolated yield; **Table 24** entry 11 with **M20**, B: (**E**)-**57a**:(**E**)-**57b**:(**Z**)-**57a** 14:15:71, 79% isolated yield). According to the Chalk-Harrod mechanism, we postulate that an isomerization should take place before the reductive elimination step in order to form the *anti*-addition product. Possibly, some interaction between the oxygen atoms of the ester group and the Rh atoms of the NPs can stabilize the corresponding intermediate and yield the *anti*-addition product as a major isomer (**Scheme 31**).

The formation of the β-*anti*-isomer was also observed with phenylacetylene **12a**, although in this case in a minor amount (**Table 24** entry 12 with **M18**, A: (**E**)-**58a**:**58b**:(**Z**)-**58a** 65:25:10, 85% isolated yield; **Table 24** entry 13 with **M19**, A: (**E**)-**58a**:**58b**:(**Z**)-**58a** 59:30:11, 79% isolated yield). It is worth to note that the formation of the *anti*-addition product with a different substrate was also described in a previous report of the group using other Rh NPs as catalyst, although in that case a spontaneous *E* to *Z* thermal isomerization was observed.[214e] Ethynylcyclohexane **12d** under Rh catalysis lead to poor yields although the regioselectivity was high towards the β-syn addition product and the β-*anti*-addition compound was not detected (**Table 24** entry 14 with **M18**, A: (**E**)-**59a**:**59b** 80:20, 36% isolated yield; **Table 24** entry 15 with **M19**, A: (**E**)-**59a**:**59b** 80:20, 47% isolated yield).

Finally, the hydrosilylation of symmetrical 1,3-diyne 2,2,7,7-tetramethylocta-3,5-diyine **54** was also successfully performed, affording exclusively the monohydrosilylation product under method A (**Table 24** entry 16 for **M18**, **60** 99% isolated yield; **Table 24** entry 17 for **M19**, **60** 64% isolated yield). This reaction was also tried under catalysis by Pt NPs without any activity after 24 h of reaction.
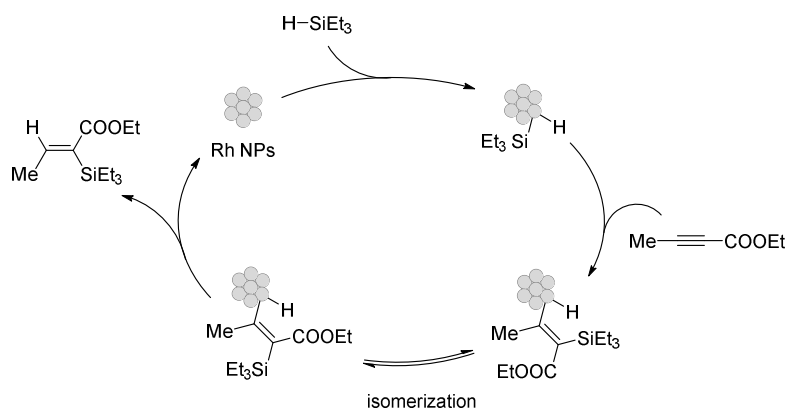
Scheme 31 Mechanism proposed for the formation of the *anti*-isomer *(Z)*-**57a** under Rh NPs catalysis according to the Chalk-Harrod cycle.

Finally, by comparing the results with the two metal based nanocatalysts (Pt and Rh), we can conclude: (a) the *syn*-addition was favoured in most cases; (b) in all cases Pt NPs present higher activity than Rh NPs (faster reactions); (c) the catalysis under Rh NPs leads to higher regioselectivities.

4.5.5 RECYCLABILITY OF THE PT AND RH NPS IN THE HYDROSILYLATION OF INTERNAL ALKYNES

As mentioned in chapter 3, the nature of the stabilizers provides different solubility to the corresponding metal NPs. Thus, the Pt NPs stabilized by **S1A-B** are soluble in CH_2Cl_2, $CHCl_3$, THF or toluene, and insoluble in hexane, diethyl ether, ethyl acetate or water. Instead, the PEG-tagged chains present in the stabilizers **S2A-B** and **S3** of the Rh NPs provide solubility in water, CH_2Cl_2 or THF and insolubility in diethyl ether, hexane or toluene. Taking profit of the solubility properties, the recyclability of the synthesized metal NPs for the hydrosilylation reaction of alkynes was studied.

Initially, the hydrosilylation of diphenylacetylene with Pt NPs (**M5**) was chosen to test the reusability under method A. The workup was the following: upon completion of the reaction diethyl ether o hexane was added to the reaction mixture, in which the Pt NPs were insoluble. This caused the precipitation of the nanocatalyst, which was separated by centrifugation/decantation (**Figure 43**). After repeating this process two more times to ensure the complete washing of the Pt NPs, the nanocatalyst was ready for another run.

Figure 43 Precipitation of the Pt NPs after the addition of hexane and centrifugation.

Using this procedure, the nanocatalyst was reused up to four times in the hydrosilylation of diphenylacetylene **13** with triethylsilane under method A (**Table 25**).

Table 25 Recycling of the Pt NPs (**M5**) in the hydrosilylation of diphenylacetylene under method A.

Ph———Ph + HSiEt₃ $\xrightarrow[\text{neat, 90 ºC}]{\text{0.5 mol % Pt (M5)}}$ Ph/Ph with H, SiEt₃

13   **39**   **40**

Cycle	Time (h)	Yield (%)
1[a]	1	99
2	1	97
3	1	98
4	1.5	95

[a] Reaction conditions: diphenylacetylene: 0.5 mmol; triethylsilane: 2 mmol; at 90 ºC in a closed vessel. [b] Full conversion in all cases. isolated yield.

In the first three runs the Pt NPs **M5** did not show a significant loss of activity, reaching full conversion after 1 h of reaction in all cases (entries 1-3 of **Table 25**). However, a higher reaction time was needed in the fourth cycle to achieve full conversion (entry 4 of **Table 25**). With the aim to explain this drop in the catalytic activity, a TEM analysis of the Pt NPs after the 4th cycle was performed. We observed in these images that the mean size of the nanoparticles was higher (5 ± 1.5 nm; **Figure 44 (B)**) than in the freshly prepared catalyst (1.6 ± 0.6 nm; **Figure 44 (A)**). Alternatively, an ICP-MS analysis of the crude product from this hydrosilylation reaction under method B (**Table 22**, entry 1) was performed. The amount of Pt present in this crude product represent

a 0.12 % of the initial amount of Pt added as catalyst. This small amount of Pt lost in each cycle and the agglomeration of the particles can explain the slight decrease of the catalytic activity.
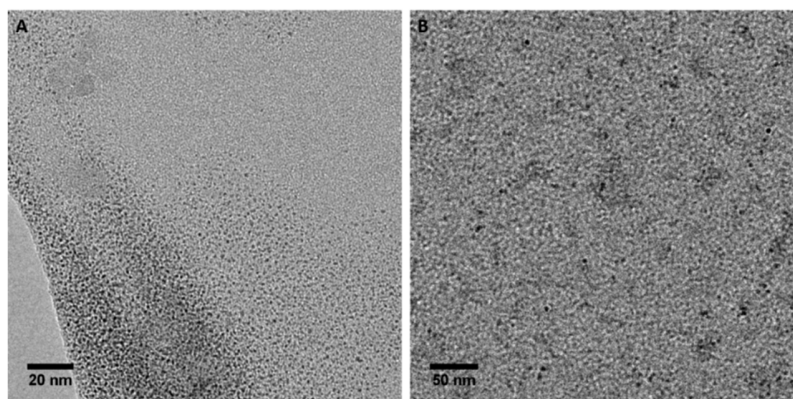
Figure 44 TEM images of Pt NPs (M5) (A) freshly prepared and (B) after four consecutive cycles of reaction.

Then, the reusability of the Pt nanocatalyst was tested with unsymmetric alkynes. Thus, ethyl 2-butynoate 53 was chosen as substrate for the reaction under method A (Table 26) and 1-phenyl-1-propyne 51 as substrate for method B (Table 27). In both cases, M5 could be reused up to five times. Whereas in the second case there was no loss of activity after all cycles, in the first case an increase of the reaction time was needed for full conversion after the first run.

Table 26 Recycling of the Pt NPs (M5) in the hydrosilylation of ethyl 2-butynoate 53 under method A.

Cycle[a]	(E)-57a:(E)-57b[b]	Time (h)	Yield (%)[c]
1	65:36	1	81
2	56:44	1.5	74
3	58:42	2	65
4	57:43	2	57
5	60:40	2	75

[a] Reaction conditions: alkyne: 0.5 mmol; triethylsilane: 2 mmol; 90 ºC in a closed vessel. [b] Molar ratio of the regioisomers determined by NMR techniques. [c] Full conversion in all cases; isolated yield of the mixture.

Table 27 Recycling of the Pt NPs (M5) in the hydrosilylation of 1-phenyl-1-propyne 51 under method B.

Cycle[a]	(E)-55a:(E)-55b[b]	Time (h)	Yield (%)[c]
1	59:41	24	90
2	61:39	24	98
3	64:36	24	99
4	60:40	24	99
5	57:43	24	97

[a] Reaction conditions: alkyne: 0.5 mmol; triethylsilane: 0.6 mmol; THF: 1 mL; 90 ºC in a closed vessel. [b] Molar ratio of the regioisomers determined by NMR techniques. [c] Full conversion in all cases; isolated yield of the mixture.

The reusability of Rh NPs (M18, M19 and M20) has also been tested, in that case only with 1-phenyl-1-propyne 51 under method B (Table 28). No significant decrease of the catalytic activity was found upon 5 cycles and the regioselectivity did not change in a significant manner.

Table 28 Recycling of the Rh NPs (**M18**, **M19** or **M20**) in the hydrosilylation of 1-phenyl-1-propyne **51** under method B.

Catalyst	Cycle[a]	(*E*)-55a:(*E*)-55b[b]	Time (h)	Yield (%)[c]
	1	76:24	24	98
	2	75:25	24	91
M18	3	76:24	24	99
	4	75:25	24	84
	5	78:22	24	80
	1	77:23	24	94
	2	77:23	24	93
M19	3	78:22	24	97
	4	79:21	24	94
	5	78:22	24	85
	1	76:24	24	80
	2	78:22	24	99
M20	3	79:21	24	99
	4	78:22	24	92
	5	77:23	24	86

[a] Reaction conditions: alkyne: 0.5 mmol; triethylsilane: 2 mmol; THF: 1 mL; 90 ºC in a closed vessel. [b] Molar ratio of the regioisomers determined by NMR techniques. [c] Full conversion in all cases; isolated yield of the mixture.

4.6 Reduction of nitroarenes catalyzed by Ni and Rh NPs

4.6.1 Introduction to reduction of nitroarenes

Nitroaryl compounds have a high environmental effect being one of the most common organic pollutants in agricultural or industrial wastewaters. This is caused by their extensive use as building blocks in the preparation of diverse products such as organic solvents, pesticides, dyes or explosives. Especially hazardous are the water-soluble nitroarenes, such as 4-nitrophenol which is carcinogenic among other health risks.[320] For this reason, the reduction process could be favourable in order to minimize the problems derived from these species in wastewater. Besides, the anilines obtained from the reduction of the nitro group of nitroarenes are very important as industrial raw materials.[321]

Historically, the production of anilines was achieved by the classical Béchamp reduction, firstly reported in 1854.[322] It consists on the reduction of nitroarenes to the corresponding aromatic amines by iron in aqueous acid. However, the slow reaction rates and the costly distillation process caused the loss of interest for this reaction in front of the most efficient catalytic hydrogenation. Transition metal heterogeneous catalysts (Pd, Pt, Ru, Ni) were the most employed for this transformation. These processes are considered environmentally desirable due to their simplicity and minimum production of waste. Nevertheless, the main drawback of the conventional heterogeneous catalytic hydrogenation is the low selectivity in front of other reducible functional groups.[323]

Recently, promising studies have found that metal NPs can be catalytically active in the reduction of nitroarenes to yield the corresponding amines in the presence of several reducing agents. As in the case of classical heterogeneous catalysts, the main drawback of the use of metal NPs in that transformation is their poor selectivity. In that way, a study published by Corma and collaborators showed that Au NPs supported on TiO_2 or Fe_2O_3 present high selectivity for the reduction of different nitroarenes, although hard reaction conditions were needed (high temperature and H_2 pressure).[324] In this work the authors also use Pt and Pd NPs supported on carbon, but these species present low selectivity in most cases. Other authors reported similar results with Au NPs supported on SiO_2.[325] Later on, several authors described the use of Pd[326] and Pt NPs[46,327] for that purpose, which exhibited good catalytic activity and selectivity under milder conditions than the Au NPs. Recently, some examples of supported Ni NPs have been reported as catalysts for the reduction of nitroarenes with different hydrogen sources, such as $NaBH_4$, high H_2 pressure, hydrazine or glycerol.[95a,328,329]

The mechanism proposed by Haber in 1898 is still an excellent description of the hydrogenation process (**Scheme 32**).[229,330] According to these mechanistic studies, the final product can be achieved by two pathways,

[320] (a) McCormick, N. G., Feeherry, F. E., Levinson, H. S. *Appl. Eviron. Microbiol.* **1976**, *31* (6), 949. (b) Kaplan, D. L., Kaplan, A. M. *Eviron. Sci. Technol.* **1982**, *16*, 566. (c) Boopathy, R., Gurgas, M., Ullian, J., Manning, J. F. *Current Microbiol.* **1998**, *37*, 127.

[321] Blaser, H.-U., Steiner, H., Studer, M. *ChemCatChem* **2009**, *1*, 210.

[322] (a) Béchamp, A. J. *Ann. Chim. Phys.* **1854**, *42*, 186. (b) Downing, R. S., Kunkeler, P. J., van Bekkum, H. *Catal. Today* **1997**, *37*, 121. (c) *Comprehensive Organic Name Reactions and Reagents. Béchamp Reduction;* Wang, Z. Ed.: John Wiley & Sons, Inc., **2010**.

[323] Dixon, D. J., Pando Morejón, O. In *Comprehensive Organic Synthesis II (second edition). Vol. 8 p. 479*; Breit, B., Diab, L., Knochel, P., Molander, G. A. Ed.: Elsevier Amsterdam, **2014**.

[324] Corma, A., Serna, P. *Science* **2006**, *313*, 332.

[325] Chen, Y., Qiu, J., Wang, X., Xiu, J. *J. Catal.* **2006**, *242*, 227.

[326] (a) Wu, H., Zhuo, L., He, Q., Liao, X., Shi, B. *Appl. Catal. A: Gen.* **2009**, *366*, 44. (b) Li, J., Shi, X.-Y., Bi, Y.-.Y., Wei, J.-F., Chen, Z.-G. *ACS Catal.* **2011**, *1*, 657.

[327] Lara, P., Philippot, K. *Catal. Sci. Technol.* **2014**, *4*, 2445.

[328] Romanazzi, G., Fiore, A. M., Mali, M., Rizzuti, A., Leonelli, C., Nacci, A., Mastrorilli, P., Dell'Anna, M. M. *Mol. Catal.* **2018**, *446*, 31.

[329] Pisiewicz, S., Formenti, D., Surkus, A.-E., Pohl, M.-M., Radnik, J., Junge, K., Topf, C., Bachmann, S., Scalone, M., Beller, M. *ChemCatChem* **2016**, *8*, 129.

[330] Song, J., Huang, Z.-F., Pan, L., Li, K., Zhang, X., Wang, L., Zou, J.-J. *Appl. Catal. B Environ.* **2018**, *227*, 386.

the direct route or the condensation route. In the direct route, the nitrobenzene **61** is reduced to the corresponding nitroso compound **A** (step **a**), which after a subsequent reduction (step **b**) yield the hydroxylamine **B**. Then, the hydroxylamine is reduced (step **c**) to give the desired aniline **62**. In the condensation route, instead, the nitroso compound **A** and the hydroxylamine **B** condensate into the azoxy compound **C** (step **d**). This compound is consecutively reduced to the azo compound **D**, hydrazo compound **E** and finally to the corresponding aniline **62**.
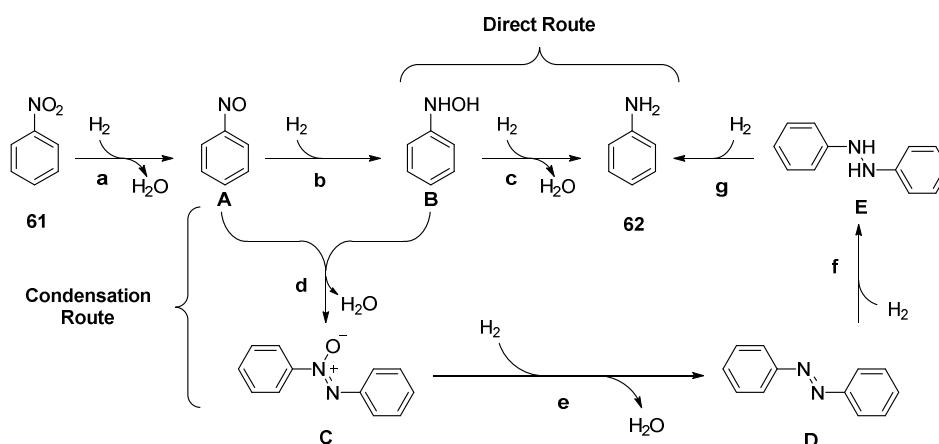
Scheme 32 Commonly accepted mechanism for the catalytic reduction of nitroarenes.

The mechanism of the reaction under catalysis by metal nanoparticles is still a source of debate. The most common theory, specially studied with supported Au NPs, involves the adsorption of the reducing agent and the nitroarenes on the surface of the material. In these cases, the adsorbed reducing agent (normally $NaBH_4$ or H_2) generates gold hydride species in the surface of the NPs, which is followed by a reversible adsorption of the nitroarene. Then, the nitroarene is reduced (following a direct or condensation route) by a hydrogen transfer process between the gold hydride species and the nitroarene.[331]

The reduction of nitroarenes catalyzed by water-soluble Au NPs stabilized by a nitrogen-rich polyoxyethylenated substrate has been previously reported in our group. The reaction was performed using an excess of $NaBH_4$ as reducing agent in water at room temperature. Due to their solubility properties, the catalyst was easily recycled up to four times.[228,229]

4.6.2 Reduction of nitroarenes catalyzed by Ni NPs stabilized by tris-imidazolium salts

Taking into account the results published in the literature (using supported Ni NPs) and the previous work made in the group with water-soluble Au NPs, we decided to test the catalytic activity of the previously synthesized soluble Ni NPs (**M11** and **M13**) for the reduction of nitroarenes. In the following **Table 29** we summarize the different conditions tested during the optimization of the reduction of nitrobenzene with hydrazine and sodium borohydride as hydrogen sources.

---

[331] (a) Corma, A., Concepción, P., Serna, P. *Angew. Chem. Int. Ed.* **2007**, *46*, 7266. (b) Khalavka, Y., Becker, J., Sönnichsen, C. *J. Am. Chem. Soc.* **2009**, *131*, 1871. (c) Wunder, S., Polzer, F., Lu, Y., Mei, Y., Ballauff, M. *J. Phys. Chem. C* **2010**, *114*, 8814. (d) Wang, C., Zou, W., Wang, J., Ge, Y., Lu, R., Zhang, S. *New J. Chem.* **2017**, *41*, 3865.

Table 29 Optimization of the conditions for the reduction of nitrobenzene catalyzed by Ni NPs (**M11** or **M13**).

Entry[a]	Catalyst	Solvent	Reductant	Temperature (ºC)	Time (h)	Products[b]
1	**M13**	EtOH	N₂H₄·H₂O	reflux	40	**62** / **63** 89:11
2[c]	**M13**	THF	N₂H₄·H₂O	reflux	20	**62** / **63** 96:4
3	**M13**	THF	N₂H₄·H₂O	r.t.	24	**62** / **63** 60:40
4	**M13**	H₂O:THF (1:4)	NaBH₄	r.t	24	**62** / **63** 46:54
5[d]	**M11**	THF	N₂H₄·H₂O	reflux	2	**62**

[a] Reaction conditions: nitrobenzene: 1 mmol; reductant: 8 mmol; 2 mol% Ni. [b] molar ratio of the products by GC-MS. [c] Aniline **62** 67% isolated yield. [d] Aniline **62** 97% isolated yield.

First, we tried the reaction in refluxing EtOH under catalysis (2 mol%) by Ni NPs stabilized by **S1B** (**M13**) using hydrazine as reductant (entry 1 of **Table 29**). After 40 h of reaction, all the initial nitrobenzene was consumed, but a mixture of aniline **62** and hydrazobenzene **63** was obtained (89:11 by GC-MS). A change of the solvent to THF, in which the catalyst was more soluble, resulted in a lower reaction time, obtaining almost full conversion of aniline after 20 h of reaction. However, still a small amount of hydrazobenzene was obtained (entry 2 of **Table 29**; **62:63** 96:4). The aniline was isolated in 67% yield. When the reaction was carried out with hydrazine in THF at room temperature for 24 h, lower selectivity was observed (entry 3 of **Table 29**, **62:63**, 60:40). Then we used NaBH₄ as reducing agent in H₂O:THF (1:4) as solvent at room temperature and these conditions resulted in poor selectivity, obtaining the aniline as minor product in front of hydrazobenzene (entry 4 of **Table 29**; **62:63**, 46:54). Finally, Ni NPs stabilized by **S1A** (**M11**) were used under the conditions of entry 2. This catalyst was found to be much more active and selective, yielding pure aniline as the only product after 2 h of reaction (entry 5 of **Table 29**; **62** 97% isolated yield). These final conditions under **M11** catalysis were chosen as optimal for the reduction of nitroarenes.

It is worth to mention that in the control experiments by GC-MS of entries 1, 2 and 3 we observed the presence of other reduction intermediates such as phenylhydroxylamine and azobenzene, besides the hydrazobenzene

present in large amount in the final product mixture. These intermediates disappeared during the progress of the reaction. According to these results, we can conclude that the condensation route is the most feasible pathway for this reduction (**Scheme 32**).

With the optimized conditions in hand, the reaction was extended to several nitroarenes bearing different functional groups, using **M11** as catalyst (**Table 30**). The hydrazine is a clean source of hydrogen as the *in situ* decomposition in the presence of metal generates H_2 and N_2.

Table 30 Scope of the reduction of nitroarenes under catalysis by Ni NPs (**M11**).

Entry[a]	Nitroarene	Aniline	ArNH$_2$:ArNO$_2$ [b]	Yield (%)[c]
1	61	62	> 99:1	97
2	64	73	> 99:1	52
3	65	74	> 99:1	77
4	66	75	> 99:1	95
5	67	76	> 99:1	87
6	68	77	97:3	45
7	69	78	> 99:1	91
8	70	79	> 99:1	63
9	71	80	89:11	74

| 10 | Ph—CH=CH—C₆H₄—NO₂ **72** | Ph—CH=CH—C₆H₄—NH₂ **81** | > 99:1 | 86 |

[a] Reaction conditions: nitrobenzene: 1 mmol; NH₂NH₂·H₂O: 8 mmol; Ni NPs (**M11**): 2 mol%, THF: 2 mL, reflux, 2 h. [b] molar ratio ArNH₂:ArNO₂ by TLC or ^{1}H NMR. [c] Isolated yield.

Thus, the Ni nanocatalyst (**M11**) has proved to be effective for the reduction of nitroarenes bearing electron-donating groups (**Table 30** entry 2, *m*-nitroaniline **64**, **73** 52% isolated yield; **Table 30** entry 3, *p*-nitroanisole **65**, **74** 77% isolated yield; **Table 30** entry 4, 3,4-dimethoxynitrobenzene **66**, **75** 95% isolated yield; **Table 30** entry 5, *p*-nitrotoluene **67**, **76** 87% isolated yield) and electron-withdrawing groups (**Table 30** entry 6, *p*-nitrobenzenesulfonamide **58**, **77** 45% isolated yield), obtaining in all cases the desired aniline in moderate to high yield. The reduction of *p*-bromonitrobenzene **69** afforded the corresponding *p*-bromoaniline **78** and the dehalogenated product was not detected (**Table 30** entry 7, **78** 91% isolated yield). We also undertook the reduction of nitroarenes bearing other reducible groups, such as *p*-nitrobenzonitrile **70** (**Table 30** entry 8, **79** 63% isolated yield), *p*-nitroacetophenone **71** (**Table 30** entry 9, **80** 74% isolated yield) and *p*-nitrostilbene **72** (**Table 30** entry 10, **81** 86% isolated yield). The corresponding anilines were isolated in moderate to good yields and the groups -CN, -CO- and -CH=CH- remained unaltered. A blank experiment of *p*-nitroacetophenone furnished a mixture of starting ketone and the corresponding hydrazone after 2 h in the absence of **M11**. This result is in sharp contrast with the 74% isolated yield of *p*-aminoacetophenone obtained under **M11** catalysis.

An ICP-MS analysis of the crude product obtained in the reduction of 3,4-dimethoxynitrobenzene **66** (entry 4, **Table 30**) was performed in order to check the metal leaching. The analysis showed a loss of 0.13% nickel with respect to the initial amount added.

4.6.3 RECYCLABILITY OF THE NI NPS IN THE REDUCTION OF NITROARENES

The reusability of Ni NPs was investigated in the reduction of nitrobenzene **61** (**Table 31**). Once the reaction was completed, the addition of diethyl ether to the crude mixture caused the precipitation of **M11**. Then, taking advantage of the magnetic properties of the NPs, the catalyst was easily separated from the crude mixture by decantation using an external magnet (**Figure 45 (B)**). Finally, after washing the Ni NPs with more diethyl ether and drying under vacuum, the catalyst was ready for another run. The reaction was repeated up to five consecutive cycles, with an increase of the reaction times needed for full conversion upon recycling. Probably, this loss of activity is caused by some loss of catalyst during the recyclability process, in addition to the small leaching of Ni in each cycle.

Table 31 Recycling of the Ni NPs (**M11**) in the reduction of nitrobenzene.

Cycle[a]	ArNH₂:ArNO₂ [b]	Time (h)	Yield (%)[c]
1	> 99:1	2	97
2	> 99:1	3	92
3	> 99:1	3	90
4	> 99:1	4	85
5	> 99:1	5	90

[a] Reaction conditions: nitrobenzene: 1 mmol; reductant: 8 mmol; THF (2 mL), reflux. [b] Molar ratio ArNO₂:ArNH₂ by TLC and ^{1}H NMR. [c] Isolated yield.
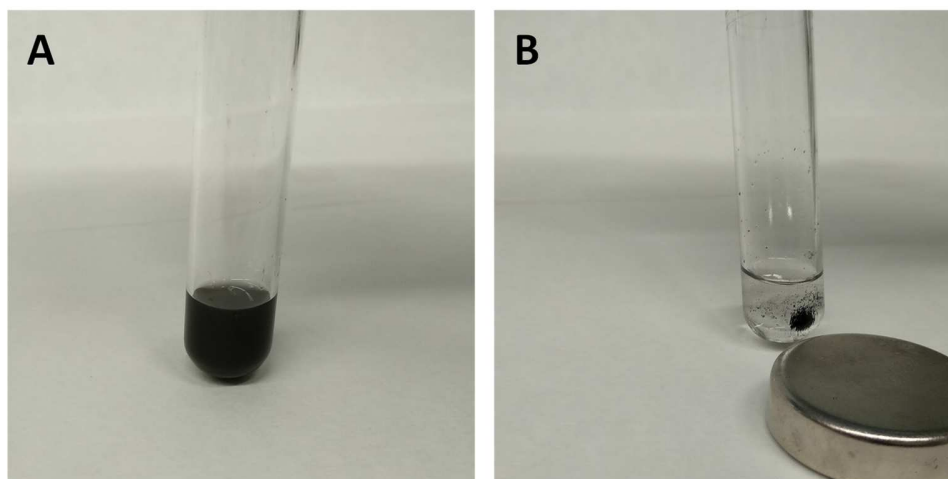
Figure 45 Ni NPs (**M11**) suspension **(A)** without an external magnetic field; **(B)** applying an external magnetic field.

4.6.4 REDUCTION OF NITROARENES CATALYZED BY RH NPS STABILIZED BY PEG-TAGGED IMIDAZOLIUM SALTS

The generation of hydrogen from the hydrolysis of ammonia borane (AB) **82** under Rh catalysis (**Scheme 33**) has recently been reported. Different supported transition metals have been used for that reaction being Rh and Co especially active.[332,333]

$$H_3N-BH_3 \ + \ 4 \cdot H_2O \ \xrightarrow{\text{Cat.}} \ 3 \cdot H_2 \ + \ NH_4^+B(OH)_4^-$$

82
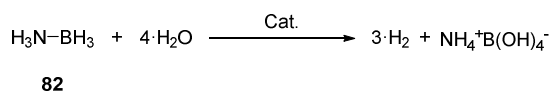
Scheme 33 Hydrolysis of ammonia borane **82** for the generation of hydrogen.

Based on these publications, we planned the generation of hydrogen from the hydrolysis of AB under catalysis by our water-soluble Rh NPs. This *in situ* generated hydrogen would be used for the reduction of nitroarenes. First, the hydrolysis of AB at room temperature was tested using a common set up to quantify the amount of H$_2$ generated (**Figure 46**). In our case, a closed vessel with an aqueous solution (8 mL) of Rh NPs was connected *via* a gas outlet to a water-filled burette. Then an AB water solution (2 mmol of AB in 2 mL water) was injected through the septum and the reaction time started counting.

---

[332] Wang, W., Ciganda, R., Wang, C., Escobar, A., Martinez-Villacorta, A. M., Ramirez, M. d. l. A., Hernández, R., Moya, S. E., Ruiz, J., Hamon, J.-R., Astruc, D. *Inorg. Chem. Front.* **2019**, *6*, 2704.

[333] (a) Zhao, T.-J., Zhang, Y.-N., Wang, K.-X., Su, J., Wei, X., Li, X.-H. *RSC Adv.* **2015**, *5*, 102736. (b) Maier, T. M., Sandl, S., Shenderovich, I. G., von Wangelin, A. J., Weigand, J. J., Wolf, R. *Chem. Eur. J.* **2019**, *25*, 238.

Figure 46 Set up to quantify the amount of H_2 generated during the hydrolysis of AB catalyzed by Rh NPs **M20**.

Ideally, 1 mmol of AB will generate 3 mmol of hydrogen (**Scheme 33**), which correspond to *ca* 75 mL of gas, volume at atmospheric pressure corrected for water vapor pressure at 20 ºC.[332] So, in our case *ca* 150 mL of hydrogen should be obtained in a complete conversion starting from 2 mmol of AB. As summarized in **Table 32**, after 1 h complete conversion of AB to H_2 was achieved (cycle 1). The Rh NPs were recycled up to four runs, but longer reaction times were required upon recycling.

Table 32 Generation of hydrogen via ammonia borane hydrolysis catalyzed by Rh NPs (**M20**).

$$H_3N-BH_3 \ + \ 4\cdot H_2O \ \xrightarrow[\text{rt}]{\text{Rh NPs (M20)}} \ 3\cdot H_2 \ + \ NH_4^+B(OH)_4^-$$

82

Cycle[a]	Time (h)	H_2 generated (mL)[b]
1	1	150
2	1.5	150
3	2	150
4	2	150

[a] Reaction conditions: AB: 2 mmol; Rh NPs: 1 mol% Rh; H_2O: 10 mL; rt; in a closed vessel with a balloon. [b] H_2 generated quantified with a water filled burette (see **Figure 46**).

After the demonstration that Rh NPs were effective for the generation of hydrogen from ammonia borane, the next step was to find the optimal conditions for the reduction of nitroarenes (**Table 33**).

Table 33 Optimization of the conditions for the reduction of nitroarenes catalyzed by Rh NPs (**M20**) with AB as hydrogen source.

Entry[a]	Solvent	Nitroarene	Time (h)	Products[b]	Yield (%)[c]
1	H₂O	61	0.25	62	92
2	H₂O	72	0.25	72 81 80:20	-
3	THF: H₂O (8:2)	72	18	72 81 50:50	-
4	THF:H₂O (2:8)	72	20	81 83 91:9	91[d]

[a] Reaction conditions: nitroarene: 0.5 mmol, AB: 2 mmol; solvent: 10 mL; rt; in a closed vessel with a balloon. [b] Products and molar ratios by ¹H NMR. [c] Isolated yield. [d] ¹H NMR yield.
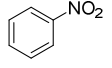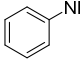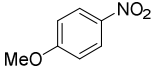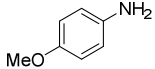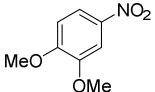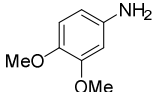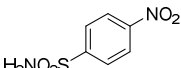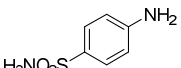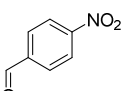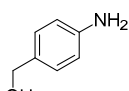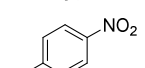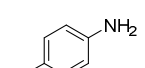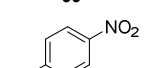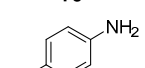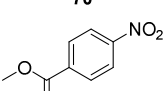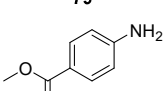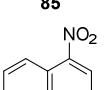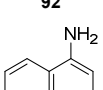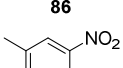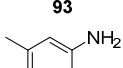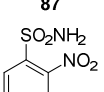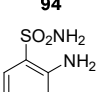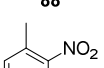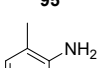
Taking advantage of the water solubility of the Rh NPs, pure water was the first choice as solvent. In that medium the reduction of nitrobenzene was performed with complete conversion after just 15 min of reaction at room temperature under catalysis by Rh NPs (**M20**, 1 mol%) (entry 1 of **Table 33**, **62** 92% isolated yield). However, some nitroarenes were not soluble in water. Thus, for *p*-nitrostilbene just a 20% conversion was achieved after 15 min of reaction in water at room temperature (Entry 2 of **Table 33**). The precipitation of the substrate in the medium prevented further evolution of the reaction. In order to increase the solubility of both the substrate and the product of the reaction, a mixture of THF:H₂O (8:2) was tried for *p*-nitrostilbene. In that case all the reactants were solubilized, but the amount of water was not enough for full conversion of AB to hydrogen, reaching just a 50% conversion after 18 h of reaction (entry 3 of **Table 33**). Finally, we decreased the amount of THF to just enough to solubilize the nitroarene. Thus, in a mixture of THF:H₂O (2:8) the nitro group of *p*-nitrostilbene **72** was completely reduced after 20 h of reaction achieving the desired product **81** and a minor amount of the aniline **83** resulting from the partial hydrogenation of the olefinic moiety (91:9 by ¹H NMR) (**Table 33** entry 4, **81** 91% ¹H NMR yield).

From this point we decided to use THF:H₂O (2:8) as solvent for the reduction of several substituted nitroarenes with AB as hydrogen source at room temperature under catalysis by all the prepared Rh NPs stabilized by PEG-tagged imidazolium salts (**M20**, **M18** and **M19**) (**Table 34**).

Table 34 Scope of the reduction of nitroarenes catalyzed by Rh NPs (**M18**, **M19** or **M20**) with AB as hydrogen source.

Ent.[a]	Cat.	Nitroarene	t (h)	ArNH$_2$: ArNO$_2$[b]	Products (selectivity)	Yield (%)[c]
1[d]		**61**	15 min	>99:1	**62**	92
2		**65**	50 min	>99:1	**74**	81
3		**66**	50 min	>99:1	**75**	89
4		**68**	50 min	>99:1	**77**	58
5		**84**	1	>99:1	**91**	64
6		**69**	1	>99:1	**78**	76
7	**M20**	**70**	18	>99:1	**79**	85
8		**85**	1	>99:1	**92**	66
9		**86**	1	>99:1	**93**	83
10		**87**	18	>99:1	**94**	53
11		**88**	24	–[f]	**95**	–[f]
12		**89**	24	–[f]	**96**	–[f]

128

Entry	Catalyst	Substrate	Time	Selectivity	Product	Yield
13		O_2N NO_2 **90**	2	>99:1	H_2N NH_2 **73**	78
14		NO_2 (acetyl) **71**	1	>99:1	**80** / **97** 77:27	64[e]
15		Ph NO_2 **72**	20	>99:1	**81** / **83** 91:9	91[e]
16	M18	MeO OMe NO_2 **66**	50 min	>99:1	MeO OMe NH_2 **75**	92
17		NO_2 (aldehyde) **84**	1	>99:1	NH_2 OH **91**	72
18		NO_2 (acetyl) **71**	1	69:31	**80** / **97** 91:9	56[e]
19		Ph NO_2 **72**	18	>99:1	Ph NH_2 **81**	85
20	M19	MeO OMe NO_2 **66**	50 min	>99:1	MeO OMe NH_2 **75**	48
21		NO_2 (aldehyde) **84**	1	>99:1	NH_2 OH **91**	55
22		NO_2 (acetyl) **71**	1	82:18	**80** / **97**	71[e]
23		Ph NO_2 **72**	18	>99:1	**81** / **83** 91:9 / 85:15	77[e]

[a] Reaction conditions: nitroarene: 0.5 mmol, AB: 2 mmol; THF:H_2O 2:8, 10 mL; rt; in a closed vessel with a balloon. [b] Molar ratio $ArNH_2$:$ArNO_2$ by TLC or ^1H NMR. [c] Isolated yield. [d] water as solvent. [e] ^1H NMR yield of the corresponding aniline. [f] No reaction.

The reaction scope was extended to several substituted nitroarenes under **M20** catalysis (entries 1-15 of **Table 34**). The protocol was found to be tolerant to the presence of electron-donating and electron-withdrawing substituents on the aromatic ring. Thus, the developed protocol was effective for the reduction of *p*-nitroanisole **65**, 3,4-dimethoxynitrobenzene **66** and *p*-nitrobenzenesulfonamide **68** (**Table 34** entries 2, 3 and 4) affording the corresponding anilines in 81, 89 and 58% isolated yields. Unfortunately, the reaction was not selective when an aldehyde function was present. In that way, *p*-nitrobenzaldehyde **84** was reduced to *p*-aminobenzylalcohol (**Table 34** entry 5, **91** 64% isolated yield). Conversely, good selectivity was found for nitroarenes bearing bromo, cyano or ester groups. Thus, *p*-bromonitrobenzene **69** furnished *p*-bromoaniline **78** in 76 % yield and the dehalogenated product was not detected (**Table 34** entry 6); *p*-nitrobenzonitrile **70** and methyl *p*-nitrobenzoate **85** gave the desired amines **79** and **92** in 85 and 66% yields, respectively (entries 7 and 8), the -CN and the -COOMe groups remaining unaltered. The heterocyclic compound 5-quinolinamine **93** was also obtained in 83% yield after 1 h of reaction (**Table 34** entry 9). The *meta* substituted *m*-nitrotoluene **87** was reduced in moderate yield after 18 h of reaction (**Table 34** entry 10, **94** 53%). However, the *ortho* substituted nitroarenes (*o*-nitrobenzenesulfonamide **88**, **Table 34** entry 11; *o*-nitrotoluene **89**, **Table 34** entry 12) remained unaltered after 24 h of reaction, possibly due to steric effects. Successful reduction of *m*-dinitrobenzene **90** to the corresponding 1,3-benzenediamine **73** was achieved after 2 h with the same amount of AB than in the other cases (**Table 34** entry 13, 78% yield). As a general trend, nitroarenes bearing electron-withdrawing groups required longer reaction times and were obtained in lower yields.

The reduction of nitroarenes containing ketone or alkene functional groups did not proceed with full selectivity. In the case of *p*-nitroacetophenone **71**, full conversion was achieved after only 1 h of reaction. Nevertheless, a certain amount of the carbonyl group was also reduced (**Table 34** entry 14, **80** 64% ^1H NMR yield). A similar result was obtained with *p*-nitrostilbene **72**, full conversion was reached after 20 h, but a minor amount of the olefinic moiety was also reduced (**Table 34** entry 15, **81** 91% ^1H NMR yield).

With the aim to compare the activity of the Rh NPs stabilized by **S3** (**M20**) with that of Rh NPs stabilized by **S2A-B** (**M18** and **M19**), some nitroarenes were also reduced under the same conditions using the Rh nanocatalysts **M18** and **M19**. In that way, similar results were obtained with 3,4-dimethoxynitrobenzene **66** (**Table 34** entry 16, **75** 92% yield with **M18**; **Table 34** entry 20, **75** 48% yield with **M19**). *p*-Nitrobenzaldehyde **84** was also reduced to 4-aminobenzylalcohol (**Table 34** entry 17, **91** 72% isolated yield for **M18**; **Table 34** entry 21, **91** 55% isolated yield for **M19**). For the case of *p*-nitroacetophenone **71** these two catalysts exhibited lower activity than **M20**. Full conversion was not reached after 1 h of reaction (**Table 34** entry 18, **80** 56% ^1H NMR yield with a 69% conversion for **M18**; **Table 34** entry 22, **80** 71% ^1H NMR yield with a 82% conversion for **M19**). However, they offered better selectivity than **M20**. It is remarkable that the reduction of *p*-nitrostilbene **72** was selective with **M18** as catalyst, obtaining *p*-aminostilbene as the only product (**Table 34** entry 19, **81** 85% isolated yield for **M18**). Conversely, **M19** was less selective and a 85:15 mixture of **81:83** was found (**Table 34** entry 23, **81** 77% ^1H NMR yield).

In order to overcome the selectivity problems encountered with some substrates, we also tested the reduction of some nitroarenes using $NaBH_4$ and hydrazine as hydrogen sources. The results of these reactions for the three Rh catalysts are summarized in tables **35** and **36**.

Table 35 Reduction of nitroarenes catalyzed by Rh NPs (**M18**, **M19** or **M20**) with NaBH$_4$ as reductant.

$$\text{R}\!-\!\!\!\!\diagup\!\!\!\!\diagdown\!\!-\text{NO}_2 \xrightarrow[\text{THF:H}_2\text{O (2:8), rt}]{\substack{\text{1 mol\% Rh (M18, M19 or M20)}\\ \text{NaBH}_4}} \text{R}\!-\!\!\!\!\diagup\!\!\!\!\diagdown\!\!-\text{NH}_2$$

Ent.[a]	Cat.	Nitroarene	t (h)	ArNH$_2$: ArNO$_2$[b]	Products (selectivity)[c]	Yield (%)[d]
1		3,4-dimethoxynitrobenzene **66**	50 min	>99:1	**75**	66
2		p-nitrobenzonitrile **70**	18	>99:1	**79**	83[e]
3	**M20**	p-nitroacetophenone **71**	30 min	>99:1	**80** / **97** (Partially reduced nitro compounds)	-
4		**72**	24	>99:1	**81** / **83** (92:8)	77[e]
5		p-nitroacetophenone **71**	1	69:31	**80** / **97** (74:26)	58[e]
6	**M18**	**72**	18	>99:1	**81** / **83** (97:3)	92[e]
7		p-nitroacetophenone **71**	1	>99:1	**80** / **97** (36:64)	10[e]
8	**M19**	**72**	18	>99:1	**81** / **83** (84:16)	70[e]

[a] Reaction conditions: nitroarene: 0.5 mmol, NaBH$_4$: 2 mmol; THF:H$_2$O 2:8: 10 mL; rt; in a closed vessel with a balloon. [b] Molar ratio ArNH$_2$:ArNO$_2$ by TLC or ^{1}H NMR. [c] Molar ratio by ^{1}H NMR. [d] Isolated yield. [e] ^{1}H NMR yield of the corresponding aniline.

When NaBH$_4$ was employed as reductant in THF:H$_2$O (2:8) at room temperature, we obtained similar results to those found with AB in the case of 3,4-dimethoxynitrobenzene **66** (entry 1 of **Table 35**, **75** 66% yield for **M20**) and p-nitrobenzonitrile **70** (entry 2 of **Table 35**, **79** 83% yield for **M20**). In the case of p-nitroacetophenone **71** higher activity was observed with the three nanocatalysts, the nitroarene being fully consumed after 1 h with **M18** (entry 5 of **Table 35**) and **M19** (entry 7 of **Table 35**), and after 30 min with **M20** (entry 3 of **Table 35**). However, in all cases low selectivity was observed, obtaining mixtures of the desired

aniline and the benzyl alcohol in different proportions. Moreover, in the case of **M20** some products derived from the partial reduction of the nitro group were detected. Finally, for *p*-nitrostilbene **72** minor amounts of the aniline derived from reduction of the olefin were formed as it was found with AB as reducing agent (entry 6 of **Table 35**, **81** 92% ^{1}H NMR yield for **M18**; entry 8 of **Table 35**, **81** 70% ^{1}H NMR yield for **M19**; entry 4 of **Table 35**, **81** 77% ^{1}H NMR yield for **M20** catalysis).

In summary, NaBH$_4$ was not found to be a better alternative to ammonia borane for the selective reduction of nitroarenes under the conditions tested.

Table 36 Reduction of nitroarenes catalyzed by Rh NPs (**M18**, **M19** or **M20**) with hydrazine as reductant.

Ent.[a]	Cat.	Nitroarene	t (h)	ArNH$_2$: ArNO$_2$[b]	Products (selectivity)[c]	Yield (%)[d]
1		**66** (3,4-dimethoxynitrobenzene)	16	>99:1	**75**	70
	M20					
2		**71**	2	>99:1	**80** Partially reduced nitro compounds	-
3		**71**	24	>99:1	**80** Partially reduced nitro compounds	-
	M18					
4		**72**	48	62:38	**81**	48[e]
5		**71**	24	87:13	**80** Partially reduced nitro compounds	-
	M19					
6		**72**	48	29:71	**81**	23[e]

[a] Reaction conditions: nitroarene: 0.5 mmol, N$_2$H$_4$·H$_2$O: 2 mmol; THF:H$_2$O 2:8: 10 mL; rt; in a closed vessel with a balloon. [b] Molar ratio ArNH$_2$:ArNO$_2$ by TLC or ^{1}H NMR. [c] Molar ratio by ^{1}H NMR. [d] Isolated yield. [e] ^{1}H NMR yield of the corresponding aniline.

When hydrazine was used as reductant in THF:H$_2$O (2:8) at room temperature, longer reaction times were needed in all cases compared with the other reductants. For instance, 3,4-dimethoxynitrobenzene **66** was completely reduced in only 50 min with AB and NaBH$_4$ under **M20** catalysis, but with hydrazine 16 h were needed to complete the reaction (entry 1 of **Table 36**, **75** 70% yield). The reaction was also slower for *p*-nitroacetophenone **71**, and mixtures of the desired aniline and compounds derived from the partial reduction of the nitro group were obtained with the three catalysts (entry 2 of **Table 36** for **M20;** entry 3 of **Table 36**, for **M18**; entry 5 of **Table 36** for **M19**;). A similar pattern of behaviour was observed with *p*-nitrostilbene **72**, obtaining low yield of the desired aniline after 48 h of reaction with **M18** (entry 4 of **Table 36**, **81** 48% ^{1}H NMR yield) and **M19** (entry 6 of **Table 36**, **81** 23% ^{1}H NMR yield).

In summary, hydrazine was not found to be a better alternative to ammonia borane for the selective reduction of nitroarenes under the conditions tested.

So, we can conclude that AB and NaBH$_4$ present a similar behaviour in the reduction of nitroarenes catalyzed by Rh NPs stabilized by PEG-tagged imidazolium salts. However, the reaction using AB was cleaner and the purification of the product was easier. Also, in the presence of certain reducible functional groups the reduction using AB as hydrogen source was found more selective. On the contrary, the use of hydrazine resulted in longer reaction times, in some cases not achieving a full conversion.

4.6.5 RECYCLABILITY OF THE RH NPS IN THE REDUCTION OF NITROARENES

Lastly, taking advantage of the water solubility of the catalyst, the recyclability of **M18** was investigated for the reduction of 3,4-dimethoxynitrobenzene **66** using AB as a hydrogen source. As we can observe in **Table 37**, five consecutive runs were successfully performed but longer reaction times were needed for full conversion after the first cycle. Some degradation of the catalyst and mechanical losses during the work-up procedure may be the reason for this decrease of activity upon recycling.

Table 37 Recycling of the Rh NPs (**M18**) in the reduction of 3,4-dimethoxynitrobenzene **66** with AB as hydrogen source.

Cycle[a]	Time (h)	Yield (%)[b]
1	50 min	92
2	75 min	88
3	18	90
4	18	85
5	24	87

[a] Reaction conditions: nitroarene: 0.5 mmol, AB: 2 mmol; THF:H$_2$O 2:8: 10 mL; rt; in a closed vessel with a balloon. [b] Complete conversion. Isolated yield.

4.7 CONCLUSIONS

The prepared metal NPs (Pt, Ni, Au and Rh) have been tested as reusable catalysts in different reactions.

The formation of new C-C bonds via coupling reactions under Ni NPs catalysis (Suzuki and Sonogashira) has been examined. Unfortunately, **M12** (Ni NPs stabilized by the tris-imidazolium iodide **S1A**) was not active in Suzuki coupling under the conditions tested. For the Sonogashira reaction with **M11** and **M12**, the desired products were only formed when secondary amines were used as bases, but as only low conversions were achieved, this type of reaction was not further investigated.

The activity of the water-soluble Rh NPs **M20** (stabilized by PEG-tagged tris-imidazolium bromide **S3**) for Heck-type reactions between arylboranes and *n*-butyl acrylate has been investigated. After some screening of conditions (base, solvent, temperature), only low conversions were observed and the reaction was not further investigated.

Water-soluble Au nanocatalyst **M16** (Au NPs stabilized by **S3**) presented high catalytic activity for the synthesis of propargylamines via A^3 coupling between aldehydes (or ketones), secondary amines and terminal alkynes under neat conditions at 100 ºC. The scope of the reaction was extended to a wide number of different aldehydes, ketones and secondary amines obtaining good yields in all cases. Different alkynes were also tested obtaining from moderate to excellent yields with the aromatic ones and poor yields or no reaction with the non-aromatic terminal alkynes. Taking advantage of the water-solubility of **M16** (and their insolubility in diethyl ether), the catalyst has been recycled up to four times for this reaction. Worse results were obtained with **M14** and **M15** (Au NPs stabilized by the PEG-tagged imidazolium bromide and tetrafluoroborate **S2A** or **S2B**, respectively). The lower activity of these catalysts in front of **M16** was attributed to different factors, such as the lower amount of Au(I) species in the nanoparticles and the structural features of the stabilizers.

Besides, the water-soluble Au NPs (**M16**) are efficient catalysts for the cycloisomerization of different γ-alkynoic acids to enol lactones in a biphasic medium toluene:water at room temperature. The Au NPs were also successfully recycled up to six runs. Lower activity was also observed for **M14** and **M15** as catalysts for this reaction.

The platinum NPs stabilized by tris-imidazolium tetrafluoroborate **S1B** (**M5**) and the water-soluble rhodium NPs stabilized by **S2A**, **S2B** and **S3** (**M18**, **M19** or **M20** respectively) were efficient catalysts for the stereoselective *syn*-hydrosilylation of symmetric and unsymmetric internal alkynes. The corresponding (*E*)-vinylsilanes were obtained with excellent yields under two different methods: (i) solvent-free conditions at 90 ºC with an excess of silane (method A) and (ii) with THF as a solvent with one equivalent of silane (method B) at 90 ºC in a closed vessel. Pt NPs gave faster reactions than Rh NPs, yielding the desired product after only 45 min in the best case. However, with Rh NPs higher regioselectivities were achieved. The major regioisomer was in all cases the one with the silyl group closest to the more electron-deficient group. For both Pt and Rh NPs, the addition of hexane upon completion of the reaction resulted in the precipitation of the nanocatalysts, which were easily separated from the crude mixture by a centrifugation/decantation process. Following this procedure both kind of catalysts (Pt and Rh NPs) have been successfully recycled up to four or five runs.

The reduction of nitroarenes was performed under catalysis by Ni (**M12**) and Rh (**M18**, **M19** and **M20**) NPs under different conditions. Regarding to Ni NPs, the nanocatalyst was found very effective in the selective reduction of nitroarenes to the corresponding anilines with hydrazine as hydrogen donor in THF at reflux. The Ni catalyst has proved to be tolerant for the presence of other reducible groups such as carbon-carbon double bonds or carbonyl groups. The magnetic properties of the Ni NPs facilitate the separation of the catalyst from the crude mixture, allowing to reuse it up to 5 cycles.

On the other hand, Rh NPs (**M18**, **M19** and **M20**) have been proved to be effective for the generation of hydrogen from the hydrolysis of ammonia borane complex. This *in situ* generated hydrogen acts as reductant

for the reduction of nitroarenes to the corresponding anilines in THF:H$_2$O (1:4) at room temperature. The reaction was carried out with a wide number of nitroarenes bearing different functional groups. Unfortunately, with nitroarenes bearing carbonyl groups or olefins, small amounts of side products derived from the reduction of these functional groups were also found. The reaction using NaBH$_4$ as a reducing agent or hydrazine as hydrogen source was also performed for some substrates under the same conditions. With ammonia borane and NaBH$_4$ fast reactions take place with similar selectivity. However, when hydrazine was used, lower conversions were observed after longer reaction times. The Rh NPs **M18** were successfully recycled up to 5 runs. Ammonia borane remained the reductant of choice.

4.8 EXPERIMENTAL SECTION

4.8.1 GENERAL REMARKS

Commercial reagents were used directly as received. Milli-Q water and HPLC grade solvents were used in the preparation and purification of products. All NMR spectra were recorded with Bruker Avance DRX-250 (250 MHz for ^{1}H NMR), Bruker Avance DPX-360 MHz (360 MHz for ^{1}H NMR) and Bruker Avance III 400SB (400 MHz for ^{1}H NMR) spectrometers. High resolution mass spectra were performed at the *Servei d'Anàlisi Química* of the *Universitat Autònoma de Barcelona* using a Bruker Daltoniks MicroTOFQ spectrometer (Bremen, Germany) equipped with an ESI inlet.

4.8.2 HECK-TYPE REACTION OF ARYLBORONIC ACIDS WITH ALKENES UNDER CATALYSIS BY Rh NANOPARTICLES

4.8.2.1 BUTYL CYNNAMATE 18[334]
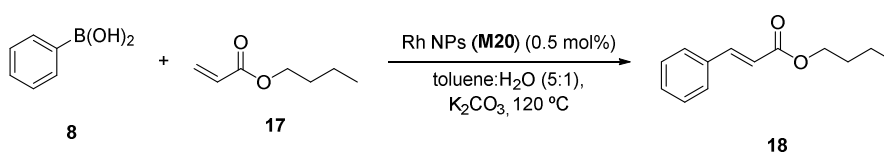
A mixture of phenylboronic acid (121.9 mg, 1.0 mmol), *n*-butyl acrylate (430 µL, ρ = 0.894 g/mL, 3.0 mmol), **M20** (0.5 mol% Rh, 2.2 mg), K_2CO_3 (41.4 mg, 0.3 mmol) in a mixture of toluene (2.5 mL) and H_2O (0.5 mL) was stirred at 100 ºC in a closed vessel for 24 h. The reaction solution was cooled to room temperature and extracted with Et_2O (3 x 5 mL), the organic layer was dried over Na_2SO_4, the solvent was evaporated under reduced pressure and the residue was purified by flash column chromatography on silica gel, eluting with hexane/ethyl acetate (9:1) to give **18** as a white solid (18.4 mg, 10%). ^{1}H NMR (360 MHz, $CDCl_3$, ppm): δ 7.68 (d, J = 16.1 Hz, 1H), 7.55-7.51 (m, 2H), 7.40-7.37 (m, 3H), 6.44 (d, J = 16.1 Hz, 1H), 4.21 (t, J = 6.8 Hz, 2H), 1.71-1.66 (m, 2H), 1.49-1.39 (m, 2H), 0.97 (t, J = 7.3 Hz, 3H).

4.8.3 GENERAL PROCEDURE FOR THE SYNTHESIS OF PROPARGYLAMINES VIA A^3 COUPLING BETWEEN ALDEHYDES, SECONDARY AMINES AND ALKYNES

Aldehyde (1 equiv.), secondary amine (1.3 equiv.), alkyne (1.3 equiv.) and Au NPs (0.5 mol% Au) were mixed into a sealed tube in the absence of solvent. The mixture was stirred at 100 ºC for 24 h. After that time, 1 equiv. of 4-methoxyphenol as internal standard was added and the yield of propargylamine was determined by ^{1}H NMR. In order to isolate the product, water was added to the mixture and the solution was extracted with Et_2O (3 x 5 mL).The organic layer was washed with water, then dried over anhydrous Na_2SO_4, and the solvent was evaporated under reduced pressure. A sample of pure product was obtained after flash chromatography on alumina (10:0.1 hexane:EtOAc).

For the recycling of the catalyst, the Au NPs were recovered by addition of diethyl ether to the crude mixture, centrifugation and decantation. The NPs, insoluble in diethyl ether, were reused in the next run. The ethereal phase was washed with water, dried over anhydrous Na_2SO_4 and the solvent was evaporated under reduced pressure to give the corresponding propargylamine.

---

[334] Nájera, C., Gil-Moltó, J., Karlström, S., Falvello, L. R. *Org. Lett.* **2003**, *5* (3), 1451.

4.8.3.1   4-(1,3-DIPHENYLPROP-2-YN-1-YL)MORPHOLINE, **23AAA**[209]
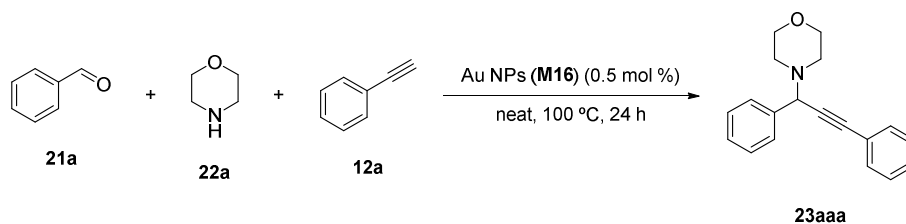
Following the typical procedure for the A[3] coupling, freshly distilled benzaldehyde **21a** (51.8 μL, ρ = 1.044 g/mL, 0.5 mmol) was allowed to react with morpholine **22a** (56.9 μL, ρ = 1.01 g/mL, 0.65 mmol) and phenylacetylene **12a** (71.4 μL, ρ = 0.930 g/mL, 0.65 mmol) at 100 ºC for 24 h. **23aaa**, Brown oil (51% isolated yield) ^{1}H NMR (250 MHz, CDCl$_3$, ppm): δ 7.64-7.70 (m, 2H), 7.52-7.57 (m, 2H), 7.32-7.40 (m, 6H), 4.81 (s, 1H), 3.70-3.80 (m, 4H), 2.62-2.69 (m, 4H).

4.8.3.2   1-(1,3-DIPHENYLPROP-2-YN-1-YL)PIPERIDINE, **23ABA**[209]
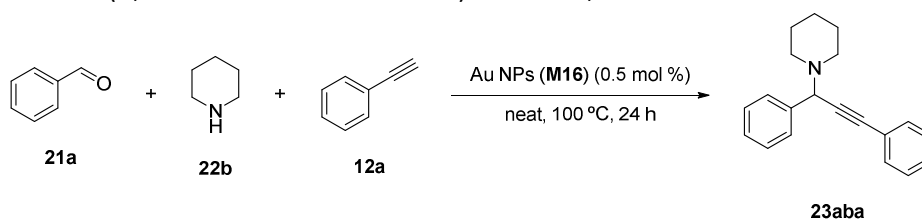
Following the typical procedure for the A[3] coupling, freshly distilled benzaldehyde **21a** (51.8 μL, ρ = 1.044 g/mL, 0.5 mmol) was allowed to react with piperidine **22b** (64.2 μL, ρ = 0.862 g/mL, 0.65 mmol) and phenylacetylene **12a** (71.4 μL, ρ = 0.930 g/mL, 0.65 mmol) at 100 ºC for 24 h. **23aba**, brown oil (56% isolated yield). ^{1}H NMR (250 MHz, CDCl$_3$, ppm): δ 7.63-7.70 (m, 2H), 7.52-7.57 (m, 2H), 7.39-7.27 (m, 6H), 4.82 (s, 1H), 2.58 (t, *J* = 5.4 Hz, 4 H), 1.54-1.68 (m, 4H), 1.42-1.53 (m, 2H).

4.8.3.3   *N*-BENZYL-*N*-METHYL-1,3-DIPHENYLPROP-2-YN-1-AMINE, **23ACA**[209]
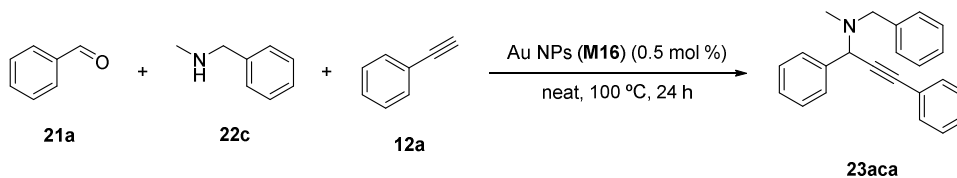
Following the typical procedure for the A[3] coupling, freshly distilled benzaldehyde **21a** (51.8 μL, ρ = 1.044 g/mL, 0.5 mmol) was allowed to react with *N*-benzylmethylamine **22c** (82.9 μL, ρ = 0.939 g/mL, 0.65 mmol) and phenylacetylene **12a** (71.4 μL, ρ = 0.930 g/mL, 0.65 mmol) at 100 ºC for 24 h. **23aca**, yellow oil. ^{1}H NMR (250 MHz, CDCl$_3$, ppm): δ 7.69-7.76 (m, 2H), 7.58-7.65 (m, 2H), 7.26-7.49 (m, 11H), 4.97 (s, 1H), 3.73 (AB system, *J* = 13.2 Hz, 2H), 2.29 (s, 3H).

4.8.3.4   *N*,*N*-DIETHYL-1,3-DIPHENYLPROP-2-YN-1-AMINE, **23ADA**[335]
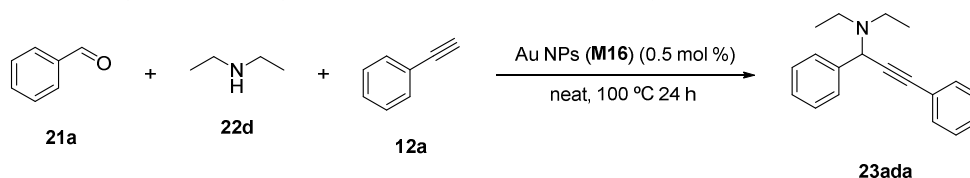
Following the typical procedure for the A[3] coupling, freshly distilled benzaldehyde **21a** (51.8 μL, ρ = 1.044 g/mL, 0.5 mmol) was allowed to react with *N*,*N*-diethylamine **22d** (67.2 μL, ρ = 0.707 g/mL, 0.65 mmol) and phenylacetylene **12a** (71.4 μL, ρ = 0.930 g/mL, 0.65 mmol) at 100 ºC for 24 h. **23ada**, brown oil (46% isolated

[335] Lin, Z., Yu, D., Zhang, Y. *Tetrahedron Lett.* **2011**, *52*, 4967.

yield). ^{1}H NMR (360 MHz, CDCl$_3$, ppm): δ 7.69-7.73 (m, 2H), 7.50-7.55 (m, 2H), 7.30-7.40 (m, 6H), 5.08 (s, 1H), 2.54-2.69 (m, 4H), 1.10 (t, *J* = 7.2 Hz, 6H).

4.8.3.5   1-(1,3-DIPHENYLPROP-2-YNYL)PYRROLIDINE, **23AEA**[336]
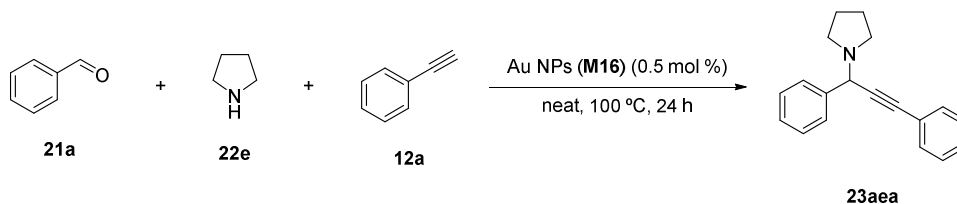
21a   **22e**   **12a**   **23aea**

Following the typical procedure for the A^3 coupling, freshly distilled benzaldehyde **21a** (51.8 µL, ρ = 1.044 g/mL, 0.5 mmol) was allowed to react with pyrrolidine **22e** (54.4 µL, ρ = 0.866 g/mL, 0.65 mmol) and phenylacetylene **12a** (71.4 µL, ρ = 0.930 g/mL, 0.65 mmol) at 100 ºC for 24 h. **23aea**, brown oil. ^{1}H NMR (360 MHz, CDCl$_3$, ppm): δ 7.59-7.64 (m, 2H), 7.46-7.51 (m, 2H), 7.28-7.38 (m, 6H), 4.93 (s, 1H), 2.69-2.77 (m, 4H), 1.70-1.86 (m, 4H).

4.8.3.6   1-(3-PHENYL-1-(*P*-TOLYL)PROP-2-YN-1-YL)PIPERIDINE, **23BBA**[337]

21b   **22b**   **12a**   **23bba**
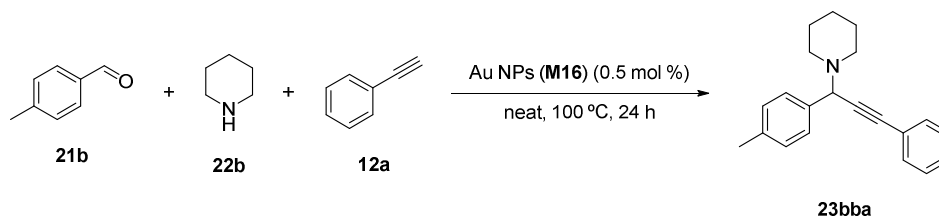
Following the typical procedure for the A^3 coupling, *p*-methylbenzaldehyde **21b** (58.9 µL, ρ = 1.019 g/mL, 0.5 mmol) was allowed to react with piperidine **22b** (64.2 µL, ρ = 0.862 g/mL, 0.65 mmol) and phenylacetylene **12a** (71.4 µL, ρ = 0.930 g/mL, 0.65 mmol) at 100 ºC for 24 h. **23bba**, brown oil. ^{1}H NMR (360 MHz, CDCl$_3$, ppm): δ 7.54-7.51 (m, 4H), 7.34-7.31 (m, 3H), 7.20-7.16 (m, 2H), 4.77 (s, 1H), 2.60-2.52 (m, 4H), 2.37 (s, 3H), 1.64-1.54 (m, 4H), 1.48-1.40 (m, 2H).

4.8.3.7   1-[1-(4-METHOXYPHENYL)-3-PHENYLPROP-2-YN-1-YL]PIPERIDINE, **23CBA**[209]

21c   **22b**   **12a**   **23cba**
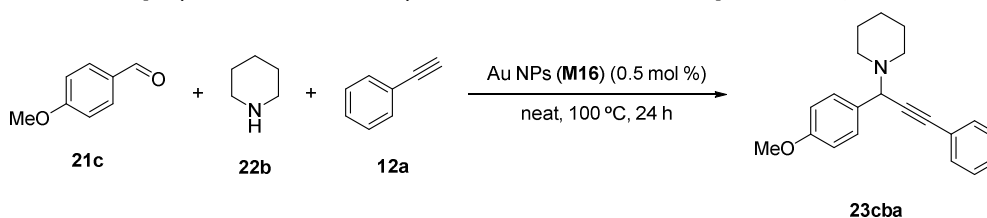
Following the typical procedure for the A^3 coupling, *p*-methoxybenzaldehyde **21c** (60.8 µL, ρ = 1.119 g/mL, 0.5 mmol) was allowed to react with piperidine **22b** (64.2 µL, ρ = 0.862 g/mL, 0.65 mmol) and phenylacetylene **12a** (71.4 µL, ρ = 0.930 g/mL, 0.65 mmol) at 100 ºC for 24 h. **23cba**, brown oil (85% isolated yield). ^{1}H NMR (250 MHz, CDCl$_3$, ppm): δ 7.56-7.48 (m, 4H), 7.34-7.30 (m, 3H), 6.91-6.86 (m, 2H), 4.75 (s, 1H), 3.82 (s, 3H), 2.59-2.52 (m, 4H), 1.64-1.54 (m, 4H), 1.48-1.40 (m, 2H).

[336] Lo, V. K.-Y., Kung, K. K.-Y., Wong, M.-K., Che, C.-M. *J. Otrganometal. Chem.* **2009**, *694*, 583.
[337] Samai, S., Nandi, G. C., Singh, M. S. *Tetrahedron Lett.* **2010**, *51*, 5555.

4.8.3.8   *N*-[4-(3-Phenyl-1-propyl-2-propynyl)]piperidine, **23dba**[338]
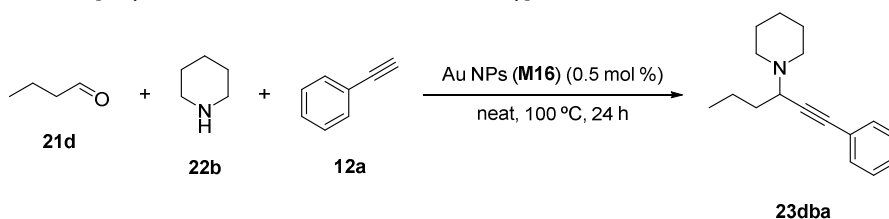
Following the typical procedure for the A^3 coupling, *n*-butanal **21d** (45.0 µL, ρ = 0.800 g/mL, 0.5 mmol) was allowed to react with piperidine **22b** (64.2 µL, ρ = 0.862 g/mL, 0.65 mmol) and phenylacetylene **12a** (71.4 µL, ρ = 0.930 g/mL, 0.65 mmol) at 100 ºC for 24 h. **23dba**, pale yellow oil (73% isolated yield). ^{1}H NMR (250 MHz, CDCl$_3$, ppm): δ 7.44-7.42 (m, 2H), 7.30-7.27 (m, 3H), 3.53-3.47 (m, 1H), 2.72-2.64 (m, 2H), 2.53-2.46 (m, 2H), 1.77-1.43 (m, 10H), 0.97 (t, *J* = 7.2 Hz, 3H).

4.8.3.9   1-(1-Phenyldodec-1-yn-3-yl)piperidine, **23eba**[209]
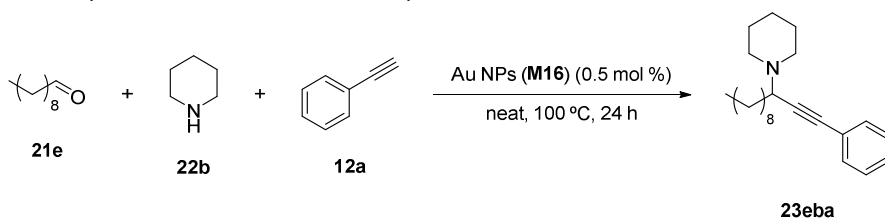
Following the typical procedure for the A^3 coupling, decanal **21e** (94.0 µL, ρ = 0.830 g/mL, 0.5 mmol) was allowed to react with piperidine **22b** (64.2 µL, ρ = 0.862 g/mL, 0.65 mmol) and phenylacetylene **12a** (71.4 µL, ρ = 0.930 g/mL, 0.65 mmol) at 100 ºC for 24 h. **23eba**, yellow oil. ^{1}H NMR (250 MHz, CDCl$_3$, ppm): δ 7.46-7.41 (m, 2H), 7.32-7.26 (m, 3H), 3.50-3.44 (m, 1H), 2.73-2.64 (m, 2H), 2.53-2.44 (m, 2H), 1.75-1.25 (m, 22H), 0.88 (t, *J* = 6.6 Hz, 3H).

4.8.3.10   1-[3-(4-Methoxyphenyl)-1-phenylprop-2-yn-1-yl]piperidine, **23abb**[209]
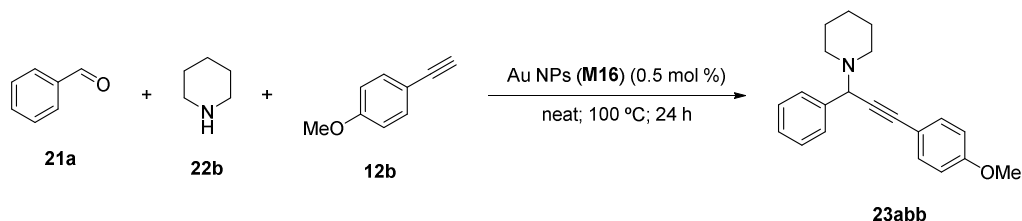
Following the typical procedure for the A^3 coupling, freshly distilled benzaldehyde **21a** (51.8 µL, ρ = 1.044 g/mL, 0.5 mmol) was allowed to react with piperidine **22b** (64.2 µL, ρ = 0.862 g/mL, 0.65 mmol) and *p*-methoxyphenylacetylene **12b** (84.3 µL, ρ = 1.019 g/mL, 0.65 mmol) at 100 ºC for 24 h. **23abb**, pale yellow oil. ^{1}H NMR (250 MHz, CDCl$_3$, ppm): δ 7.69-7.65 (m, 2H), 7.51-7.45 (m, 2H), 7.42-7.27 (m, 3H), 6.86-6.90 (m, 2H), 4.80 (s, 1H), 3.83 (s, 3H), 2.59 (t, J = 5.3 Hz, 4H), 1.67-1.57 (m, 4H), 1.51-1.42 (m, 2H).

4.8.3.11   1-[3-(4-Fluorophenyl)-1-phenylprop-2-yn-1-yl]piperidine, **23abc**[339]

---
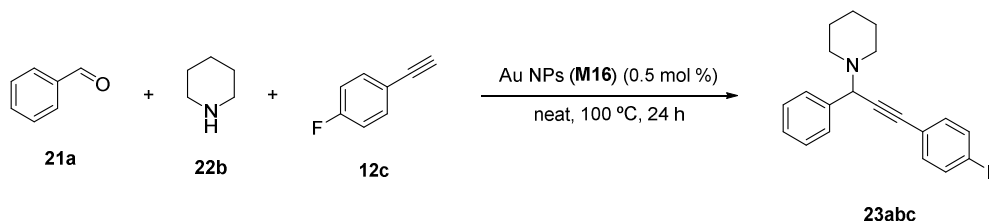
[338] Wang, M., Li, P., Wang, L. *Eur. J. Org. Chem.* **2008**, 2255.

[339] Chng, L. L., Yang, J., Wei, Y., Ying, J. Y. *Adv. Synth. Catal.* **2009**, *351*, 2887.

Following the typical procedure for the A[3] coupling, freshly distilled benzaldehyde **21a** (51.8 µL, ρ = 1.044 g/mL, 0.5 mmol) was allowed to react with piperidine **22b** (64.2 µL, ρ = 0.862 g/mL, 0.65 mmol) and *p*-fluorophenylacetylene **12c** (57.3 µL, ρ = 1.098 g/mL, 0.65 mmol) at 100 ºC for 24 h. **23abb**, yellow oil. ¹H NMR (250 MHz, CDCl₃, ppm): δ 7.65-7.61 (m, 2H), 7.53-7.47 (m, 2H), 7.40-7.30 (m, 3H), 7.06-6.99 (m, 2H), 4.78 (s, 1H), 2.56 (t, *J* = 5.1 Hz, 4H), 1.64-1.56 (m, 4H), 1.47-1.43 (m, 2H).

4.8.4 GENERAL PROCEDURE FOR THE SYNTHESIS OF PROPARGYLAMINES VIA A[3] COUPLING BETWEEN KETONES, SECONDARY AMINES AND ALKYNES.

Ketone (1.3 equiv.), secondary amine (1 equiv.), alkyne (1.3 equiv.) and Au NPs (0.5 mol% Au) were mixed into a sealed tube in the absence of solvent. The mixture was stirred at 100 ºC for 24 h. After that time, 1 equiv. of 4-methoxyphenol was added as internal standard and the yield of propargylamine was determined by ¹H NMR. In order to isolate the product, water was added to the mixture and the solution was extracted with Et₂O (3 x 5 mL). The organic layer was washed with water, dried over Na₂SO₄, filtered and the solvent evaporated under reduced pressure. A sample of pure product was obtained after flash chromatography on alumina (10:0.1 hexane:EtOAc).

4.8.4.1   1-[1-(PHENYLETHYNYL)CYCLOHEXYL]MORPHOLINE, **25AAA**[209]
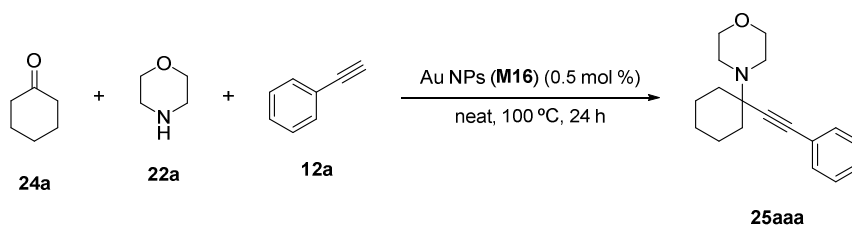
24a   **22a**   **12a**   **25aaa**

Following the typical procedure for the A[3] coupling, cyclohexanone **24a** (67.3 µL, ρ = 0.948 g/mL, 0.65 mmol) was allowed to react with morpholine **22a** (43.5 µL, ρ = 1.01 g/mL, 0.5 mmol) and phenylacetylene **12a** (71.4 µL, ρ = 0.930 g/mL, 0.65 mmol) at 100 ºC for 24 h. **25aaa**, pale yellow oil. ¹H NMR (250 MHz, CDCl₃, ppm): δ 7.50-7.20 (m, 5H), 3.85-7.69 (m, 4H), 2.77-2.65 (m, 4H), 2.08-1.98 (m, 2H), 1.75-1.43 (m, 7H), 1.31-1.22 (m, 1H).

4.8.4.2   1-(1-(PHENYLETHYNYL)CYCLOHEXYL)PIPERIDINE, **25ABA**[288A]
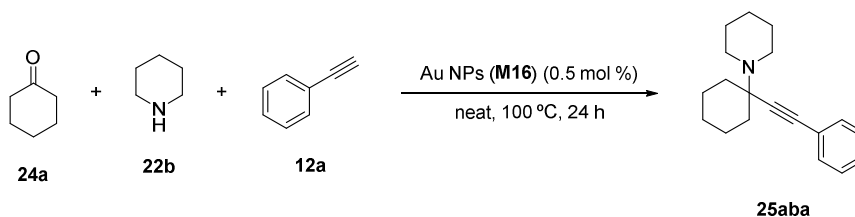
24a   **22b**   **12a**   **25aba**

Following the typical procedure for the A[3] coupling, cyclohexanone **24a** (67.3 µL, ρ = 0.948 g/mL, 0.65 mmol) was allowed to react with piperidine **22b** (49.4 µL, ρ = 0.862 g/mL, 0.5 mmol) and phenylacetylene **12a** (71.4 µL, ρ = 0.930 g/mL, 0.65 mmol) at 100 ºC for 24 h. **25aba**, pale yellow oil. ¹H NMR (360 MHz, CDCl₃, ppm): δ 7.48-7.42 (m, 2H), 7.31-7.27 (m, 3H), 2.73-2.64 (m, 4H), 2.17-2.03 (m, 2H), 1.86-1.44 (m, 13H), 1.28-1.21 (m, 1H).

4.8.4.3 1-(1-(Phenylethynyl)cyclopentyl)piperidine 25bba[288b]

24b **22b** **12a** **25bba**
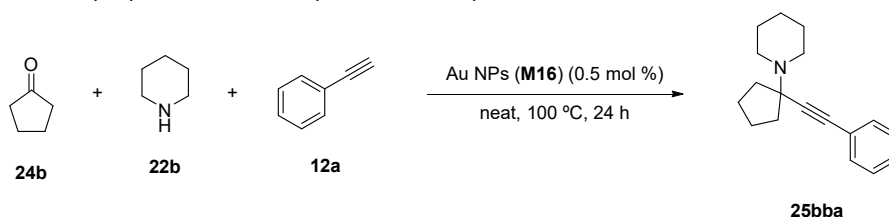
Following the typical procedure for the A^3 coupling, cyclopentanone **24b** (57.6 µL, ρ = 0.950 g/mL, 0.65 mmol) was allowed to react with piperidine **22b** (49.4 µL, ρ = 0.862 g/mL, 0.5 mmol) and phenylacetylene **12a** (71.4 µL, ρ = 0.930 g/mL, 0.65 mmol) at 100 ºC for 24 h. **25bba**, pale yellow oil. ^{1}H NMR (360 MHz, CDCl$_3$, ppm): δ 7.47-7.42 (m, 2H), 7.33-7.27 (m, 3H), 2.70-2.64 (m, 4H), 2.15-2.06 (m, 2H), 1.74-1.57 (m, 10H), 1.50-1.42 (m, 2H).

4.8.4.4 4-(1,1-diethyl-3-phenyl-2-propyn-1-yl)morpholine, 25caa[340]

24c **22a** **12a** **25caa**
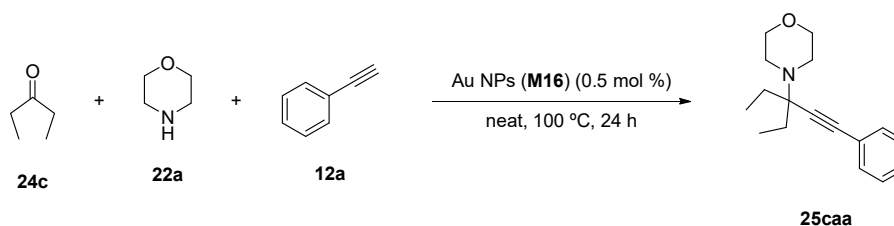
Following the typical procedure for the A^3 coupling, diethylketone **24c** (57.6 µL, ρ = 0.815 g/mL, 0.65 mmol) was allowed to react with morpholine **22a** (43.5 µL, ρ = 1.01 g/mL, 0.5 mmol) and phenylacetylene **12a** (71.4 µL, ρ = 0.930 g/mL, 0.65 mmol) at 100 ºC for 24 h. **25caa**, colorless oil. ^{1}H NMR (250 MHz, CDCl$_3$, ppm): δ 7.44-7.40 (m, 2H), 7.30-7.26 (m, 3H), 3.76-3.72 (m, 4H), 2.70-2.66 (m, 4H), 1.77-1.68 (m, 4H), 0.97 (t, J = 7.5 Hz, 6H).

4.8.5 General procedure for the cycloisomerization of γ-alkynoic acids into enol lactones

To a biphasic system of toluene/water 1:1 (1 mL), the corresponding γ-alkynoic acid (0.15 mmol) and Au NPs (1 mol%) were added. The resulted mixture was stirred with a wrist type laboratory shaker apparatus at room temperature until full conversion of alkynoic acid (monitored by ^{1}H NMR using 4-methoxyphenol as internal standard). The organic phase was then separated, and the aqueous layer was extracted with Et$_2$O (3 x 1 mL). The combined organic layers were washed with water, dried over anhydrous Na$_2$SO$_4$, filtered and the solvent was evaporated. A sample of pure enol lactone was obtained after flash chromatography (hexane: EtOAc, 4:1).

4.8.5.1 5-Methylenedihydrofuran-2(3H)-one, 29[297]

27 **29**
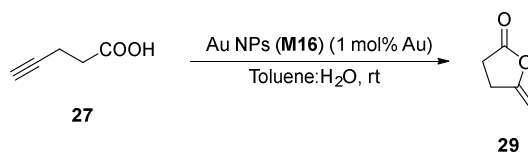
Following the typical procedure for the cycloisomerization of γ-alkynoic acids, 4-pentynoic acid **27** (13.4 µL, ρ = 1.096 g/mL, 0.15 mmol) was stirred in the presence of **M16** at room temperature for 50 min. **29**, colorless oil. ^{1}H NMR (360 MHz, CDCl$_3$, ppm): δ 4.82 (m, 1H), 4.39 (m, 1H), 2.98-2.93 (m, 2H), 2.78-2.73 (m, 2H).

---

[340] Katritzky, A. R., Yang, H., Singh, S. K. *J. Org. Chem.* **2005**, *70*, 286.

4.8.5.2 METHYL 5-METHYLENE-2-OXO-3-(PROP-2-YN-1-YL)TETRAHYDROFURAN-3-CARBOXYLATE, 33[297]
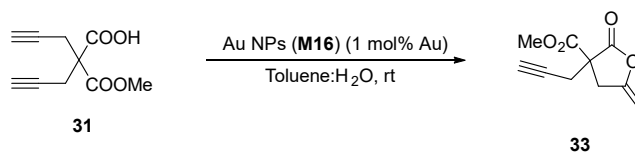
Following the typical procedure for the cycloisomerization of γ-alkynoic acids, 2-(methoxycarbonyl)-2-(prop-2-yn-1-yl)pent-4-ynoic acid **31** (29.1 mg, 0.15 mmol) was stirred in the presence of **M16** at room temperature for 24 min. **33**, colorless oil. ^{1}H NMR (360 MHz, CDCl$_3$, ppm): δ 4.84 (m, 1H), 4.42 (m, 1H), 3.80 (s, 3H), 3.29-3.24 (m, 2H), 2.89 (d, J = 2.6 Hz, 2H), 2.08 (t, J = 2.6 Hz, 1H).

4.8.5.3 2,2-DI(PROP-2-YNYL)MALONIC ACID, 34[299]
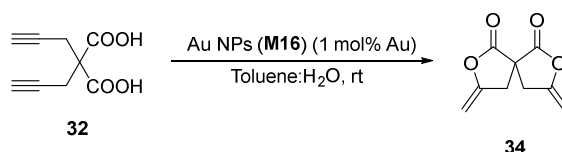
Following the typical procedure for the cycloisomerization of γ-alkynoic acids, 2,2-di(prop-2-ynyl)malonic acid **32** (13.5 mg, 0.15 mmol) was stirred in the presence of **M16** at room temperature for 24 min. **34**, colorless oil. ^{1}H NMR (360 MHz, CDCl$_3$, ppm): δ 4.94-4.91 (m, 1H), 4.51-4.49 (m, 1H), 3.47 (d, J = 16.2 Hz, 1H), 2.95 (d, J = 16.2 Hz, 1H).

4.8.6 PREPARATION OF INTERNAL ALKYNES

4.8.6.1 1-NITRO-4-(PHENYLETHYNYL)BENZENE, 37[318]
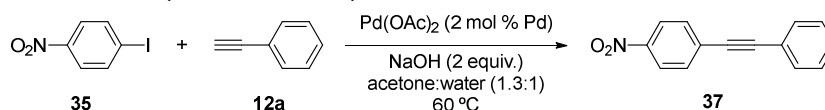
A mixture of *p*-nitrobenzene **35** (747 mg, 3.0 mmol), phenylacetylene **12a** (430 µL, ρ = 0.93 g/mL, 3.9 mmol), Pd(OAc)$_2$ (13.5 mg, 0.06 mmol), NaOH (240 mg, 6.0 mmol) in acetone (12 mL) and H$_2$O (9 mL) was stirred at 60 ºC in a closed vessel for 3 h (100% conv., GC). The reaction solution was cooled to room temperature and extracted with Et$_2$O (4 x 10 mL), the organic layer was washed with water, dried over Na$_2$SO$_4$, the solvent was evaporated under reduced pressure and the residue was purified by flash column chromatography on silica gel (hexane:EtOAc, 4:1) to give **37** as a yellow solid (348 mg, 51%). ^{1}H NMR (250 MHz, CDCl$_3$, ppm): δ 8.23 (d, J = 9.0 Hz, 2H), 7.67 (d, J = 9.0 Hz, 2H), 7.61-7.50 (m, 2H), 7.45-7.31 (m, 3H).

4.8.6.2 1-[4-(PHENYLETHYNYL)PHENYL]ETHANONE, 14[318]
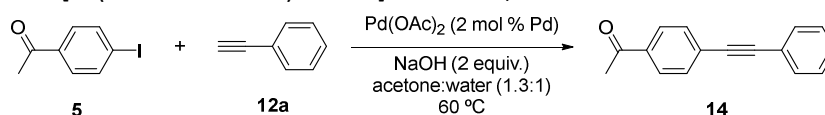
A mixture of *p*-iodoacetophenone **5** (738 mg, 3.0 mmol), phenylacetylene **12a** (430 µL, ρ = 0.93 g/mL, 3.9 mmol), Pd(OAc)$_2$ (13.5 mg, 0.06 mmol), NaOH (240 mg, 6.0 mmol) in acetone (12 mL) and H$_2$O (9 mL) was stirred at 60 ºC in a closed vessel for 2.5 h (100% conv., GC). The reaction solution was cooled to room temperature and extracted with Et$_2$O (4 x 10 mL), the organic layer was washed with water, dried over Na$_2$SO$_4$, the solvent was evaporated under reduced pressure and the residue was purified by flash column chromatography on silica gel (hexane:EtOAc, 100:0 → 98:2) to give **14** as a white solid (344 mg, 52%). ^{1}H NMR (360 MHz, CDCl$_3$, ppm): δ 7.95 (d, J = 8.7 Hz, 2H), 7.61 (d, J = 8.7 Hz, 2H), 7.58-7.52 (m, 2H), 7.40-7.33 (m, 3H), 2.62 (s, 3H).

4.8.6.3 1-METHOXY-4-(PHENYLETHYNYL)BENZENE, 38[318]
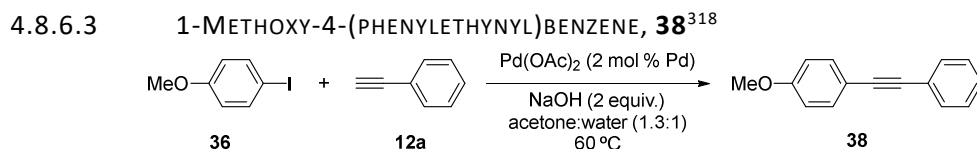
A mixture of *p*-iodoanisole **36** (1.20 g, 5.1 mmol), phenylacetylene **12a** (733 μL, ρ = 0.93 g/mL, 6.6 mmol), Pd(OAc)$_2$ (22.9 mg, 0.102 mmol), NaOH (408 mg, 10.2 mmol) in acetone (24 mL) and H$_2$O (18 mL) was stirred at 60 ºC in a closed vessel for 2.5 h (100% conv., GC). The reaction solution was cooled to room temperature and extracted with Et$_2$O (4 x 10 mL), the organic layer was washed with water, dried over Na$_2$SO$_4$, the solvent was evaporated under reduced pressure and the residue was purified by flash column chromatography on silica gel(hexane:EtOAc, 99.5:0.5) to give **38** as a pale yellow solid (815 mg, 77%). ^{1}H NMR (360 MHz, CDCl$_3$, ppm): δ 7.53-7.50 (m, 2H), 7.47 (d, *J* = 9.0 Hz, 2H), 7.36-7.31 (m, 3H), 6.88 (d, *J* = 9.0 Hz, 2H), 3.83 (s, 3H).

4.8.7 HYDROSILYLATION OF INTERNAL ALKYNES

4.8.7.1 GENERAL PROCEDURE FOR THE HYDROSILYLATION OF ALKYNES BY PT OR RH NPS WITHOUT SOLVENT (METHOD A)

To a mixture of alkyne (0.5 mmol) and nanocatalyst (**M5**, **M18**, **M19** or **M20**) (0.5 mol% Pt or Rh) into a screw-top sealable tube, triethylsilane (2 mmol) was added. The resulting solution was then heated under stirring at 90ºC until total conversion of the alkyne (GC monitoring). Hexane was added to the mixture to precipitate the Pt or Rh NPs and the catalyst was separated by centrifugation/decantation. The supernatant was filtered through a plug of silica-gel eluting with hexane and the solvent was removed under an air flow to afford the corresponding vinylsilane.

4.8.7.2 GENERAL PROCEDURE FOR THE HYDROSILYLATION OF ALKYNES BY PT OR RH NPS IN THF (METHOD B)

A mixture of alkyne (0.5 mmol) and nanocatalyst (**M5**, **M18**, **M19** or **M20**) (0.5 mol% Pt or Rh) into a screw-top sealable tube was subjected to three evacuate-refill cycles with argon. Then the corresponding silane (0.6 mmol) and anhydrous and degassed THF (1 mL) were added under argon atmosphere. The reaction mixture was heated under stirring at 90 ºC until total conversion of the alkyne (GC monitoring). Hexane was added to the mixture to precipitate the Pt or Rh NPs and the catalyst was separated by centrifugation/decantation. The supernatant was filtered through a plug of silica-gel eluting with hexane and the solvent was removed under an air flow to afford the corresponding vinylsilane. When the non-volatile triphenylsilane was used, the crude mixture was purified by column chromatography.
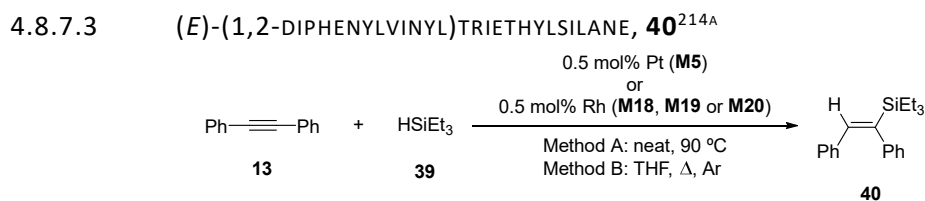
4.8.7.3 (*E*)-(1,2-DIPHENYLVINYL)TRIETHYLSILANE, 40[214A]

Following the general procedure for the hydrosilylation, diphenylacetylene (89 mg, 0.5 mmol), was allowed to react with triethylsilane (Method A: 320 μL, ρ = 0.73 g/mL, 2 mmol; Method B: 100 μL, ρ = 0.73 g/mL, 0.6 mmol) at 90 ºC until total conversion (GC monitoring). **40**, pale yellow oil (84% isolated yield with **M5** under Method A). ^{1}H NMR (360 MHz, CDCl$_3$, ppm): δ 7.27 (t, *J* = 7.2 Hz, 2H), 7.17 (t, *J* = 7.2 Hz, 1H), 7.11-7.02 (m, 3H), 7.01-6.91 (m, 4H), 6.77 (s, 1H), 0.95 (t, *J* = 7.9 Hz, 9H), 0.65 (q, *J* = 7.9 Hz, 6H).

4.8.7.4   (*E*)-(1,2-DIPHENYLVINYL)TRIPHENYLSILANE, **42**[214A]
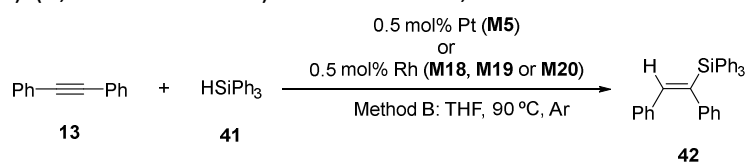
Following the general method B for the hydrosilylation, diphenylacetylene (89 mg, 0.5 mmol), was reacted with triphenylsilane (156 mg, 0.6 mmol) in THF at 90 ºC until total conversion (GC-MS monitoring). **42**, white solid (82% isolated yield with **M5**). ^{1}H NMR (360 MHz, CDCl$_3$, ppm): δ 7.50-7.38 (m, 9H), 7.37-7.30 (m, 6H), 7.17-7.08 (m, 6H), 7.03 (s, 1H), 7.00-6.96 (m, 2H), 6.92-6.89 (m, 2H).

4.8.7.5   (*E*)-5-TRIETHYLSILYL-5-DECENE, **45**[214A]
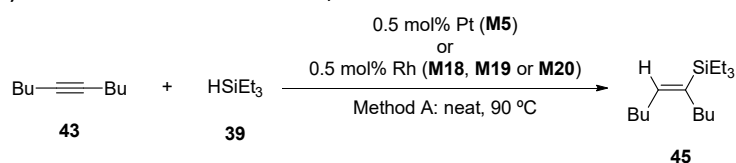
Following the general procedure for the hydrosilylation, 5-decyne (69 mg, 0.5 mmol), reacted with triethylsilane (320 μL, ρ = 0.73 g/mL, 2 mmol) at 90 ºC until total conversion (GC monitoring). **45**, colorless oil (82% isolated yield with **M5** under Method A). ^{1}H NMR (250 MHz, CDCl$_3$, ppm): δ 5.67 (t, *J* = 6.7 Hz, 1H), 2.14-2.02 (m, 4H), 1.37-1.21 (m, 8H), 0.97-0.84 (m, 15H), 0.57 (q, *J* = 7.5 Hz, 6H).

4.8.7.6   (*E*)-(1,4-DIMETHOXYBUT-3-EN-2-YL)TRIETHYLSILANE, **46**
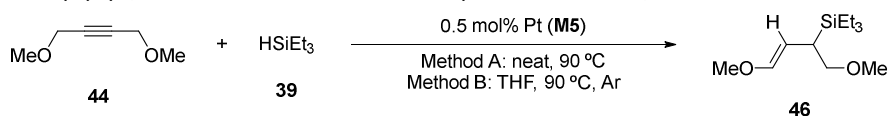
Following the general procedure for the hydrosilylation, 1,4-dimethoxy-2-butyne (57 mg, 0.5 mmol), was allowed to react with triethylsilane (Method A: 320 μL, ρ = 0.73 g/mL, 2 mmol; Method B: 100 μL, ρ = 0.73 g/mL, 0.6 mmol) at 90 ºC until total conversion (GC monitoring). **46**, colorless oil (79% isolated yield under Method A). ^{1}H NMR (400 MHz, CDCl$_3$, ppm): δ 6.19 (d, *J* = 12.6 Hz, 1H =C**H**), 4.66 (dd, *J* = 12.5, 10.2 Hz, 1H =C**H**), 3.48 (s, 3H –OC**H$_3$**), 3.42-3.41 (m, 2H, -C**H$_2$**-), 3.28 (s, 3H –OC**H$_3$**), 1.92-1.84 (m, 1H, -C**H**Si), 0.93 (t, *J* = 7.9 Hz, 9H, –SiCH$_2$C**H$_3$**), 0.56 (q, *J* = 7.9 Hz, 6H, –SiC**H$_2$**CH$_3$). ^{13}C NMR (100 MHz, CDCl$_3$, ppm): δ 146.05, 102.59, 74.08, 58.31, 56.11, 26.65, 7.59, 2.53. MS (m/z): 201.2 (M$^+$- Et). HRMS (ESI): calculated for C$_{12}$H$_{26}$O$_2$Si.H$_2$O+Na m/z = 271.1700; found m/z = 271.1701.

4.8.7.7   (*E*)-(1,4-DIMETHOXYBUT-2-EN-2-YL)TRIETHYLSILANE, **47**[214E]
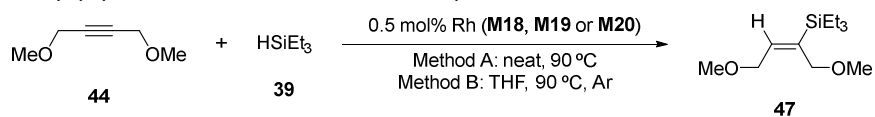
Following the general procedure for the hydrosilylation, 1,4-dimethoxy-2-butyne (57 mg, 0.5 mmol), was reacted with triethylsilane (Method A: 320 μL, ρ = 0.73 g/mL, 2 mmol; Method B: 100 μL, ρ = 0.73 g/mL, 0.6 mmol) at 90 ºC until total conversion (GC monitoring). **47**, colorless oil (97% isolated yield with **M18** under Method B). ^{1}H NMR (250 MHz, CDCl$_3$, ppm): δ 5.95 (t, *J* = 5.5 Hz, 1H), 4.09 (d, *J* = 5.5 Hz, 2H), 3.99 (s, 2H), 3.35 (s, 3H), 3.28 (s, 3H), 0.93 (t, *J* = 7.9 Hz, 9H), 0.56 (q, *J* = 7.9 Hz, 6H).

4.8.7.8 (*E*)-(1-(4-NITROPHENYL)-2-PHENYLVINYL)TRIETHYLSILANE, (*E*)-48A[214E]
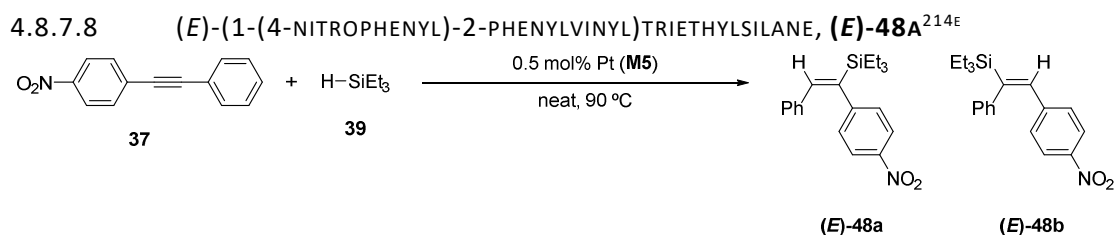
(*E*)-48a   **(*E*)-48b**

Following the general procedure for the hydrosilylation, 1-nitro-4-(phenylethynyl)benzene (112 mg, 0.5 mmol), was allowed to react with triethylsilane (320 µL, ρ = 0.73 g/mL, 2 mmol) at 90 ºC until total conversion (GC monitoring). Mixture of isomers (*E*)-48a:(*E*)-48b 68:32 (^{1}H NMR), yellow liquid (71% solated yield). Selected spectroscopic data from the mixture: ^{1}H NMR (400 MHz, CDCl$_3$, ppm): δ (*E*)-48a: 8.17 (d, *J* = 9.0 Hz, 2H, Ar**H**), 6.87 (s, 1H, =C**H**); (*E*)-48a: 7.94 (d, *J* = 9.0 Hz, 2H, Ar**H**), 6.83 (s, 1H =C**H**); 1.00-0.93 (two triplets overlapped from SiCH$_2$C**H$_3$**), 0.72-0.61 (two quartets overlapped from SiC**H$_2$**CH$_3$).

4.8.7.9 (*E*)-1-(4-(2-PHENYL-1-(TRIETHYLSILYL)VINYL)PHENYL)ETHANONE, (*E*)-49A[214E]

(*E*)-49a   **(*E*)-49b**
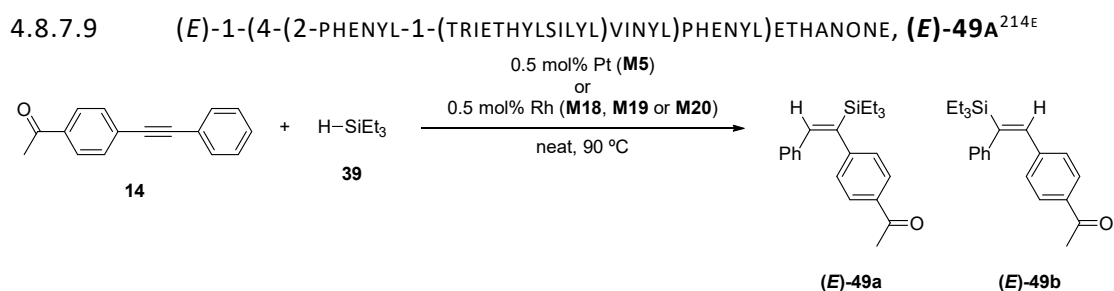
Following the general procedure for the hydrosilylation, 1-(4-(phenylethynyl)phenyl)ethanone (110 mg, 0.5 mmol), was allowed to react with triethylsilane (320 µL, ρ = 0.73 g/mL, 2 mmol) at 90 ºC until total conversion (GC monitoring). Mixture of isomers (for **M5**) (*E*)-49a:(*E*)-49b 58:52 (^{1}H NMR), yellow liquid (88% isolated yield for **M5**). Selected spectroscopic data from the mixture: ^{1}H NMR (400 MHz, CDCl$_3$, ppm): δ (*E*)-49a: 7.91 (d, *J* = 7.8 Hz, 2H, Ar**H**), 6.82 (s, 1H, =C**H**), 2.61 (s, 3H, COC**H$_3$**); (*E*)-49b: 7.68 (d, *J* = 8.1 Hz, 2H, Ar**H**), 2.50 (s, 3H COC**H$_3$**); 1.03-0.89 (two triplets overlapped from SiCH$_2$C**H$_3$**), 0.72-0.61 (two quartets overlapped from SiC**H$_2$**CH$_3$).

4.8.7.10 (*E*)-TRIETHYL(2-P-METHOXYPHENYL-1-PHENYLVINYL)SILANE, (*E*)-50B[214A]

(*E*)-50a   **(*E*)-50b**
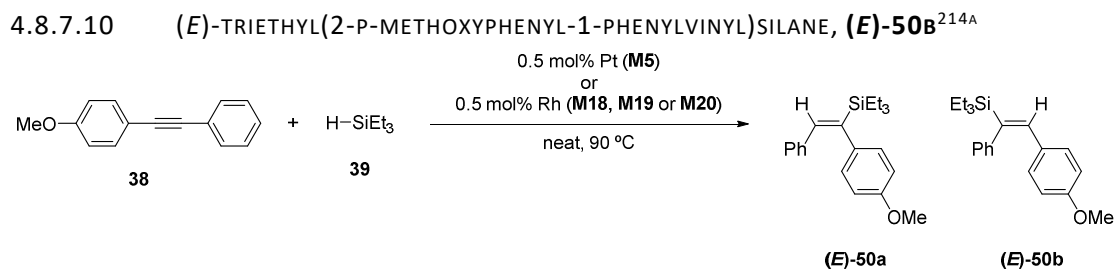
Following the general procedure for the hydrosilylation, 1-methoxy-4-(phenylethynyl)benzene (104 mg, 0.5 mmol), was allowed to react with triethylsilane (320 µL, ρ = 0.73 g/mL, 2 mmol) at 90 ºC until total conversion (GC monitoring). Mixture of isomers (for **M5**) (*E*)-50a:(*E*)-50b 47:53 (^{1}H NMR), yellow oil (99% isolated yield for **M5**). Selected spectroscopic data from the mixture: ^{1}H NMR (360 MHz, CDCl$_3$, ppm): δ (*E*)-50a: 6.77 (s, 1H, =C**H**), 3.83 (s, 3H, OC**H$_3$**); (*E*)-50b: 6.71 (s, 1H, =C**H**), 3.73 (s, 3H, OC**H$_3$**), 1.00-0.94 (two triplets overlapped from SiCH$_2$C**H$_3$**), 0.69-0.61 (two quartets overlapped from SiC**H$_2$**CH$_3$) (for other signals see the spectrum).
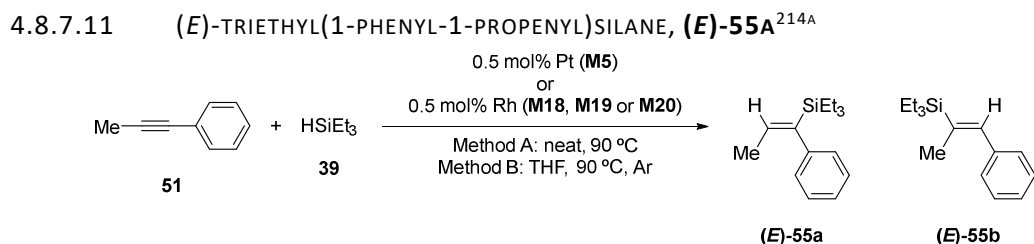
4.8.7.11 (*E*)-TRIETHYL(1-PHENYL-1-PROPENYL)SILANE, (*E*)-55A[214A]

(*E*)-55a   **(*E*)-55b**

Following the general procedure for the hydrosilylation, 1-phenyl-1-propyne (58 mg, 0.5 mmol), was allowed to react with triethylsilane (Method A: 320 μL, ρ = 0.73 g/mL, 2 mmol; Method B: 100 μL, ρ = 0.73 g/mL, 0.6 mmol) at 90 ºC until total conversion (GC monitoring). Mixture of isomers (for **M5**) **(E)-55a:(E)-55b** 58:42 (^{1}H NMR), pale yellow oil (84% isolated yield for **M5**). Selected spectroscopic data from the mixture: ^{1}H NMR (250 MHz, CDCl$_3$, ppm): δ **(E)-55a**: 6.94 (d, J = 7.0 Hz, 2H, Ar**H**), 6.07 (q, J = 6.5 Hz, 1H, =C**H**), 1.57 (d, J = 6.5 Hz, 3H, −C**H₃**), 0.91 (t, J = 7.9 Hz, 9H, SiCH₂C**H₃**), 0.69 (q, J = 7.9 Hz, 6H, SiC**H₂**CH₃); **(E)-55b**: 6.72 (s, 1H =C**H**), 1.95 (s, 3H, −C**H₃**), 0.99 (t, J = 7.8 Hz, 9H, SiCH₂C**H₃**), 0.69 (q, J = 7.8 Hz, 6H, SiC**H₂**CH₃) (for other signals see the spectrum).

4.8.7.12   (E)-METHYL 2-(TRIETHYLSILYL)OCT-2-ENOATE, (E)-56A[214A]
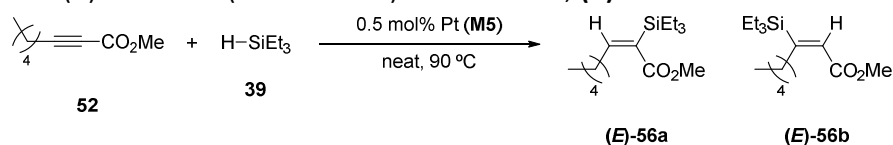
Following the general procedure for the hydrosilylation, methyl-2-octynoate (77 mg, 0.5 mmol), was reacted with triethylsilane (320 μL, ρ = 0.73 g/mL, 2 mmol) at 90 ºC until total conversion (GC monitoring). Mixture of isomers **(E)-56a:(E)-56b** 85:15 (^{1}H NMR), colorless oil (72% isolated yield). Selected spectroscopic data from the mixture: ^{1}H NMR (250 MHz, CDCl$_3$, ppm): δ **(E)-56a**: 6.08 (t, J = 7.2 Hz, 1H, =C**H**), 3.70 (s, 3H, COOC**H₃**), 2.30 (apparent q, J = 7.2 Hz, 2H, CH₂C**H₂**CH=); **(E)-56b**: 5.99 (s, 1H, =C**H**), 3.69 (s, 3H, COOC**H₃**) (for other signals see the spectrum).

4.8.7.13   (E)-ETHYL 2-(TRIETHYLSILYL)-2-BUTENOATE, (E)-57A[214A]
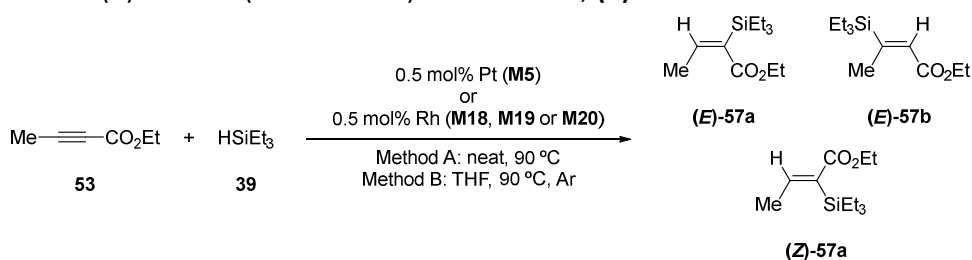
Following the general procedure for the hydrosilylation, ethyl-2-butynoate (56 mg, 0.5 mmol), was reacted with triethylsilane (Method A: 320 μL, ρ = 0.73 g/mL, 2 mmol; Method B: 100 μL, ρ = 0.73 g/mL, 0.6 mmol) at 90 ºC until total conversion (GC monitoring). Mixture of isomers (for **M5**) **(E)-57a:(E)-57b** 64:36 (^{1}H NMR), yellow oil (81% isolated yield). Selected spectroscopic data from the mixture: ^{1}H NMR (250 MHz, CDCl$_3$, ppm): δ **(E)-57a**: 6.21 (q, J = 6.8 Hz, 1H, =C**H**), 4.16 (q, J = 7.1 Hz, 2H, COOC**H₂**CH₃), 1.93 (d, J = 6.8 Hz, 3H, C**H₃**CH=), 1.29 (t, J = 7.1 Hz, 3H, COOCH₂C**H₃**); **(E)-57b**: 6.00 (q, J = 1.8 Hz, 1H, =C**H**), 2.19 (d, J = 1.8 Hz, 3H, C**H₃**CH=) (for other signals see the spectrum).

4.8.7.14   (E)-2-PHENYL-1-(TRIETHYLSILYL)ETHENE, (E)-58A[341]
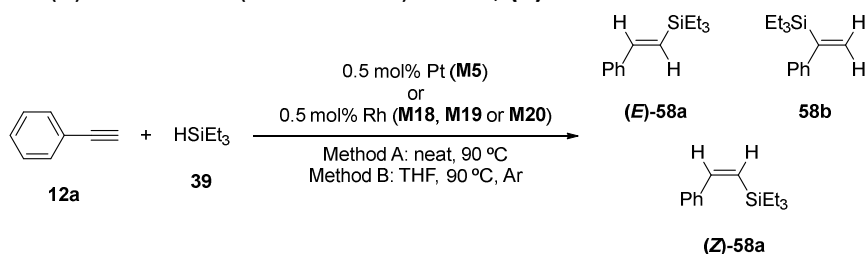
Following the general procedure for the hydrosilylation, phenylacetylene (51 mg, 0.5 mmol), was reacted with triethylsilane (Method A: 320 μL, ρ = 0.73 g/mL, 2 mmol; Method B: 100 μL, ρ = 0.73 g/mL, 0.6 mmol) at 90 ºC until total conversion (GC monitoring). Mixture of isomers (for **M5**) **(E)-58a:58b** 83:17 (^{1}H NMR), colorless oil

---

[341] Yong, L., Kirels, K., Butenschön, H. *Adv. Synth. Catal.* **2006**, *348*, 833.

(82% isolated yield). Selected spectroscopic data from the mixture: ^{1}H NMR (250 MHz, CDCl$_3$, ppm): δ (E)-**58a**: 6.99 (d, J = 19.3 Hz, 1H, =C**H**), 6.51 (d, J =19.3 Hz, 1H, =C**H**); **58b**: 5.96 (d, J = 2.6 Hz, 1H, =C**H**), 5.66 (d, J = 2.6 Hz, 1H, =C**H**) (for other signals see the spectrum).

4.8.7.15 (E)-(2-CYCLOHEXYLVINYL)TRIETHYLSILANE, (E)-59A[214E]
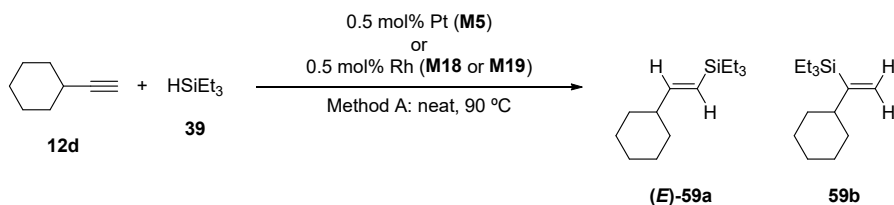
Following the general procedure for the hydrosilylation, ethynylcyclohexane (55 mg, 0.5 mmol), was reacted with triethylsilane (320 µL, ρ = 0.73 g/mL, 2 mmol) at 90 ºC until total conversion (GC monitoring). Mixture of isomers (for **M5**) (E)-**59a:59b** 62:38 (^{1}H NMR), colorless oil (80% isolated yield). Selected spectroscopic data from the mixture: ^{1}H NMR (400 MHz, CDCl$_3$, ppm): δ (E)-**59a:** 5.99 (dd, J = 18.9, 6.0 Hz, 1H, =C**H**), 5.49 (d, J = 18.9 Hz, 1H, =C**H**); **59b**: 5.68 (d, J = 2.3 Hz, 1H, =C**H**), 5.31 (d, J = 2.3 Hz, 1H, =C**H**) (for other signals see the spectrum).

4.8.7.16 (E)-TRIETHYL(2,2,7,7-TETRAMETHYLOCT-3-EN-5-YN-4-YL)SILANE, 60[214E]
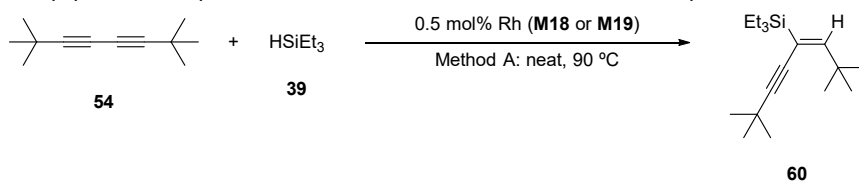
Following the general procedure for the hydrosilylation, 2,2,7,7-tetramethylocta-3,5-diyne (81 mg, 0.5 mmol), was reacted with triethylsilane (320 µL, ρ = 0.73 g/mL, 2 mmol) at 90 ºC until total conversion (GC monitoring). **60**, colorless oil (99% isolated yield with **M18**). ^{1}H NMR (250 MHz, CDCl$_3$, ppm): δ 5.86 (s, 1H), 1.24 (s, 9H), 1.20 (s, 9H), 0.95 (t, J = 7.9 Hz, 9H), 0.63 (q, J = 7.9 Hz, 6H).

4.8.8 REDUCTION OF NITROARENES

4.8.8.1 GENERAL PROCEDURE FOR THE REDUCTION OF NITROARENES CATALYZED BY NI NPS.

Hydrazine monohydrate (8 mmol) was added dropwise to a stirred solution of catalyst **M11** (2 mol% Ni) and nitroarene (1 mmol) in anhydrous and degassed THF (2 mL), and the mixture was heated at reflux. Upon completion of the reaction (TLC monitoring), diethyl ether was added (2 mL), **M11** precipitated and the liquid phase was separated by decantation from the solid magnetic catalyst **M11** by use of an external magnet. The magnetic Ni NPs were washed twice with diethyl ether. At this point the catalyst was dried and it was ready for a second cycle. The combined organic fractions were evaporated to dryness and the residue was partitioned between water and dichloromethane. The organic phase was dried with anhydrous Na$_2$SO$_4$ and then the solvent was evaporated under reduced pressure to afford the corresponding pure aniline.

When some starting nitroarene was observed in the ^{1}H NMR spectrum of the crude mixture, this residue was partitioned between 4 M HCl and dichloromethane. The organic phase was discarded, the aqueous phase was basified with 4 M NaOH and it was extracted with dichloromethane. The organic phase was dried with anhydrous Na$_2$SO$_4$ and then the solvent was evaporated under reduced pressure to afford the corresponding amine.

4.8.8.2 GENERAL PROCEDURE FOR THE REDUCTION OF NITROARENES CATALYZED BY RH NPS.

A solution of ammonia borane (2 mmol) in 8 mL of H$_2$O was added dropwise to a stirred solution of catalyst **M20** (1 mol% Rh) and nitroarene (0.5 mmol) in THF (2 mL) into a sealed tube with an empty balloon to maintain

the pressure. Upon completion of the reaction (TLC monitoring), diethyl ether was added (5 mL), **M20** was maintained in the aqueous phase and the product in the ether phase. The two phases were separated by decantation, the aqueous phase was extracted with more diethyl ether (2 x 5 mL). For the recycling of the catalyst the aqueous layer was then extracted with CH$_2$Cl$_2$ (3 x 5 mL), dried over Na$_2$SO$_4$ and the solvent was evaporated under reduced pressure to obtain the Rh NPs ready for another cycle. The combined fractions of diethyl ether were washed with water (2 x 5 mL). The organic phase was dried with anhydrous Na$_2$SO$_4$ and then the solvent was evaporated under reduced pressure to afford the corresponding pure aniline.

4.8.8.3   ANILINE, **62**[342]
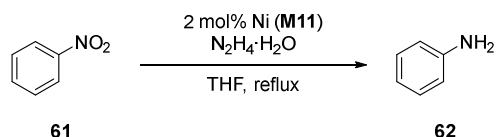
Following the general procedure for the reduction of nitroarenes catalyzed by Ni NPs, nitrobenzene (123 mg, 1 mmol) reacted with hydrazine (256 mg, 251 μL, 8 mmol) in THF at reflux temperature until total conversion (TLC monitoring). **62**, pale yellow liquid (90 mg, 97% isolated yield).[343] ^{1}H NMR (250 MHz, CDCl$_3$, ppm): δ 7.23-7.15 (m, 2 H), 6.86-6.72 (m, 3 H), 3.65 (br s, 2H).

4.8.8.4   *M*-PHENYLENEDIAMINE, **73**[342]
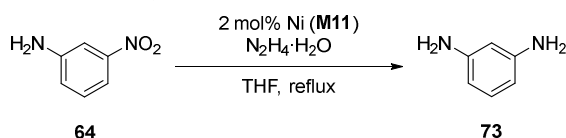
Following the general procedure for the reduction of nitroarenes catalyzed by Ni NPs, *m*-nitroaniline (138 mg, 1 mmol) reacted with hydrazine (256 mg, 251 μL, 8 mmol) in THF at reflux temperature until total conversion (TLC monitoring). **73**, brownish liquid (56 mg, 52% isolated yield).[344] ^{1}H NMR (250 MHz, CDCl$_3$, ppm): δ 6.95 (t, *J* = 7.8 Hz, 1H), 6.12 (dd, *J* = 7.9, 2.2 Hz, 2 H), 6.01 (t, *J* = 2.2 Hz, 1H), 3.52 (br s, 4H).

4.8.8.5   *P*-METHOXYANILINE, **74**[342]
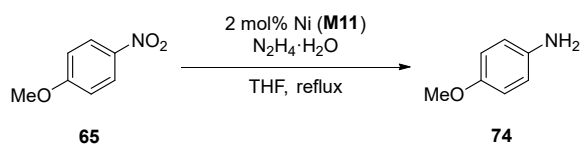
Following the general procedure for the reduction of nitroarenes catalyzed by Ni NPs, 1-methoxy-4-nitrobenzene (153 mg, 1 mmol) reacted with hydrazine (256 mg, 251 μL, 8 mmol) in THF at reflux temperature until total conversion (TLC monitoring). **74**, white solid (95 mg, 77% isolated yield). [343] ^{1}H NMR (250 MHz, CDCl$_3$, ppm): δ 6.75 (d, *J* = 8.6 Hz, 2H), 6.65 (d, *J* = 8.6 Hz, 2H), 3.75 (s, 3H), 3.42 (br s, 2 H).

4.8.8.6   3,4-DIMETHOXYANILINE, **75**[345]

---
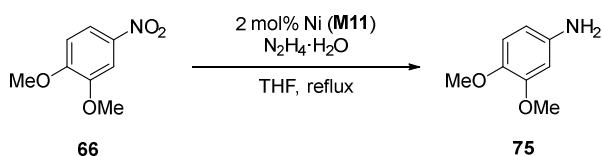
[342] Layek, K., Kantam, M. L., Shirai, M., Nishio-Hamame, D., Sasaki, T., Maheswaran, H. *Green Chem.* **2012**, *14*, 3164.

[343] This product was also obtained following the general procedure for the reduction of nitroarenes catalyzed by Rh NPs (section 4.8.8.2).

[344] This product was also obtained from 3,4-dimethoxynitrobenzene following the general procedure for the reduction of nitroarenes catalyzed by Rh NPs (section 4.8.8.2).

[345] Aksenov, A. V., Aksenov, N. A., Nadein, O. N., Aksenova, I. V. *Synlett* **2010**, *17*, 2628.

Following the general procedure for the reduction of nitroarenes catalyzed by Ni NPs, 1,2-dimethoxy-4-nitrobenzene (169 mg, 1 mmol) reacted with hydrazine (256 mg, 251 μL, 8 mmol) in THF at reflux temperature until total conversion (TLC monitoring). **75**, brownish solid (145 mg, 95% isolated yield).[343] ^{1}H NMR (250 MHz, CDCl$_3$, ppm): δ 6.67 (d, *J* = 8.4 Hz, 1H), 6.28 (d, *J* = 2.6 Hz, 1H), 6.20 (dd, *J* = 8.4, 2.6 Hz, 1H), 3.79 (s, 3H), 3.76 (s, 3H), 3.48 (br s, 2H).

4.8.8.7   *P*-TOLUIDINE, **76**[346]
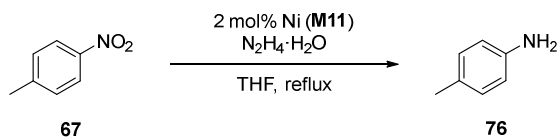
Following the general procedure for the reduction of nitroarenes catalyzed by Ni NPs, 1-methyl-4-nitrobenzene (137 mg, 1 mmol) reacted with hydrazine (256 mg, 251 μL, 8 mmol) in THF at reflux temperature until total conversion (TLC monitoring). **76**, brownish solid (93 mg, 97% isolated yield). ^{1}H NMR (250 MHz, CDCl$_3$, ppm): δ 7.0 (d, *J* = 8.0 Hz, 2H), 6.63 (d, *J* = 8.0 Hz, 2H), 3.55 (br s, 2H), 2.27 (s, 3H).

4.8.8.8   *P*-AMINOBENZENESULFONAMIDE, **77**[228]
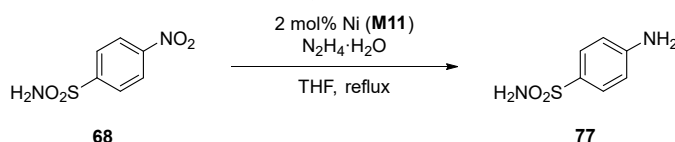
Following the general procedure for the reduction of nitroarenes catalyzed by Ni NPs, *p*-nitrobenzenesulfonamide (202 mg, 1 mmol) reacted with hydrazine (256 mg, 251 μL, 8 mmol) in THF at reflux temperature until total conversion (TLC monitoring). **77**, pale yellow solid (76 mg, 45% isolated yield).[343] ^{1}H NMR (250 MHz, (CD$_3$)$_2$CO, ppm): δ 7.56 (d, *J* = 8.9 Hz, 2H), 6.72 (d, *J* = 8.9 Hz, 2H), 6.15 (br s, 2H), 5.34 (br s, 2H).

4.8.8.9   *P*-BROMOANILINE, **78**[342]
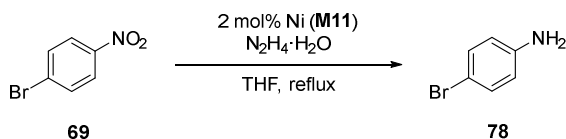
Following the general procedure for the reduction of nitroarenes catalyzed by Ni NPs, 1-bromo-4-nitrobenzene (202 mg, 1 mmol) reacted with hydrazine (256 mg, 251 μL, 8 mmol) in THF at reflux temperature until total conversion (TLC monitoring). **78**, pale yellow solid (156 mg, 91% isolated yield).[343] ^{1}H NMR (250 MHz, CDCl$_3$, ppm): δ 7.25 (d, *J* = 8.7 Hz, 2H), 6.56 (d, *J* = 8.7 Hz, 2H), 3.69 (br s, 2H).

4.8.8.10   *P*-AMINOBENZONITRILE, **79**[342]
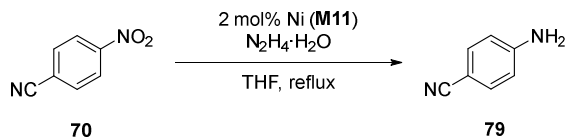
Following the general procedure for the reduction of nitroarenes catalyzed by Ni NPs, *p*-nitrobenzonitrile (148 mg, 1 mmol) reacted with hydrazine (256 mg, 251 μL, 8 mmol) in THF at reflux temperature until total conversion (TLC monitoring). **79**, white solid (75 mg, 63% isolated yield).[343] ^{1}H NMR (250 MHz, CDCl$_3$, ppm): δ 7.39 (d, *J* = 8.6 Hz, 2H), 6.64 (d, *J* = 8.6 Hz, 2H), 4.2 (br s, 2H).

---

[346] Kim, J., Chang, S. *Chem. Commun.* **2008**, 3052.

4.8.8.11   P-AMINOACETOPHENONE, 80[347]
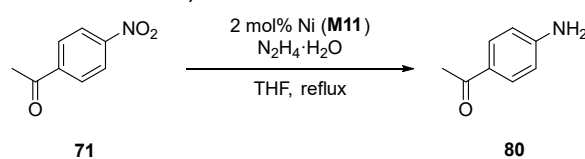
71 → **80**

Following the general procedure for the reduction of nitroarenes catalyzed by Ni NPs, *p*-nitrobenzophenone (165 mg, 1 mmol) reacted with hydrazine (256 mg, 251 µL, 8 mmol) in THF at reflux temperature until total conversion (TLC monitoring). **80**, white solid (100 mg, 74% isolated yield).[343] ^{1}H NMR (250 MHz, CDCl$_3$, ppm): δ 7.79 (d, *J* = 8.6 Hz, 2H), 6.63 (d, *J* = 8.6 Hz, 2H), 4.22 (br s, 2H), 2.49 (s, 3H). ^{13}C NMR (90 MHz, CDCl$_3$, ppm): δ 196.5, 151.1, 130.7, 127.7, 113.6, 26.0. IR (ATR): 3389, 3328, 3222, 1650 cm^{-1}.

4.8.8.12   P-AMINOSTILBENE, 81
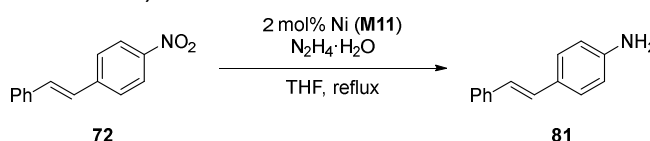
72 → **81**

Following the general procedure for the reduction of nitroarenes catalyzed by Ni NPs, *p*-nitrostilbene (225 mg, 1 mmol) reacted with hydrazine (256 mg, 251 µL, 8 mmol) in THF at reflux temperature until total conversion (TLC monitoring). **81**, pale yellow solid (168 mg, 86% isolated yield).[343] ^{1}H NMR (250 MHz, CDCl$_3$, ppm): δ 7.51-7.47 (m, 2H), 7.38-7.32 (m, 4H), 7.26-7.22 (m, 1H), 7.05 (d, *J* = 16.3 Hz, 1H), 6.93 (d, *J* = 16.3 Hz, 1H), 6.68 (d, *J* = 8.5 Hz, 2H), 3.74 (br s, 2H); ^{13}C NMR (90 MHz, CDCl$_3$, ppm): δ 146.1, 137.9, 128.6, 128.5, 127.9, 127.7, 126.8, 126.0, 125.0, 115,1. HRMS-ESI (m/z): [M+H]$^+$ calculated for C$_{14}$H$_{14}$N: 196.1121 found: 196.1121.

4.8.8.13   P-AMINOBENZYALCOHOL, 91[346]

84 → **91**
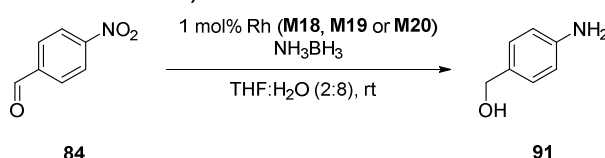
Following the general procedure for the reduction of nitroarenes catalyzed by Rh NPs, *p*-nitrobenzaldehyde (76 mg, 0.5 mmol) reacted with ammonia borane (69 mg, 2 mmol) in THF:H$_2$O (1:4) at room temperature until total conversion (TLC monitoring). **91**, brown solid (39 mg, 64% isolated yield with **M20**). ^{1}H NMR (250 MHz, CDCl$_3$, ppm): δ 7.16 (d, *J* = 8.4 Hz, 2H), 6.67 (d, *J* = 8.4 Hz, 2H), 4.56 (s, 2H).

4.8.8.14   METHYL P-AMINOBENZOATE, 92[228]

85 → **92**
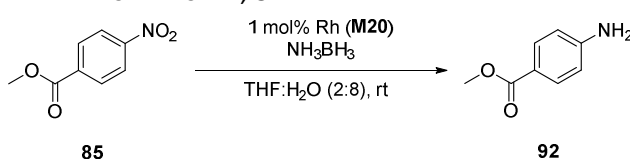
Following the general procedure for the reduction of nitroarenes catalyzed by Rh NPs, methyl *p*-nitrobenzoate (91 mg, 0.5 mmol) reacted with ammonia borane (69 mg, 2 mmol) in THF:H$_2$O (1:4) at room temperature until total conversion (TLC monitoring). **92**, white solid (50 mg, 66% isolated yield with **M20**). ^{1}H NMR (250 MHz, CDCl$_3$, ppm): δ 7.85 (d, *J* = 8.6 Hz, 2H), 6.64 (d, *J* = 8.6 Hz, 2H), 4.06 (br s, 2H), 3.85 (s, 3H).

4.8.8.15   5-QUINOLINAMINE, 93[348]

---

[347] Wang, C., Pan, Y., Wu, A. *Tetrahedron* **2007**, *63*, 429.

[348] Rashidi, A., Afghan, A., Baradarani, M. M., Joule, J. A. *J. Heterocyclic Chem.* **2009**, *46*, 428.
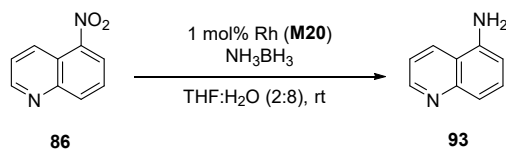
Following the general procedure for the reduction of nitroarenes catalyzed by Rh NPs, 5-nitroquinolone (97 mg, 0.5 mmol) reacted with ammonia borane (69 mg, 2 mmol) in THF:H_2O (1:4) at room temperature until total conversion (TLC monitoring). **93**, yellow solid (60 mg, 83% isolated yield with **M20**). ^{1}H NMR (360 MHz, CDCl$_3$, ppm): δ 8.89 (dd, J = 4.2, 1.7 Hz, 1H), 8.18 (dd, J = 8.5, 1.7 Hz, 1H), 7.59-7.49 (m, 2H), 7.35 (dd, J = 8.5, 4.2 Hz, 1H), 6.82 (d, J = 8.5 Hz, 1H), 4.21 (br s, 2H).

4.8.8.16 *M*-TOLUIDINE, **94**[349]
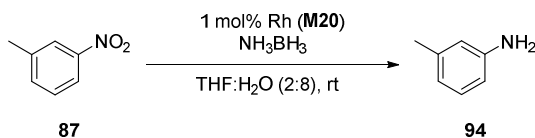
Following the general procedure for the reduction of nitroarenes catalyzed by Rh NPs, 3-methyl-4-nitrobenzene (69 mg, 0.5 mmol) reacted with ammonia borane (69 mg, 2 mmol) in THF:H_2O (1:4) at room temperature until total conversion (TLC monitoring). **94**, yellow solid (29 mg, 53% isolated yield with **M20**). ^{1}H NMR (360 MHz, CDCl$_3$, ppm): δ 7.06 (t, J = 7.4 Hz, 1H), 6.60 (d, J = 7.5, 1.7 Hz, 1H), 6.54-6.50 (m, 2H), 3.58 (br s, 2H), 2.28 (s, 3H).

---

[349] Spectral Database for Organic Compounds (SDBS); ^{1}HNMR; No. 1156HSP-00-727

Chapter 5.   GENERAL CONCLUSIONS

Following the interest of our group in the preparation of soluble metal NPs for their use in catalysis, we have synthesized novel metal NPs stabilized by imidazolium salts soluble in organic solvents (Pt and Ni NPs) or in water (Rh and Au NPs). The activity of the prepared nanomaterials as reusable catalysts has been evaluated in different organic reactions.

Three new PEG-tagged imidazolium salts have been designed and successfully synthesized via a copper-catalyzed azide-alkyne cycloaddition reaction, namely bromide **S2A**, tetrafluoroborate **S2B** and the tris-imidazolium bromide **S3** (**Figure 47**). These salts were soluble in water and some organic solvents (CH$_2$Cl$_2$, THF) and insoluble in diethyl ether, toluene or hexane.

The previously reported tris-imidazolium iodide (**S1A**) and tetrafluoroborate (**S1B**) containing hexadecyl chains (**Figure 47**) have been successfully applied as stabilizers for the preparation of novel Pt (**S1B**) and Ni (**S1A** and **S1B**) NPs.
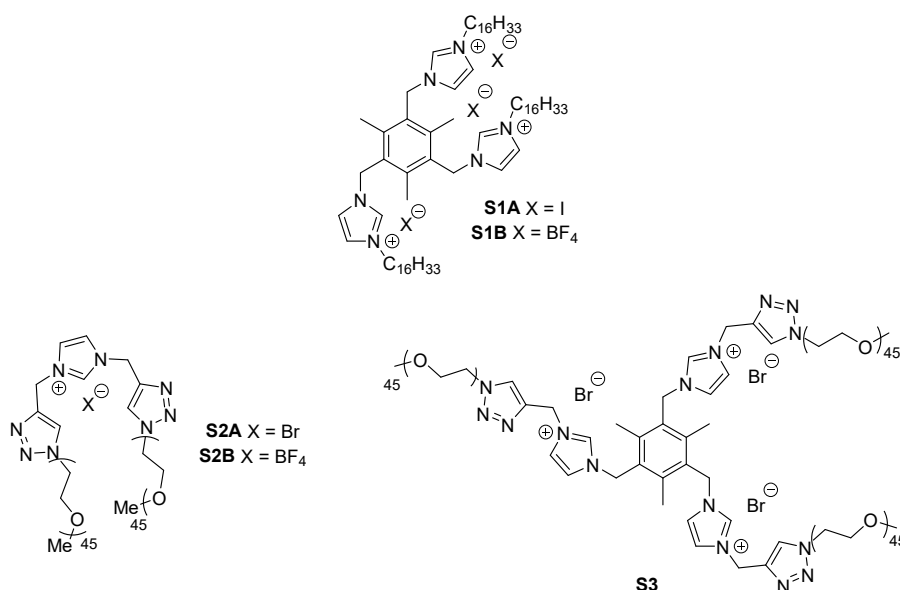
Figure 47 Imidazolium salts (**S1A**, **S1B**, **S2A**, **S2B** and **S3**) developed for the stabilization of metal NPs.

Platinum NPs have been obtained by a two-step process involving the reduction of H$_2$PtCl$_6$ with ethylene glycol:NaOH at 160 ºC and subsequent treatment with a THF solution of **S1B** at room temperature. Depending on the **S1B**:Pt initial molar ratio, two different Pt(0) nanomaterials were prepared (**M5** for 1:1 **S1B**:Pt and **M6** for 0.5:1 **S1B**:Pt). The Pt NPs have been fully characterized by TEM, HRTEM, ED, EDS and ICP-OES (crystalline FCC lattice, average size of 1.6 ± 0.6 nm for **M5**). They were soluble in some organic solvents such as toluene, THF, CH$_2$Cl$_2$, CHCl$_3$ and insoluble in pentane, diethyl ether, ethyl acetate, methanol and water. Unfortunately, the tris-imidazolium iodide **S1A** failed as stabilizer of Pt NPs.

Nickel NPs stabilized by **S1A** and **S1B** have been successfully obtained by the *organometallic approach*. Thus, the hydrogenation (3 bar H$_2$) of Ni(COD)$_2$ at 70 ºC in the presence of **S1A** or **S1B** gave stable magnetic Ni NPs which were kept under inert atmosphere. However, the iodide **S1A** has been found better stabilizer than the tetrafluoroborate **S1B** for Ni NPs. Two different nanomaterials were obtained depending on the initial molar ratio between the nickel precursor and the stabilizer (**M11** for 1:1 **S1A**:Ni and **M12** for 0.05:1 **S1A**:Ni). They were characterized by TEM, HRTEM, ED, EDS, XPS and ICP-OES, revealing Ni(0) NPs of 10.1 ± 5 nm for **M11**. A study of the magnetic properties of the materials was also performed (hysteresis loops and ZFC/FC), revealing a superparamagnetic behaviour at room temperature. This property is desirable for these nanomaterials, because they do not aggregate in the absence of an external magnetic field. The Ni NPs presented the same pattern of solubility as the Pt NPs. The magnetic and solubility properties facilitate the recycling of the NPs when used in catalysis.

Chapter 5. General Conclusions

The synthesized PEG-tagged imidazolium salts (**S2A**, **S2B** or **S3**) have been successfully employed as stabilizers for the preparation of Au and Rh NPs. These stabilizers will provide to the derived metal NPs solubility in water and insolubility in diethyl ether.

Gold NPs have been prepared by the reduction of tetrachloroauric acid with sodium borohydride in the presence of the stabilizer in water at room temperature. Depending on the stabilizer used four different nanomaterials were obtained (**M14** with **S2A**; **M15** with **S2B**; and **M16** and **M17** with **S3**) with average sizes around 4.5 nm. The Au NPs were characterized by TEM, HRTEM, EDS, ED, XPS, UV-vis and ICP-OES. Two valence states of gold (Au(0) and Au(I)) were present in the nanoparticles according to the XPS spectra, being the oxidized Au(I) species the major one in the nanomaterials derived from **S3** (**M16** and **M17**). Also, the ^{1}H NMR spectra suggested a stronger interaction between the imidazolium ring and the metal surface when bromide was the counter anion (**S2A** and **S3**).

Rhodium NPs have been prepared following the reduction method. Rh(III) chloride was reduced with NaBH$_4$ in the presence of the corresponding stabilizer in water at room temperature. They have been characterized by TEM, HRTEM, ^{1}H NMR, EDS, ED, XPS and ICP-OES. Small Rh NPs were obtained with tendency to form flower-like aggregates with sizes around 25 nm. However, most part of the NPs remained well dispersed presenting an FCC crystalline structure. The absence of oxidized Rh species was confirmed by XPS analyses.

The formation of new C-C bonds via coupling reactions has been tested with Ni (Suzuki and Sonogashira) and Rh (Heck-type reaction between arylboronic acids and butyl acrylate) NPs. Unfortunately, no conversion or low conversions have been obtained under the conditions studied. For this reason, these reactions were not further investigated. The previously reported Pd NPs stabilized by **S1A** have been found active for different cross-coupling reactions (Suzuki, Heck, Sonogashira and Hiyama) obtaining good yields in all cases with a wide number of substrates.

Successful results have been achieved for the A^3 coupling between aldehydes, secondary amines and terminal alkynes catalyzed by Au NPs (**Figure 48 (A)**). Gold NPs stabilized by **S3** (**M16**) resulted much more active than **M14** and **M15** stabilized by **S1A** and **S1B,** respectively. This difference may be due to the higher amount of Au(I) species present in **M16** with respect to **M14** and **M15** nanomaterials. The structural features of the stabilizers may also have an influence in these results. Under **M16** catalysis twelve different propargylamines have been obtained with moderate to good yields. The reaction has also been extended to ketones, obtaining four derived propargylamines. Taking advantage of the solubility properties, the nanocatalyst has been recycled up to four times.

The gold nanocatalyst has been also active in the cycloisomerization of diverse γ-alkynoic acids to enol lactones in a biphasic medium toluene:water at room temperature (**Figure 48 (B)**), obtaining excellent yields in all cases. The Au NPs were successfully reused up to six cycles. As in the case of the A^3 coupling, Au NPs **M14** and **M15** present lower activity than **M16** and **M17** for this reaction.

The Pt (**M5**) and Rh (**M18**, **M19** and **M20**) NPs have been found very effective in the stereoselective *syn*-hydrosilylation of symmetric and unsymmetric internal alkynes for the preparation of the corresponding (*E*)-vinylsilanes (**Figure 48 (C)**). Excellent yields were obtained in all cases under two different methods: (i) neat conditions at 90 ºC with an excess of silane (method A) and (ii) with THF as a solvent at 90 ºC with one equivalent of silane in a closed vessel (method B). Lower reaction times were needed with Pt NPs compared to the Rh NPs. However, Rh NPs presented higher regioselectivities with asymmetric alkynes. In all cases the nanocatalyst could be reused several times without a significant loss of activity. Previously, our group had reported this reaction with Pd NPs stabilized by **S1B**. However, strict anhydrous conditions were needed to prevent the formation of the reduced products. The Rh NPs stabilized by a N-rich PEG-tagged substrate had also been found active for this reaction. In that case anhydrous conditions were not necessary. The Pt NPs described in this thesis provide faster reactions than the previously reported Pd NPs and Rh NPs and

competitive transfer hydrogenation of the alkyne was not found with traces of water. Moreover, terminal alkynes have been found to react in the presence of Pt and Rh NPs and not in the presence of Pd NPs.

The reduction of nitroarenes has been performed under Ni (**M12**) and Rh (**M18**, **M19** and **M20**) catalysis. Ni(0) NPs have been found very effective for the reduction of differently substituted nitroarenes with hydrazine as hydrogen donor in refluxing THF (**Figure 48 (D)**). The nanocatalyst was chemoselective and other reducible groups (bromo, carbonyl, ester, cyano, olefin) present in the nitroarene were recovered unaltered. The Ni NPs were recycled up to 5 runs for the reduction of nitrobenzene to aniline.

Finally, the Rh NPs (**M18**, **M19** and **M20**) have been found catalytically active for the generation of hydrogen from the hydrolysis of ammonia-borane complex (AB) at room temperature. Thus, with this *in situ* generated hydrogen as reductant, Rh NPs have been able to reduce a wide number of different nitroarenes to the corresponding anilines in a toluene:water medium at room temperature (**Figure 48 (E)**). In all cases good yields of the reduced products were obtained. Nevertheless, the chemoselectivity was lower than with Ni NPs and certain reducible groups present in the nitroarene were also fully (aldehyde) or partially reduced (olefin). Other reductants (NaBH$_4$ and hydrazine) have also been tested with some substrates, obtaining similar results with NaBH$_4$ and lower conversions with hydrazine. The Rh NPs (**M18**) were successfully recycled up to 5 runs for this reaction using AB as hydrogen source. The previously reported Au NPs stabilized by a *N*-rich PEG-tagged substrate were also catalytically active for the reduction of nitroarenes, in that case with a great excess of NaBH$_4$ as reductant in water at room temperature. In the present work we have reacted nitroarenes bearing olefin and carbonyl groups not previously tested with Au NPs. Ni NPs and hydrazine as reductant were found to be selective towards the nitro group. Although the selectivity in front of these reducible groups was lower with Rh NPs in the presence of ammonia-borane as source of hydrogen, this method constitutes a clean and mild transfer hydrogenation for a wide number of nitro aromatics. Thus, the results of the procedures developed here compete well with the results previously described with Au NPs for this type of reaction.
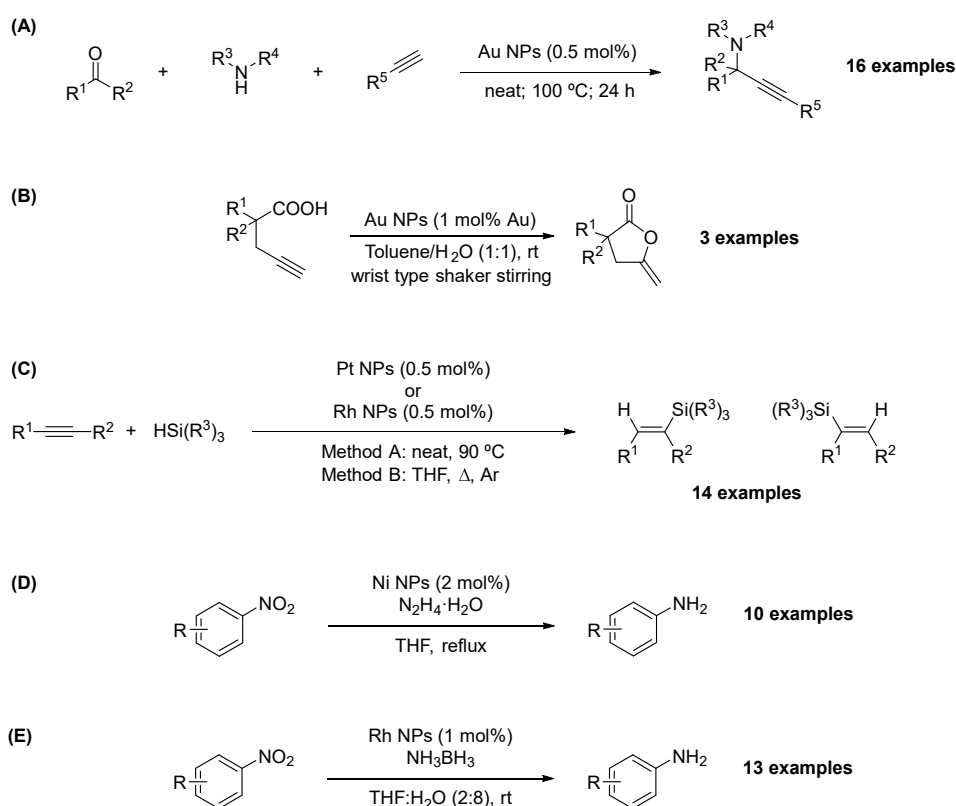
Figure 48 Summary of the reactions catalyzed by the different soluble metal NPs synthesized.

SPECTRA COLLECTION

1

^{1}H NMR (250 MHz, CDCl$_3$)

7.31
7.26
7.06
6.74

5.24

2.32

1.64

0.07

2.98
2.77
2.84

5.98

9.00

10.5 10.0 9.5 9.0 8.5 8.0 7.5 7.0 6.5 6.0 5.5 5.0 4.5 4.0 3.5 3.0 2.5 2.0 1.5 1.0 0.5 0.0 -0.5
ppm
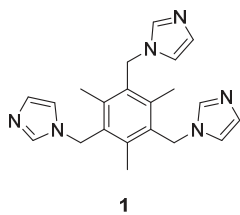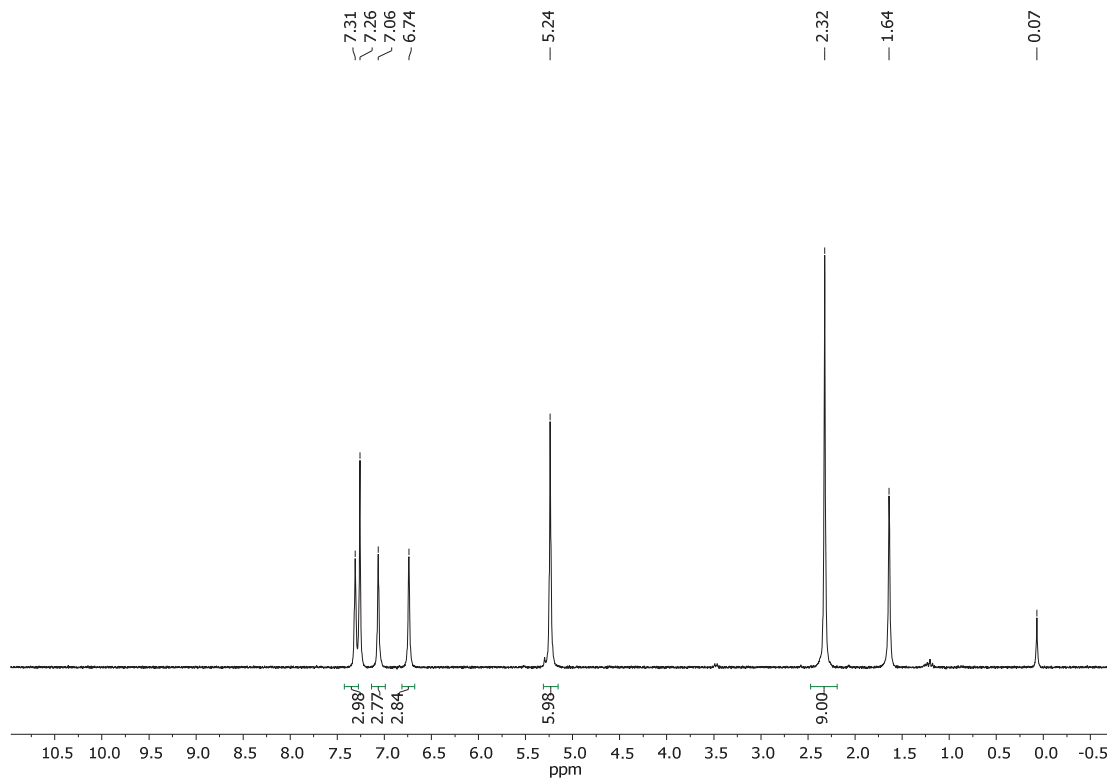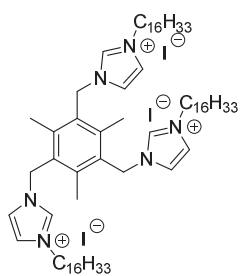
S1A
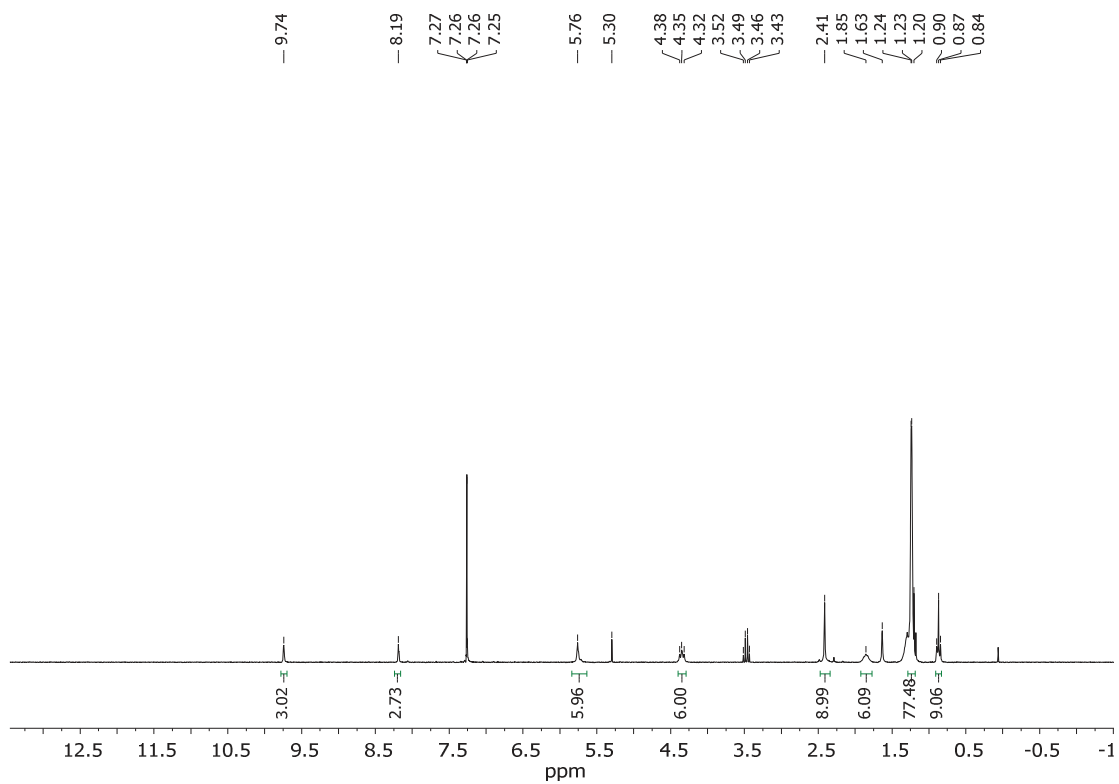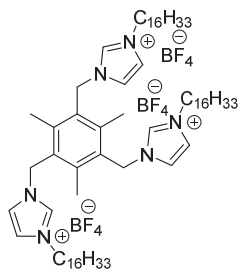
^{1}H NMR (250 MHz, CDCl$_3$)

S1B

^{1}H NMR (360 MHz, CDCl$_3$)
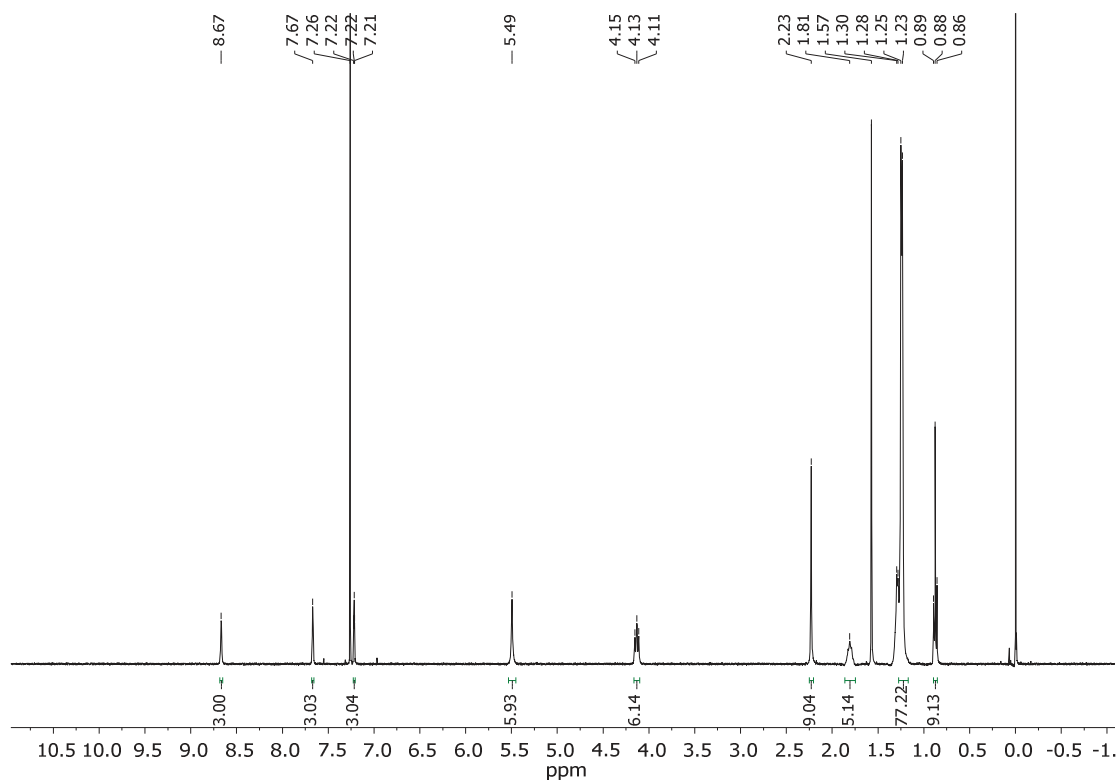
Spectra Collection
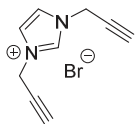
2a

^{1}H NMR (250 MHz, CD$_3$CN)
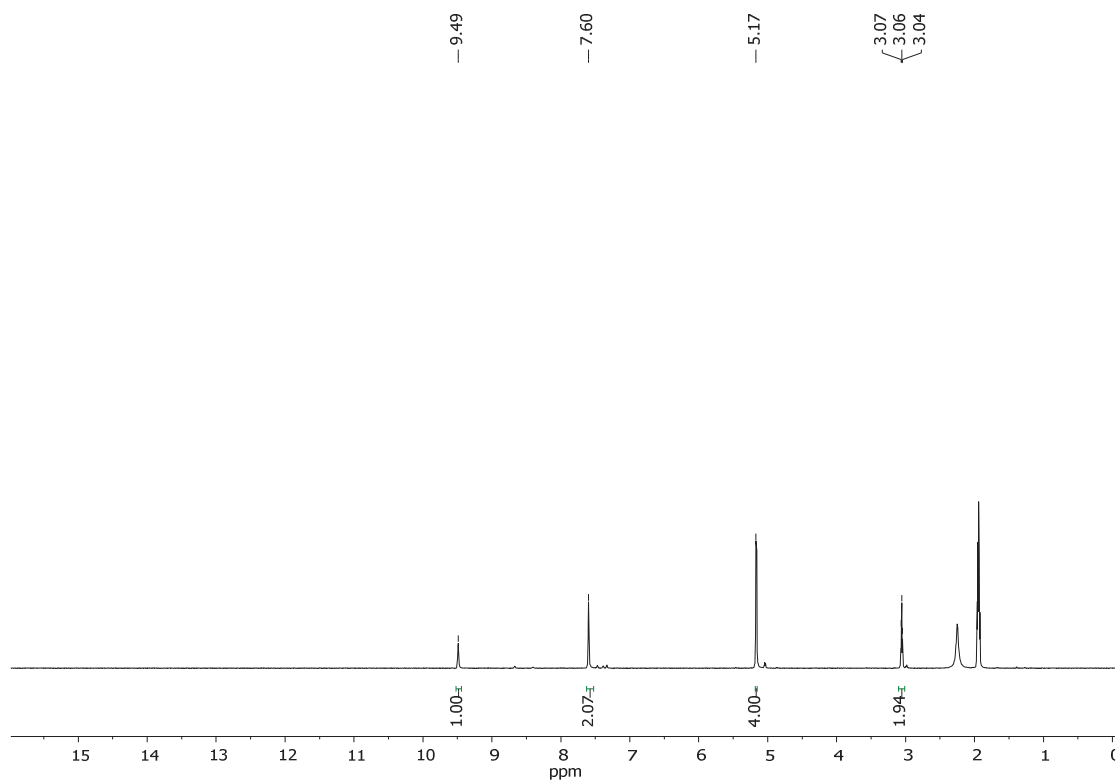
^{13}C NMR (62.5 MHz, CD$_3$CN)

ESI-HRMS

#	m/z	I	I %
1	145.0761	462219	100.0
2	146.0787	48338	10.5
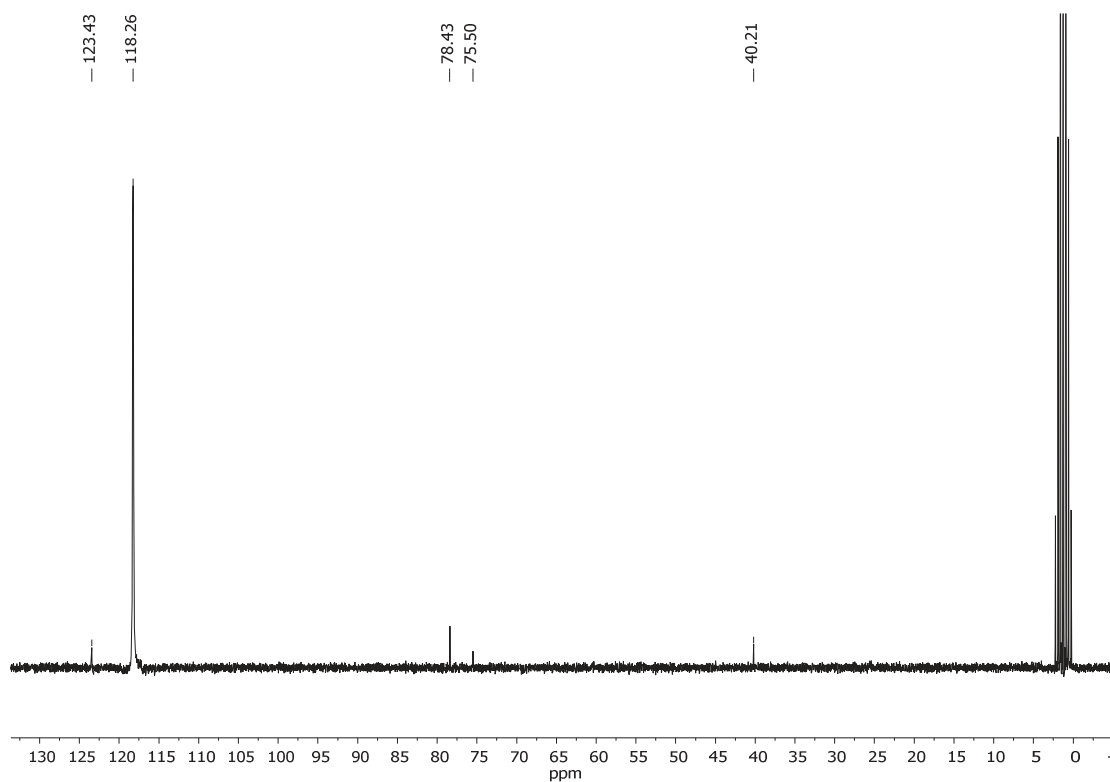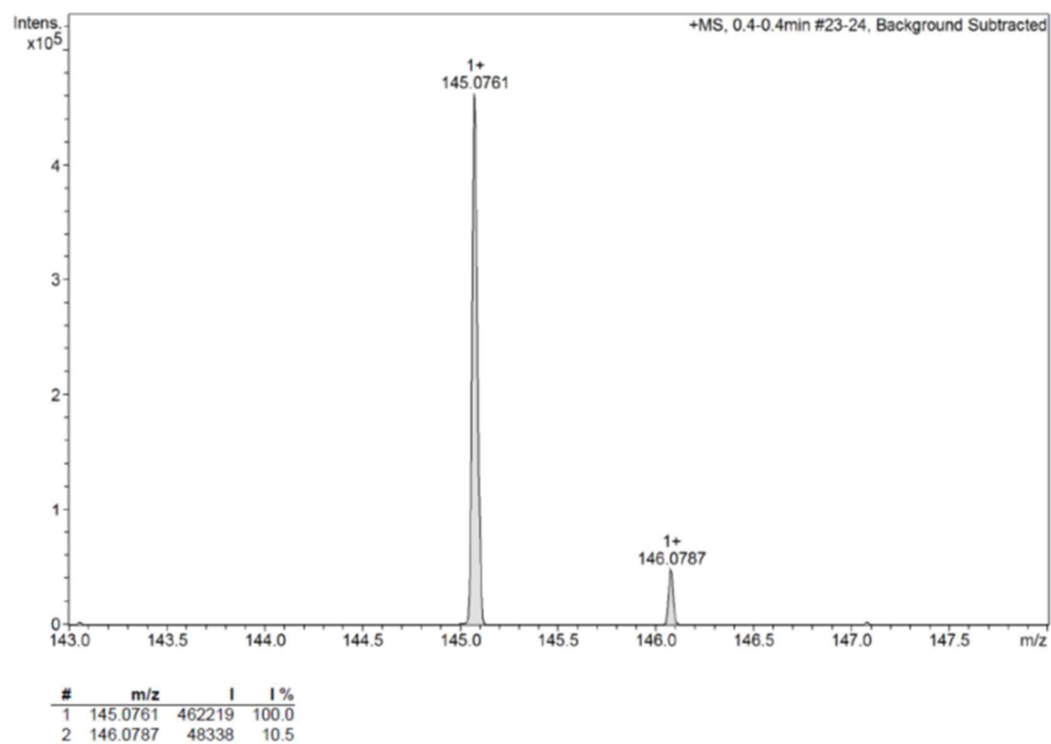
Spectra Collection
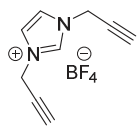
2b

^{1}H NMR (250 MHz, CD$_3$CN)
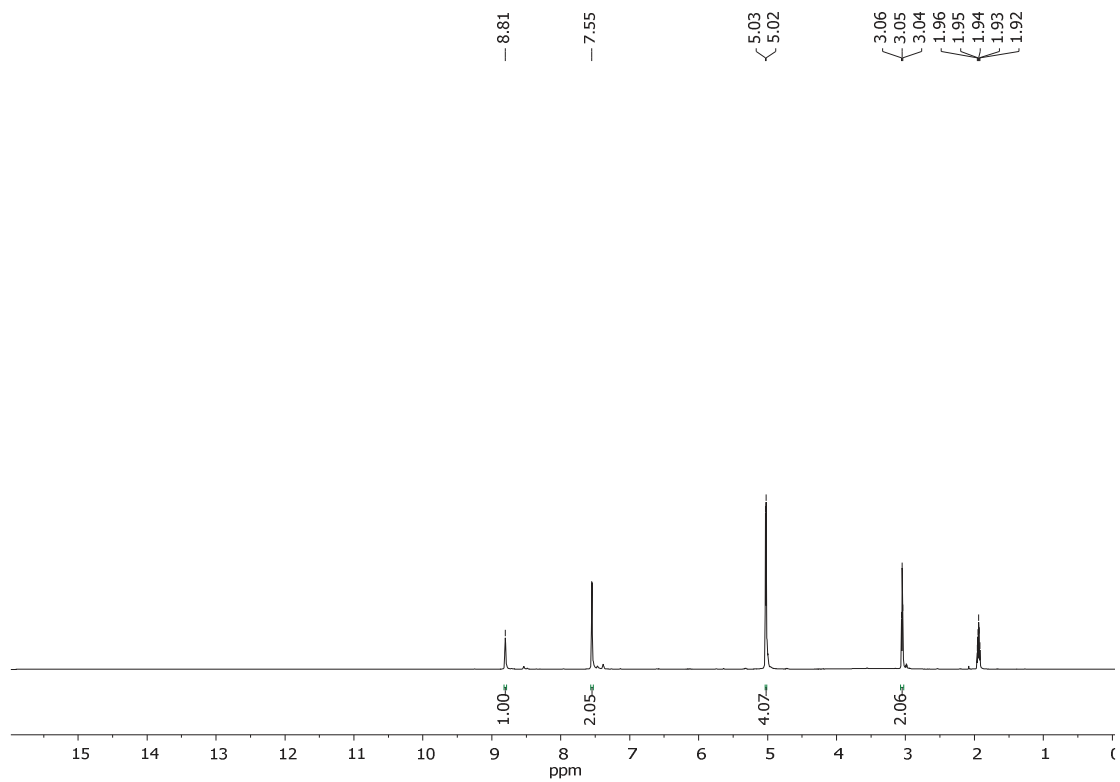
^{13}C NMR (62.5 MHz, CD$_3$CN)
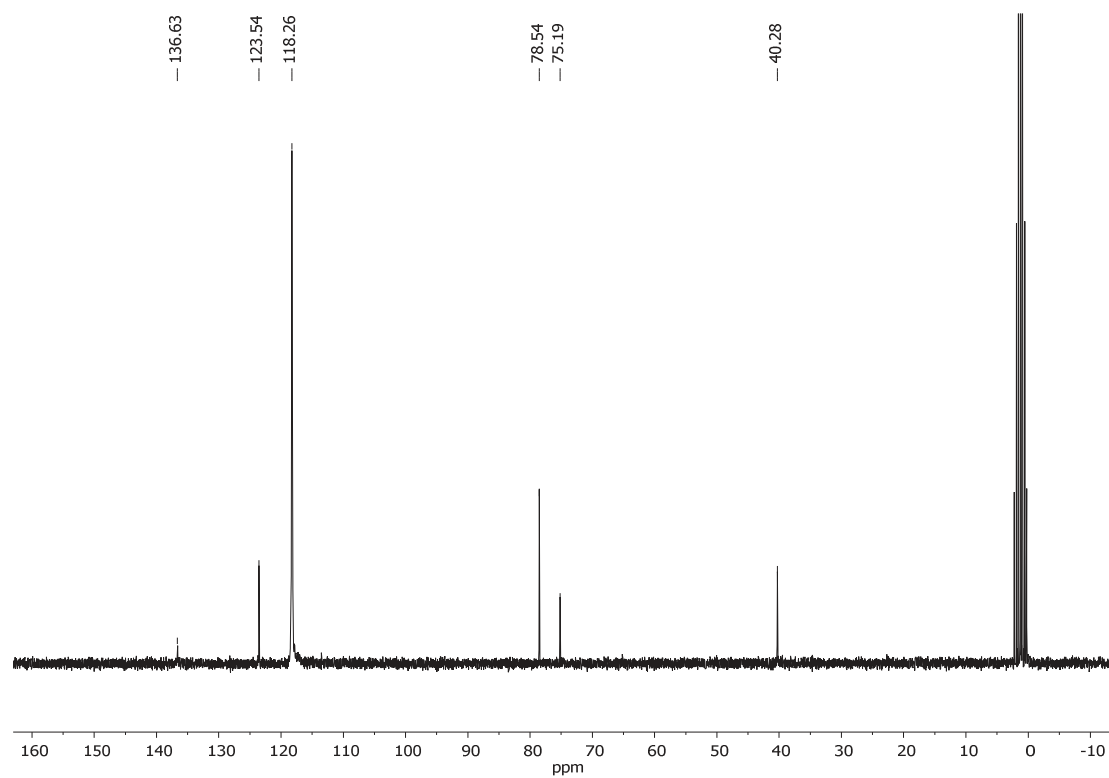
Spectra Collection

3
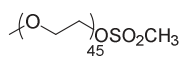
^{1}H NMR (250 MHz, CDCl$_3$)
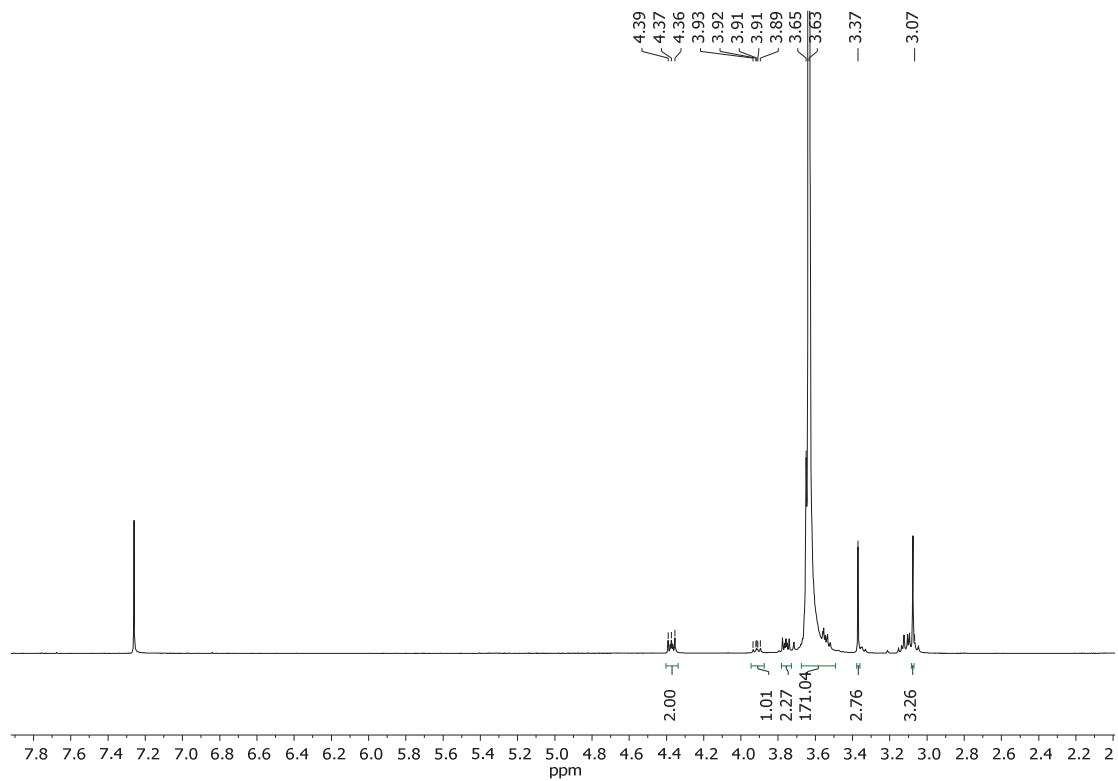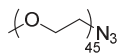
4

^{1}H NMR (250 MHz, CDCl$_3$)
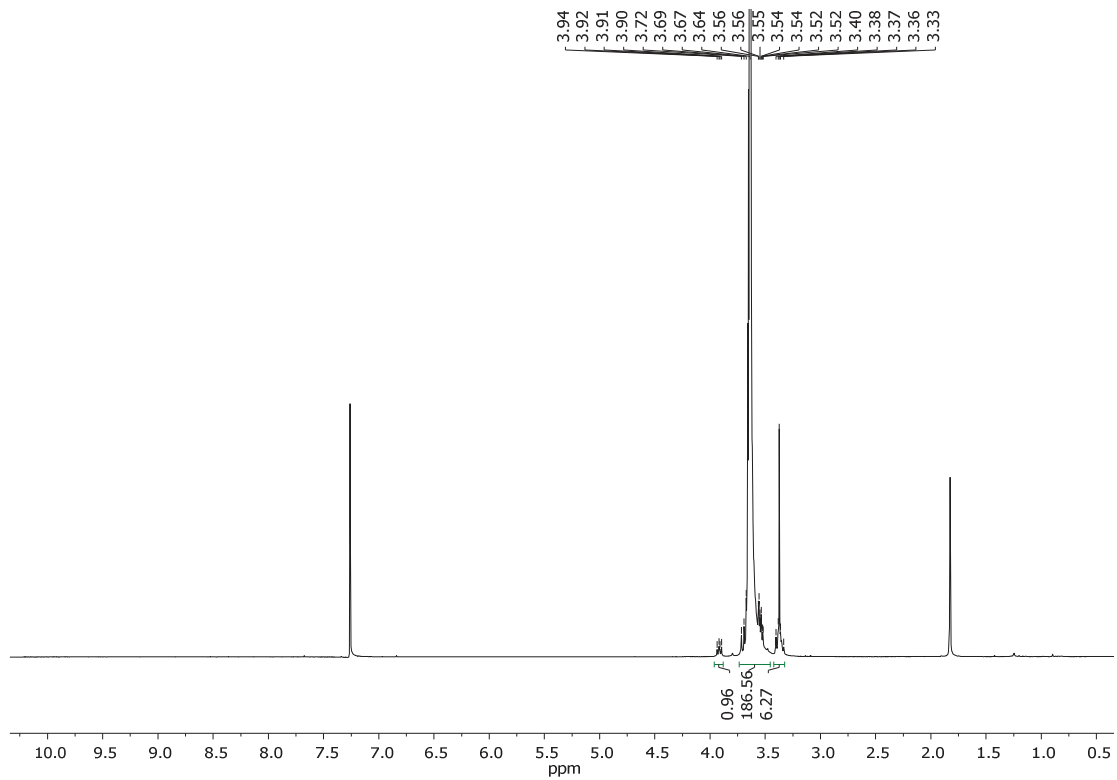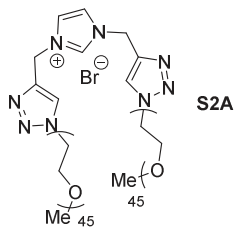
Spectra Collection

S2A

^{1}H NMR (250 MHz, CDCl$_3$)

ESI-TOF-MS

+MS, 0.5-0.7min #31-39

2+
4047.7

S2B

^{1}H NMR (250 MHz, CDCl$_3$)

ESI-TOF-MS

5
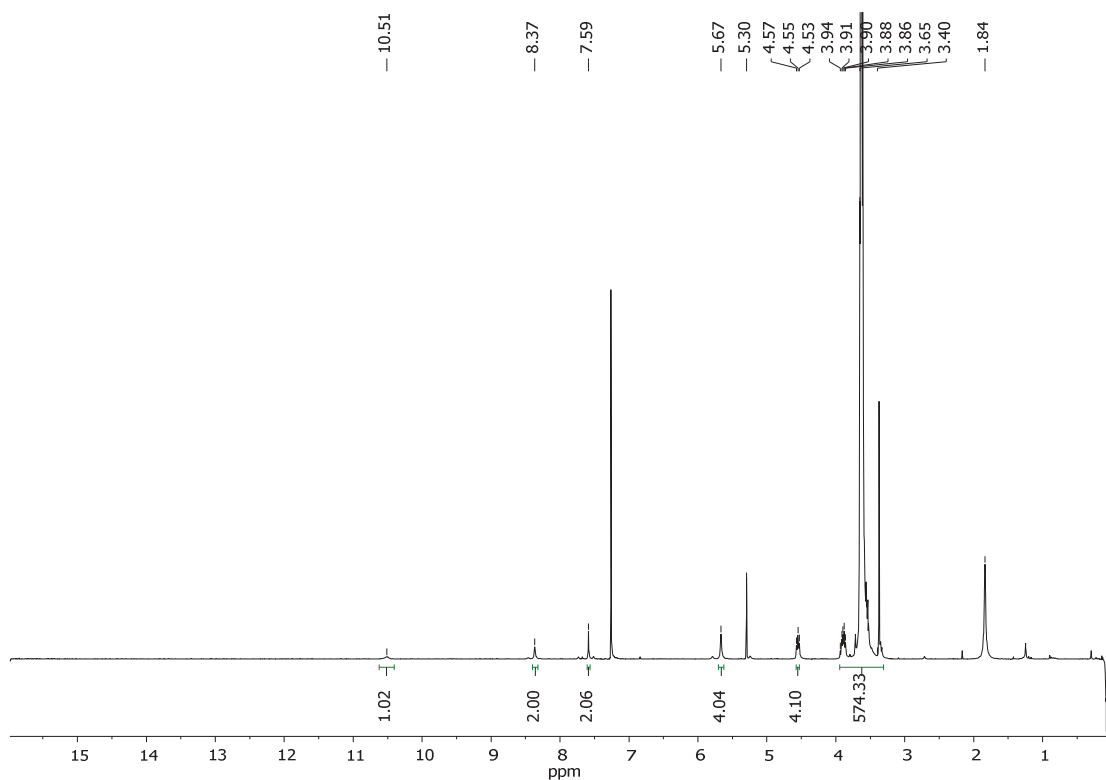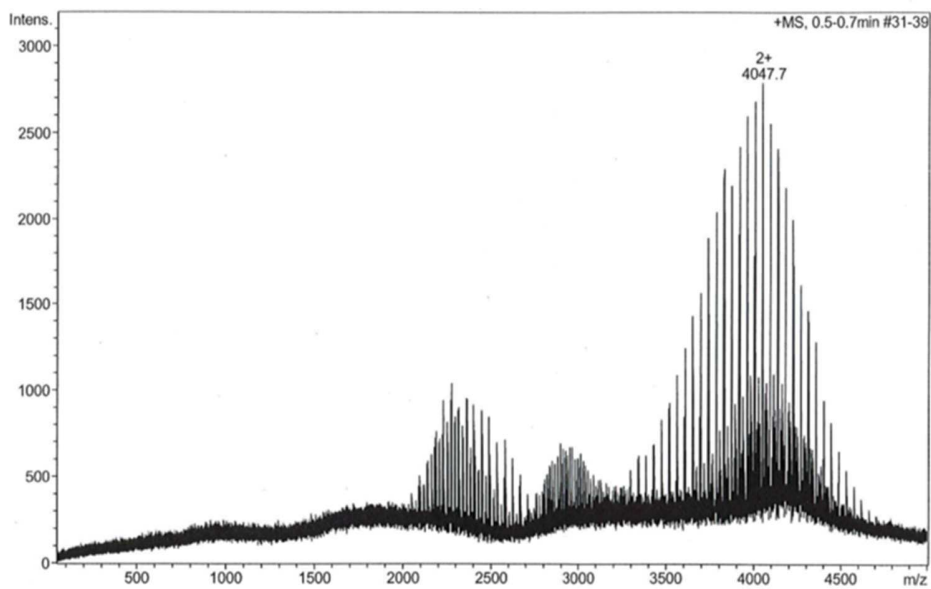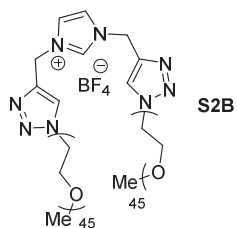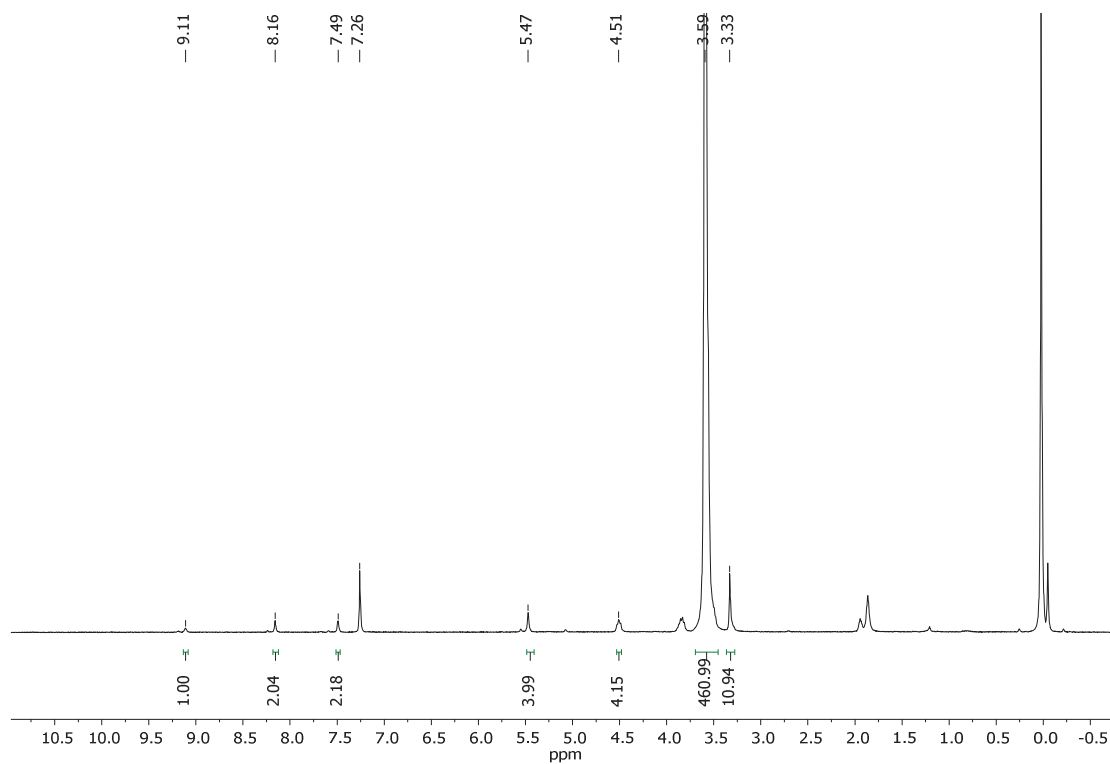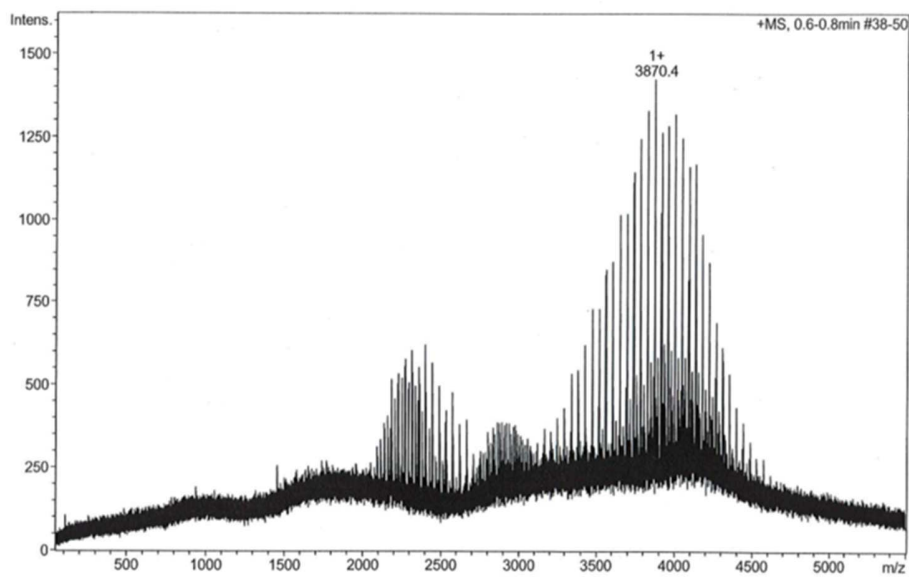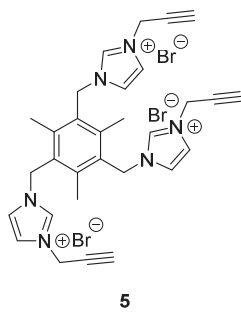
^{1}H NMR (360 MHz, (CD$_3$)$_2$SO)
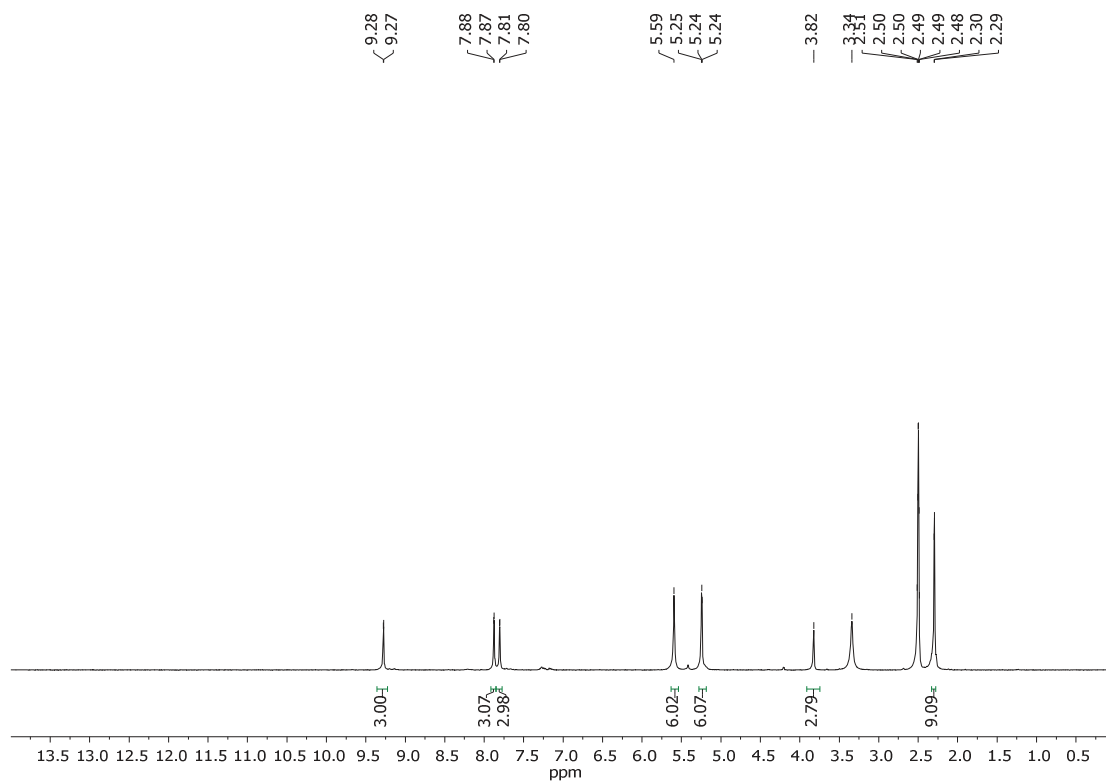
^{13}C NMR (100. MHz, (CD$_3$)$_2$SO)
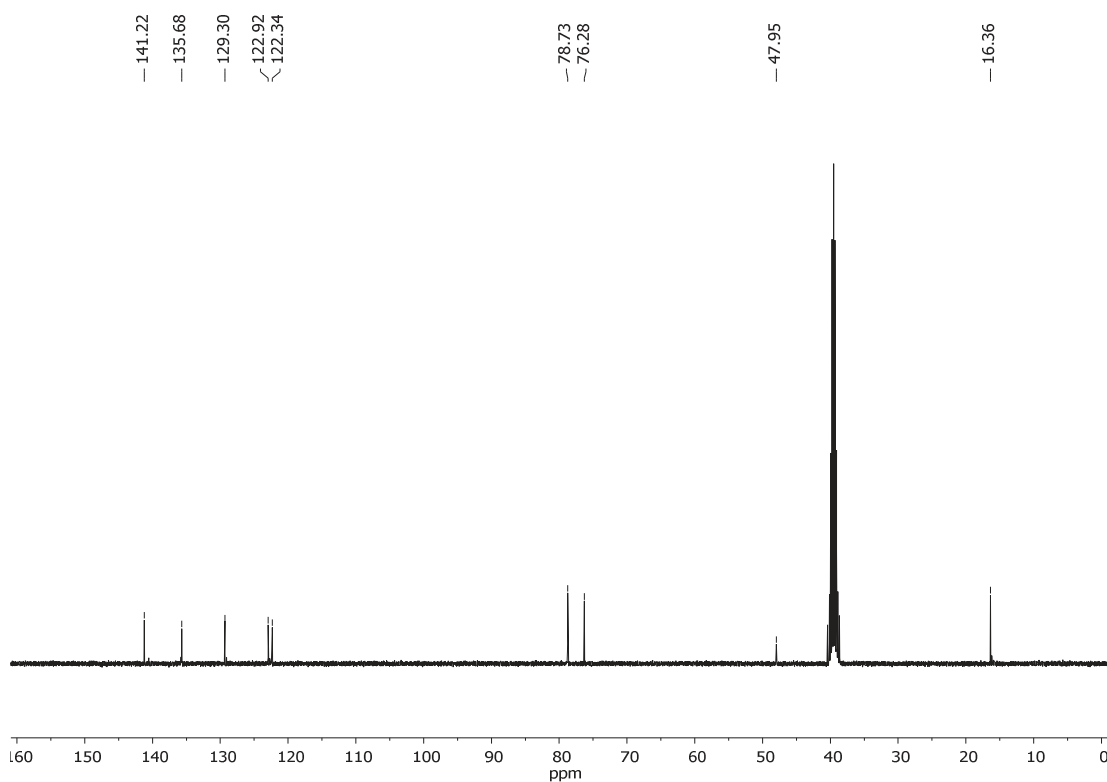
ESI-TOF-HRMS

Spectra Collection

S3
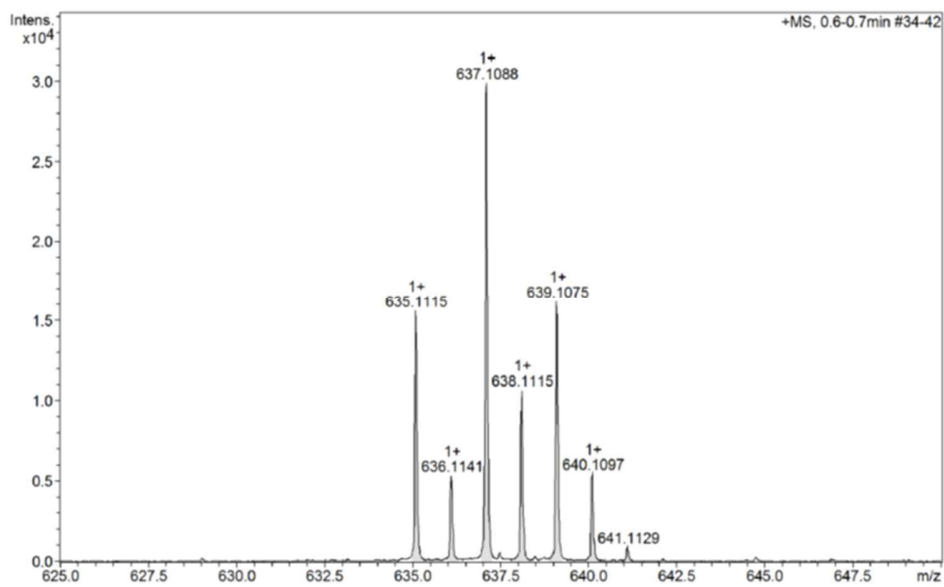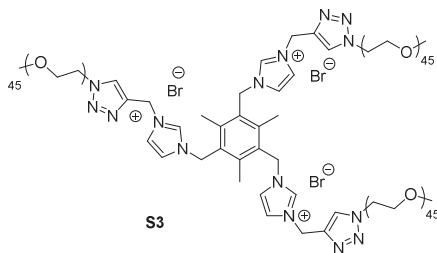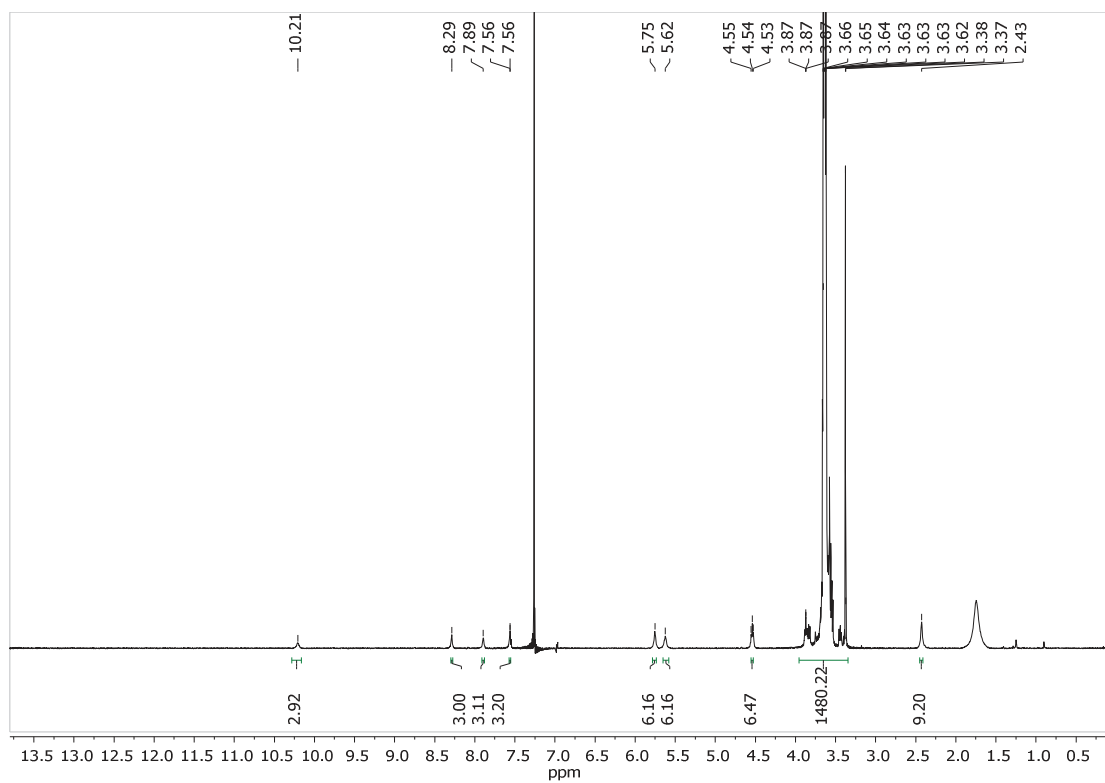
^{1}H NMR (360 MHz, CDCl$_3$)

MALDI-TOF-MS
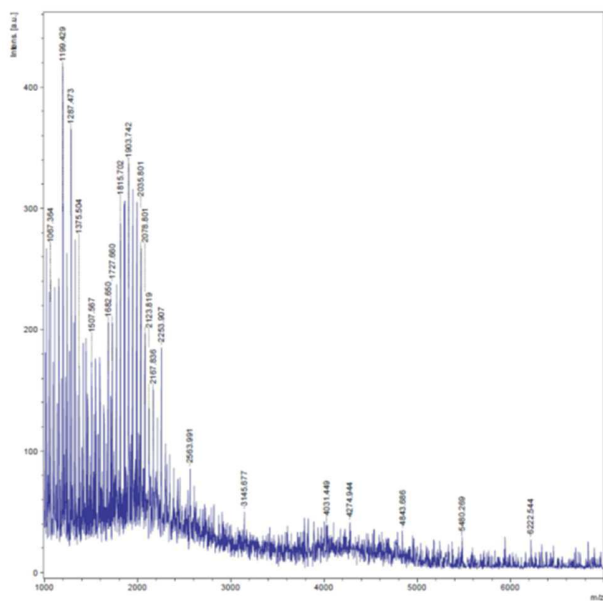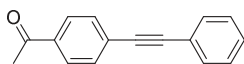
14

^{1}H NMR (250 MHz, CDCl$_3$)

18
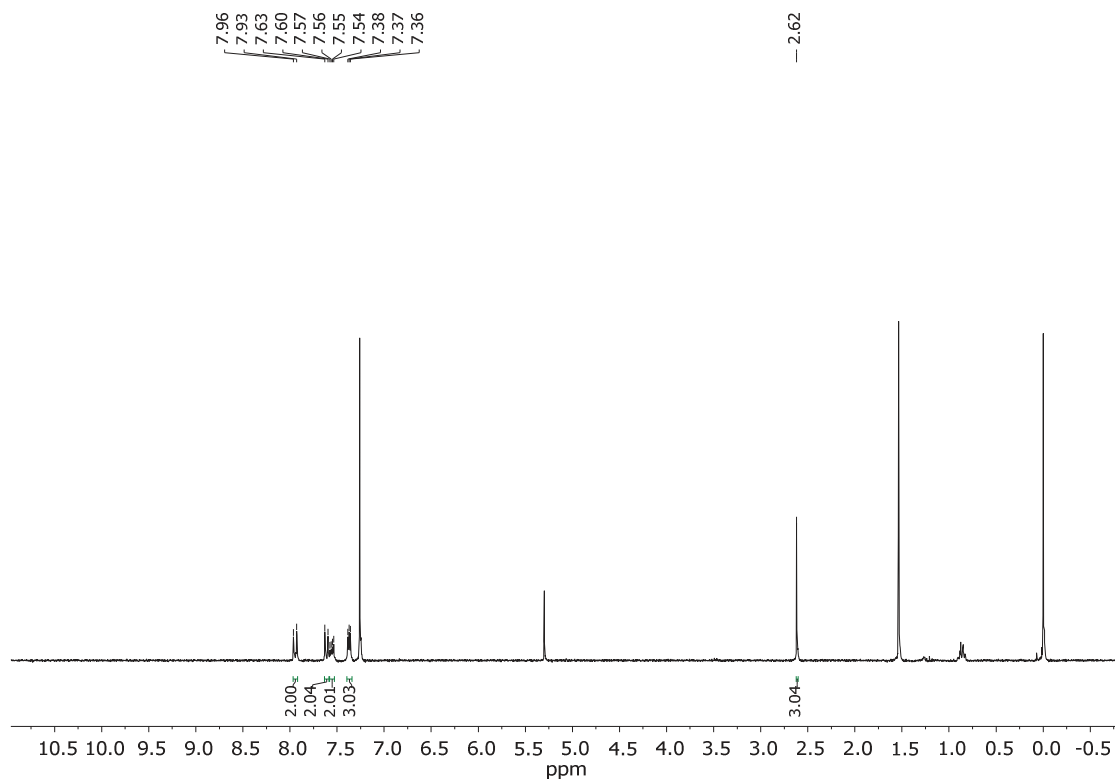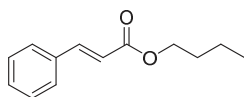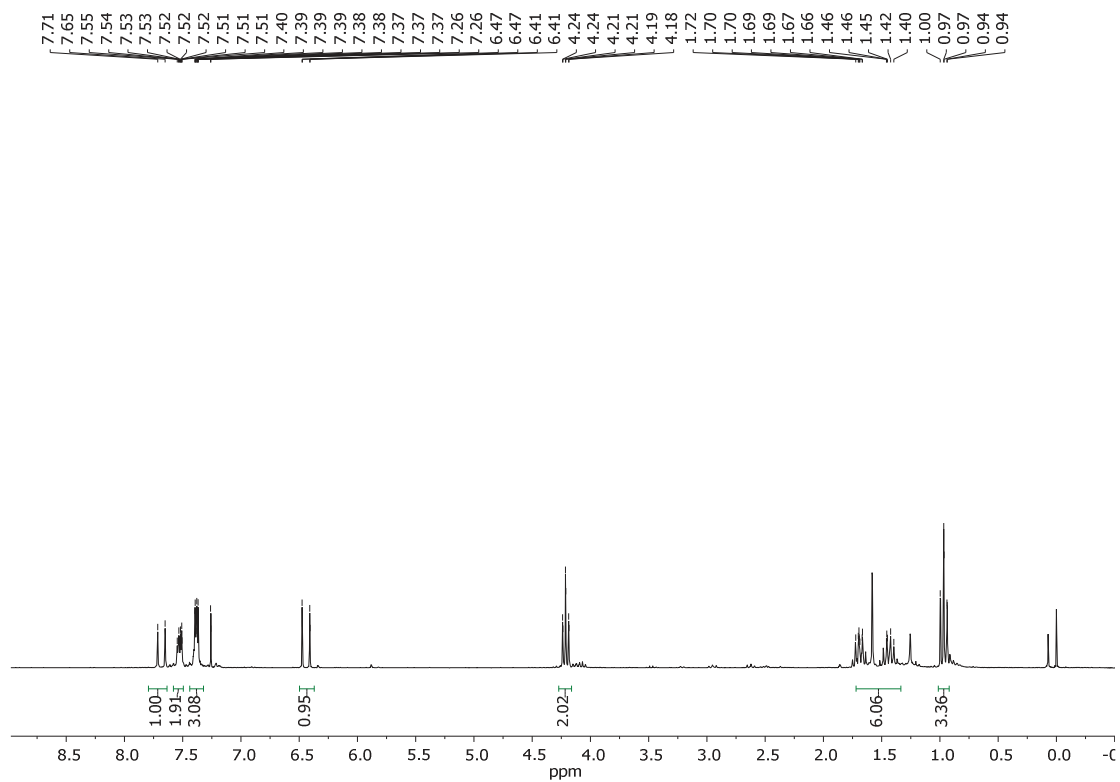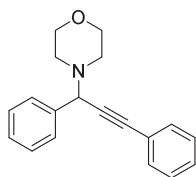
^{1}H NMR (250 MHz, CDCl$_3$)

23aaa

^{1}H NMR (250 MHz, CDCl$_3$)
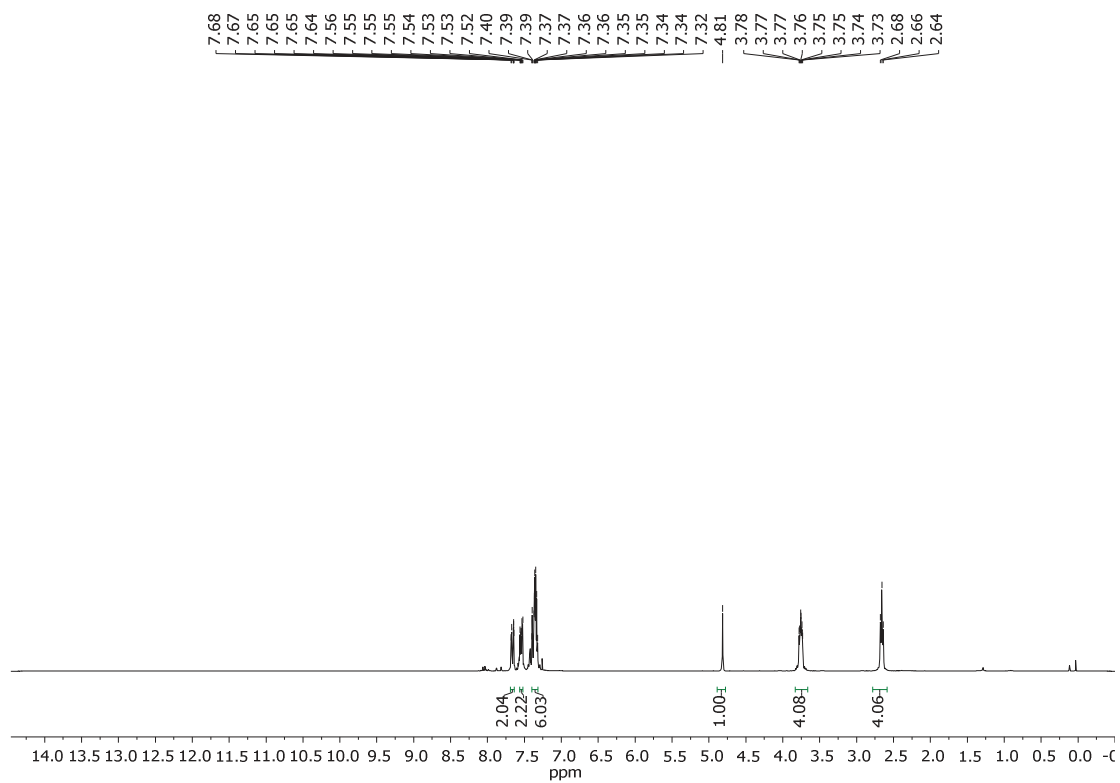
Spectra Collection

23aba

^{1}H NMR (250 MHz, CDCl$_{3}$)

7.67
7.65
7.64
7.64
7.55
7.53
7.52
7.38
7.35
7.35
7.35
7.34
7.33

— 4.82

2.60
2.58
2.56
1.64
1.63
1.62
1.61
1.60
1.58
1.48
1.46
1.28

2.07
2.02
6.02

1.00

4.00

4.05
2.07

23aca

^{1}H NMR (250 MHz, CDCl$_3$)

7.74
7.74
7.74
7.71
7.71
7.71
7.70
7.64
7.62
7.62
7.61
7.60
7.48
7.45
7.45
7.45
7.43
7.41
7.40
7.40
7.39
7.38
7.37
7.37
7.36
7.35
7.34
7.34
7.32
7.32
7.31
7.29
4.97
3.81
3.75
3.71
3.65
2.29

4.02
11.18
1.00
2.06
3.02

14.0 13.5 13.0 12.5 12.0 11.5 11.0 10.5 10.0 9.5 9.0 8.5 8.0 7.5 7.0 6.5 6.0 5.5 5.0 4.5 4.0 3.5 3.0 2.5 2.0 1.5 1.0 0.5 0.0 -0
ppm
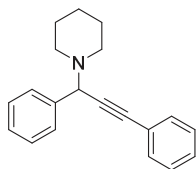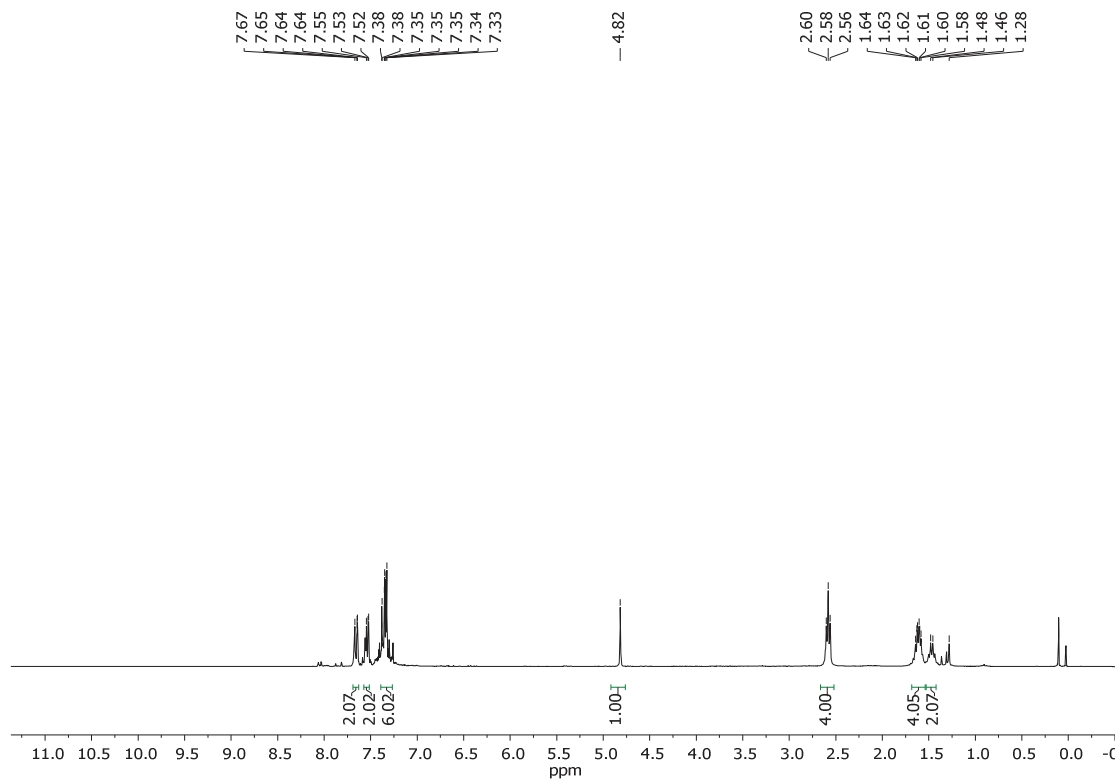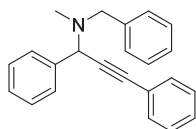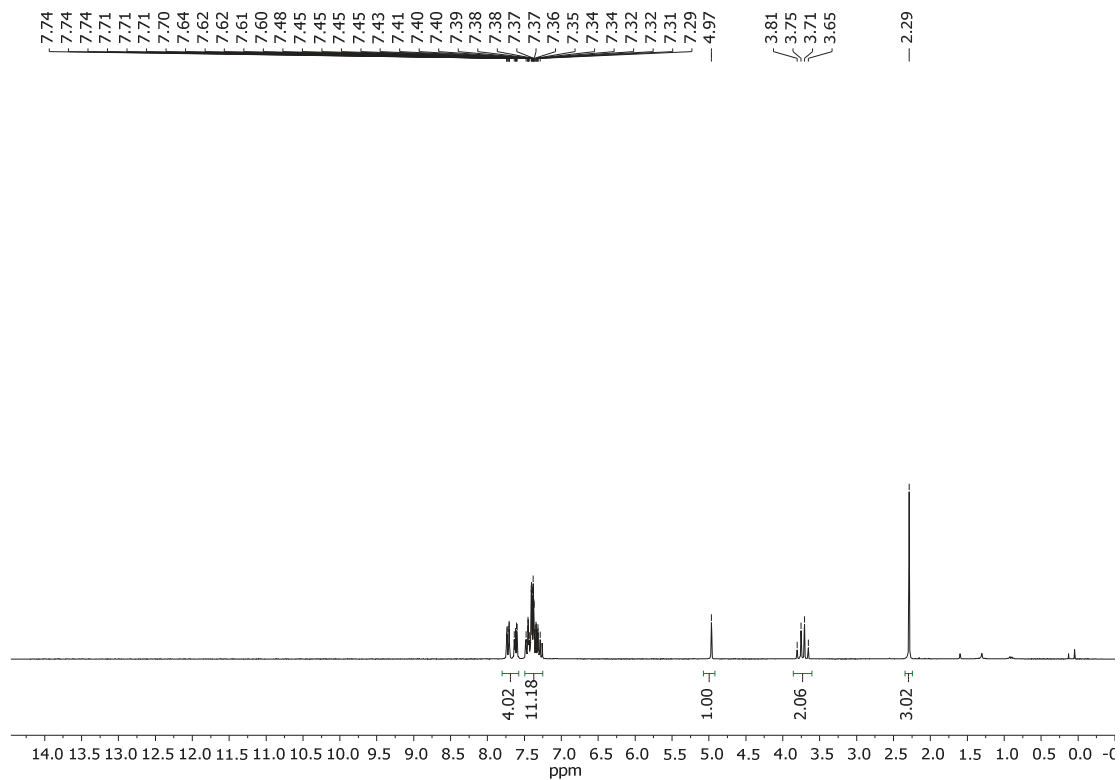
Spectra Collection
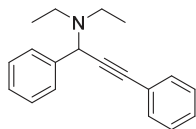
23ada

^{1}H NMR (360 MHz, CDCl$_3$)

23aea

^{1}H NMR (360 MHz, CDCl$_3$)

7.62
7.60
7.50
7.49
7.48
7.36
7.36
7.34
7.33
7.32
7.31
7.30
7.26

—4.93

2.75
2.73
2.73
2.72
2.71
1.83
1.81
1.80

1.94
2.07
6.03
1.00
3.99
3.97

13.5 13.0 12.5 12.0 11.5 11.0 10.5 10.0 9.5 9.0 8.5 8.0 7.5 7.0 6.5 6.0 5.5 5.0 4.5 4.0 3.5 3.0 2.5 2.0 1.5 1.0 0.5 0
ppm
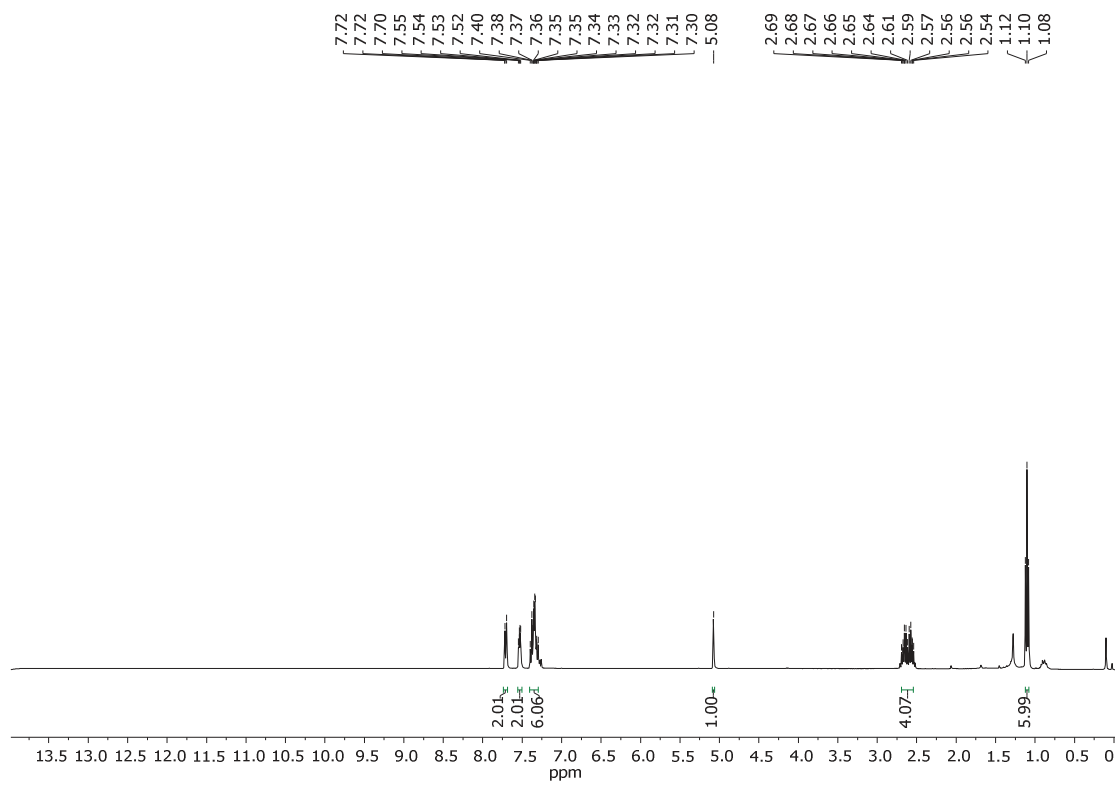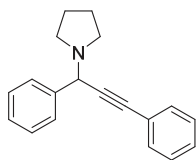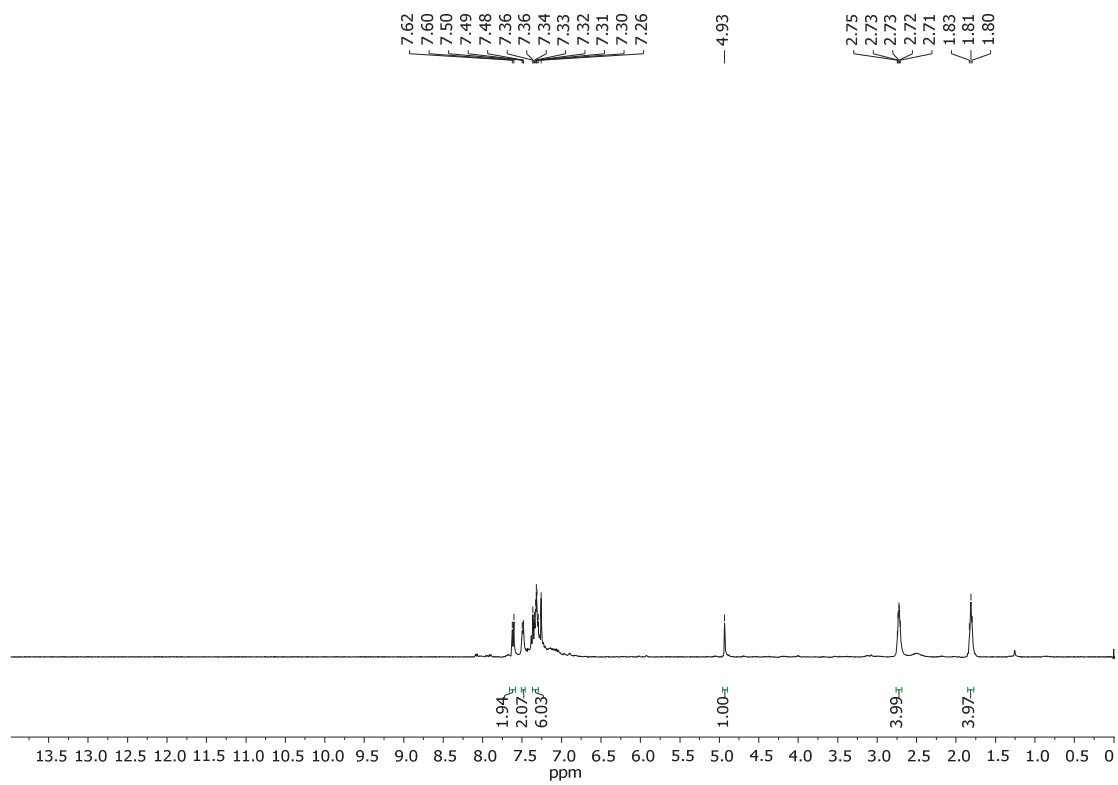
Spectra Collection
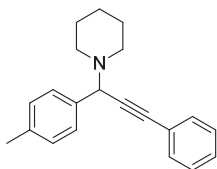
23bba

^{1}H NMR (360 MHz, CDCl$_3$)
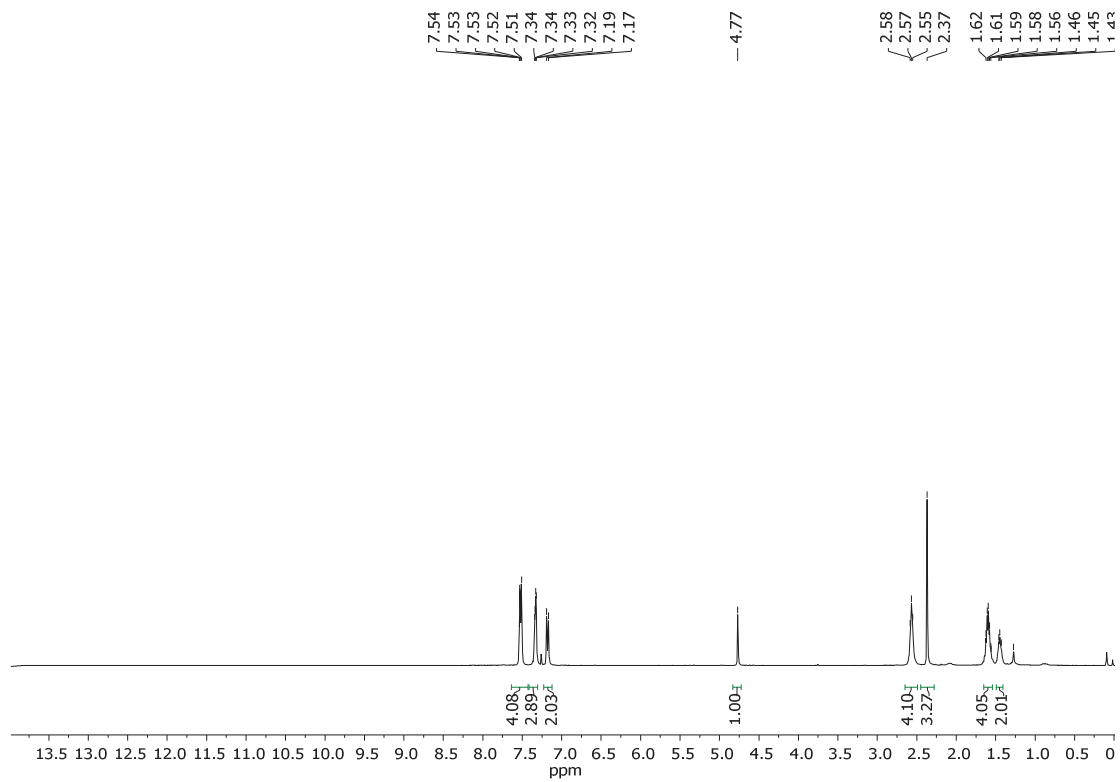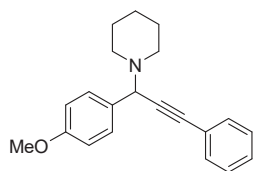
23cba

^{1}H NMR (250 MHz, CDCl$_3$)

23dba

^{1}H NMR (250 MHz, CDCl$_3$)

7.44
7.44
7.43
7.43
7.42
7.30
7.30
7.29
7.28
7.27
7.27

3.53
3.51
3.49
3.47
2.72
2.71
2.69
2.67
2.66
2.64
2.53
2.52
2.51
2.49
2.47
2.46
1.77
1.65
1.64
1.63
1.61
1.60
1.59
1.48
1.43
1.00
0.97
0.96
0.94

1.98
3.02

1.00

2.09
2.04

10.09

3.04

ppm
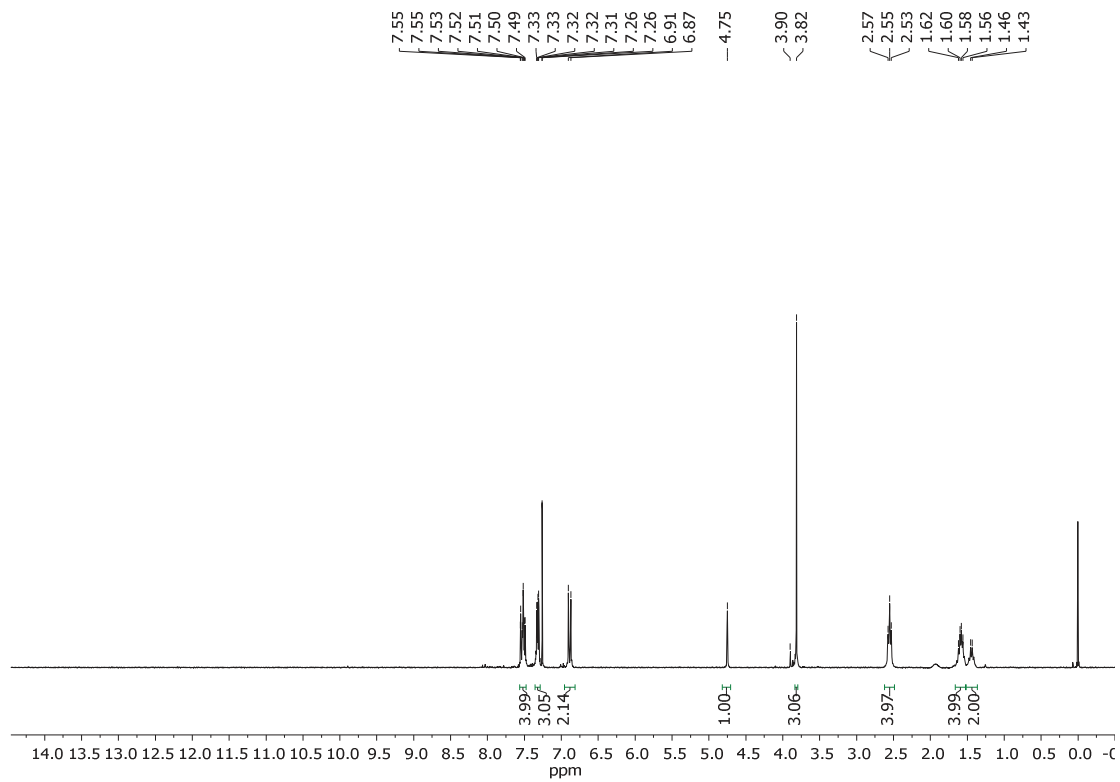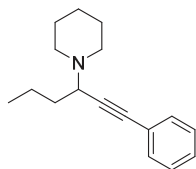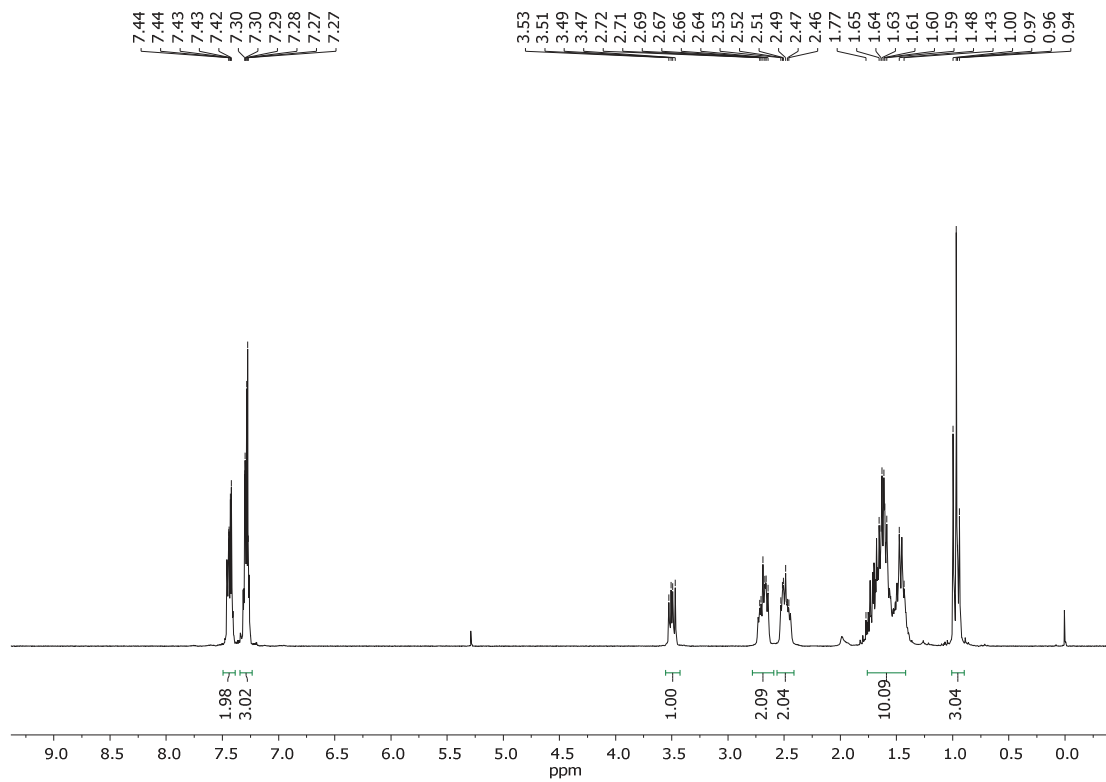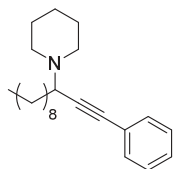
23eba
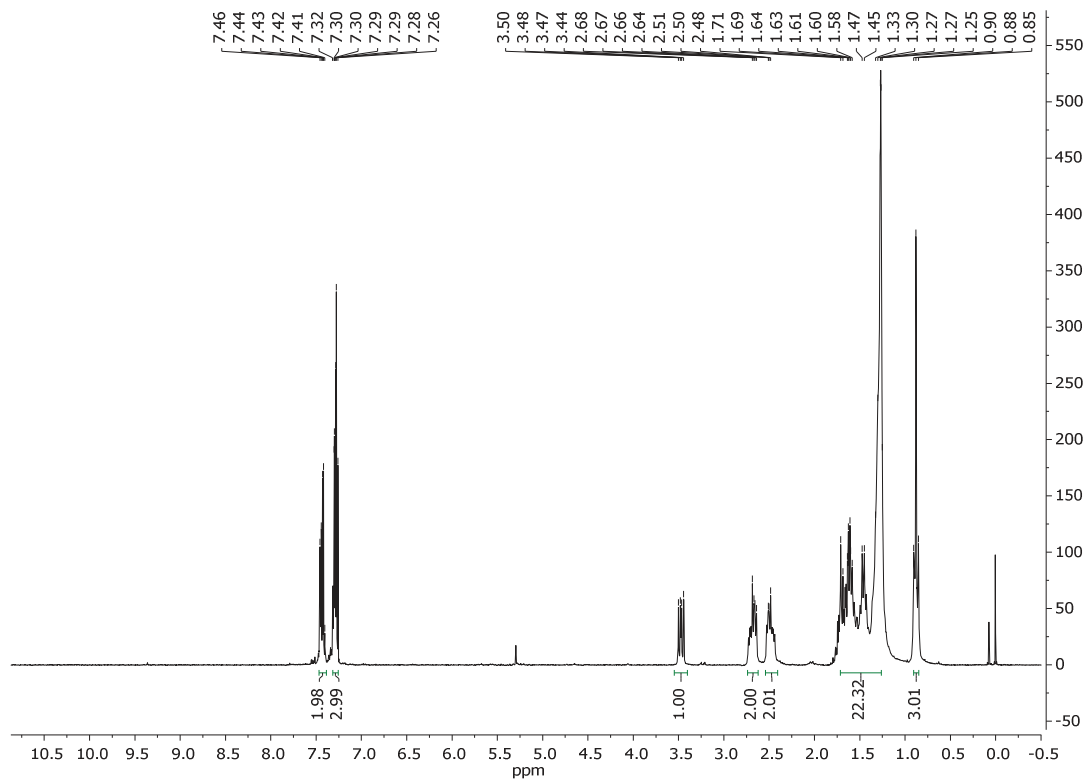
^{1}H NMR (250 MHz, CDCl$_3$)

Spectra Collection

23abb

^{1}H NMR (250 MHz, CDCl$_3$)

7.68, 7.68, 7.68, 7.65, 7.65, 7.65, 7.50, 7.48, 7.47, 7.39, 7.38, 7.36, 7.35, 6.90, 6.89, 6.87, 6.86 — 4.80 — 3.83 — 2.61, 2.59, 2.56, 1.67, 1.66, 1.65, 1.64, 1.63, 1.61, 1.61, 1.59, 1.57, 1.51, 1.49, 1.46, 1.44, 1.42

1.98, 2.04, 3.07, 2.07, 1.00, 3.02, 4.01, 4.03, 2.02

ppm: 9.5, 9.0, 8.5, 8.0, 7.5, 7.0, 6.5, 6.0, 5.5, 5.0, 4.5, 4.0, 3.5, 3.0, 2.5, 2.0, 1.5, 1.0, 0.5, 0.0
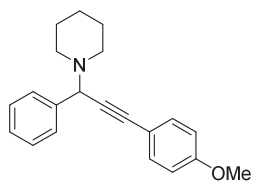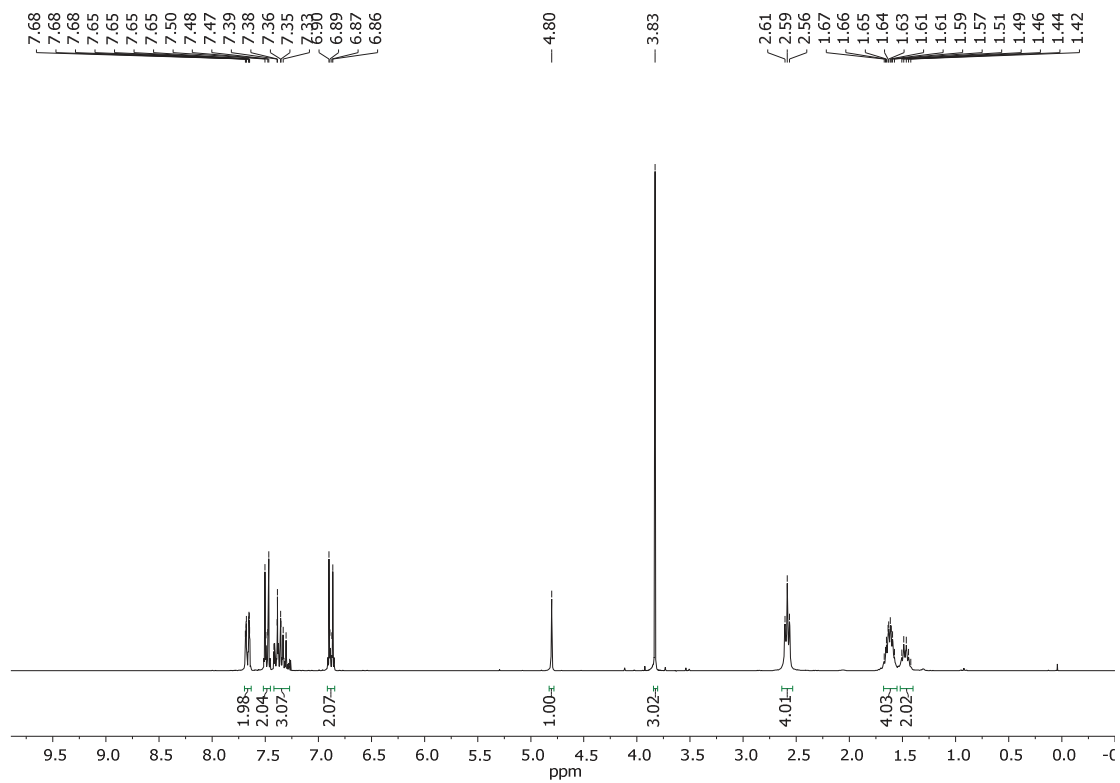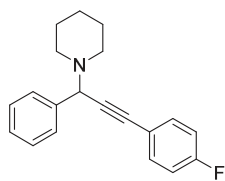
23abc
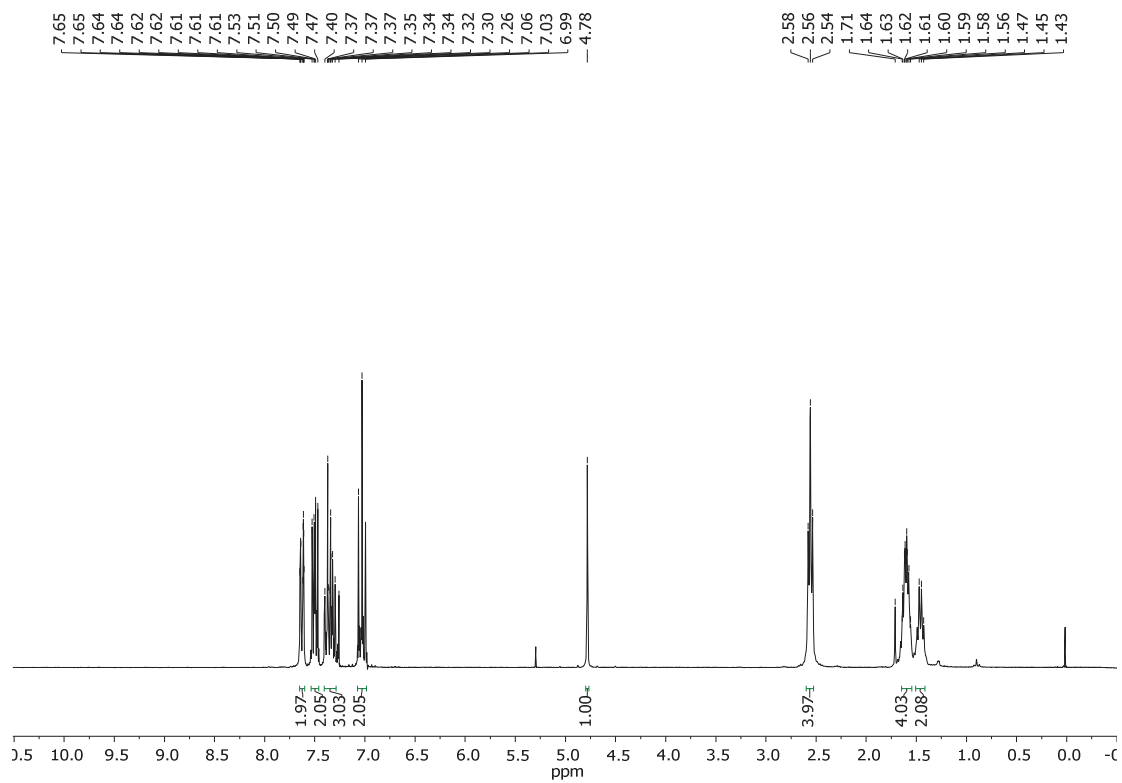
¹H NMR (250 MHz, CDCl₃)

Spectra Collection
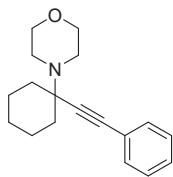
25aaa

^{1}H NMR (250 MHz, CDCl$_3$)
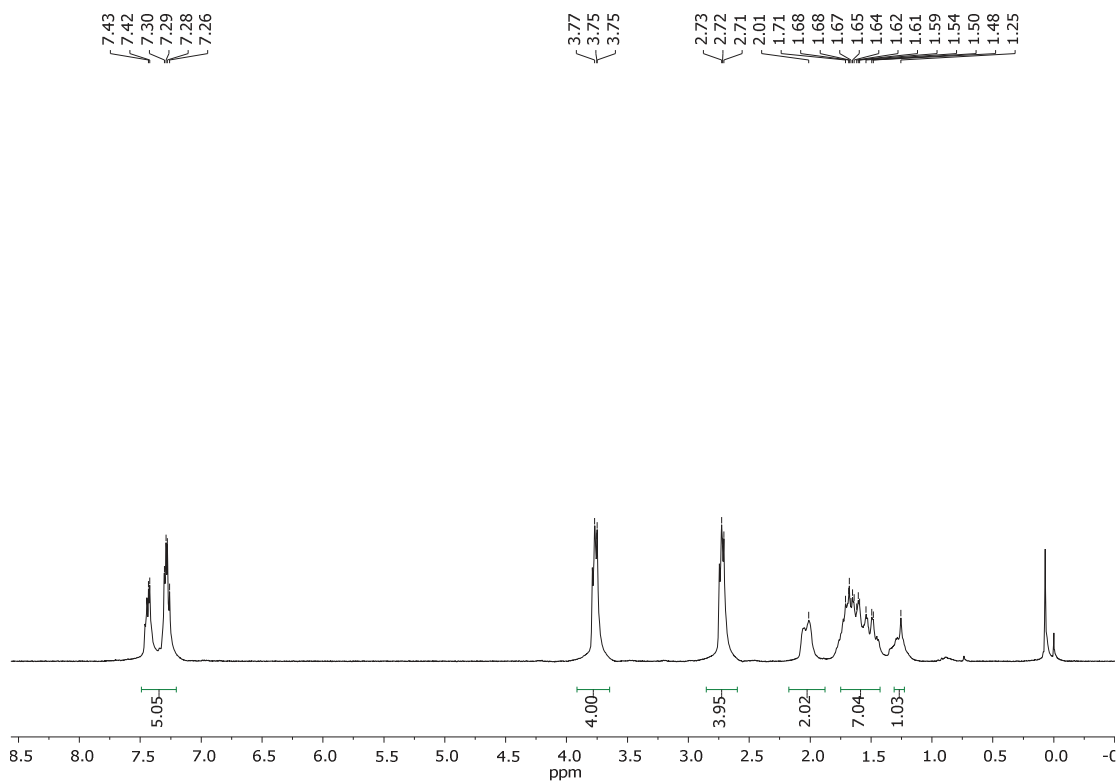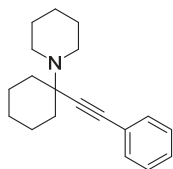
25aba

^{1}H NMR (250 MHz, CDCl$_3$)
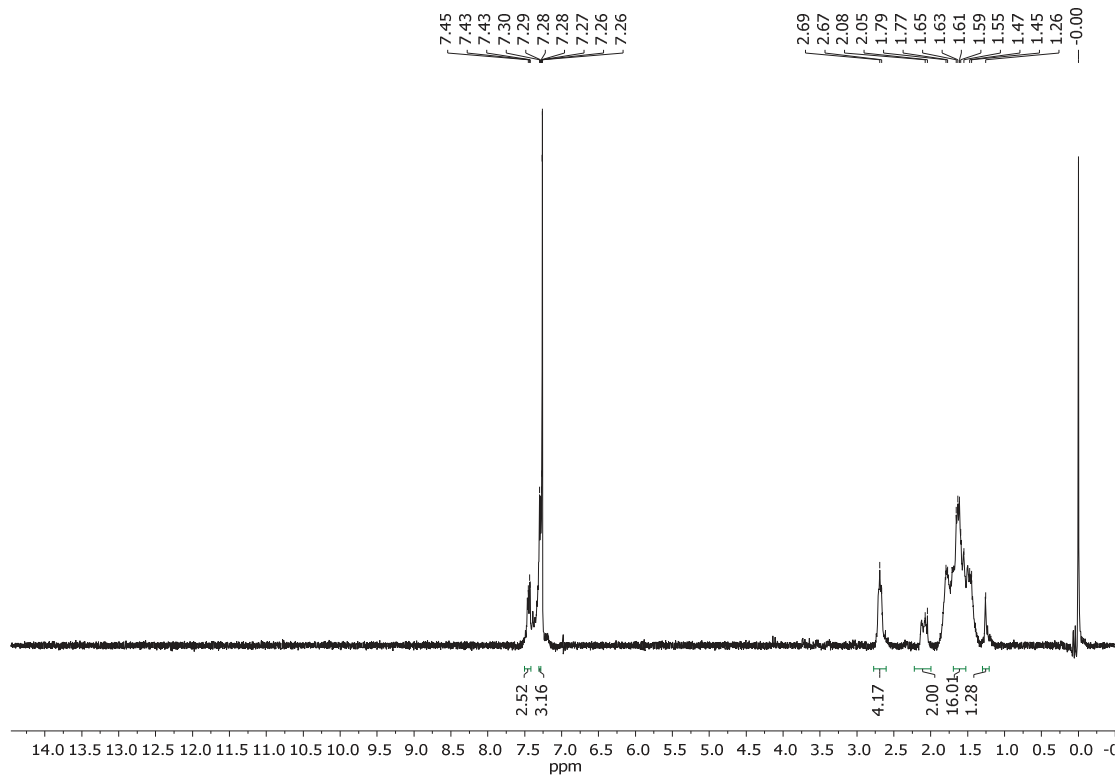
Spectra Collection
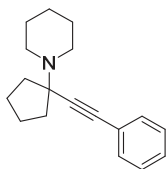
25bba

^{1}H NMR (360 MHz, CDCl$_3$)
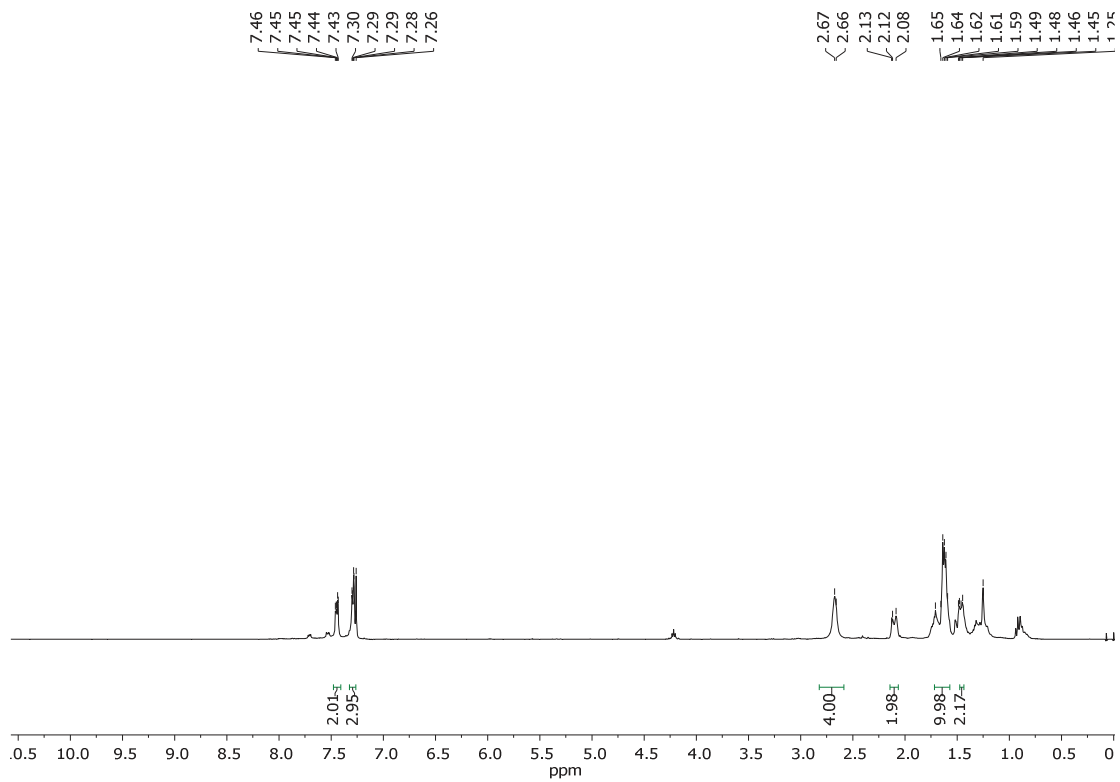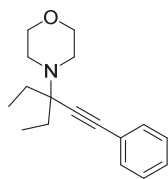
25caa

^{1}H NMR (250 MHz, CDCl$_3$)
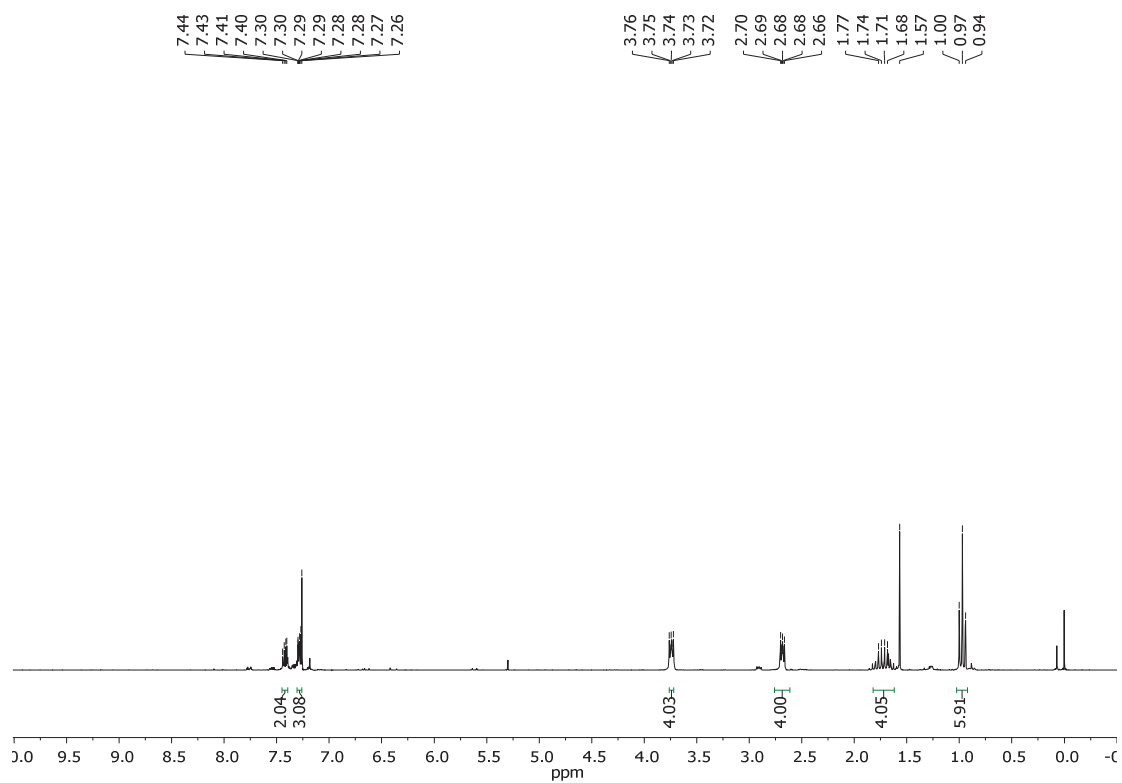
Spectra Collection

29

^{1}H NMR (360 MHz, CDCl$_3$)

4.83
4.82
4.40
4.39

2.99
2.98
2.96
2.94
2.78
2.75
2.73
2.73

1.00
1.01
2.06
2.01

4.0 13.5 13.0 12.5 12.0 11.5 11.0 10.5 10.0 9.5 9.0 8.5 8.0 7.5 7.0 6.5 6.0 5.5 5.0 4.5 4.0 3.5 3.0 2.5 2.0 1.5 1.0 0.5
ppm
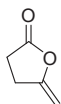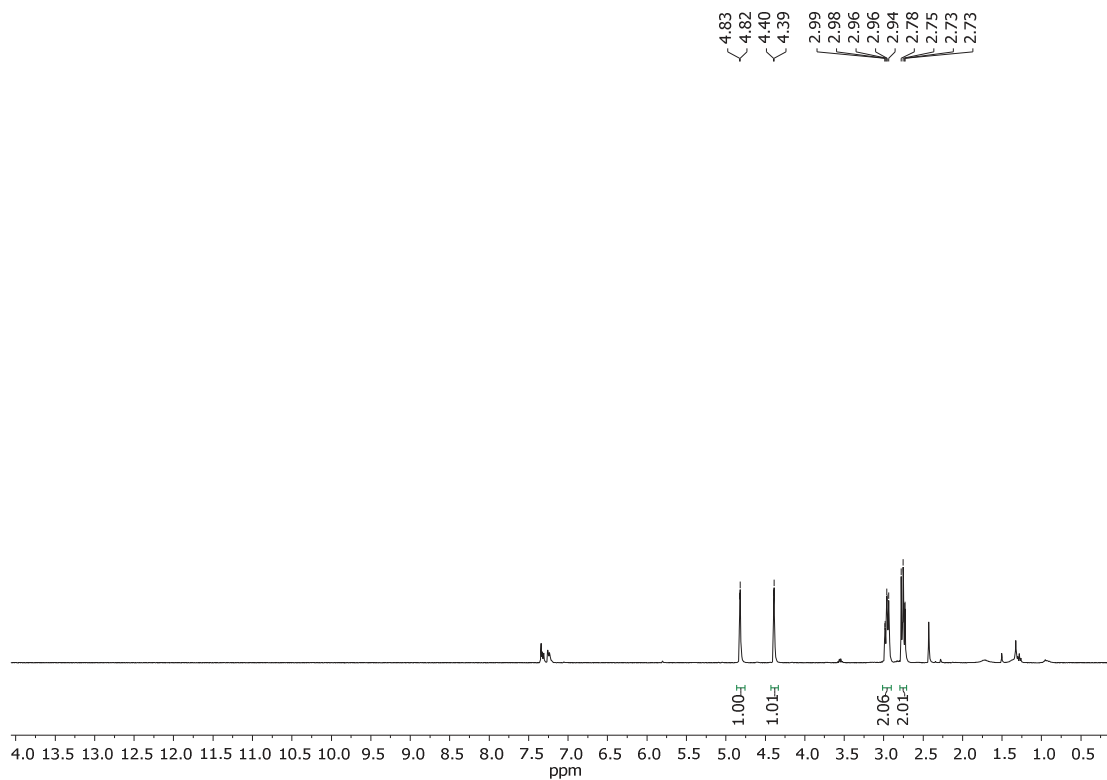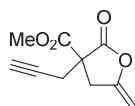
33
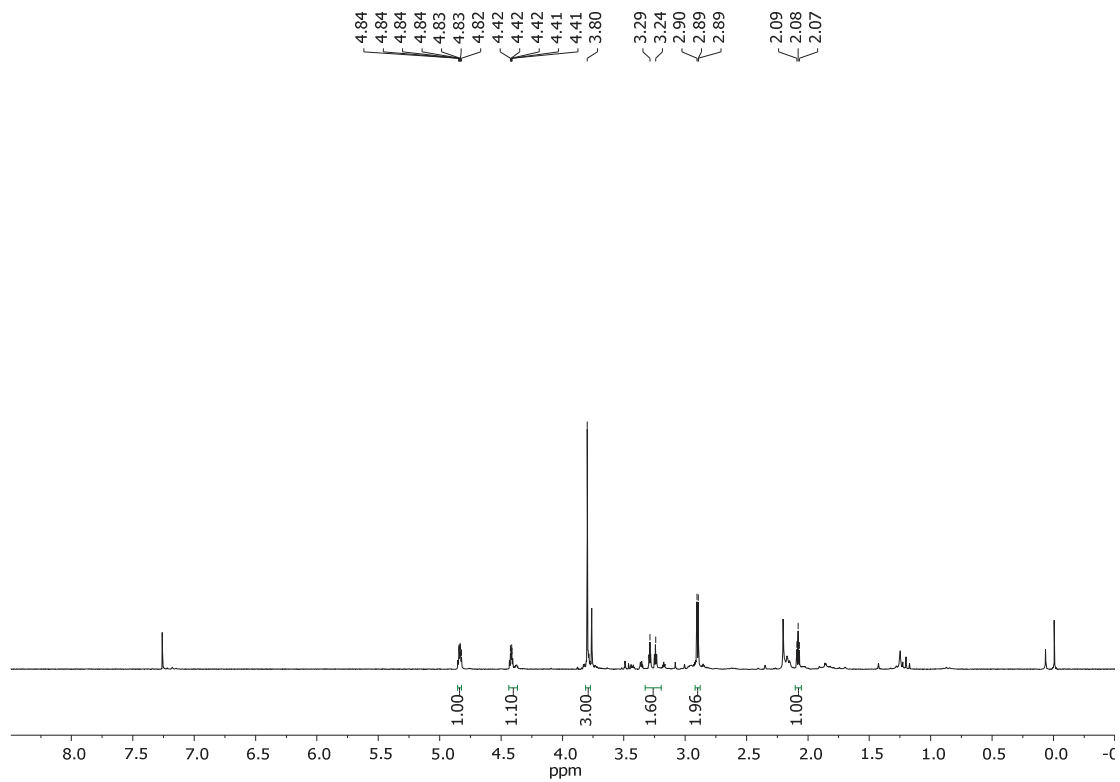
¹H NMR (250 MHz, CDCl₃)

Spectra Collection

34
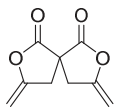
^{1}H NMR (250 MHz, CDCl$_3$)
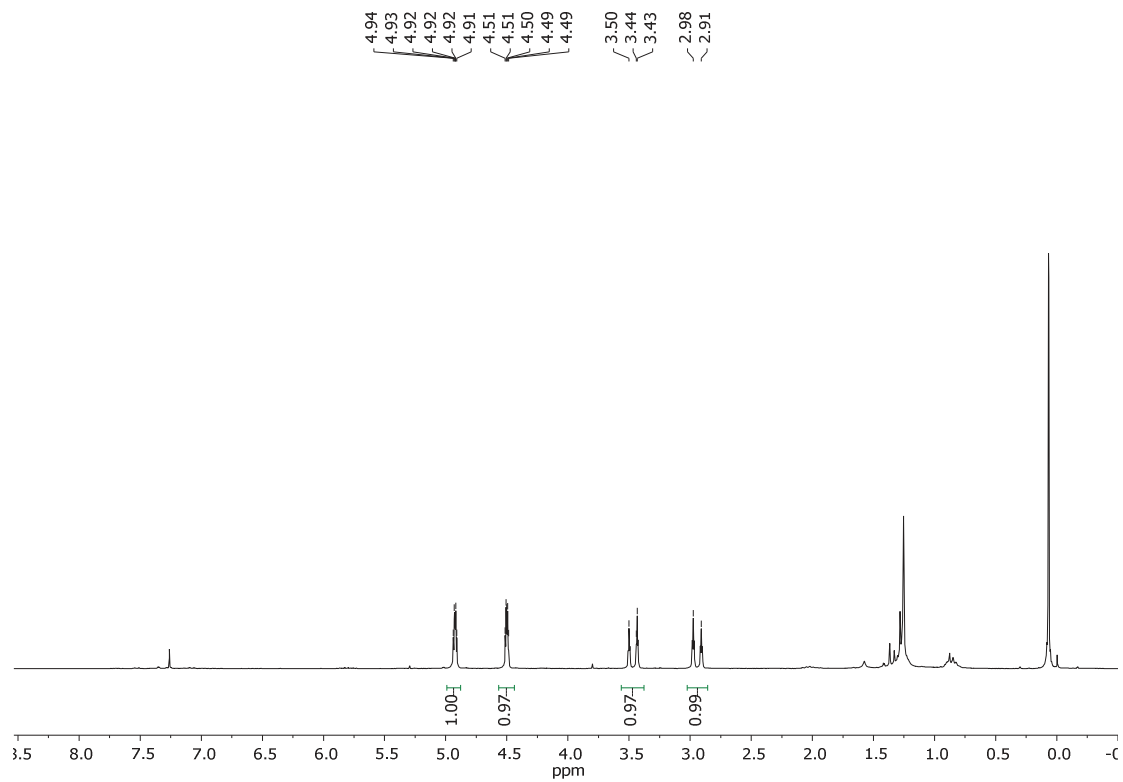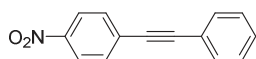
37

^{1}H NMR (250 MHz, CDCl$_3$)
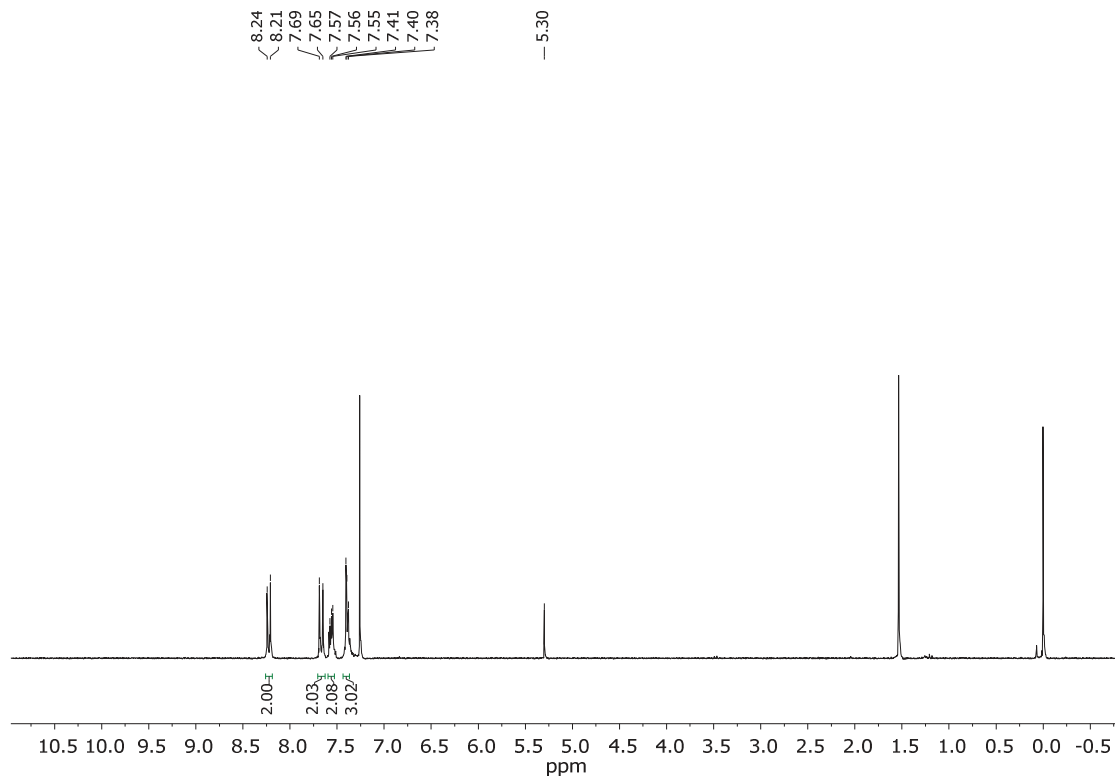
Spectra Collection

MeO—[benzene ring]—C≡C—[benzene ring]

38

^{1}H NMR (360 MHz, CDCl$_3$)

H—SiEt₃

Ph   Ph

40

^{1}H NMR (360 MHz, CDCl₃)

Spectra Collection

H   SiPh₃

Ph   Ph
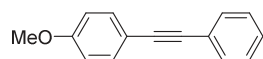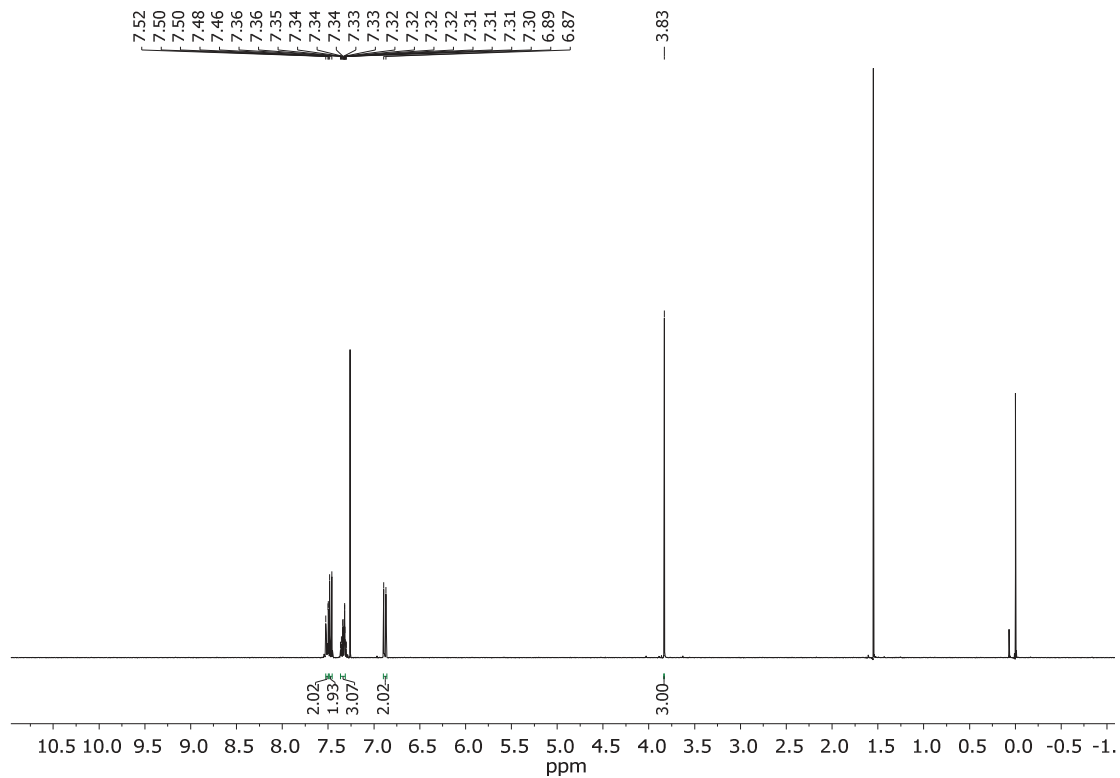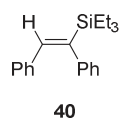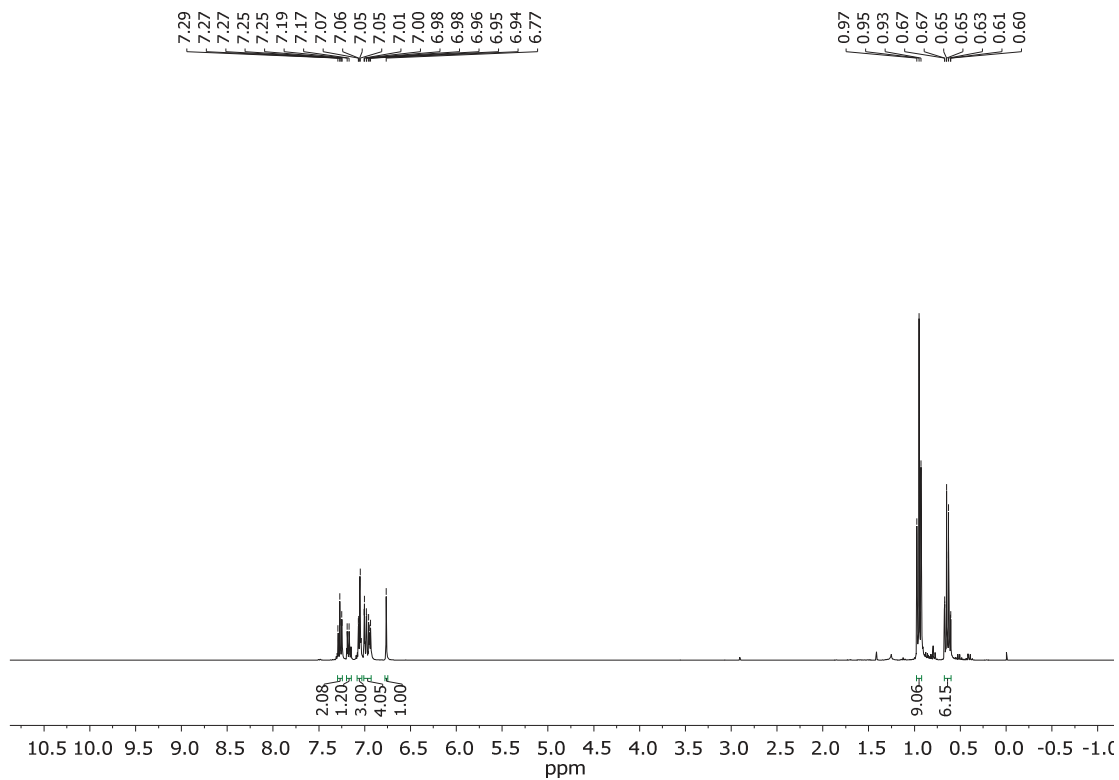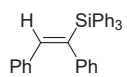
42

¹H NMR (360 MHz, CDCl₃)

45

^{1}H NMR (250 MHz, CDCl$_3$)

Spectra Collection

H   SiEt₃

MeO—   —OMe

46

¹H NMR (400 MHz, CDCl₃)

6.21, 6.21, 6.18, 6.17, 4.69, 4.67, 4.66, 4.63, 3.48, 3.42, 3.41, 3.40, 3.28, 1.91, 1.91, 1.90, 1.90, 1.89, 1.89, 1.89, 1.88, 1.88, 1.87, 1.87, 1.87, 1.86, 1.86, 1.85, 1.85, 0.95, 0.93, 0.93, 0.93, 0.91, 0.58, 0.56, 0.55, 0.54, 0.53

1.00, 1.02, 3.01, 0.99, 0.95, 3.01, 1.06, 9.15, 6.30

¹³C NMR (100 MHz, CDCl₃)

145.88, 102.43, 73.92, 58.15, 55.95, 26.49, 7.43, 2.38
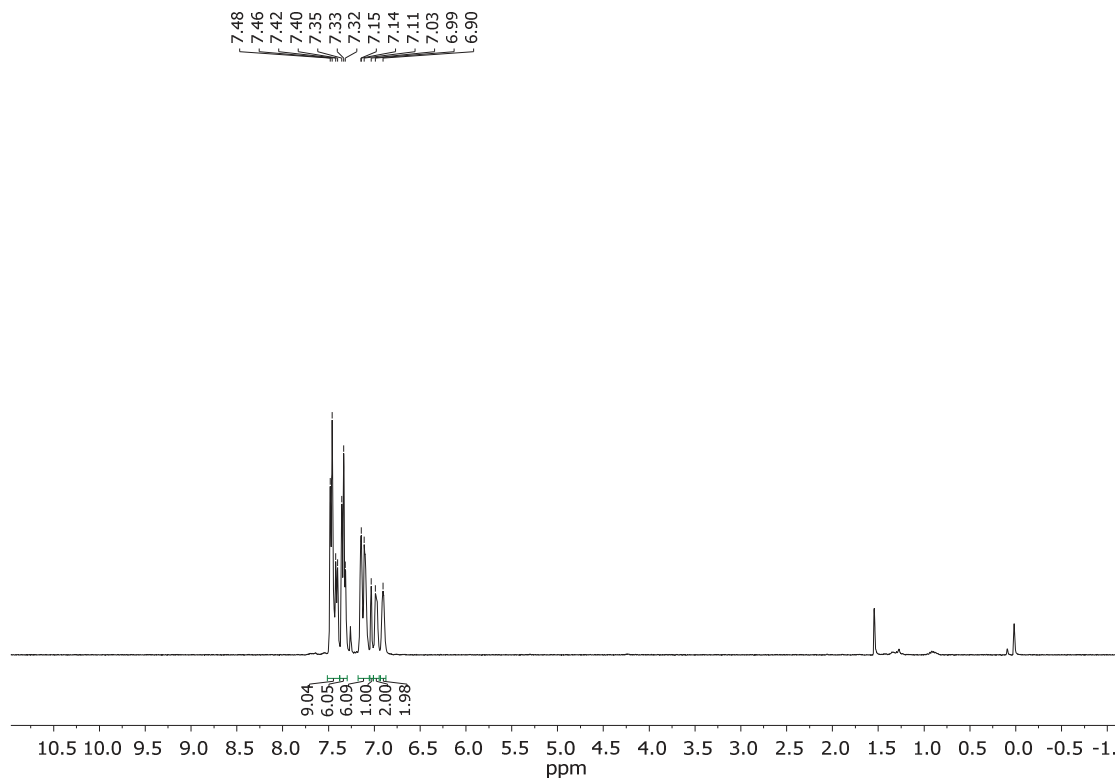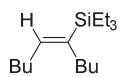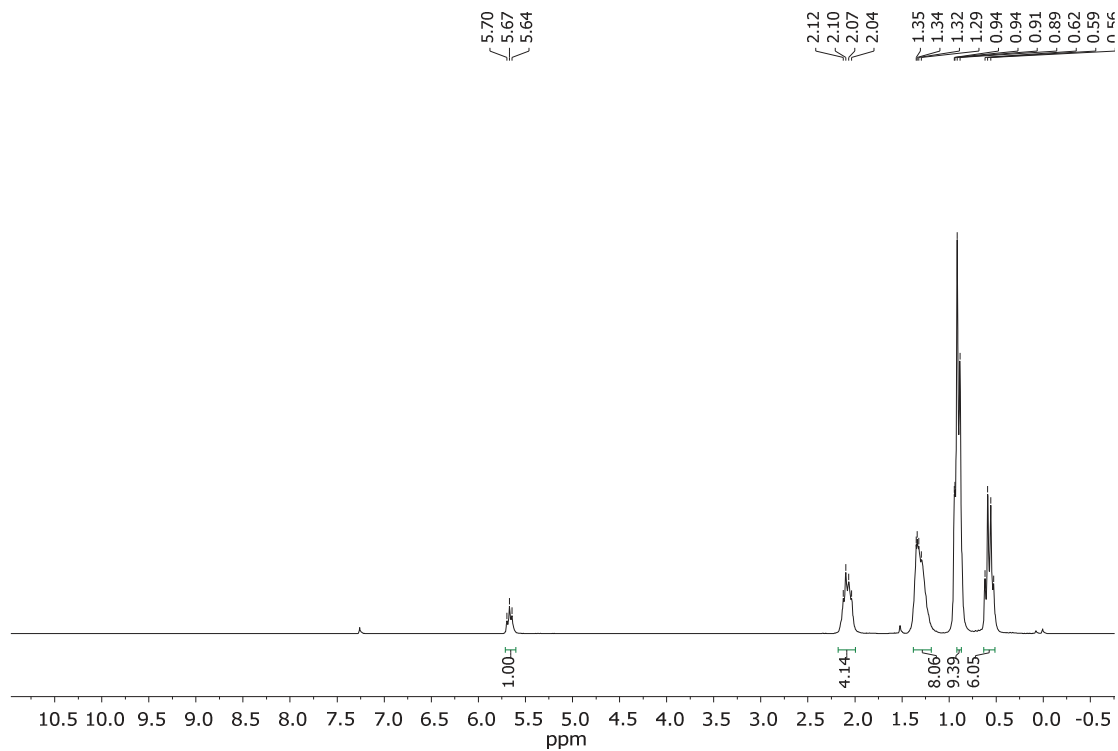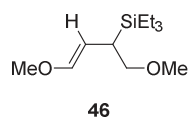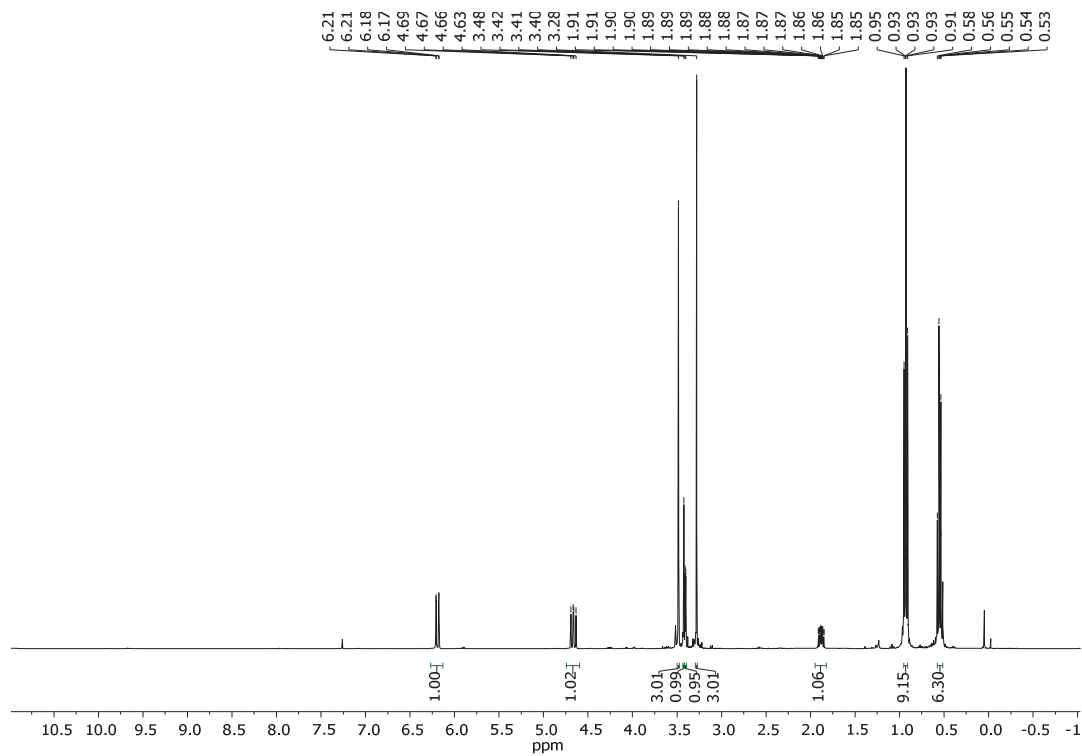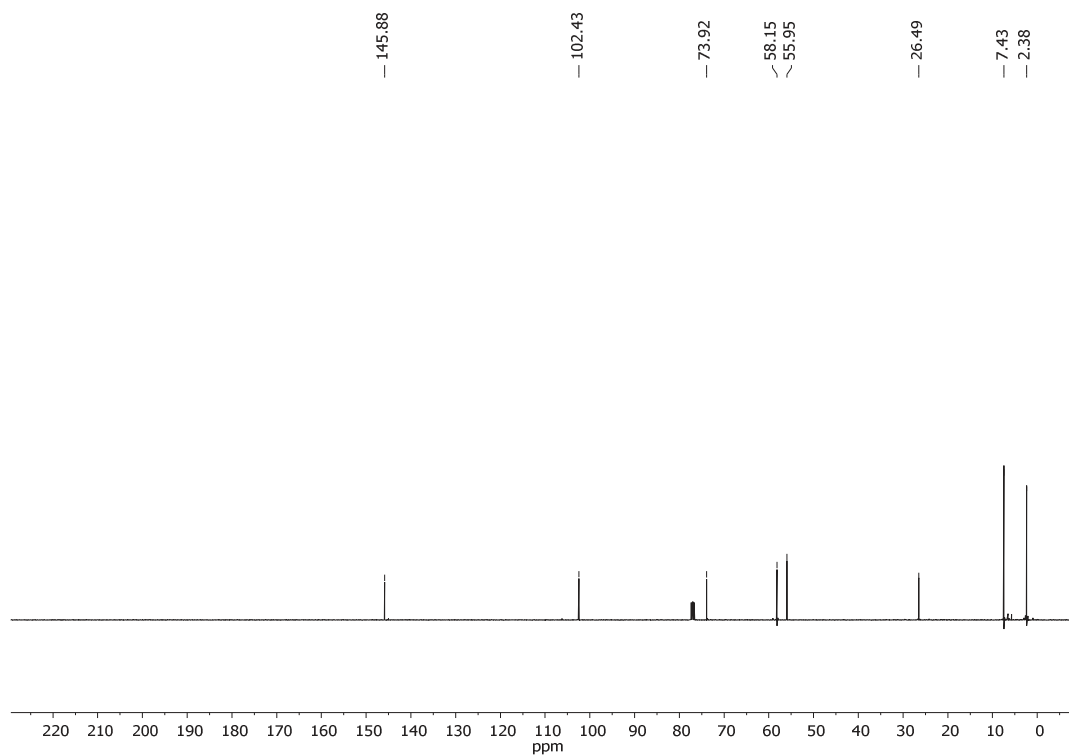
COSY ^{1}H – ^{1}H
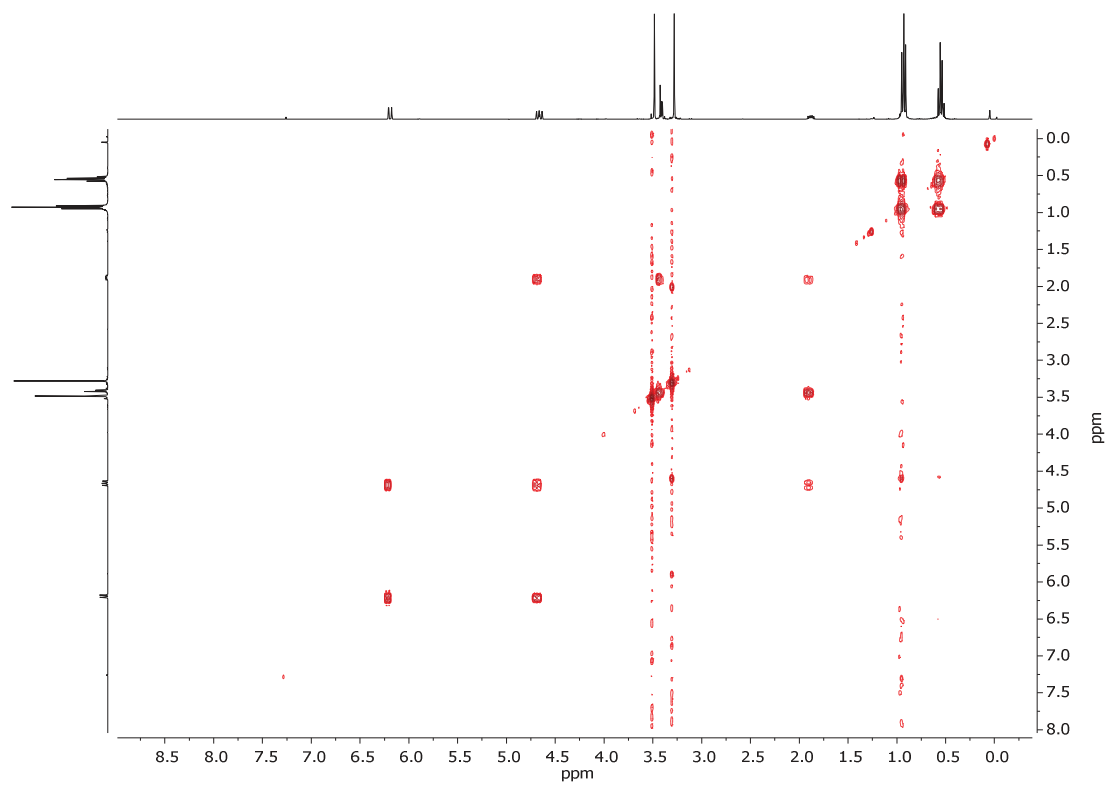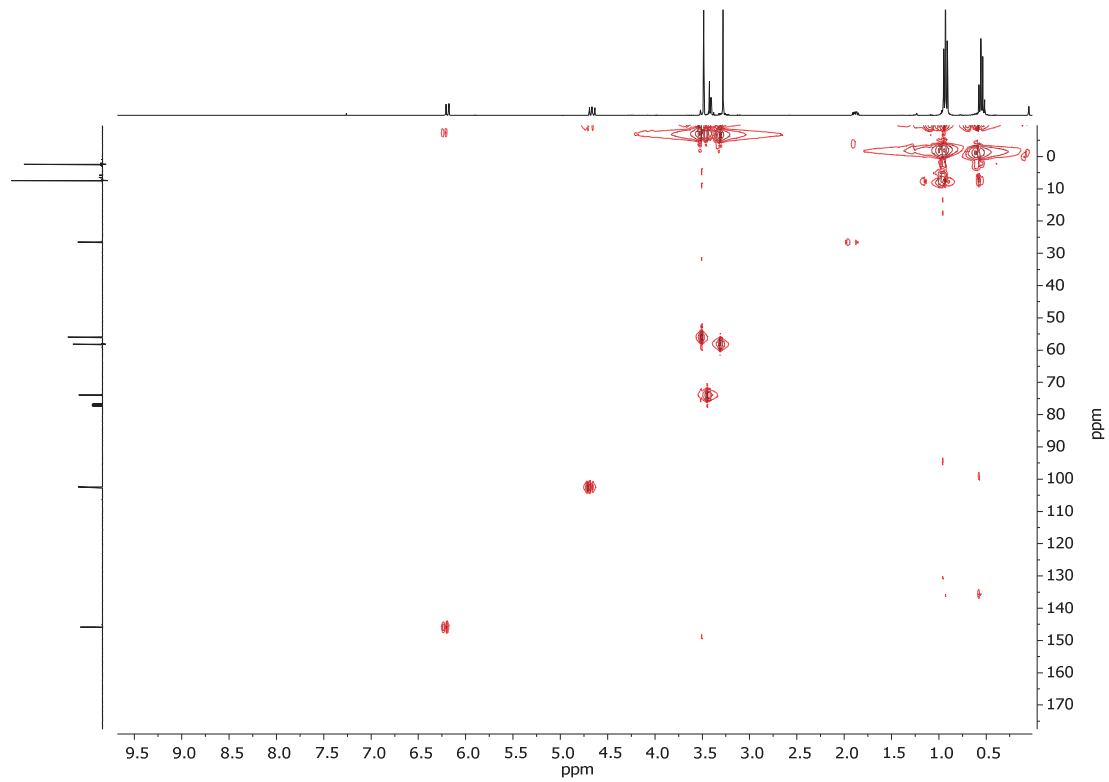
HSQC ^{1}H – ^{13}C

Spectra Collection

HMQC $^1H - ^{13}C$
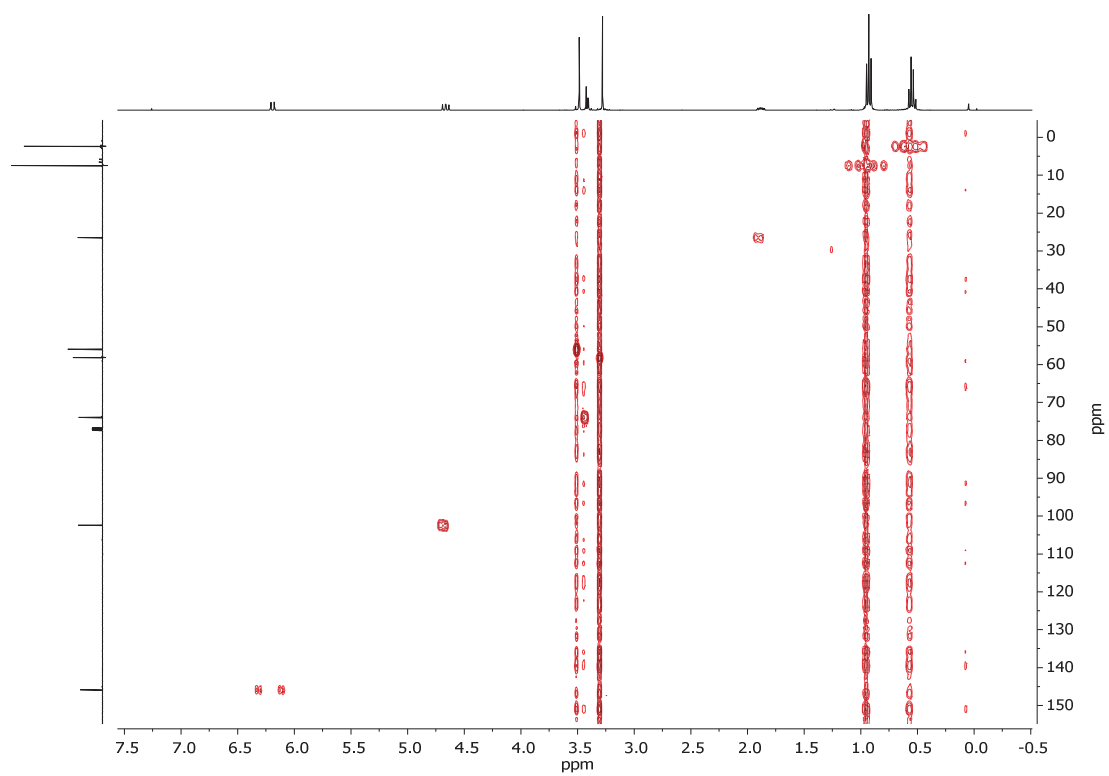
HMBC $^1H - ^{13}C$
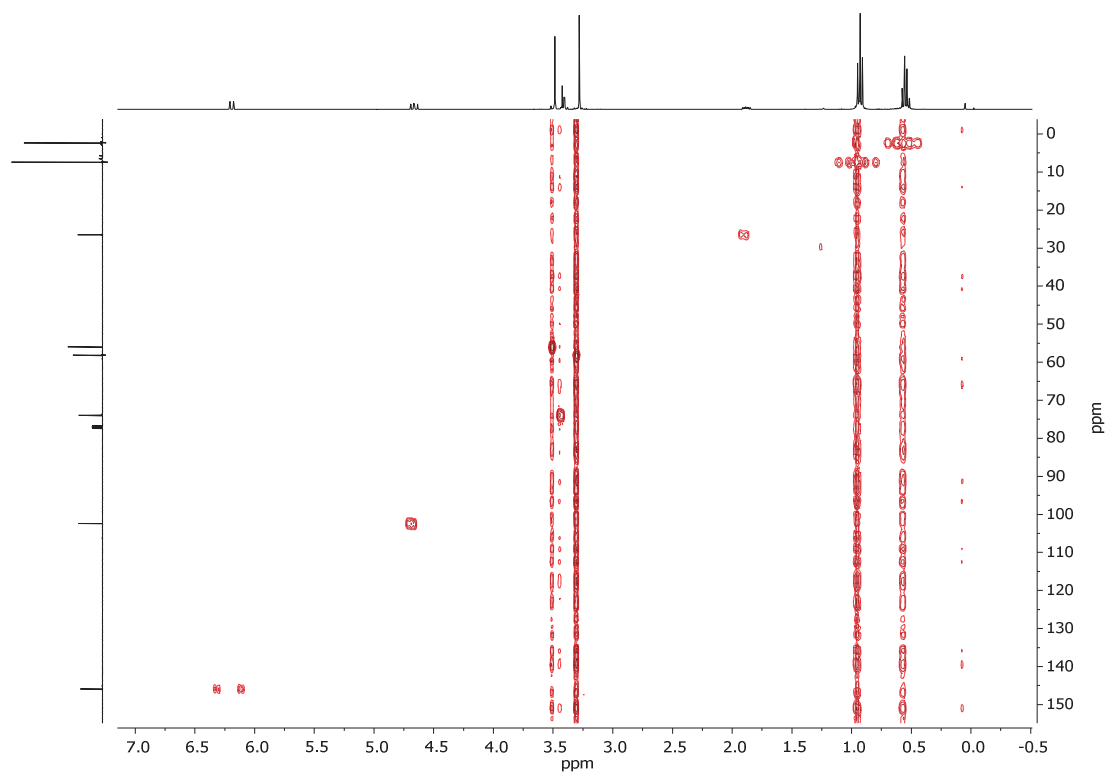
NOE (select. 6.2 ppm)
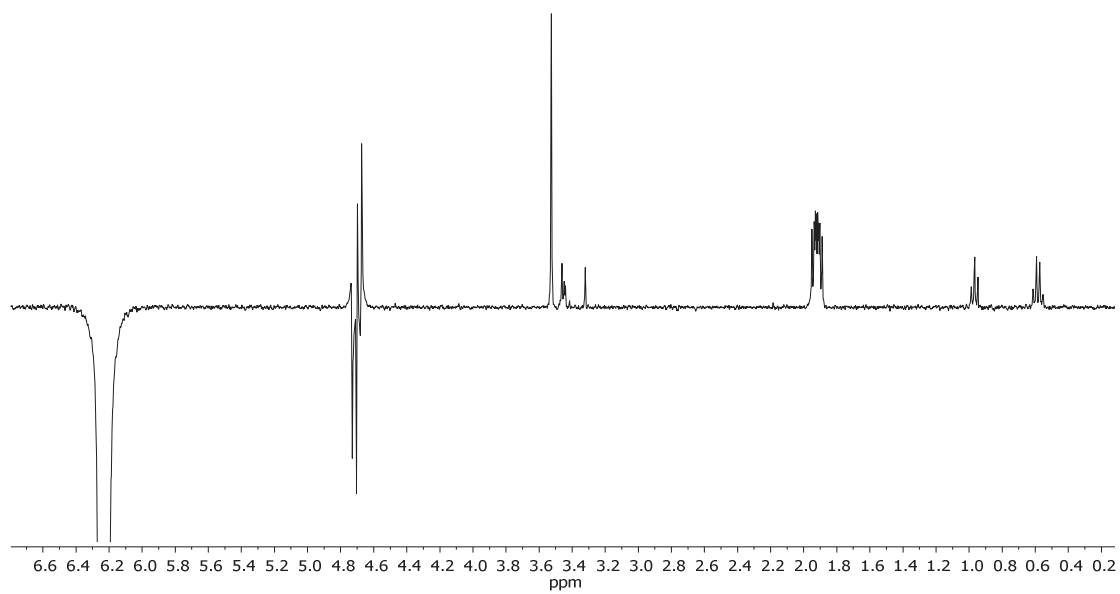
NOE (select. 4.7 ppm)
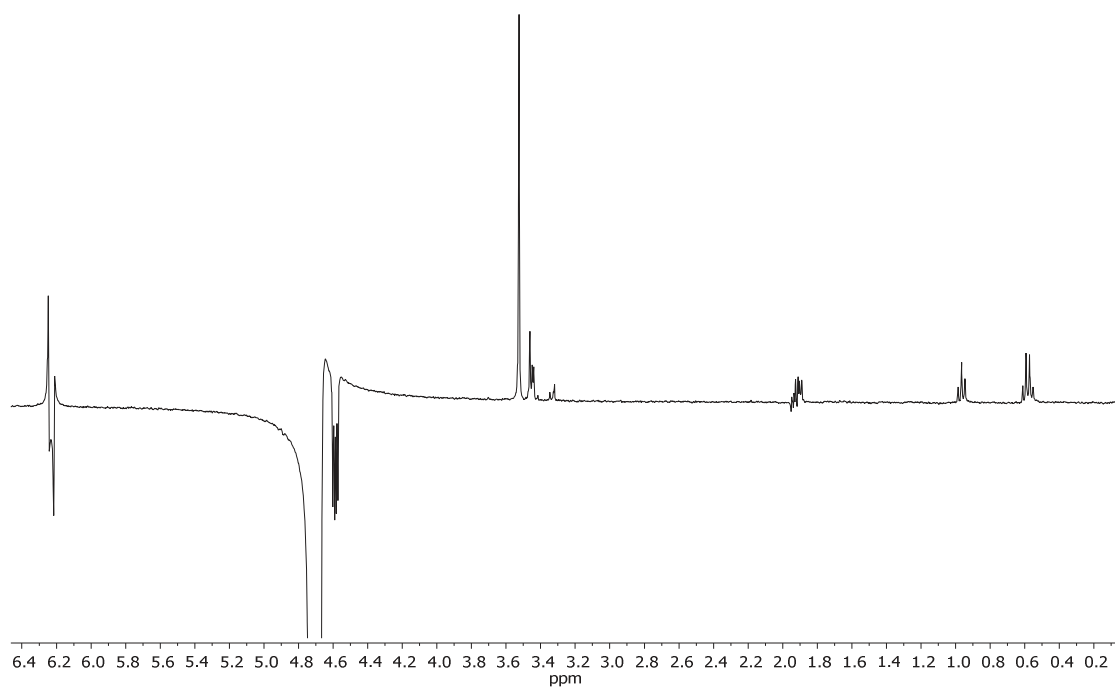
Spectra Collection

ESI-HRMS (experimental)

#	m/z	I	I %
1	271.1701	279226	100.0
2	272.1723	48725	17.5
3	273.1688	18910	6.8
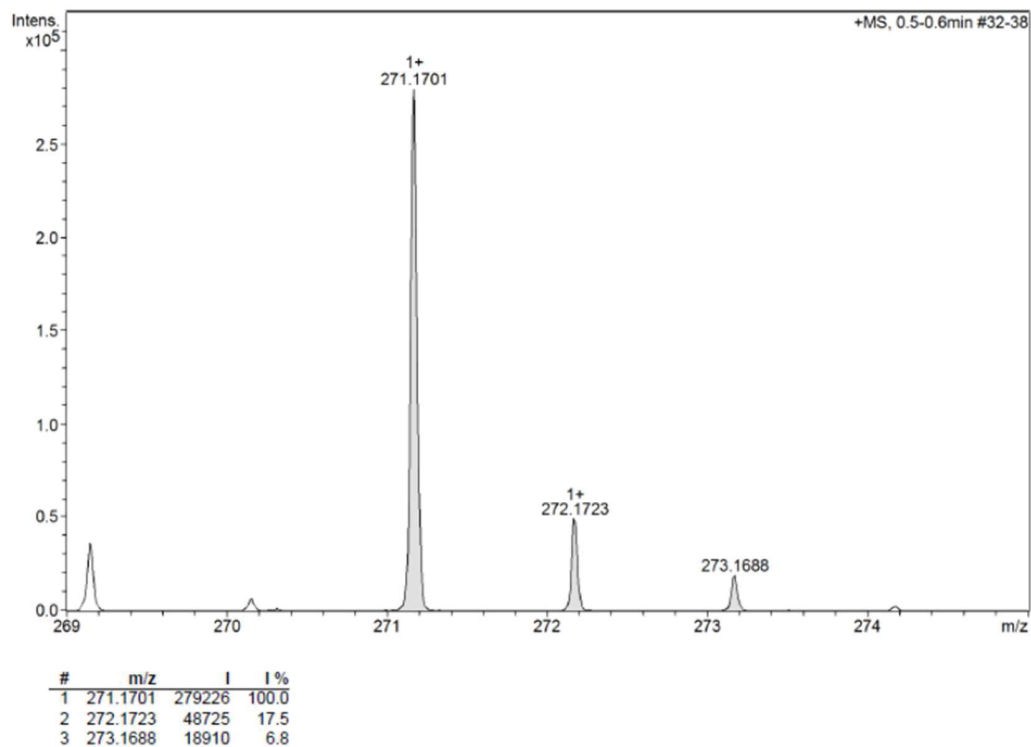
ESI-HRMS (Calculated for $C_{12}H_{26}O_2Si.H_2O+Na$)

#	m/z	I	I %
1	271.1700	1000	100.0
2	272.1724	185	18.5
3	273.1698	55	5.5

47
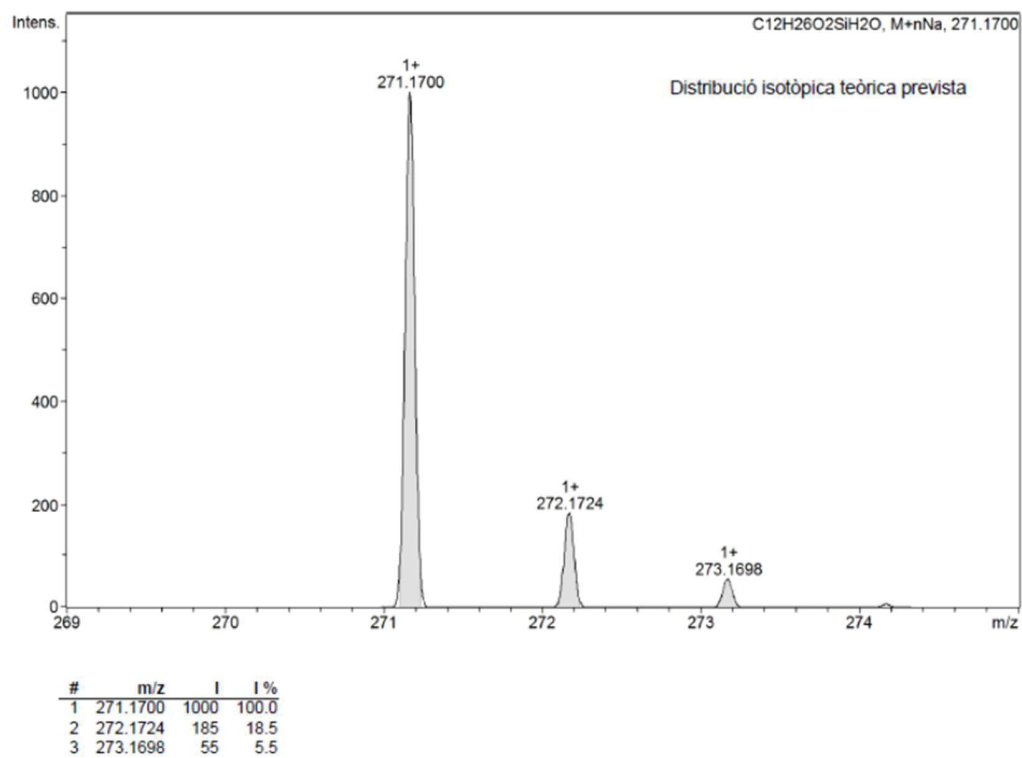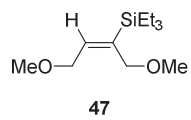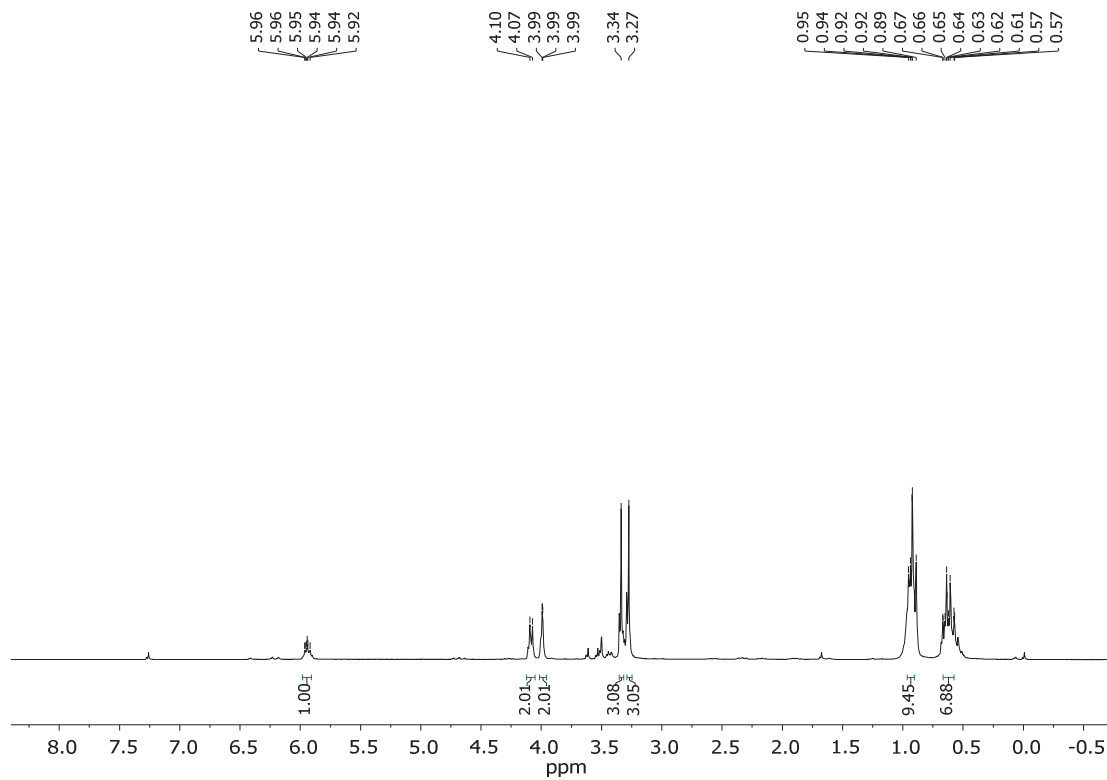
^{1}H NMR (250 MHz, CDCl$_3$)

Spectra Collection
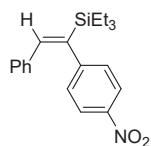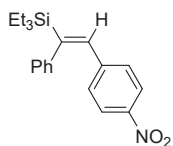
(**E**)-48a   (**E**)-48b

^{1}H NMR (360 MHz, CDCl$_3$)

(E)-49a   **(E)-49b**

^{1}H NMR (400 MHz, CDCl$_3$)

Spectra Collection

(**E**)-50a   (**E**)-50b
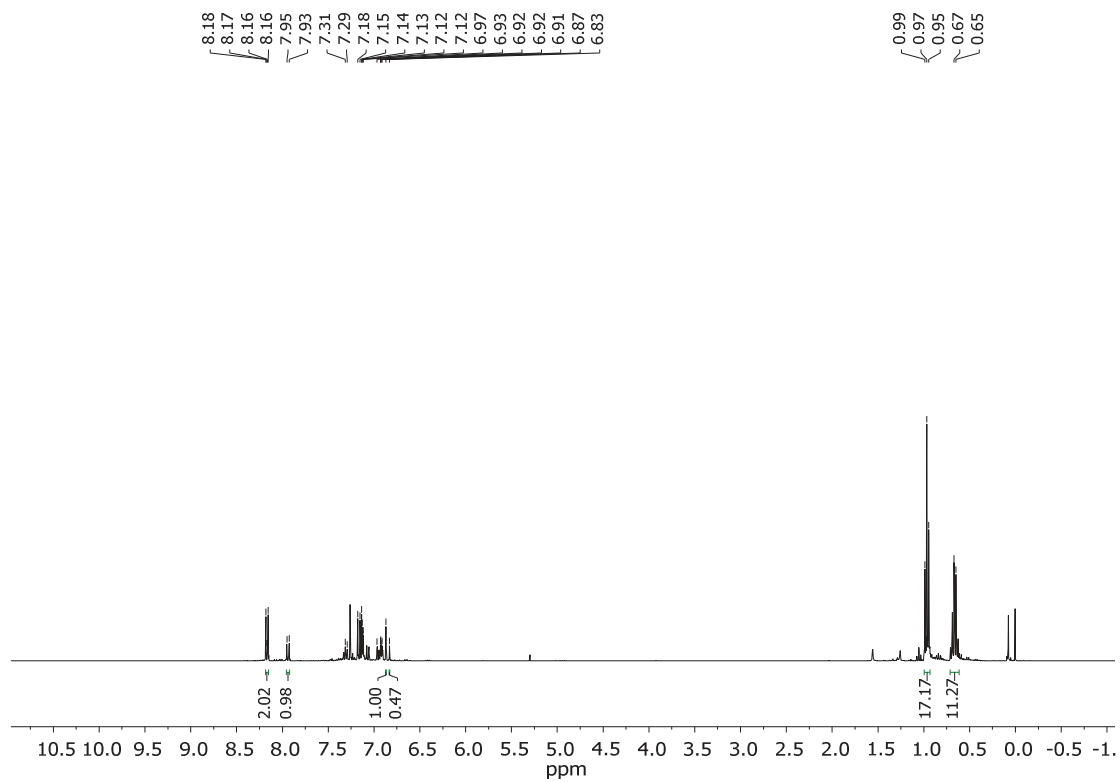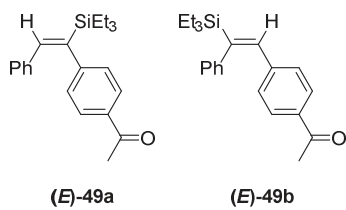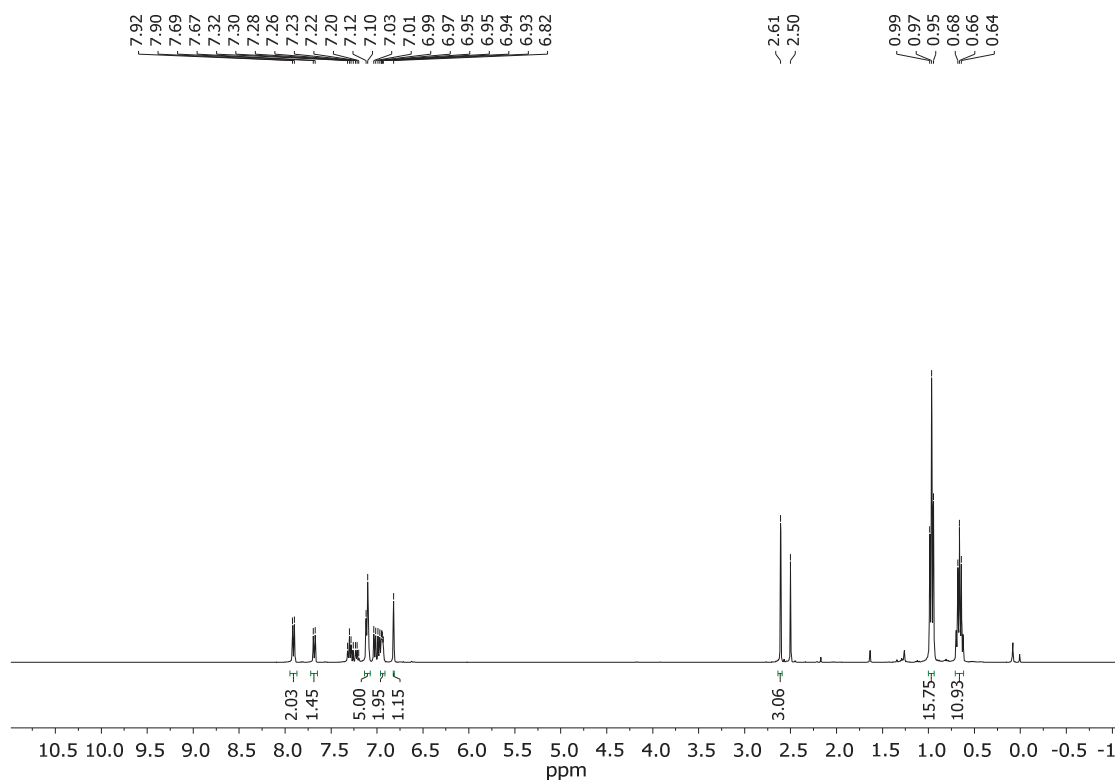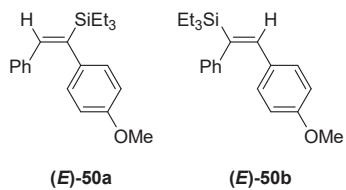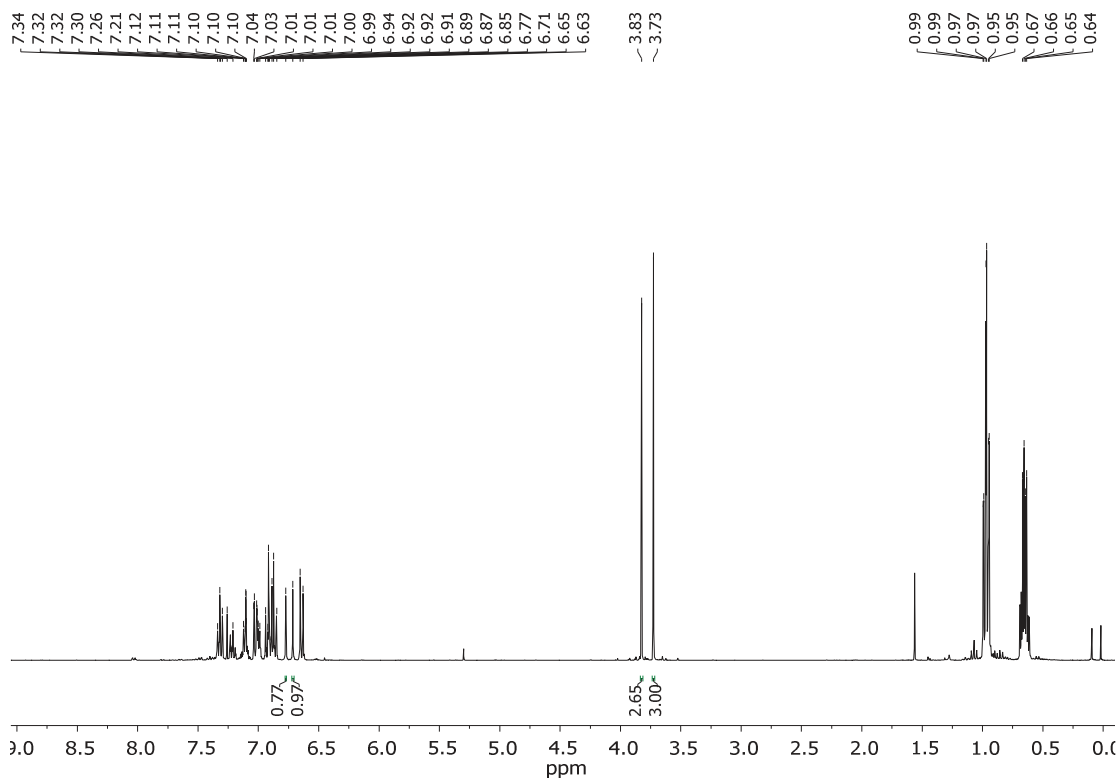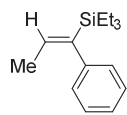
^{1}H NMR (360 MHz, CDCl$_3$)

(*E*)-55a   (*E*)-55b
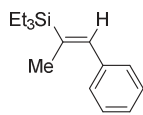
^{1}H NMR (250 MHz, CDCl$_3$)
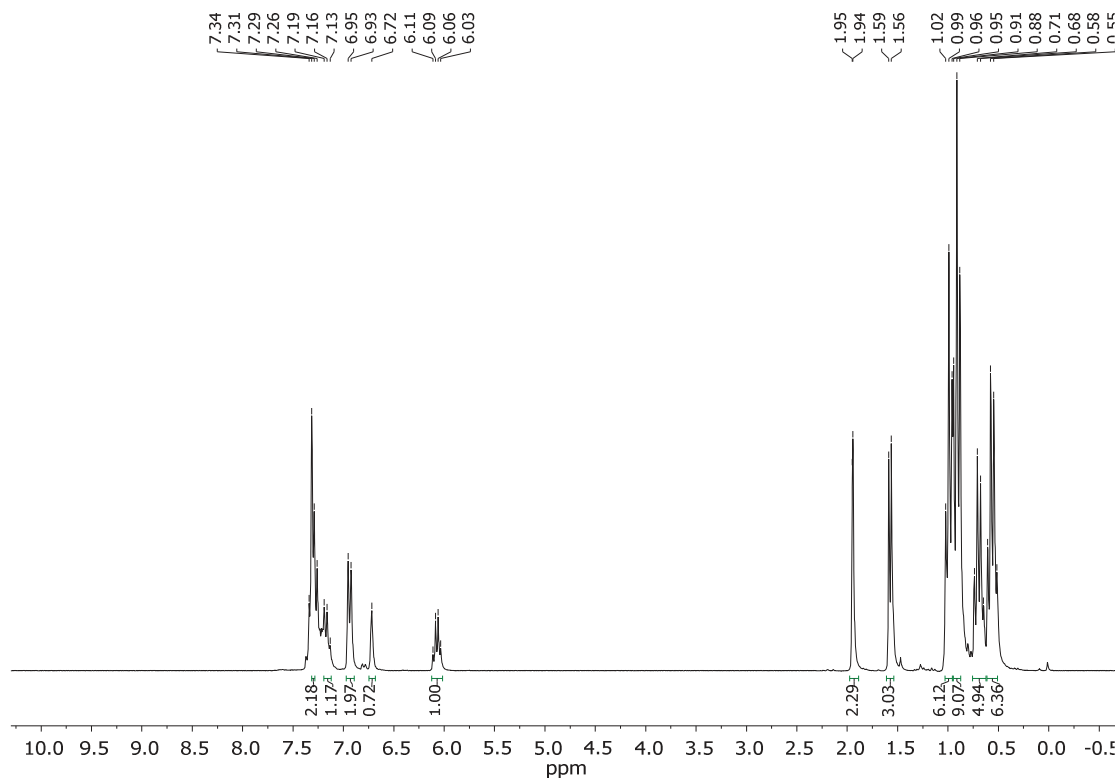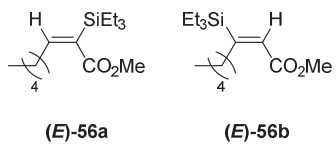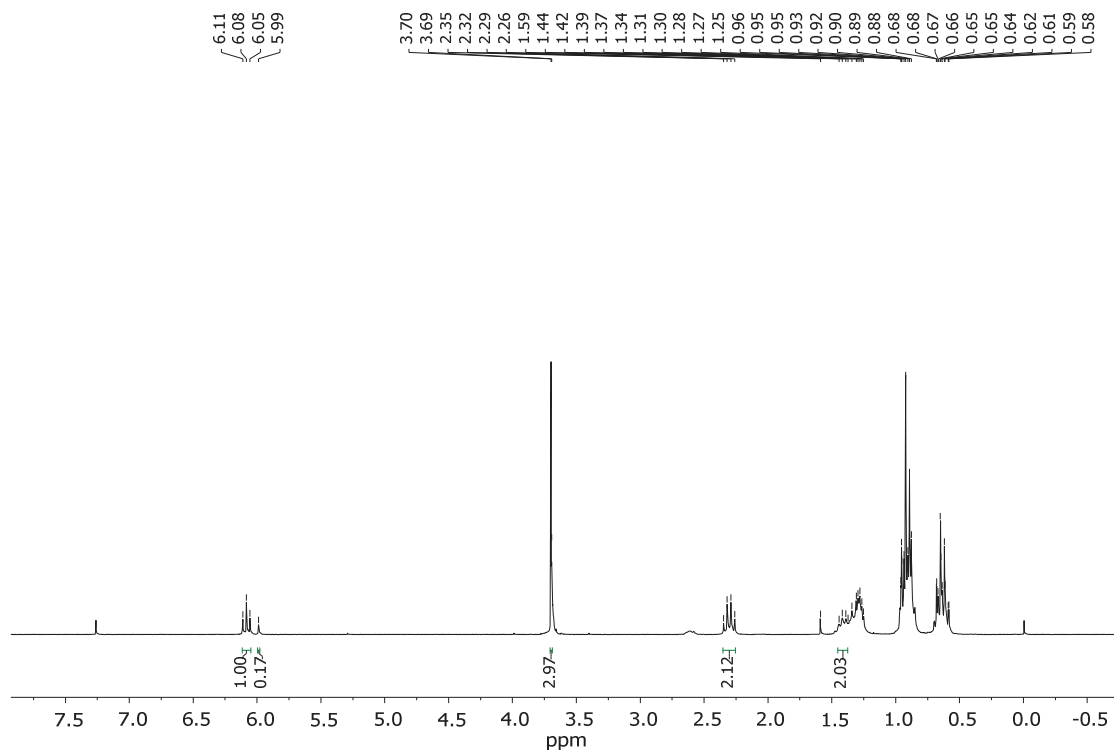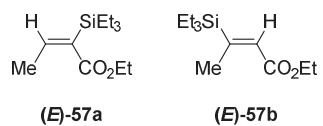
Spectra Collection

(*E*)-56a   (*E*)-56b

^{1}H NMR (250 MHz, CDCl$_3$)

(E)-57a   **(E)-57b**

^{1}H NMR (250 MHz, CDCl$_3$)

Spectra Collection

(E)-58a   58b

^{1}H NMR (250 MHz, CDCl$_3$)

(E)-59a   **59b**
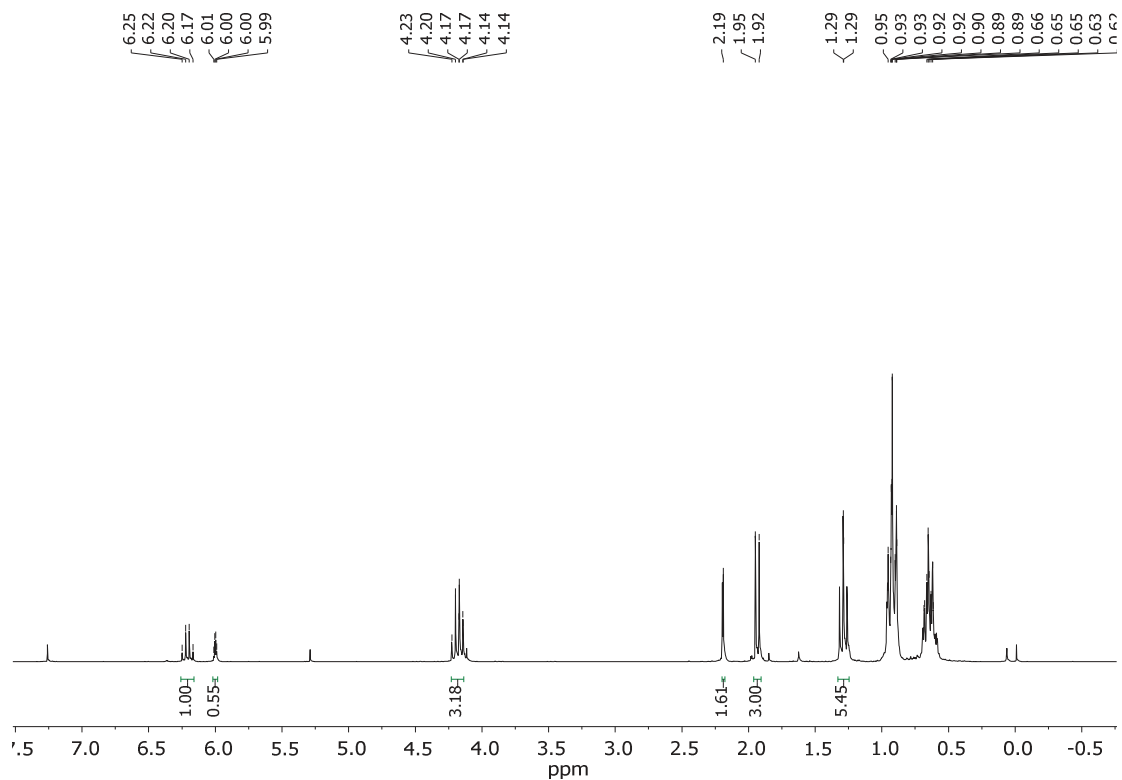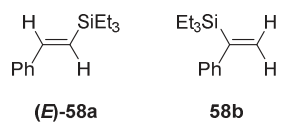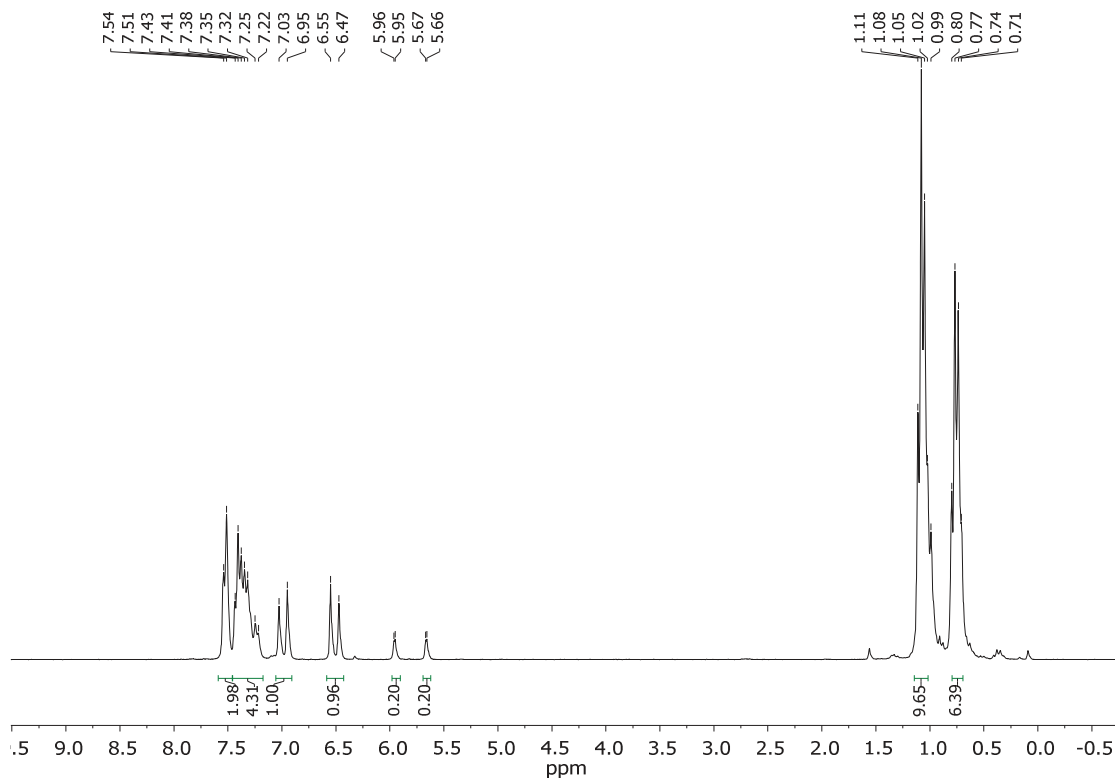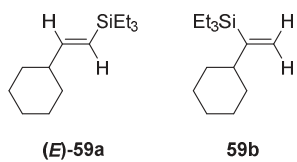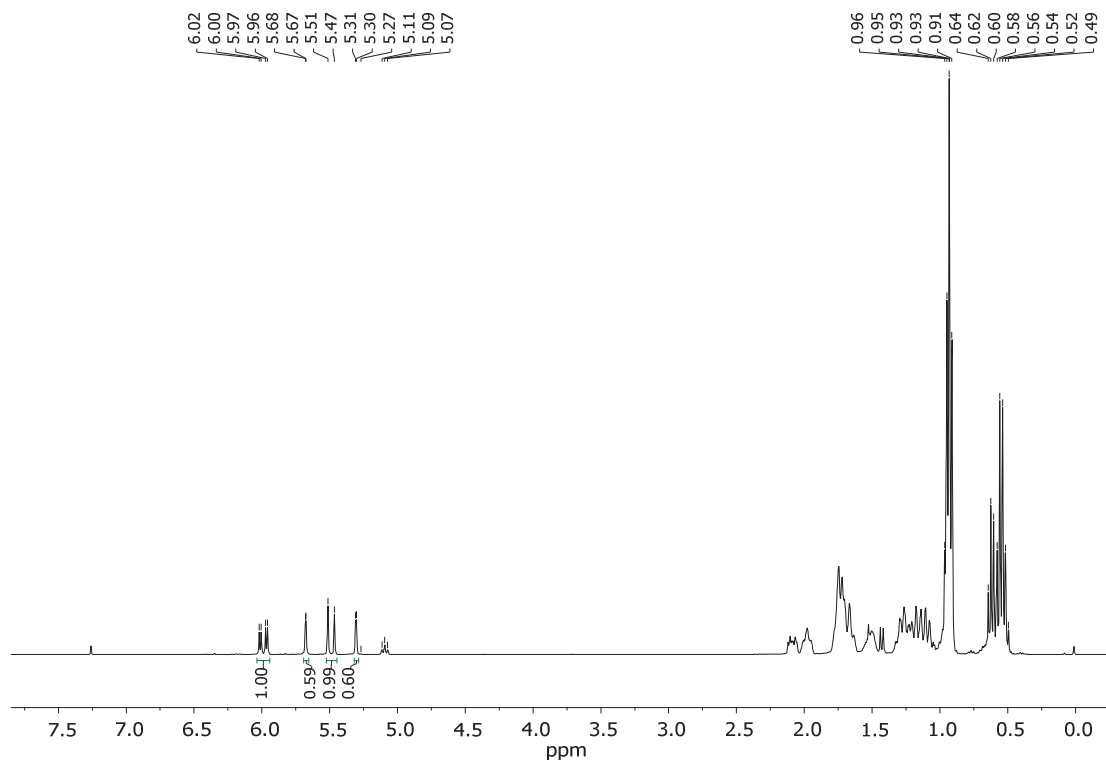
^{1}H NMR (400 MHz, CDCl$_3$)

Spectra Collection

60

^{1}H NMR (250 MHz, CDCl$_3$)
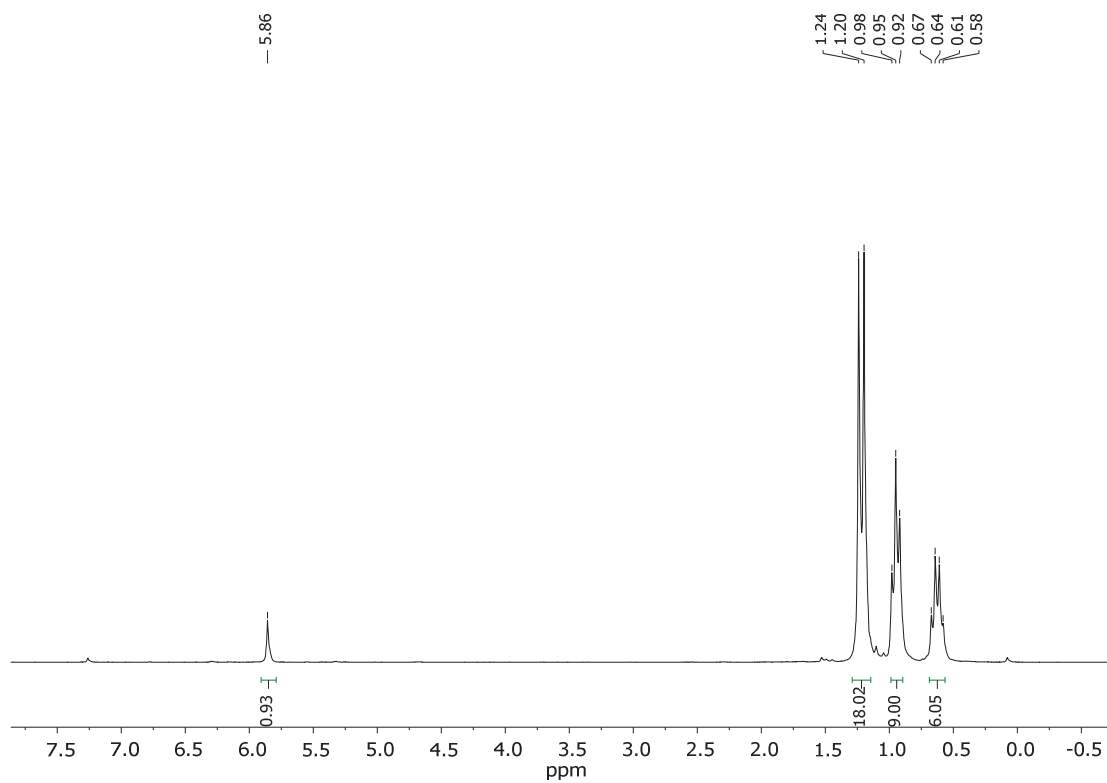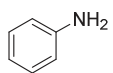
NH$_2$

62

^{1}H NMR (250 MHz, CDCl$_3$)

H$_2$N — ⬡ — NH$_2$

73

^{1}H NMR (250 MHz, CDCl$_3$)

6.95
6.91

6.14
6.13
6.11
6.10
6.02
6.01
6.00

3.52

0.99   2.98   4.00

8.0   7.5   7.0   6.5   6.0   5.5   5.0   4.5   4.0   3.5   3.0   2.5   2.0   1.5   1.0   0.5   0.0
ppm

74

^{1}H NMR (250 MHz, CDCl$_3$)

6.77
6.77
6.73
6.67
6.63

3.75
3.74

3.42

2.00
2.02

3.00

1.84

ppm
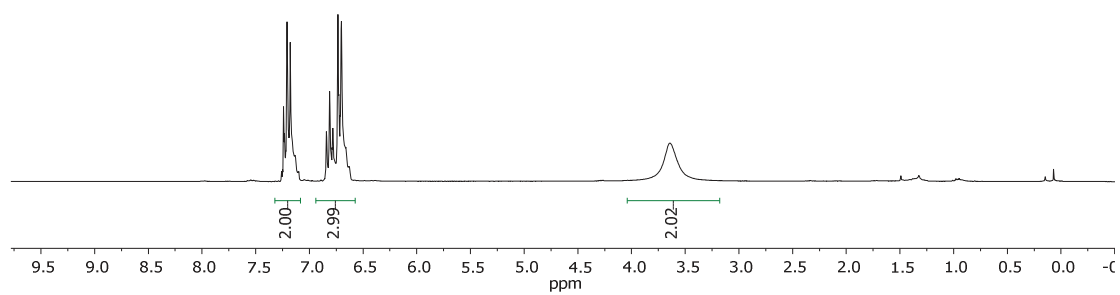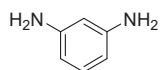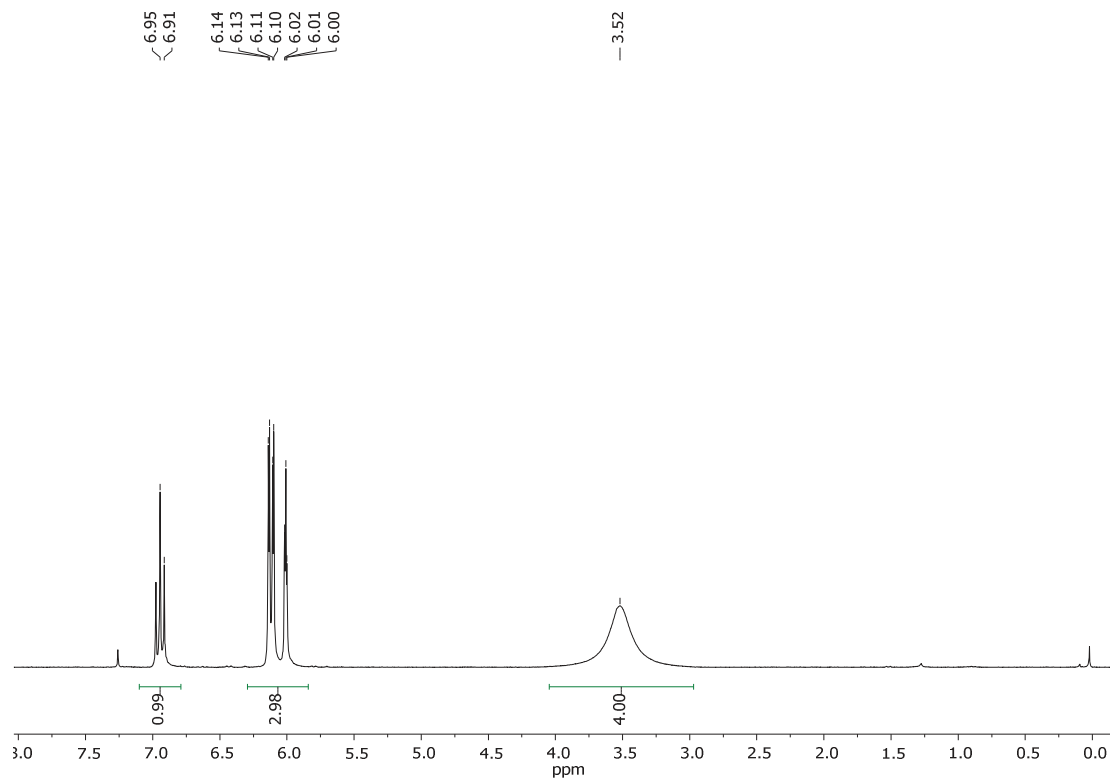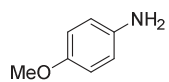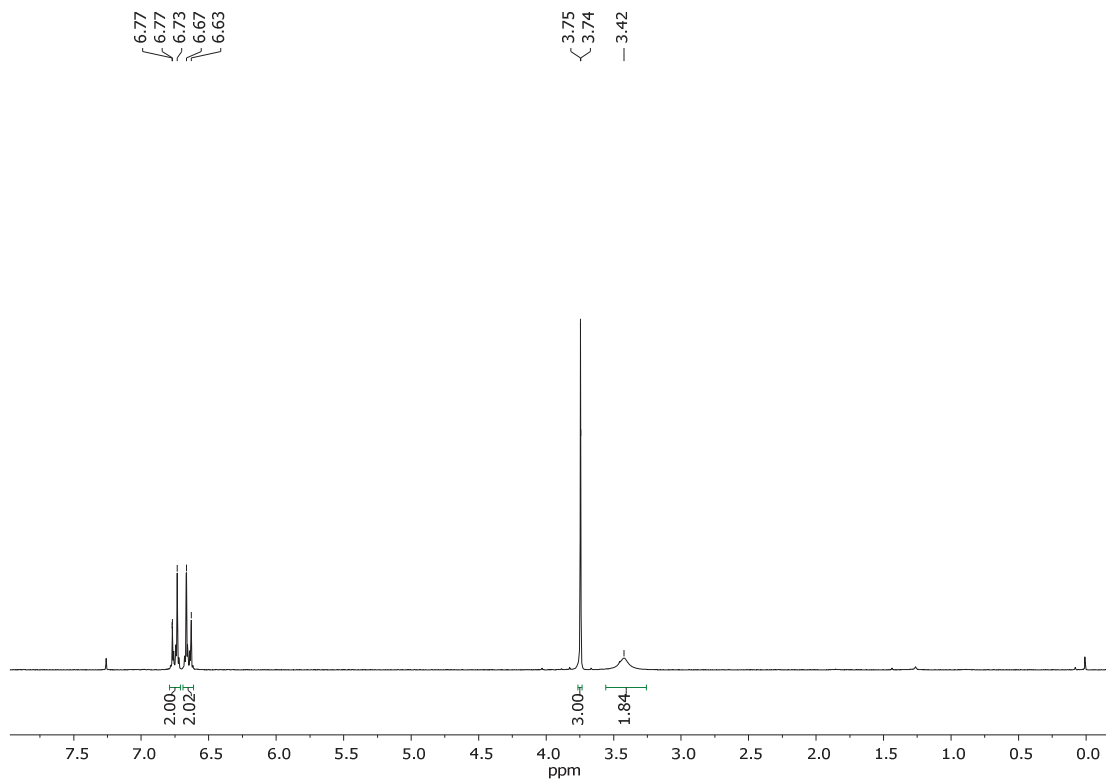
Spectra Collection
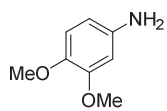
75

^{1}H NMR (250 MHz, CDCl$_3$)

76

^{1}H NMR (250 MHz, CDCl$_3$)

77

^{1}H NMR (360 MHz, (CD$_3$)$_2$CO)

78

^{1}H NMR (250 MHz, CDCl$_3$)

7.27
7.26
7.24
7.23
6.58
6.57
6.56
6.55

3.77
3.76
3.75
3.70
3.69

1.97
1.88
2.00

14.0 13.5 13.0 12.5 12.0 11.5 11.0 10.5 10.0 9.5 9.0 8.5 8.0 7.5 7.0 6.5 6.0 5.5 5.0 4.5 4.0 3.5 3.0 2.5 2.0 1.5 1.0 0.5 0.0
ppm

NC—⟨benzene ring⟩—NH$_2$

79

^{1}H NMR (250 MHz, CDCl$_3$)

7.39
7.36
7.35

6.65
6.61
6.61

4.26

2.02
2.06
2.00

9.0 8.5 8.0 7.5 7.0 6.5 6.0 5.5 5.0 4.5 4.0 3.5 3.0 2.5 2.0 1.5 1.0 0.5 0.0
ppm

80

^{1}H NMR (250 MHz, CDCl$_3$)

7.81
7.77

6.65
6.61

4.22
4.22

2.49

2.00

2.01

2.00

3.03

9.0 8.5 8.0 7.5 7.0 6.5 6.0 5.5 5.0 4.5 4.0 3.5 3.0 2.5 2.0 1.5 1.0 0.5 0.0
ppm

Spectra Collection

^{13}C NMR (90 MHz, CDCl$_3$)

— 196.49

— 151.15

∖ 130.74
/ 127.66

— 113.62

∖ 29.64
/ 26.04

| 230 | 220 | 210 | 200 | 190 | 180 | 170 | 160 | 150 | 140 | 130 | 120 | 110 | 100 | 90 | 80 | 70 | 60 | 50 | 40 | 30 | 20 | 10 | 0 | -10 |

ppm

IR (ATR)

3389.48
3328.77
3222.60
2922.16
2852.46
2363.97
1736.67
1650.03
1586.13
1563.47
1513.25
1437.94
1358.66
1303.65
1260.14
1176.47
1092.30
1023.64
959.31
836.14
818.37
736.65
696.34

Transmittance [%]

Wavenumber cm-1

224

81

^{1}H NMR (250 MHz, CDCl$_3$)

Spectra Collection

^{13}C NMR (90 MHz, CDCl$_3$)

146.10

137.86
128.61
128.52
127.87
127.66
126.81
126.03
124.98

115.11

150	140	130	120	110	100	90	80	70	60	50	40	30	20	10	0

ppm

ESI-HRMS

+MS, 0.4-0.5min #26-27

1+
196.1121

1+
197.1148

#	m/z	I	I %
1	196.1121	383288	100.0
2	197.1148	60354	15.7
3	198.1189	4320	1.1

226

90

^{1}H NMR (250 MHz, CDCl$_3$)

7.26 7.26 7.18 7.18 7.15 7.15 7.14   6.69 6.66   4.55

1.00 1.09 1.03

9.0 8.5 8.0 7.5 7.0 6.5 6.0 5.5 5.0 4.5 4.0 3.5 3.0 2.5 2.0 1.5 1.0 0.5 0.0

ppm

Spectra Collection

91

^{1}H NMR (360 MHz, CDCl$_3$)
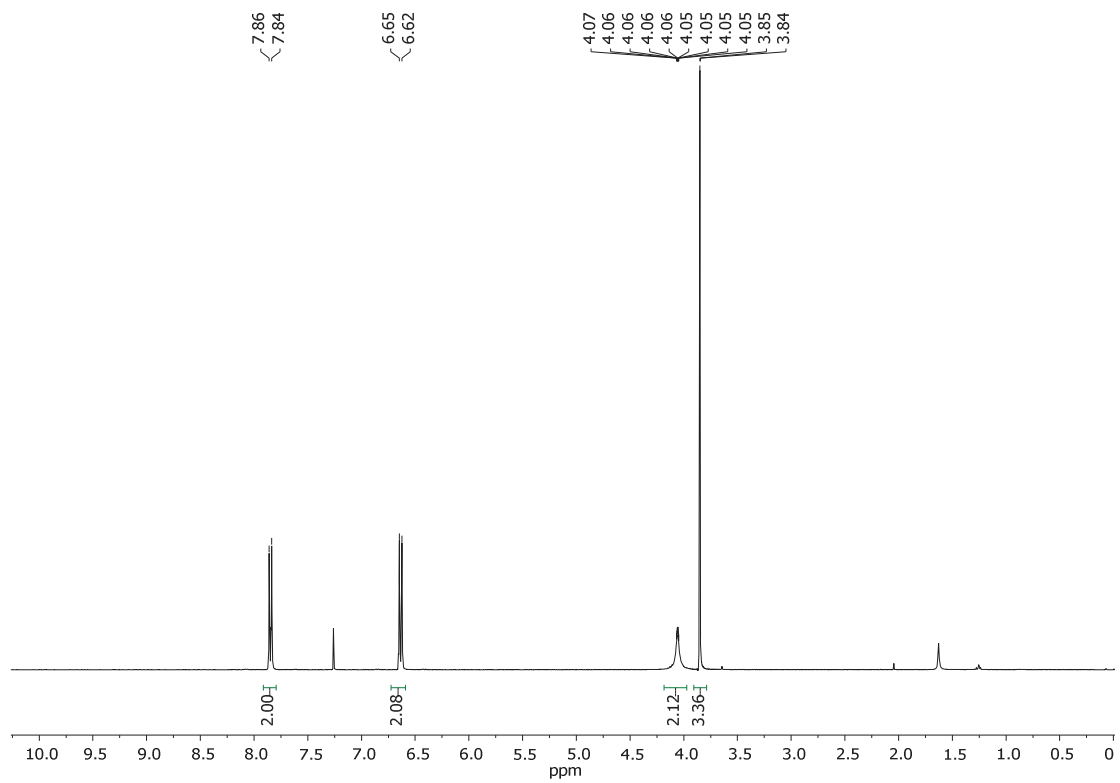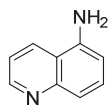
92

^{1}H NMR (360 MHz, CDCl$_3$)
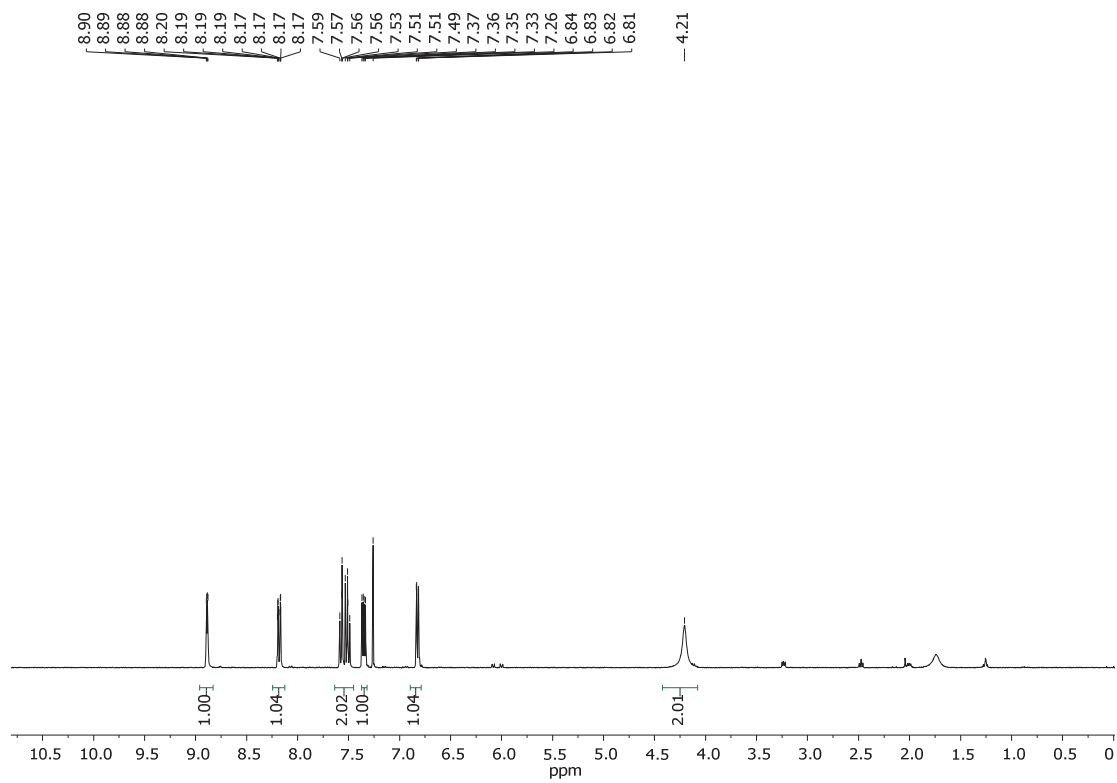
Spectra Collection

93

^{1}H NMR (360 MHz, CDCl$_3$)

7.08
7.06
7.04
6.62
6.61
6.61
6.61
6.60
6.60
6.59
6.59
6.59
6.54
6.53
6.53
6.51
6.50

3.58
3.58

2.28

0.98
0.95
1.93
1.86
3.07

9.0 8.5 8.0 7.5 7.0 6.5 6.0 5.5 5.0 4.5 4.0 3.5 3.0 2.5 2.0 1.5 1.0 0.5 0

ppm